# THE EFFECT OF ISCHAEMIA ON CAVERNOSAL SMOOTH MUSCLE

A thesis submitted to University College London, University of London in part fulfilment of the requirement for the degree of;

## DOCTOR OF PHILOSOPHY

by

## Pardeep Kumar

Department of Applied Physiology

The Institute of Urology

UCL

2012

# ABSTRACT

Ischaemic priapism is a pathological condition characterised by a prolonged painful penile erection. Corporal blood aspirates show a combination of hypoxia, acidosis and glucopenia. Initial treatment includes ice packs, corporal aspiration and subsequent washout with room temperature fluids. The effect of ischaemia on cavernosal smooth function was examined.

*In vitro* guinea-pig cavernosal smooth muscle strip experiments showed that simulated ischaemia caused a significant and marked reduction in phenylephrine-induced (PE) contraction (plateau $PE_{30}$ response 35±19%, plateau $PE_{60}$ response 29±16% of control). The degree of depression was similar to that seen in nerve-contraction although there appeared to be some metabolic reserve as shown by early preservation of the peak PE response (peak $PE_{30}$ response 83±31%, peak $PE_{60}$ response 36±35% of control). Nerve-contraction did not recover upon reperfusion whereas agonist-contractures demonstrated complete recovery. Experiments recording the effect of the elements of ischaemia showed this depression to be secondary to combined hypoxia and substrate depletion (absence of superfusate glucose and Na pyruvate). Isolated muscle cells showed a significant reduction in agonist-induced calcium transients during similar interventions.

Simulated ischaemia markedly reduced nerve- and abolished agonist-relaxation. These detrimental effects were completely reversible upon reperfusion. Nerve-relaxation recovered whereas nerve-contraction did not. This effect was again secondary to the combination of hypoxia and substrate depletion. This suggests that relaxatory nerves are more resistant to ischaemic damage, a finding which would contribute to the pathogenesis of ischaemic priapism and the contractile failure observed in this condition.

Intracellular acidification caused a significant and reversible increase in nerve-mediated contraction. Intracellular acidification also augmented PE contractures at 30 min. (peak $PE_{30}$ response 120±12%, plateau $PE_{30}$ response 117±9%). Intracellular acidification induced a significant and reversible increase in PE-induced calcium transients in isolated cells. This augmentation of function was via an oxygen-dependent mechanism.

Reduction in superfusate temperature significantly suppressed nerve-contraction. This was not due to reduced recruitment of nerve fibres at low temperature. The time-course of phasic nerve-contractions and agonist-contractures was prolonged, slowing responses significantly. Nerve-relaxation was significantly ameliorated at low temperatures. The phasic relaxation was also prolonged with the return to pre-contracted tension following EFS-mediated relaxation slowed to a greater degree than the initial relaxatory response. No change in magnitude of agonist-induced relaxation was observed. Overall reduced temperature interventions affect contraction to a greater degree than relaxatory mechanisms. These effects were not due to changes in the visco-elastic properties of the tissue at low temperature.

Prolonged ischaemia is detrimental to contractile function before relaxatory responses. Substrate depletion is a late finding in ischaemic priapism, with undetectable blood glucose after 6-12 hours of priapism. Depletion of the energy substrates glucose and Na pyruvate, combined with hypoxia, is central to the contractile failure seen in ischaemic priapism. This depression is irreversible on contractile nerves at an earlier stage when compared to relaxatory nerves and the smooth muscle itself, propagating the ischaemic priapic state. Reversal of these conditions should form part of any treatment regimen for patients who have priapism. Low temperature interventions do not improve CSM function with nerve-mediated function significantly reduced at low temperature as well as slowing CSM contractile responses. It may be beneficial to use oxygenated washout fluids at body temperature which contain energy substrates such as glucose and Na pyruvate to treat ischaemic priapism.

# ACKNOWLEDGEMENTS

'Obstacles are those frightful things you see when you take your eyes off the goal' *Henry Ford*

'The journey is the reward' *Chinese Proverb*

# CONTENTS

# LIST OF FIGURES

# LIST OF TABLES

# ABBREVIATIONS

| | |
|---|---|
| A | acidosis |
| $\alpha$-AR | $\alpha$-adrenergic receptor |
| Ach | acetylcholine |
| $\beta$-AR | $\beta$-adrenergic receptor |
| BCECF | 2'7'bis(carboxyethyl)-5,6-carboxyfluorescein |
| $Ca^{2+}$ | free ionised calcium |
| $[Ca^{2+}]$ | concentration of free ionised calcium |
| $[Ca^{2+}]_i$ | intracellular concentration of free ionised calcium |
| csa | cross-sectional area |
| CSM | cavernosal smooth muscle |
| DMSO | dimethyl sulphoxide |
| ET-1 | endothelin 1 |
| EGTA | ethylene glycol tetraacetic acid |
| eNOS | endothelial nitric oxide synthase |
| cGMP | 3',5'-cyclic guanosine monophosphate |
| GTP | guanosine triphosphate |
| H | hypoxia |
| $[H^+]$ | concentration of free ionised hydrogen |
| I | intra-cellular acidosis |
| IA | intra and extra-cellular acidosis |
| $IP_3$ | inositol 1,4,5-triphosphate |
| $IP_3R$ | inositol 1,4,5-trisphosphate receptor |
| $K_{ATP}$ | ATP sensitive potassium channels |
| $K_{Ca}$ | calcium sensitive potassium channels |
| $K_d$ | dissociation constant |
| MLCK | myosin light chain kinase |
| MLCP | myosin light chain phosphatase |
| mRNA | messenger ribonucleic acid |
| NA | noradrenaline |
| NADPH | nicotinamide adenine dinucleotide phosphate |
| $NADPH_i$ | intracellular nicotinamide adenine dinucleotide phosphate |
| NANC | non-adrenergic, non-cholinergic |
| NO | nitric oxide |
| NOS | nitric oxide synthase |
| nNOS | neuronal nitric oxide synthase |
| ODQ | 1H-[1,2,4]oxadiazolo-[4,3-a]quinoxalin-1-one |
| PE | phenylephrine |
| $pH_i$ | intracellular pH |
| $pH_e$ | extracellular pH |
| PKA | protein kinase A |
| PKC | protein kinase C |
| PKG | protein kinase G |
| PMT | photomultiplier tube |
| $pO_2$ | partial pressure of oxygen |
| S | substrate depletion – absence of sodium pyruvate and glucose |
| SR | sarcoplasmic reticulum |
| sGC | soluble guanyl cyclase |
| TTX | tetrodotoxin |

**1.0    Introduction**

1.1    **Priapism**

Priapism is defined as a pathological condition where penile erection persists beyond, or is unrelated to sexual stimulation. Priapism often affects young men who frequently develop severe erectile dysfunction as a consequence with its resultant effects on both physical and psychological wellbeing. Priapism is a relatively uncommon condition with an incidence of 1.5 per 100,000 person-years rising to 2.9 per 100,000 person-years in men 40 years and older[1, 2]. In certain population groups the reported incidence is much higher. In an international multi-centre study of men with sickle-cell anaemia, 35% of men questioned reported at least one episode of priapism[3].

The term priapism is derived from the Greek demi-god Priapus. Priapus was cursed by the goddess Hera to be impotent, ugly and of unpleasant personality whilst in the womb of his mother Aphrodite. Born with a disproportionately enlarged phallus, Priapus became a symbol of the vitality of the animal and plant kingdoms. Interestingly, Priapus was often frustrated by his impotence, the subject of many songs and comedies. The first mention of Priapus in existence is in the eponymous comedy *Priapus*, written in the 4th century BC by Xenarchus[4]. "Gonorrhoea, Satyriasi et Priapisme" by Petraens contains the earliest account of priapism in the medical literature. Research into the condition in the 20th century consisted of personal case series of patients with priapism where it was recognised as a difficult condition to treat.

Hinman in the early 20th century attempted to classify the disease into either mechanical or nervous types and suggested an approach to management based on this[5]. The mechanical subtype was described as being related to thrombosis of the veins of the corpora. Conditions

associated with this condition included pelvic abscesses, penile tumours, perineal and genital injuries and blood dyscrasias. The nervous subtype related to intracerebral disorders affecting the erectile process such as syphilis, brain tumours, epilepsy and spinal cord injuries. Dysfunction of venous outflow was hypothesised as the primary reason for failure of detumescence in priapism by Hinman Jr.(6). He proposed that the dark viscous blood seen following aspiration or incision of the corpus cavernosum during a bout of priapism had a reduced oxygen tension with elevated carbon dioxide levels and that these factors enhanced blood viscosity, particularly in patients with abnormal erythrocytes such as in sickle cell anaemia(6).

The contemporary view is that priapism encompasses two distinct clinical entities, high flow arterial and low flow ischaemic priapism, both exhibiting the phenotype of prolonged penile erection(7). The terms high and low flow describe the status of the blood flow in the penis; the differing clinical presentation and treatments of these groups is outlined below.

### 1.1.1    High flow priapism

High flow priapism is due to unregulated arterial blood flow within the lacunar spaces of the corpora cavernosae of the penis(8, 9). This results in a localised hyperdynamic circulation with penile tumescence secondary to a pressure effect and release of localised relaxant factors. High flow priapism occurs most commonly following penile or perineal trauma ('saddle' or 'fall astride' type injuries). This results in a cavernosal artery laceration which may present acutely or after several days or weeks. Delayed presentation is postulated to occur due to the original injury causing a localised area of arterial wall weakness which subsequently 'gives way' resulting in unrestricted arterial flow within the penis(8). Microvascular trauma secondary to the injection

needle used in intracavernosal therapy for erectile dysfunction may also create an arterio-lacunar fistula resulting in high flow priapism(9, 10).

High flow priapism has also been described in association with sickle cell anaemia(11), cavernosal artery pseudoaneurysms(12) and Fabry's disease(13, 14). Fabry's disease is an inherited disorder which results in an α-galactosidase A deficiency. This leads to a glycolipid accumulation in vascular endothelium such as that lining the lacunar spaces of the penis. It is postulated that this leads to derangement of the nitric-oxide pathway, especially when associated with a concurrent glucose-6-phosphate dehydrogenase deficiency (15-17).

High flow priapism is typically painless; the penis is well oxygenated and not subject to the localised ischaemia present in the low-flow subtype where smooth muscle damage and corporal fibrosis predominate(7, 18). Erectile function is preserved in 77%-86% of patients on long term follow up(8, 18). Corporal blood aspiration shows well oxygenated blood and colour Doppler ultrasound shows good arterial penile blood flow. These diagnostic tests are interpreted with caution as the simple act of inserting a needle into the corpus cavernosum of an *ischaemic* priapism may produce a localised iatrogenic arteriovenous shunt. This can erroneously infer the diagnosis of a safe high flow priapism in a patient who actually has an ischaemic priapism which has a poorly oxygenated, acidotic microenvironment and is a surgical emergency(19, 20).

Conservative measures to treat high flow priapism have been reported with limited success. These include observation, ice packs/baths and intracavernosal injection of methylene blue (a monoamine oxidase inhibitor which may act as a non-selective inhibitor of nitric oxide synthase)(18, 21, 22). The mainstay of current management is superselective internal pudendal angiography. This modality allows confirmation of the diagnosis as well as intervention by means

of injection at the site of the lacunar fistula with either absorbable gelfoam or permanent metallic coils(23-26). Metallic coils are no longer recommended due to their permanent nature being implicated in long term erectile dysfunction in these patients. Although spontaneous resolution can occur after observation, immediate embolisation is both successful and avoids the risk of long term venous leakage(24). Open arterial ligation using intraoperative ultrasound to localise the abnormality has also been described(27).

## 1.1.2    Ischaemic priapism

The commonest subtype, ischaemic priapism, is characterised by a prolonged painful penile erection often lasting for more than 8 hours(28). The condition is a surgical emergency as it is a form of compartment syndrome(10, 29, 30). The corpora cavernosae are turgid and painful with dark ischaemic blood, the glans is characteristically soft as it is uninvolved in the pathophysiology due to its differing blood supply. Blood is trapped within the lacunar spaces of the penis, with little or no arterial inflow or venous outflow. As the priapism episode progresses, the cavernosal microenvironment becomes progressively more ischaemic(31). Blood gas analysis of cavernosal aspirates typically demonstrates hypoxia and acidosis, typical values are outlined in table 1.1(10, 32). A subtype of ischaemic priapism is termed 'stuttering' priapism. This is characterised by recurrent short lived painful erections which may precede a full blown ischaemic priapism episode(33, 34).

*Table 1.1 – Typical cavernosal blood gas values. Adapted from (31, 35)*

*14 patients developed prolonged painful erections following prostaglandin $E_1$ ($PGE_1$) injection administered in a hospital environment. Corporal aspiration and blood gas analysis demonstrated a clear trend towards hypoxia, acidosis and hypercarbia with prolonged erections lasting between 105 and 342 minutes(31). In addition 6 patients with prolonged ischaemic priapism lasting 60-240 hours also demonstrated severe glucopenia on corporal blood aspirates(35).*

|  | Normal flaccid penis | Normal erect penis | High flow priapism | Ischaemic priapism |
|---|---|---|---|---|
| pH | 7.35 | 7.35 | 7.4 | <7.25 |
| $pO_2$ (mmHg) | 40 | 100 | 60 -100 | <30 |
| $pCO_2$ (mmHg) | 50 | 40 | 40-50 | >60 |
| blood glucose (BM) | 4-8 | 4-8 | 4-8 | <4 |

There are several causes of ischaemic priapism with early therapy aimed at preventing cavernosal smooth muscle necrosis and preserving long-term erectile function (Table 1.2). The mechanisms underlying prolonged penile tumescence in this clinical scenario are unclear but are thought to be a combination of both veno-occlusive and smooth muscle dysfunction.

Several haematological conditions are associated with priapism. Postulated mechanisms include increased blood viscosity and abnormal erythrocyte function. Sickle cell anaemia is the commonest blood dyscrasia associated with ischaemic priapism; 38-42% of patients report at least one episode of priapism(3, 36). It is seen more commonly in homozygous patients and is associated with sickle cell crises where abnormal deformation of red cells occur causing occlusion of the microvasculature and localised ischaemia. There may also be chronic changes

within the cavernosum of these patients resulting in disordered contractile regulatory mechanisms within the smooth muscle(27, 37). Other associated conditions include leukaemia, thalassemia, polycythaemia, fat emboli and Fabry's disease(38, 39).

Drug therapy is also associated with low flow ischaemic priapism (Table 1.2). This may be secondary to α-adrenergic blockade resulting in impaired cavernosal smooth muscle contraction. Intracavernosal agents utilised in erectile dysfunction and directly instilled into the corpora (e.g. papaverine, prostaglandin $E_1$ and phentolamine) are associated with low-flow priapism and account for 0.5-6% of cases. Drug classes associated with priapism include α-adrenergic blockers, serotonin agonists and dopamine antagonists(40-42).

Primary penile cancer, local invasion from adjacent organs and metastases from distant sites have been reported as causing priapism. Local invasion occurs from the prostate, bladder and urethra(43-48). Priapism associated with neurological disorders is well described. An imbalance of parasympathetic and sympathetic outflow from the spinal cord is postulated as the underlying pathology however this is far from clear. Examples include cauda equina syndrome, spinal cord lesions and spinal stenosis(49-54). Amyloidosis, rabies and scorpion stings are rare conditions described in case reports as causing ischaemic priapism(55-57).

*Table 1.2 - Causes of ischaemic priapism*

*In Europe and the U.S.A the commonest cause of priapism is intra-cavernosal therapy for erectile dysfunction. Worldwide sickle cell anaemia predominates(30).*

| Category | Subtypes |
|---|---|
| Drug therapy for ED | Intra-urethral prostaglandin $E_1$ (MUSE) |
| | Intra-cavernosal prostaglandin $E_1$ (Caverject) |
| | PDE-5 inhibitors (Sildenafil, Tadalafil, Vardenafil) |
| | Intracavernosal phentolamine - α-AR antagonist |
| | Papaverine – intracavernosal vasodilator |
| Haematological | Sickle cell anaemia |
| | Thrombophilia |
| | Other Haemoglobinopathies inc. Thalassemia |
| | Leukaemia |
| | Myeloma |
| Pharmacotherapy and other drugs | Phenothiazines |
| | Selective Serotonin Reuptake Inhibitors (SSRIs) |
| | Anticoagulants (heparin) |
| | Anti-hypertensives |
| | Alcohol |
| | Marijuana |
| | Cocaine |
| Solid Tumours | Locally advanced bladder cancer |
| | Locally advanced prostate cancer |
| | Metastatic renal cancer |
| Systemic disease | Hypertension |
| | Diabetes |
| | Rheumatoid Arthritis |
| Idiopathic | |
| Others | Total parenteral nutrition, amyloid, rabies, appendicitis |

Regardless of the underlying cause, urgent treatment is indicated as smooth muscle death and subsequent impairment of function are the inevitable sequelae of delayed or inappropriate treatment(58, 59). This may leave young, previously fit men, with severe organic erectile dysfunction and its' associated physical and psychological morbidity. It is therefore essential that the goals of any treatment regimen should not only take into account penile detumescence but also preservation of long term sexual function(60).

Patients with recurrent 'stuttering' priapism describe the use of masturbation and ejaculation, cold baths and ice packs in managing short lived episodes of priapism and avoiding presentation to their medical practitioner(61). The primary medical treatment of ischaemic priapism involves analgesia followed by aspiration of blood from the corpora and irrigation with 0.9 % NaCl solution at room temperature should initial non-invasive measures fail. Aspiration of the stagnant blood may be enough to re-establish penile blood flow and terminate the priapic episode with penile detumescence(10, 28). The aspirate is typically dark and viscous and should be sent for blood gas analysis to confirm the diagnosis. Aspiration and washout is often combined with the use of ice-packs and cold compresses. There is no evidence for the use of these reduced temperature interventions.

Should these measures be unsuccessful in effecting detumescence, α-adrenergic agonists (usually phenylephrine) injected into the corpora cavernosae are recommended(60, 62). Careful cardiovascular monitoring is instigated during treatment to monitor for the systemic effects of α-agonists (cardiac arrythmias, hypertension). The aim of treatment is to cause contraction of the cavernosal smooth muscle and helicine arteries. This then relieves pressure on the venous outflow with the aim of re-establishing penile blood flow and penile detumescence(60, 62). Alternative α-agonists have been described in the literature including epinephrine, norepinephrine

and metaraminol(32). Several other oral and intracavernosal agents have been described although none has gained widespread use in the initial treatment of priapism. These include the cyclic guanosine monophosphate (cGMP) inhibitor methylene blue (stains penis bright blue), etilefrine (oral and intracavernous α-agonist) and intracavernosal thrombolysis(63-68). Oral terbutaline has been reported to be successful although it does also have β-agonist effects(69, 70).

It is clear from clinical studies that intra-cavernosal injection of α-agonists becomes less efficacious with increasing duration of ischaemia(35). Cavernosal smooth muscle biopsies from patients with ischaemic priapism show evidence of apoptosis and necrosis(71, 72). In addition, functional *in vitro* studies on this tissue have shown it to be increasingly resistant to phenylephrine-induced contraction in a time-dependent manner(35).

Failure of intra-cavernosal therapy is considered when detumescence has not occurred despite up to one hour of repeated intracavernosal injections in conjunction with systemic treatment where indicated (e.g. intravenous fluid resuscitation and oxygen in sickle cell crisis)(62). Invasive surgical intervention is indicated at this stage. The aim of shunt surgery is to create an iatrogenic fistula between the corpora cavernosae and the systemic circulation, bypassing the dysfunctional veno-occlusive mechanism and providing venous outflow for blood within the corpus cavernosae(73). Shunts are indicated where there is a possibility of salvage of some degree of long term erectile function. In prolonged cases of priapism (>72 hours) penile implant insertion is the preferred option in the acute phase(74).

Various shunt procedures have been described and these are summarised in table 1.3(75-81). Shunts are reported to effect detumescence in up to 50% of patients(28). However, long-term

erectile dysfunction is common in up to 80% of patients(73). When shunt surgery has failed the placement of a penile prosthesis is considered in order to minimise penile shortening secondary to fibrosis and preserve sexual function. Implant surgery may be considered at an earlier stage in those with pre-existing erectile dysfunction or those who present at a late stage of their priapic episode(74).

The mechanisms underlying priapism are unclear. An outline of penile anatomy, cavernosal smooth muscle physiology and the normal mechanisms of penile erection and detumescence follow.

Table 1.3 – Summary of shunt surgery

## 1.2 **The penis**

### 1.2.1 Macroscopic structure

The human penis acts as the common conduit for both urine and semen. In addition, when erect, the penis is the male copulatory organ. Anatomically the penis is described when erect therefore the dorsal aspect is the surface closest to the abdominal wall and the ventral surface that where the urethra is palpable. It is predominately formed by 3 'tubes'. The paired corpora cavernosae dorsally and the corpus spongiosum (surrounding the anterior urethra) ventrally. These three erectile bodies are anchored proximally to both fasciae and bone within the superficial perineal pouch (the 'root' of the penis). The two corpora cavernosae attach to the inferior pubic rami and perineal membrane surrounded by the ischiocavernosus muscles. The single corpus spongiosum is attached to the centre of the perineal membrane. From there it enlarges distally to incorporate the bulbar urethra and is surrounded by the bulbospongiosus muscle. The corpus spongiosum runs along the ventral aspect of the penis and expands distally to 'cap' the paired corpora cavernosae as the glans penis, separated from them by the penile corona(29, 82-84).

The paired corpora cavernosae join in the midline beneath the pubis to form the major portion of the penile body. These 'pressure barrels' are surrounded by the tunica albuginea, a thick collagenous layer formed of inner circular and outer longitudinal fibres. These are elastic and change orientation to accommodate the enclosed spongy tissue during penile erection. There is a midline septum between the two cavernosae which is fenestrated, allowing free communication between the two chambers. Each corpus cavernosum encloses a lacunar meshwork of smooth muscle (50%) and connective tissue (45%)(72). The spaces within this spongy tissue are lined by vascular endothelium which, in response to appropriate stimuli, releases vaso-active factors

resulting in smooth muscle relaxation and penile tumescence. The spongy network is interspersed with collagen and elastin (fig. 1.1).
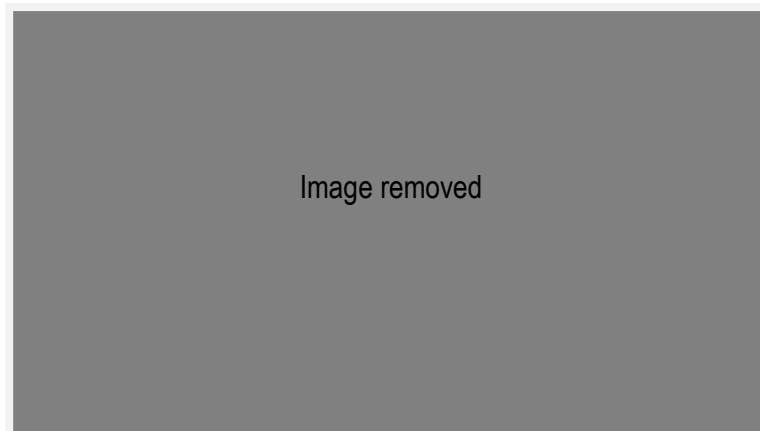


*Figure 1.1 – Cross section of the human penis at the mid-shaft level*

The corpus spongiosum and contiguous glans penis are similar in structure to the corpora cavernosae. However, the vascular spaces within the smooth muscle meshwork are larger and the surrounding tunica is thinner around the corpus spongiosum. This is due to an absent outer tunical longitudinal layer and ensures a low pressure system in this part of the penis during erection. The tunica is absent over the glans penis.

Bucks' fascia surrounds all three penile corpora and extends proximally to join with fibres from the anterior rectus sheath to form the fundiform ligament of the penis. Fibres arise from the pubis itself and merge with the fundiform ligament to form the penile suspensory ligament. This acts to hold the penis in an upright position during penile erection(82). Bucks' fascia extends distally and fuses with the penile corona, just proximal to the glans penis. Surrounding Bucks' fascia is a further superficial fascial layer just beneath the skin. This layer of dartos confers the mobility required to accommodate the changes of penile size during tumescence. The blood supply to this skin is independent to that of the erectile bodies(84).

## 1.2.2 Blood supply of the penis

The penile artery is the terminal branch of the internal pudendal artery, itself arising from the anterior branch of the internal iliac artery. The internal pudendal artery passes through the perineum supplying the anus and scrotum. It then passes through Alcock's canal as the penile artery and forms three terminal branches. The *bulbourethral* artery supplies the urethra, corpus spongiosum and glans penis. The *cavernosal* artery, responsible for cavernosal tumescence, traverses the corpus cavernosum giving rise to many branches which supply the spongy corporal tissue (fig. 1.2).


Image removed
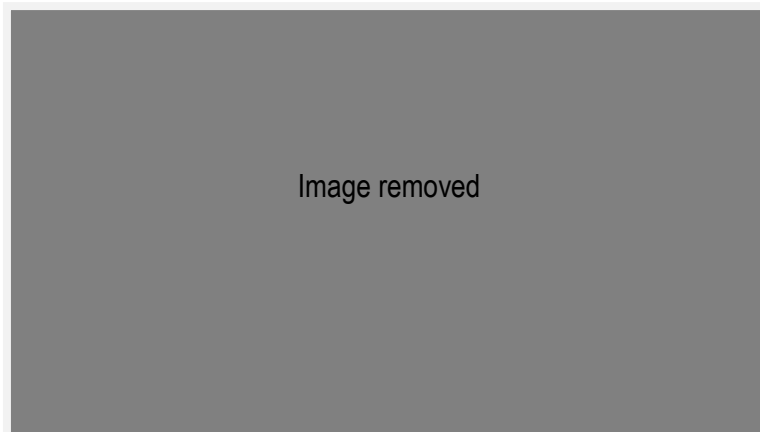
*Figure 1.2 – Arterial blood supply to the penis (withealth.net)*
*The penis has an extensive arterial supply. It is important to note that the supply to the corpora cavernosae differs from that of the glans and corpus spongiosum as well as the overlying skin.*

The terminal helicine arteries of the cavernosal artery are intimally associated with the trabeculated smooth muscle along with the terminal cavernosal nerves (fig 1.3)(84, 85). These helicine arteries are tortuous in the flaccid state becoming straight during penile erection. The *dorsal* artery of the penis, responsible for tumescence of the glans, runs along the dorsal aspect of the penis with the dorsal vein and nerve below Buck's fascia in the main neurovascular bundle of the penis. This third artery gives rise to circumferential branches to the cavernosum,

spongiosum and urethra. These branches take a direct route when piercing the tunica, resulting in minimal occlusion during penile erection (fig. 1.1).
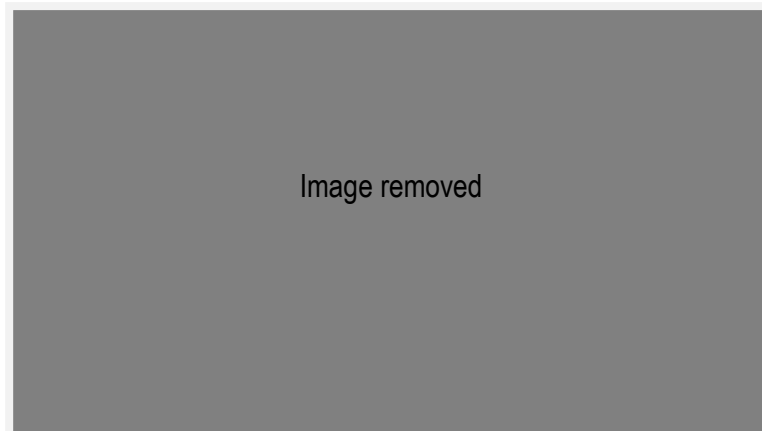


*Figure 1.3 – Scanning electron micrograph of arterial supply to lacunar space* Modified from(85)

The main venous drainage of the penis is via the deep dorsal penile vein (fig. 1.4). This arises from several venous channels just proximal to the glans penis (the retro coronal venous plexus). It traverses the ventral aspect of the penis with tributaries from the corpus spongiosum (circumflex veins present in the distal two thirds of the penis). The vascular spaces of the corpora cavernosae drain into venules which coalesce beneath the tunica to form the subtunical venous plexus before exiting as the emissary veins (fig. 1.5)(84). These emissary veins follow an oblique path between the layers of the tunica and drain into the circumflex veins dorsolaterally. This oblique path changes orientation during penile erection resulting in venular occlusion and contributing to penile erection. In the proximal one third of the penis, veins draining the cavernous bodies, crura and penile bulb join the dorsal penile vein to drain into the internal pudendal veins.
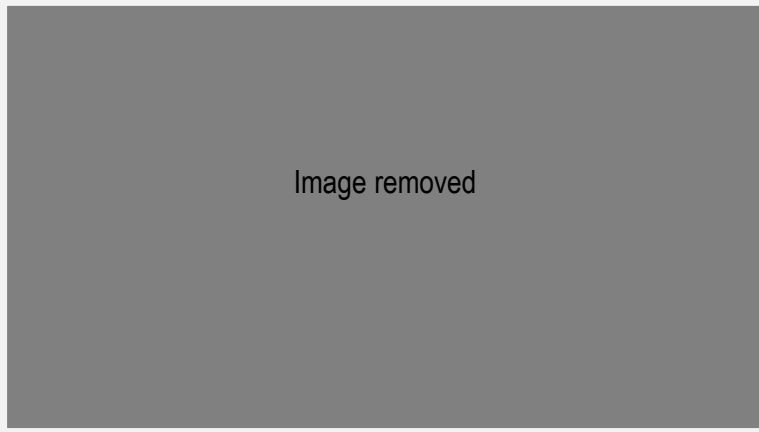
*Figure 1.4 – Venous drainage of the penis (withealth.net)*

*Draining veins coalesce into a sub-tunical plexus such that as penile tumescence occurs, venular compression occurs. This 'traps' blood within the penis and contributes to the veno-occlusive mechanism of penile erection.*
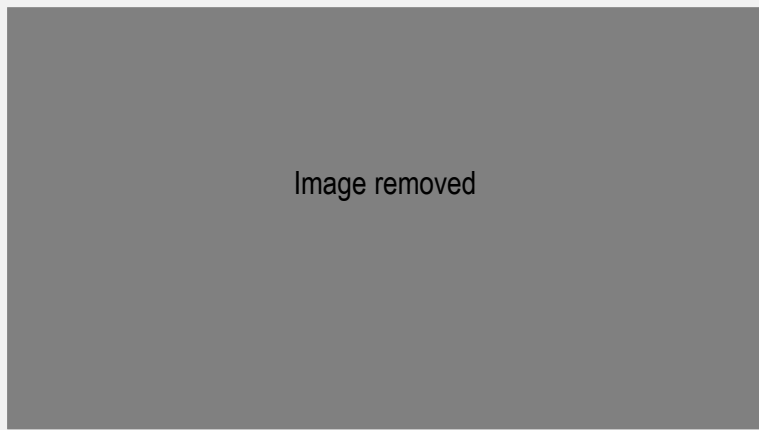


*Figure 1.5 – Scanning electron micrograph of venous drainage of subtunical plexus(85)*

*Draining emissary veins pass through the tunica albuginea in an oblique fashion becoming occluded as penile erection occurs.*

## 1.2.3   Innervation of the penis

The penis has both autonomic (parasympathetic and sympathetic) and somatic (sensory and motor) innervation. The autonomic nerve populations have been divided into three categories; adrenergic, cholinergic and non-adrenergic, non-cholinergic (NANC)(86-88).

The parasympathetic pathway arises from the second to the fourth sacral spinal segments (fig. 1.6, S2-S4). Pre-ganglionic fibres travel via the pelvic nerves to the pelvic plexus. The sympathetic pathway arises from eleventh thoracic to the second lumbar spinal segments (T11-L2), passing through the white rami to the sympathetic chain ganglia. Fibres travel via the lumbar splanchnic nerves to the inferior mesenteric and superior hypogastric plexuses. The hypogastric nerves contribute to the pelvic plexus and together with the parasympathetic fibres, form the cavernosal nerves (fig. 1.6). The cavernosal nerves supply the corpora to effect the neurovascular events seen during erection and detumescence(29, 83, 84, 86).

The somatosensory pathway originates at the sensory receptors in the penile skin, glans, urethra and within the corpora cavernosae. These free nerve endings are derived from both thin myelinated $A_\delta$ fibres and unmyelinated C fibres. They converge to form the dorsal nerve of the penis. This in turn merges with the perineal and inferior rectal nerves to form the pudendal nerve, entering the spinal cord as the second, third and fourth sacral nerves (S2-S4). The dorsal nerve also contains autonomic elements enabling it to regulate both erectile and ejaculatory function. Somatomotor innervation arises from Onuf's nucleus located in the ventral part (lamina IX) of the anterior horn in the sacral region of the spinal cord (S2-S4). Fibres originating here travel as the pudendal nerve, via the sacral nerves, to innervate the ischiocavernosus and bulbocavernosus

muscles. Contraction of these produces the rigid erection phase, with contraction of bulbocavernosus required for ejaculation(83, 84, 86).
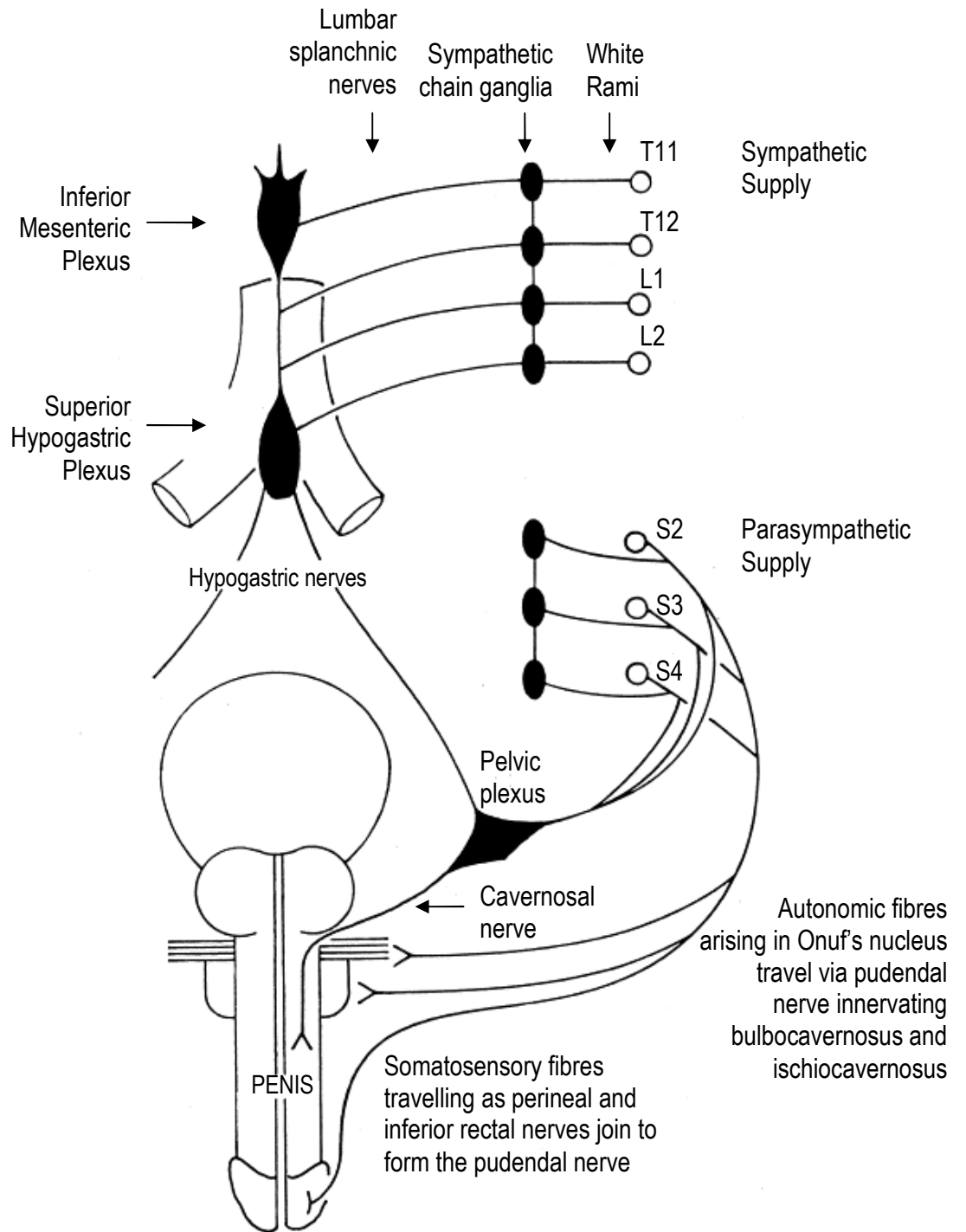


*Fig. 1.6 – Diagrammatic representation of penile neural pathways.* Adapted from(89)

1.2.4    Central pathways involved in penile erection

Penile erection is a process which, in health, is initiated centrally at the level of the hypothalamus. The predominant areas involved are the medial preoptic area (MPOA) and the paraventricular nucleus (PVN)(90). Sensory stimuli originating at the somatosensory nerve terminals are processed here and integrated with multiple other stimuli including audiovisual, cognitive, olfactory and tactile sensation. Dopaminergic neurons arising from the caudal hypothalamus synapse with oxytocinergic neurones within the PVN(91, 92). Stimuli are integrated within these two centres and result in activation of the autonomic pathways which mediate penile erection. Pro-erectile neurotransmitters include dopamine, adrenocorticotrophic hormone (ACTH) and oxytocin. Those inhibiting penile erection are 5-Hydroxytryptamine (5-HT), γ-aminobutyric acid (GABA), neuropeptide Y and prolactin(83, 84).

## 1.3    Mechanism of penile erection and detumescence

1.3.1    Corpora cavernosae

The state of the penis is predominantly influenced by the arteriolar and trabecular smooth muscle tone. In the flaccid state, these muscles are tonically contracted, allowing enough penile blood flow to maintain homeostasis. In response to appropriate stimuli, neurotransmitters are released from the cavernous nerve terminals resulting in smooth muscle relaxation. Six phases in the cycle of penile erection and detumescence are described (fig. 1.7)(93, 94):

1. *Flaccid phase*

   Minimal arterial and venous blood flow with cavernosal blood gas values similar to those of venous blood. Flow rate 2.5-8 mL/100 g/min(95); 0.5-6.5 mL/100 g/min(94). Arteriolar and cavernosal smooth muscle is tonically contracted due to basal release of NA from sympathetic nerves and endothelin form the endothelium.

2. *Latent (filling) phase*

   Arterial smooth muscle relaxation in the internal pudendal artery during both systolic and diastolic phases results in increased blood flow into the penis. The lacunar spaces within the corpora fill with blood and expand, facilitated by relaxation of the trabeculated smooth muscle. Intracavernous pressure remains unchanged and there is some lengthening of the penis.

3. *Tumescent phase*

   As the trabecular meshwork expands the subtunical venular plexus is compressed against the inner layer of the tunica albuginea resulting in decreased venous outflow. Intracavernous pressure rises until full erection is achieved. The penis expands and elongates. The arterial blood flow rate decreases as the pressure rises.

4. *Full erection phase*

   As the tunica albuginea expands, the inner circular and outer longitudinal layers expand in slightly differing directions secondary to the orientation of the connective tissue fibres. The emissary veins which traverse the tunica in an oblique fashion are occluded as the tunica expands, resulting in a further reduction in venous outflow. These changes result in an increase in intracavernous pressure. In the adult this can rise to as much as 80-90% of the systolic pressure (~100 mmHg). Pressure in the internal pudendal artery increases but remains slightly below systemic pressure. Arterial blood flow is much less than in the initial filling phase but is still higher than in the flaccid phase. Although the

venous channels are mostly compressed, the venous flow rate is slightly higher than during the flaccid phase. Due to these pressure changes, blood flow occurs only in systole. Cavernosal blood gas values approach those of arterial blood.

5. *Rigid erection phase*

As a result of contraction of the ischiocavernosus muscle (which surround the bony attachment of the corpora cavernosae), the intracavernous pressure rises well above the systolic pressure, resulting in rigid erection. During this phase, almost no blood flows through the cavernous artery; however, the short duration prevents the development of ischaemia or tissue damage.

6. *Detumescent phase*

After ejaculation or cessation of erotic stimuli, smooth muscle contraction occurs as a result of increased sympathetic tone. This effectively diminishes the arterial flow to flaccid levels. The penis returns to its flaccid length.

Image removed
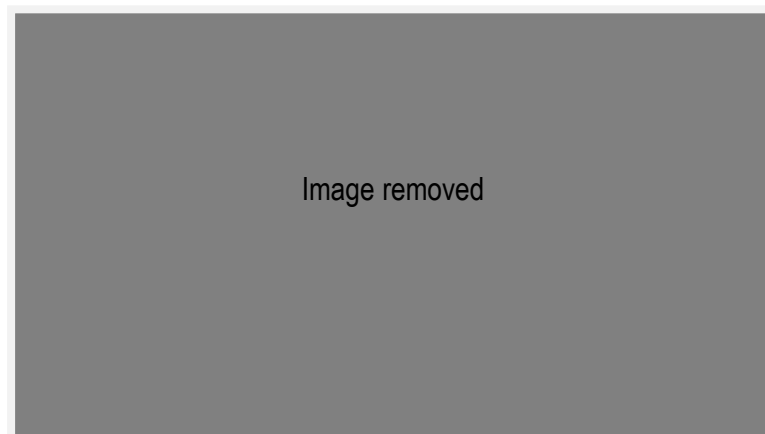
*Figure 1.7 – Graph showing penile haemodynamic changes during erection and detumescence*

*Recordings made in monkeys with erections induced by neurostimulation.*

*Numbers along the top correlate with phases of penile erection.*

*Upper trace – pudendal arterial blood flow, Lower trace – intracavernosal pressure(93).*

Penile erection is thus a combination of arterial dilatation, sinusoidal relaxation and venous compression(93).

## 1.3.2    Corpus spongiosum and glans penis

Arterial inflow to the glans and corpus spongiosum increases in a similar manner to that seen in the corpora cavernosae. However, the absence of tunical covering of the glans and lack of tunical longitudinal fibres over the spongiosum results in minimal venous occlusion and a lower pressure system during erection (typically one third to one half that seen in the corpora cavernosae). During erection, compression of the dorsal and circumflex veins contributes to engorgement of the glans and spongiosum. In the rigid erection phase, contraction of the ischiocavernosus and bulbocavernosus muscles compress the spongiosum and penile veins, increasing pressure within the glans(96).

## 1.4      Mechanisms of cavernosal smooth muscle contraction

### 1.4.1    Cavernosal smooth muscle cell structure

Cavernosal smooth muscle fibres are spindle shaped and have the ability to both contract and relax. The smooth muscle cells contain the proteins calmodulin, caldesmon and calponin. The cytoskeleton consists of the intermediate filament proteins vimentin and desmin, along with actin filaments. The actin filaments attach to the sarcolemma by focal adhesions. The contractile proteins actin and myosin organise into zones along the long axis of the cell. The sarcolemma possesses invaginations containing receptors (including muscarinic and adrenergic receptors), G proteins (Rho A, G alpha), second messenger generators (adenylate cyclase, phopholipase C)

and ion channels (L-type calcium channels, ATP sensitive potassium channels - $K_{ATP}$, calcium sensitive potassium channels - $K_{Ca}$)(86).

To maintain the trabeculated structure found within the corpora, cells are attached to one another by adherens junctions. Because of this, contraction of one cell causes contraction of adjacent cells simply by transmission of mechanical force. In addition, electrical activity within the corpus cavernosum is coordinated, with cells behaving as a functional syncytium(86). Gap junctions couple adjacent cells both chemically and electrically, facilitating propagation of smooth muscle cell contraction and relaxation. Connexin 43 is the predominant gap junction protein found in cavernosal tissue. These intercellular channels promote co-ordinated smooth muscle contraction and relaxation(97).

### 1.4.2 Neurotransmitters involved in penile detumescence and maintenance of penile flaccidity

#### 1.4.2.1 Noradrenaline

Penile flaccidity is achieved when corporal smooth muscle is tonically contracted. A-adrenergic nerve fibres and receptors present in the trabeculated cavernosal smooth muscle and cavernosal arteries are thought to mediate this contraction. The α-adrenoceptor (α-AR) is ten times more prevalent within the corporal smooth muscle than the β-adrenoceptor (β-AR) with around 650,000 α-AR binding sites per cell(98, 99). Both the $α_1$–AR and $α_2$–AR sub-types are present in CSM however the former is functionally more important(100-104).

It is postulated that $α_{1A}$-, $α_{1B}$- and $α_{1D}$-AR subtypes mediate smooth muscle contraction, the $α_{1b}$ subtype conferring a degree of pre-synaptic modulation(103, 105, 106). Both phenylephrine and

noradrenaline contract human corpus cavernosum smooth muscle(107). Non-selective α-AR antagonists abolished these contractions (phentolamine) as did the $\alpha_1$-AR antagonist prazosin(107, 108). These same contractions were also sensitive to the L-type $Ca^{2+}$ channel antagonists nifedipine and rauwolscine(107, 108). $A_1$-adrenoceptor mediated contraction results in the release of intracellular $Ca^{2+}$ stores followed by the extracellular entry of $Ca^{2+}$ for the maintenance of tone (Fig. 1.8).

Receptor localisation studies have shown that $\alpha_2$-ARs are present on the helicine arterioles supplying the cavernosal spaces(102, 109). In addition $\alpha_2$-ARs have been demonstrated on the autonomic nerves (pre-junctional) and smooth muscle itself (post-junctional)(100). Selective $\alpha_2$-agonists elicit contraction of corpus cavernosum strips *in vitro* as well as inhibiting NO release from autonomic nerves(102, 110). The role of these receptors in health and disease in the *in vivo* setting are unclear.

Both $\beta_1$ and $\beta_2$ adrenoceptors are expressed in cavernosal smooth muscle(99). Both procaterol (selective $\beta_2$ adrenoceptor agonist) and isoprenaline ($\beta_1$ and $\beta_2$ adrenoceptor agonist) produce relaxation in CSM strips pre-contracted with NA(107). Selective β-adrenergic stimulation produces relaxation of both corporal and penile arteriolar vascular smooth muscle(107). This effect was abolished in the presence of the β antagonist propranolol. These results suggest that both $\beta_1$ and $\beta_2$ adrenoceptor activation cause relaxation of corporal smooth muscle. However, β receptors are markedly outnumbered by α receptors on cavernosal smooth muscle and their functional role in the maintenance of smooth muscle tone is still largely unknown(99).

## 1.4.2.2 Calcium sensitisation and maintenance of CSM tone

Tension generated for a given intracellular $[Ca^{2+}]$ ($[Ca^{2+}]_i$) is variable. For example, tension generated in response to α-adrenoceptor stimulation is greater than that generated secondary to membrane depolarisation (e.g. by KCl)(111). Force of contraction does not always correlate with the degree of elevation in $[Ca^{2+}]_i$(112). This would suggest a possible calcium-sensitizing effect of contractile-agonists. Simultaneous *in vitro* measurement of $[Ca^{2+}]_i$ and tension in cavernosal smooth muscle strips during $\alpha_1$-adrenoceptor stimulation showed increase in force to correlate with both $[Ca^{2+}]_i$ and sensitivity of the contractile apparatus(111). These sensitizing effects are due to inhibition of myosin phosphatase via guanosine triphosphate (GTP) binding proteins that generate protein kinase C or arachidonic acid(113). This reduction in phosphatase activity results in a net increase of phosphorylated $MLC_{20}$ and therefore smooth muscle contraction independent of an increase in $[Ca^{2+}]_i$. The calcium sensitizing Rho-A/Rho-kinase pathway plays a role in maintaining penile detumescence(114). In addition to inhibiting myosin phosphatase, Rho-A can itself directly phosphorylate $MLC_{20}$, resulting in an increase in activated myosin and therefore CSM contraction(86). An additional pathway contributing to this calcium sensitisation involves protein phosphatase-1 inhibitory protein (CPI-17)(111). This protein also inhibits myosin phosphatase when phosphorylated by protein kinase C. Again an increase or maintenance of tone can be seen independent of $[Ca^{2+}]_i$ increase(111).

## 1.4.2.3 Endothelins

Endothelins are potent vasoconstrictors produced by vascular endothelium and contribute to maintenance of the penis in the flaccid state. Endothelin-1 is not stored in vesicles, it is synthesised directly from mRNA in response to stimuli such as hypoxia, ischaemia,

catecholamines, angiotensin II, thrombin or sheer stress. Human corpus cavernosum endothelial

cells express endothelin 1 (ET-1) mRNA and ET receptors ($ET_A$ and $ET_B$) have been

demonstrated in penile vascular and trabecular CSM(115). $ET_A$ receptors are present in the

endothelium lining the lacunar spaces and appear to mediate relaxatory responses, possible via

the action of NO(116, 117). $ET_B$ receptors are localised to vascular endothelium and appear to

mediate vaso-constriction(116, 118). Despite these contrasting effects on stimulation of $ET_A$ and

$ET_B$ receptors, ET-1 itself induces slowly developing, long-lasting contractions in cavernosal

arteries and smooth muscle(115, 119, 120). The main role of endothelins in penile smooth

muscle physiology in health is to sustain smooth muscle tone and maintain penile

detumescence(121).
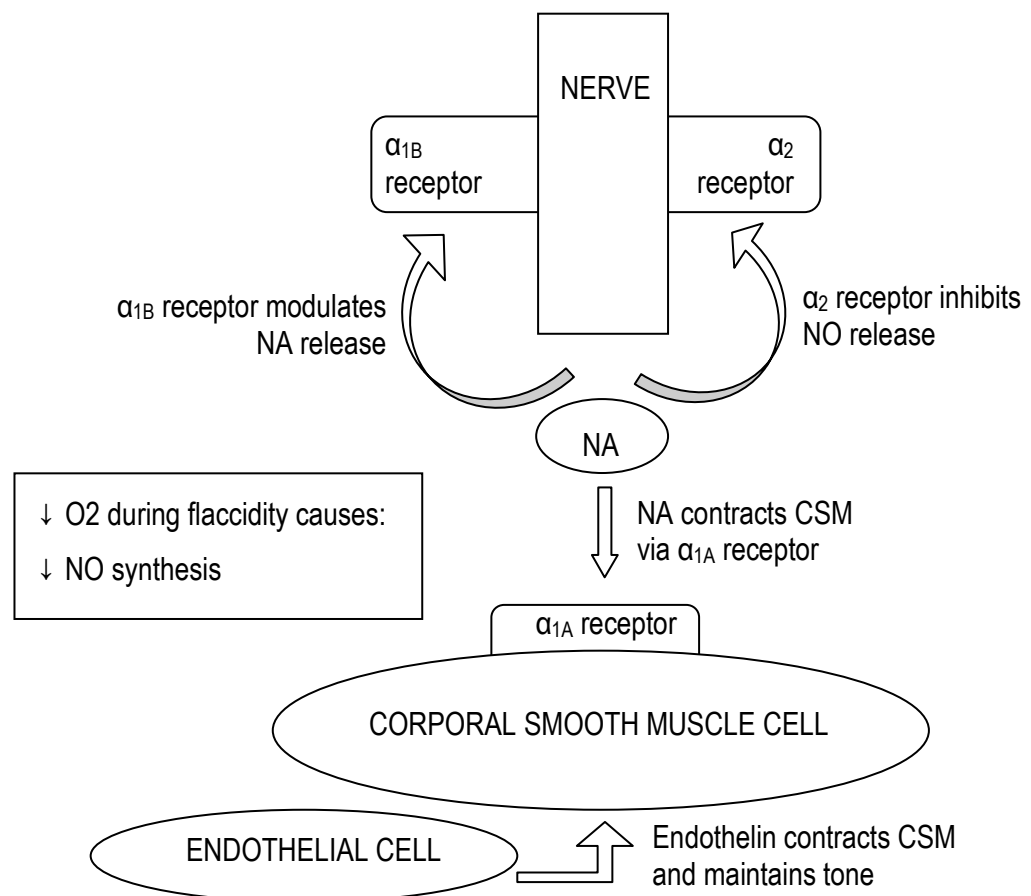


*Fig. 1.8 – Diagram of CSM contractile factors*

1.4.2.4   Oxygen tension and maintenance of penile flaccidity

There is also evidence to suggest that the corporal microenvironment itself may contribute to maintenance of flaccidity. The oxygen tension ($pO_2$) within the flaccid penis is around 25-43 mmHg(122, 123). This is similar to mixed venous blood. During penile erection, oxygen tension increases to around 100 mmHg(123). Production of NO requires oxygen and the reduction in $PaO_2$ in the flaccid penis in itself inhibits the basal release of nitric oxide, the principal mediator of CSM relaxation and penile tumescence(122-124). As penile tumescence begins, $PaO_2$ increases due to increased arterial flow, NO production becoming maximal at $pO_2$ levels above 60 mmHg(122). Prostaglandin formation is also reduced at low oxygen tension. $PGE_2$ contributes to CSM relaxation and therefore reduction in production will help maintain detumescence(Fig. 1.8)(125).

1.4.3   Molecular mechanism of smooth muscle contraction

Contraction of human penile arteries and trabecular smooth muscle is largely mediated by the stimulation of $\alpha_1$-ARs by circulating NA, NA release from autonomic nerves and endothelins from endothelium (fig. 1.8)(103, 126, 127). Cavernosal smooth muscle contraction is brought about by a sliding filament mechanism. Smooth muscle cell stimulation results in an increase in $[Ca^{2+}]_i$. These calcium ions bind to calmodulin forming a calcium-calmodulin complex. This complex in turn activates myosin light chain kinase (MLCK). Activated MLCK catalyses phosphorylation of the regulatory light chain subunits of myosin ($MLC_{20}$). Phosphorylated $MLC_{20}$ activates myosin ATPase. The myosin filaments then hydrolyse ATP to release energy. This enables the myosin filament to undergo a conformational change. The globular heads protruding from the myosin filament form crossbridges with the actin filaments. These myosin heads shift at the time of this

conformational change to slide along the actin filament. The heads then release and adopt their

original conformation prior to rebinding and shifting again should the stimulus for contraction

continue. This process is called crossbridge cycling (fig. 1.9)(128).
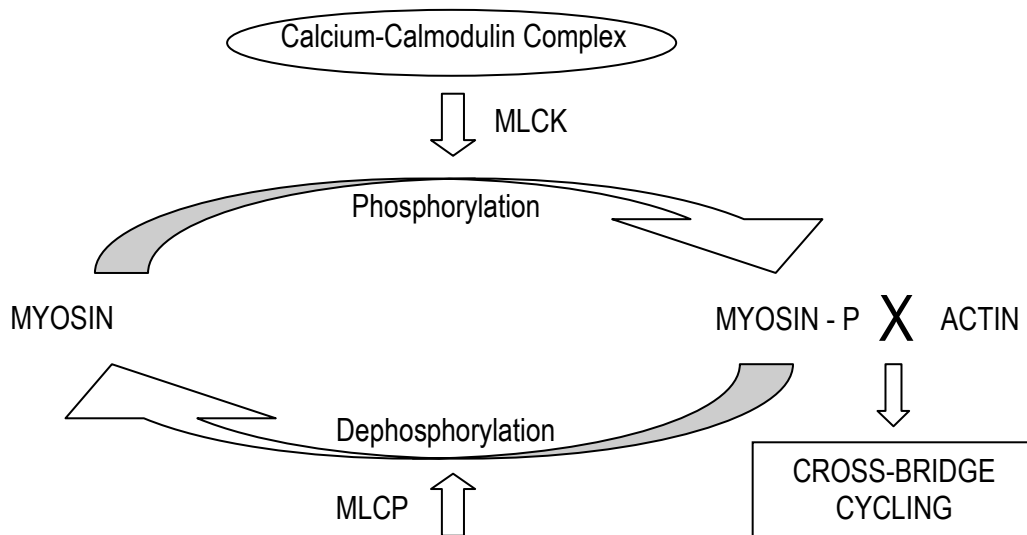


_Fig. 1.9 – Mechanism of contraction of CSM_
_The Calcium-Calmodulin complex brings about myosin phosphorylation via MLCK. This_
_Myosin-P then hydrolyses ATP and undergoes a conformational change moving along the_
_actin filament. These cross bridges continue forming and releasing as long as the stimulus for_
_contraction continues. Slowly cycling cross bridges and actin polymerisation contribute to the_
_maintenance of tone at low energy cost to the cell._

1.4.4    Energy consumption during smooth muscle contraction

Myosin light chain phosphorylation correlates well with the shortening velocity of smooth muscle.

This is accompanied by a rapid burst of energy as measured by oxygen consumption. Sustaining

this force of contraction is expensive in terms of energy and, soon after initiation, myosin light

chain phosphorylation decreases and the muscle relaxes. However, it is clear that in cavernosal

smooth muscle, a sustained level of smooth muscle tone is maintained to ensure that the penis

remains flaccid. This baseline tone may be attributed to slowly cycling de-phosphorylated myosin

crossbridges ('latch-bridges') and to actin polymerisation stiffening the cell. This type of contraction maintains a degree of force at low energy costs(129-134).

Maintenance of penile flaccidity is therefore an active process. Noradrenaline-induced smooth muscle contraction along with intrinsic myogenic activity and endothelium-derived contracting factors such as endothelin all contribute.

## 1.5 Mechanisms of cavernosal smooth muscle relaxation

### 1.5.1 Neurotransmitters involved in penile detumescence

#### 1.5.1.1 Acetylcholine

The penile vasculature and corporal smooth muscle receive a rich cholinergic innervation(129, 135, 136). Acetylcholine (Ach) acts on muscarinic receptors on both corporal smooth muscle and endothelium. $M_1$-$M_4$ receptor subtypes have been demonstrated in human corpus cavernosum with the $M_2$ subtype predominating on the smooth muscle and the $M_3$ subtype on the endothelium(137, 138). Isolated CSM cells have ~45,000 binding sites for Ach, approximately 15 times fewer than the number of α-ARs(98). Muscarinic receptor agonists cause contraction of *isolated* CSM. It is therefore postulated that the relaxant effects of ACh on CSM tissue are via pre-synaptic inhibition of adrenergic neurones which mediate smooth muscle contraction and by stimulation of the release of nitric oxide from endothelial cells(86, 107, 127, 135, 139, 140).

1.5.1.2  Nitric Oxide and the Guanyl Cyclase/cGMP pathway

Penile erection is a result of arteriolar and corporal smooth muscle relaxation. The principle neurotransmitter mediating this process is nitric oxide (NO)(86, 141). NO is synthesised from the terminal nitrogen atom of arginine by nitric oxide synthase (NOS) in the presence of NADPH and oxygen (fig. 1.10). It is therefore an oxygen dependent mechanism. There are several forms of NOS. Neuronal NOS (nNOS or NOS-1), is found in the cavernous nerves (postganglionic parasympathetic nerve fibres) and penile arteries(142). nNOS has also been demonstrated in pre-ganglionic parasympathetic nerves as well as pre-ganglionic sympathetic nerves(143-145). Endothelial NOS (eNOS or NOS-3) is present in the cells lining the cavernous spaces and in those lining the small intra-cavernosal helicine arteries(135, 142, 146, 147).

In response to stimuli from higher centres, electrical impulses are transmitted along efferent 'nitrergic' nerve fibres which terminate within the corporal bodies(148). The term 'nitrergic' applies to nerves whose transmitter function depends on the release of NO or to transmission mechanisms that are brought about by NO(149). This neuronal depolarisation causes the production of NO via nNOS. In addition, endothelial production of NO via eNOS is directly stimulated by acetylcholine as well as other neurotransmitters such as substance P and bradykinin(150, 151). Acute increases in shear stress (the term used to describe pressure forces exerted on endothelial cells by the flow of blood over them) act to drive rapid but limited amounts of NO release by similar biochemical mechanisms(152, 153).

NO diffuses into corporal smooth muscle cells where it catalyses the conversion of GTP into cyclic GMP (cGMP) and pyrophosphate via activation of the enzyme soluble guanyl cyclase (sGC). Cyclic GMP in cavernosal smooth muscle is metabolised by the iso-enzyme

phosphodiesterase-5. Inhibition of this enzyme (by drugs such as sildenafil - Viagra™) results in potentiation of the relaxatory effects of cGMP and penile erection.
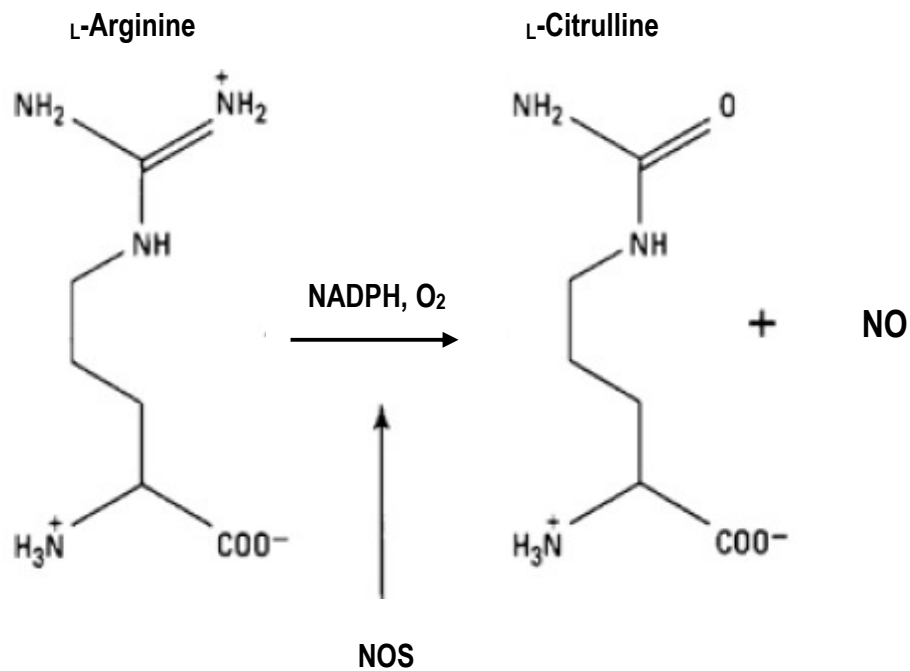


*Figure 1.10 – Nitric oxide generation from L-arginine*
*NO generation from L-arginine. Nitric oxide synthase (NOS), in the presence of $O_2$ converts arginine to NO, with the formation of citrulline.*

1.5.2    Molecular mechanism of cavernosal smooth muscle relaxation

As previously outlined, NO produced as a result of stimulation of endothelium by Ach diffuses into corporal smooth muscle cells. This catalyses the conversion of GTP into cGMP via activation of the enzyme sGC. The increase in cGMP activates a cGMP-dependent protein kinase (protein kinase G – PKG) and to a much lesser extent, protein kinase A (PKA). These activated protein kinases bring about smooth muscle relaxation by several mechanisms:

- PKG activates myosin light chain phosphatase, dephosphorylating myosin light chains and leading to smooth muscle relaxation.

- PKA phosphorylates phospholamban, a protein that inhibits the $Ca^{2+}$ pump of the SR. The pump is therefore activated and intracellular $Ca^{2+}$ is taken back into the SR, reducing $[Ca^{2+}]_i$(154).

- Both cGMP and PKG activate $K^+$ channels resulting in smooth muscle cell hyperpolarisation. This closes membrane-bound voltage-dependent calcium channels resulting in a decrease in $[Ca^{2+}]_i$(154, 155).

- cGMP may inhibit the L-type $Ca^{2+}$ channel and thereby reduce $[Ca^{2+}]_i$(156).

Cellular hyperpolarisation may also be brought about by the direct effect of NO on membrane-bound Na-K-ATPase channels, i.e. a cGMP independent pathway(157). The net effect of these mechanisms is to reduce sarcoplasmic $[Ca^{2+}]$ and therefore cause CSM relaxation.
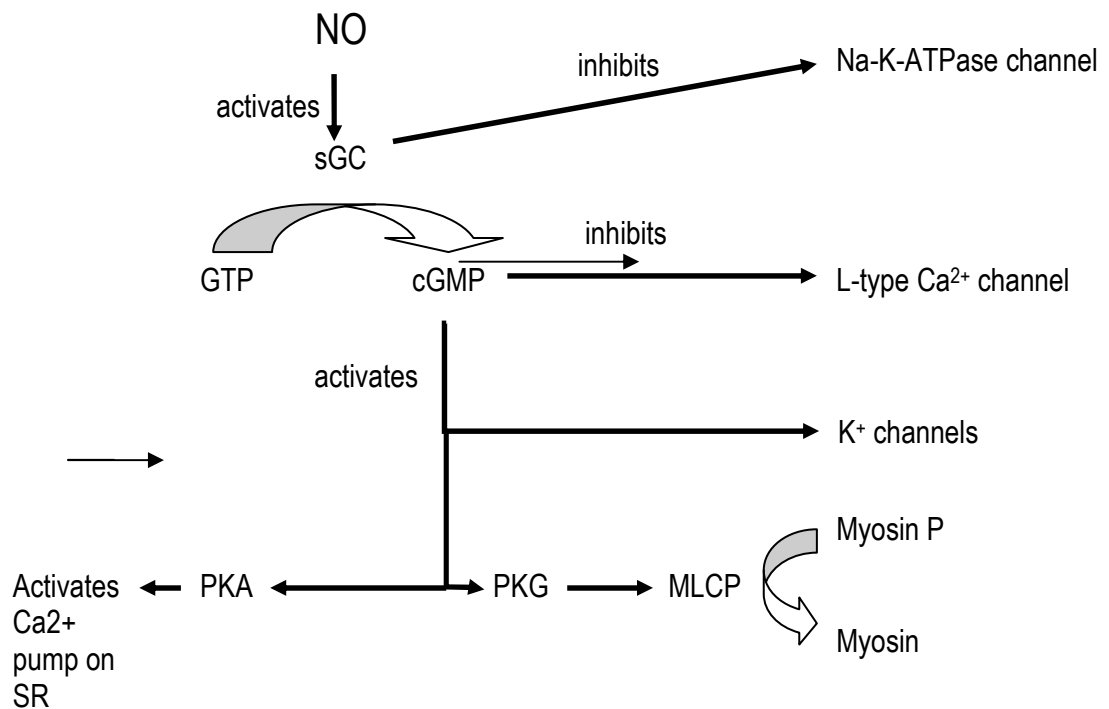


*Fig. 1.11 – Line diagram showing methods by which NO causes CSM relaxation*

### 1.5.3    Other endogenous mediators of CSM tone

Several other mediators of CSM tone have been identified in human CSM. They are thought to have a modulatory effect rather than be the predominant mechanisms involved in effecting penile erection and detumescence.

Immunohistochemical studies have identified vaso-active intestinal polypeptide (VIP) in human cavernosal tissue biopsies(158). VIP in human cavernosal nerves has been co-localised with NOS(159, 160). In addition, intracavernosal injection of VIP causes penile tumescence in some patients(161). However, it has been difficult to show that VIP directly causes CSM relaxation. Some studies have shown that an antagonist of VIP ameliorated EFS-mediated contractions in rabbit CSM. The authors concluded that relaxation was dependent upon prostanoids and the production of NO(162).

Intracavernosal injection of histamine produces a short lived penile erection. Histamine produced dose dependent relaxation in human corpus cavernosum samples(163). However, not all studies have shown consistent relaxatory effects. The predominant histamine receptor sub-type is the $H_1$ receptor ($H_{1-3}$ have been categorised). Stimulation of the $H_1$ receptor elicits contraction in isolated corpus cavernosum(164).

Stimulation of serotonin (5-hydroxytryptamine, 5-HT) type 1 and 2 subtypes mediates contraction in rabbit CSM. $5-HT_4$ stimulation elicits relaxation in the same *in vitro* model(165). However, further studies using human corpus cavernosum show an overall tendency towards smooth muscle contraction(166). The physiological role of peripheral serotonin remains unclear.

The role of purines such as ATP and adenosine in CSM contraction are not established. Both compounds produce relaxation in pre-contracted rabbit CSM and canine penile arteries(167). The purinergic system is the focus of considerable interest at present and further developments may reveal new therapeutic targets for the treatment of erectile dysfunction.

Vascular smooth muscle relaxation is mediated by endothelium-dependent mechanisms which include NO(168). Relaxation still occurs in vascular tissue with intact endothelium despite blockade of NOS and cyclo-oxygenase (inhibiting the NO-cGMP and prostaglandin pathways respectively) and is thought to be mediated by endothelial cell hyperpolarisation. The alternative endothelial derived hyperpolarising factors (EDHFs) involved in relaxation pathways may be related to products of arachidonic acid metabolism or metabolites of P-450(169). EDHFs have an important role in the relaxation of arteriolar smooth muscle as opposed to cavernosal smooth muscle(170).

## 1.6    Cavernosal smooth muscle cell calcium regulation

Corporal smooth muscle contraction is a result of an increase in $[Ca^{2+}]_i$. Transient changes in $[Ca^{2+}]_i$ are critical to the contractile state of CSM. An outline of cellular $Ca^{2+}$ regulation follows.

*$Ca^{2+}$ entry pathways*

CSM cells exhibit a variety of voltage and ligand-gated ion channels that normally serve as the principle $Ca^{2+}$ entry pathway. At rest, sarcoplasmic free $[Ca^{2+}]$ is ~100 nM. Extracellular fluid $[Ca^{2+}]$ is ~10,000 times higher than this (~1.5 to 2 mM). This concentration gradient is maintained by the $Ca^{2+}$ pump and $Na^+/Ca^{2+}$ exchanger, both located on the cell membrane. Channel activation causes movement of $Ca^{2+}$ down an electrochemical gradient and results in a 5-fold

increase in $[Ca^{2+}]_i$ to ~550 – 700 nM(171). This results in myosin phosphorylation and smooth muscle contraction.

The predominant voltage gated channel in CSM is the L-type $Ca^{2+}$ channel. Cell membrabe depolarisation due to an action potential opens these voltage-gated L-type $Ca^{2+}$ channels, resulting in $Ca^{2+}$ influx along the concentration gradient into the cell. These channels may be blocked by drugs such as nifedipine.

It is postulated that Transient receptor (TRP) channels are also present on the cell membrane, TRPM8 (a subtype of TRP channel) having been shown in rat CSM(172). Transient receptor (TRP) channels are present on the plasma membrane of many smooth muscles and are relatively non-selectively permeable to cations including $Ca^{2+}$.

## $Ca^{2+}$ release mechanisms

An important mechanism for $[Ca^{2+}]_i$ elevation involves release of $Ca^{2+}$ from intracellular stores. These can increase $[Ca^{2+}]_i$ with or without a change in membrane potential i.e. with or without an influx of $Ca^{2+}$ *into* the cell. The sarcoplasmic reticulum facilitates the storage and release of $Ca^{2+}$(173). Accumulation of $Ca^{2+}$ into these stores is accomplished by a $Ca^{2+}$ ATPase. Release of these stores occurs secondary to release of inositol 1,4,5-trisphosphate ($IP_3$)(174). The $IP_3$ pathway is stimulated when noradrenaline binds to the $\alpha_1$-adrenoceptor which is coupled to phosphoinositide-specific phospholipase C via GTP-binding proteins. Phospholipase C then hydrolyses phosphatidylinositol 4,5-biphosphate ($PIP_2$) to 1,2-diacylglycerol (this is membrane bound and activates protein kinase C) and $IP_3$. $IP_3$ (which is soluble and diffuses through the cell) binds to its receptor ($IP_3R$) on the sarcoplasmic reticulum (SR). The SR concentration of $Ca^{2+}$ is around 1 mM. $IP_3$ binding opens calcium channels in the SR resulting in $Ca^{2+}$ efflux into the

sarcoplasm and subsequent smooth muscle contraction. This increase in $Ca^{2+}$ activates the ryanodine receptor-operated channel on the SR, leading to a further increase in sarcoplasmic $[Ca^{2+}]$(i.e. calcium-induced calcium release-CICR)(84, 112, 128, 175-177). Caffeine may be used to activate CICR in intact cells(178).

*$Ca^{2+}$ efflux pathways*

To maintain homeostasis, $Ca^{2+}$ influx must be balanced by efflux across the cell membrane. This is accomplished via a $Ca^{2+}$ ATPase (the calcium 'pump') and the $Na^+/Ca^{2+}$ exchanger. The former may be sensitive to pH change whilst the latter is sensitive to amiloride(179).

## 1.7    Effect of ischaemia on cavernosal smooth muscle

As previously outlined, the process of penile erection and detumescence is secondary to haemodynamic changes within the penis. During penile erection, there is a degree of reduced blood flow within the penis secondary to the reduction in venous outflow (fig. 1.7 – penile haemodynamic changes during erection and detumescence and detumescence, page 38). As the duration of penile erection increases, the corporal microenvironment will change. Serial cavernosal blood gases in men with pharmacologically induced penile erection demonstrate a time-dependent decrease in oxygen tension and pH, and an increase in carbon dioxide levels(31). In addition, corporal blood aspirates during priapism show a time dependent decrease in blood glucose levels(31, 35, 93, 180, 181). Various researchers have examined the effect of these metabolic changes in isolation and in combination on cavernosal smooth muscle with a view to examining the effect of acute and chronic ischaemia on corporal smooth muscle.

## 1.7.1  The effect of hypoxia on CSM contraction

Broderick *et al.* subjected rabbit cavernosal smooth muscle strips to anoxia and examined the effect of EFS-mediated and agonist-induced contraction and relaxation. Both aspects of CSM function were severely affected; relaxatory responses were abolished in the absence of oxygen(182). Kim *et al*. examined the effect of hypoxia on nerve-mediated and agonist-induced contraction in an *in vitro* model of CSM(183). Noradrenaline (NA) and endothelin evoked contractions were significantly attenuated after 180 min of hypoxia. Responses returned to normal upon return to control conditions. Interestingly, EFS-mediated contractions appeared to be augmented during hypoxia, an effect which was reversed when experiments were repeated in the presence of the NOS inhibitor L-NOARG. Potassium induced tonic contraction was also examined, with a sustained relaxation observed during up to 180 min of hypoxia. This was fully reversible on return to control conditions. Additional experiments found similar responses between muscle strips with intact *vs.* denuded endothelium as well as in the presence of indomethacin (cyclo-oxygenase inhibitor) and methylene blue (guanyl cylcase inhibitor). This paper concluded that 'the effects of hypoxia are not restricted to a specific receptor pathway, but that there is a failure of the contractile mechanism of the smooth muscle to respond to any agonist or to the depolarisation that follows exposure to high $[K^+]$'. The finding that EFS-mediated contraction was increased during hypoxia was attributed to the differential effect of low oxygen tension on the various nerve types present.

Kim et al. also examined the effect of hypoxia on relaxatory responses in an *in vitro* model of CSM using both human and rabbit tissue samples(122). At oxygen tensions similar to that found in the erect penis (~ 100 mmHg), Acetylcholine and electrical field stimulation elicited increasing concentration-dependent and frequency-dependent relaxations in pre-contracted muscle strips

mounted in organ baths. Reduction in oxygen tension to that found in the flaccid penis (44-57 mmHg) resulted in significant amelioration of both Ach and EFS-mediated relaxation in the rabbit CSM preparation. EFS-mediated relaxatory responses in human CSM were significantly reduced under similar hypoxic conditions; however, more severe hypoxia was required to significantly reduce Ach mediated responses. Responses returned to normal on return to normoxia. Interestingly, during hypoxia, responses similar those seen at $PO_2$ ~ 100 mmHg were observed in response to exogenous NO.

1.7.2    The effect of acidosis on CSM contraction

Saenz de Tejada and co-workers examined the effect of acidosis on contraction in an *in vitro* model of CSM(184). Smooth muscle strips equilibrated at pH 7.4 were exposed to 30 min. of acidosis (pH 6.9) generated using a 25% $O_2$/75% $O_2$ gas mix. Responses to EFS, NA and $[K^+]$ were recorded. Acidosis caused a right shift in the dose response curve to NA i.e. higher doses of NA were required to elicit the same response under acidic conditions. The maximal response to NA was unchanged. EFS mediated contractions were significantly suppressed throughout the frequency response range at pH 6.9. Acidosis had no effect on the maximal contraction in response to high $[K^+]$. However, at $[K^+]$ less than maximal tension generated was reduced under acidotic conditions. EFS and agonist mediated relaxation in tissue strips precontracted with a non-maximal $[K^+]$ were relatively preserved under acidotic conditions. Moon *et al.* induced a metabolic acidosis in anaesthetised cats using hyperventilation. Intracavernous pressure measurements were reduced during stimulated penile erections indicating a degree of CSM failure(185).

## 1.7.3 The effect of combined elements of ischaemia

In an *in vitro* model of low flow priapism, Muneer *et al.* examined the effect of elements of ischaemia - hypoxia, acidosis and hypoglycaemia, individually and in combination on cavernosal smooth muscle(71). The absence of *glucose* markedly reduced both nerve-mediated and agonist-induced contractions when compared to the effects of acidosis and hypoxia alone. The combination of hypoxia and glucopenia, with our without simultaneous acidosis, significantly attenuated contractile function when compared to each factor in isolation. Hypoglycaemia during the period of ischaemia also reduced the ability of the tissue to recover following a period of reperfusion. In the same study it was found that nitrergic nerve-mediated relaxation was relatively spared during ischaemia when compared to adrenergic nerve-mediated contraction, a finding that could help explain the failure of detumescence in low flow priapism.

Munarriz *et al.* used an animal model to examine the effects of ischaemia and reperfusion on cavernosal smooth muscle(186). Penile erection was induced in anaesthetised rabbits and maintained using a penile clamp to mimic priapism. Varying periods of reperfusion were applied by removal of the clamp prior to tissue fixation and removal for analysis. As expected, a time dependent reduction in intracavernosal oxygen tension was noted during the priapic episode. Interestingly, increases in myeloperoxidase activity and lipid peroxidation (markers of oxidative injury) were noted with reperfusion. This would suggest that not only is corporal smooth muscle injured during the ischaemic insult but that damage occurs on reperfusion with arterial blood.

Cavernosal blood aspirates during ischaemic episodes show evidence of metabolic depletion as evidenced by low $pO_2$, low pH and low glucose. CSM contractile failure is integral to the

mechanisms underlying ischaemic priapism. The relative contributions of these elements of ischaemia to CSM dysfunction are not clearly defined.

## 1.8     Experimental models for the study of ischaemia on CSM

As described above, various animal models have been used to study the effects of ischaemia *in vitro* and *in vivo*(187). The origin of tissue for experimentation is influenced by several variables including availability and cost, as well as relevance to the condition being studied. Ideally, normal human CSM would be used for experimentation as this would most closely resemble the pathological condition. There are no operations during which *normal* human CSM may be retrieved without causing a detrimental effect to the patient. *Abnormal* CSM may be retrieved (with full ethical approval and patient consent) during implantation of penile prostheses(35, 72, 74). However, this tissue is abnormal due to the underlying processes causing the erectile dysfunction prompting the implant insertion. These are usually conditions such as diabetes and cardiovascular disease, both of which are associated with chronic corpus cavernosal ischaemic change.

A second potential source of human tissue would be during penectomy for penile cancer. Again, the patient group affected are elderly with multiple comorbidities often resulting in erectile dysfunction. In addition, due to a trend towards penile preserving surgery where possible, only small amounts of tissue are usually available. Finally penectomy during male to female gender reassignment surgery would be an excellent source of tissue for experimentation, the volume of tissue available is large and surgery is elective allowing for scheduling of experiments. However, patients undergo surgery after a prolonged period of oestrogen administration, usually for several years prior to penectomy. This in itself may induce cavernosal smooth muscle change(104).

Animal models have formed the usual basis for experiments examining CSM function. The majority of studies utilise rabbit CSM for both muscle strip and single cell experiments, the characteristics of this tissue source are well established(71, 122, 183, 184). Mouse and rat models are also described. The advantage of these is their relative ease of use and cost as well as steady supply for experimentation. In addition various pharmacological parameters are comparable to human tissue (smooth muscle to collagen ratios, $EC_{50}$ to contractile agonists). However, within our own laboratory, guinea-pig tissue has been used for experiments on both cardiac and lower urinary tract smooth muscle(188, 189). In order to maintain efficiency and enable the large number of experiments proposed we decided to define a novel guinea-pig model for examining the effect of ischaemia on CSM.

The mechanism by which researchers simulate ischaemia varies markedly. The components of ischaemia will be considered in turn.

*Glucopenia*

Glucose is broken down in the cytoplasm by the process of glycolysis(190, 191). Pyruvate is produced in a chain of events within the cytosol with the additional production of energy in the form of two molecules of adenosine-triphosphate (ATP). In the presence of oxygen, mitochondria are able to undergo aerobic respiration. Pyruvate drives the electron transport chain of the citric acid (Krebs) cycle to create further ATP as part of oxidative phosphorylation(192). In the absence of oxygen, the pyruvic acid produced by glycolysis undergoes lactic acid fermentation within the cytoplasm. In terms of energy production, aerobic respiration is far more efficient, liberating 38 ATP from each glucose molecule compared to 2 ATP for anaerobic metabolism(193). Omission of glucose (and Na pyruvate if present) from superfusing solutions during experimentation allows

the effect of prolonged glucopenia as well as the presence and effectiveness of glycogen stores at maintaining contractile function to be examined(71).

*Hypoxia*

Oxygen is required by smooth muscle to generate energy via oxidative phosphorylation. Tissues increasingly rely upon anaerobic metabolism during hypoxic interventions; this is expensive in terms of glucose expenditure. In general researchers generate hypoxia by substituting nitrogen for oxygen in gas mixtures used to perfuse solutions bathing tissue strips/isolated cell preparations. It is methodologically difficult to conduct experiments in completely anoxic conditions unless completely enclosed tissue chambers are used due to the diffusion of atmospheric oxygen into the surface of liquids. This effect is increased with greater surface area to volume ratios of fluid and reduced flow rates.

*Acidosis*

In health, extracellular acidosis induces intracellular acidification due to buffering and equilibration of $H^+$ across the cell membrane by both active and passive mechanisms(188, 194, 195). In broad terms, researchers may generate a reduction in pH in one of two ways.

1. Increasing $PaCO_2$ in the perfusing gas mixture. In solution this will generate an increase in free $[H^+]$. Changes in pH occur quickly and extracellular pH may be adjusted by increasing the concentration of available buffer for $H^+$ in solution(188, 194).

2. The use of weak acids (e.g butyrate) in perfusing solutions acts as a source of $H^+$ ions which will equilibrate across the cell membrane(195). This method allows pH to be manipulated in both intra and extracellular compartments by altering the buffering solute (bicarbonate) concentration. This mechanism typically produces smaller changes in $pH_i$ than method 1.

## 1.9    Effect of low temperature on smooth muscle

Washout of the turgid corporal bodies with fluids is a recommended intervention in the management of priapism(60, 62). These fluids are usually at room temperature and may be combined with ice packs and cold compresses to help reduce the oedema and pain that accompanies prolonged ischaemic priapism. However, there is no evidence for these reduced temperature interventions in improving cavernosal smooth muscle contraction and therefore facilitating detumesence.

In the respiratory tract reduced temperature appears to potentiate smooth muscle contraction. In human nasal smooth muscle, nerve-mediated phasic contractions were prolonged although the magnitude remained unchanged. Agonist-induced contractures mediated via α-adrenoceptors were augmented in the same preparation (196). Tracheal smooth muscle demonstrated a left shift in the nerve-mediated force-frequency relationship. Overall magnitude was not increased. In addition, agonist-induced relaxation mediated via β-adrenoceptors was abolished (197). Small intestine smooth muscle showed an increase in magnitude of contraction in response to acetylcholine with no alteration on in the $EC_{50}$ of the preparation. Researchers proposed these changes to be secondary to increases in $[Ca^{2+}]_i$ at low temperature(198). Vascular smooth muscle also demonstrates augmentation of contraction at reduced temperature. An increase in nerve-mediated contraction was noted in saphenous vein which was maintained in the presence of the $α_1$-adrenoceptor antagonist prazosin(199). Augmentation was abolished in the presence of the $α_2$-adrenoceptor rauwolscine supporting the hypothesis that this receptor mediates cold-induced vasospasm in peripheral vessels.

Reduced temperature shows a marked effect in the lower urinary tract. Cooling from 37 °C to 5 °C in a stepwise fashion evoked contraction of rat bladder muscle strips. Responses were postulated to be secondary to an increase in $[Ca^{2+}]_i$ shown by the sensitivity of the recorded response to the Ca-channel blocker nifedipine and to perfusion with $Ca^{2+}$-free solution(200). Vas deferens showed an increase in agonist-induced contraction with a left-shift of the force-concentration relationship with a reduction in temperature. Contractions were elicited by the $\alpha_1$-adrenoceptor agonist phenylephrine; augmentation at low temperature was abolished when perfusing solution $[Ca^{2+}]$ was reduced by 50%(200).

Responses to cooling differ between species. Guinea-pig ureter showed a reduction in magnitude of the agonist-induced contracture in addition to slowing of the response. The fast sarcoplasmic reticulum related $[Ca^{2+}]$ changes appeared to be affected to a greater extent when compared to the slower membrane bound mechanisms (Na/$Ca^{2+}$ exchange and $Ca^{2+}$ pump)(201). Rat ureter by contrast showed an increase in force generated in response to stimulation during reduced temperature interventions. This was attributed to an increase in the $Ca^{2+}$ transient secondary to a prolonged action potential(202). These differences were secondary to varying contributions of ion channels to the action potential. Cooling appeared to potentiate $Ca^{2+}$ activated $Cl^-$ currents (present in rat ureter, absent in guinea-pig ureter) with a resultant prolonged plateau phase of the action potential. In the rat this augmented action potential was sufficient to overcome kinetic lag. In addition and in contrast to other researchers, $Ca^{2+}$ entry and SR release of $Ca^{2+}$ appeared to be relatively insensitive to cooling whereas MLCP activity was markedly affected by reduced temperature therefore increasing the amount of phosphorylated myosin for any given $[Ca^{2+}]_i$(202). Maintenance of smooth muscle tone at low energy costs is essential in promoting penile detumescence. Smooth muscle may have a reduced capacity to maintain tone

during a reduction in temperature using slowly cycling cross-bridges (latch state). This has also been postulated to be secondary to a reduction in myosin phosphorylation(134).

It is clear that cooling can modulate force production and has differing effects in varying smooth muscles. The effect of a reduction in temperature on cavernosal smooth muscle has not been reported. In addition to experiments examining the effect of ischaemia on CSM function, the effect of cooling was recorded on various aspects of CSM function.

## 1.10    Aims and objectives of thesis

Hypothesis:

1       The combination of hypoxia, acidosis and glucopenia causes cavernosal smooth muscle failure in a time-dependent manner. The contribution of the various elements of ischaemia is variable however glucopenia is central to irreversible smooth muscle dysfunction.

2       Low temperature washout fluids do not improve CSM contractile function.

Aims of the thesis:

The aim of this project was to investigate the role of the various elements of ischaemia on cavernosal smooth muscle cell contractile function. The effect of hypoxia, acidosis and glucopenia, individually and in combination, were investigated on the contractile activity of CSM preparations. Both nerve-mediated and agonist-induced contraction and relaxation were examined. Guinea-pig cavernosal smooth muscle strips and single cell preparations were used.

Objectives:

The following objectives were addressed through the experiments performed in this study, to determine the effect of the various elements of ischaemia on CSM.

1. To establish the viability of guinea-pig CSM as a model for the study of corporal smooth muscle function

2. To determine the effect of hypoxia, acidosis and glucopenia on nerve-mediated and agonist-induced contractions and relaxations in guinea-pig CSM muscle strips. Intra- and extra-cellular acidosis was examined as well as a reduction in pH in both compartments. The elements of ischaemia were applied in isolation and in combination. The recovery of preparations on return to normal conditions was also recorded.

3. The effect of the above conditions on $[Ca^{2+}]_i$ was recorded in an isolated CSM cell model.

4. The effect of a reduction in temperature on CSM function was also examined.

**2.0      Materials and Methods**


**2.1      Solutions and chemicals**


2.1.1     Tyrode's solution


Tyrode's physiological solution was used in all experiments to superfuse preparations. The constituents of the solution and their concentrations are listed in Table 2.1. AnalaR® grade reagents were added to de-ionised water (RO water - minimum 18 M$\Omega$ resistance, reverse osmosis filter, Purite Ltd, UK) in their solid form (NaCl, $NaHCO_3$, glucose and Na pyruvate) or from 1 M stock solutions (KCl, $MgCl_2$ and $NaH_2PO_4$) made up in the laboratory, with the exception of $CaCl_2$ which was obtained as a 1 M stock solution (BDH Ltd, UK). Solid compounds were weighed using a fine balance (Sartorius Ltd, UK) and liquids measured using calibrated variable volumetric pipettes. Tyrode's solution was stored at 21°C for use on the day of production, or at 4°C if kept overnight for use the next day. A HEPES-buffered Ca-free Tyrode's solution was used for tissue storage and cell isolation (table 2.1). This Ca-free solution was adjusted to pH 7.4 with 1 M NaOH to compensate for the absence of $CO_2$ gas perfusion.


2.1.2     Chemicals and drugs


All chemicals used in interventions were freshly made up daily to the required concentration in Tyrode's or modified Tyrode's solution. The AnalaR® grade solid chemicals phenylephrine, carbachol and tetrodotoxin (Sigma, UK) were made up in RO water. 1H-[1,2,4]oxadiazolo-[4,3-a]quinoxalin-1-one (ODQ - Sigma, UK) and Fura-2 (Invitrogen Molecular Probes Inc, USA) were

dissolved in the organic solvent dimethyl sulphoxide (DMSO – BDH, UK). Stock solutions were made up in the laboratory and stored at 4 °C or drawn up into aliquots and stored at -20 °C.

### 2.1.3    Simulation of ischaemia

Modification of Tyrode's solution enabled the various components of ischaemia to be simulated. All perfusing gases were stored at room temperature and sourced from BOC, UK. The various components of simulated ischaemia are shown in Table 2.1 and are summarised here:

*Hypoxia (H)* The superfusate $PO_2$ was reduced by gassing the solution with a $N_2/CO_2$ mixture, rather than an $O_2/CO_2$ mixture. Samples were taken at the superfusion bath during experiments to estimate the partial pressure of oxygen within the solution using an oxygen-electrode ($PO_2$ from 10 kPa to 4 kPa)(203).

*Substrate depletion (S)* Glucose and sodium pyruvate were omitted from the solution.

*Intracellular acidification and extracellular acidosis (IA)* The pH was reduced as a result of increasing superfusate $PCO_2$ by using a 10% $CO_2$ gas mixture rather than a 5% $CO_2$ mixture.

*Extracellular acidosis (A)* A decrease of extracellular pH was achieved by reducing the $[HCO_3^-]$ of the superfusate (a reduction in concentration of $[NaHCO_3]$ from 24 mM to 9.6 mM). The $[Na^+]$ was maintained by increasing the $[NaCl]$ added (from 118 mM to 132.4 mM). The availability of free $Ca^{2+}$ was maintained by decreasing the $[CaCl_2]$ added (from 1.8 mM to 1.55 mM)(188).

*Intracellular acidification (I)* A decrease of intracellular pH, at constant extracellular pH, was achieved by increasing the $[HCO_3^-]$ and $PCO_2$ in proportion. This was achieved by doubling the $[NaHCO_3]$ added to the solution (from 24 mM to 48 mM) and using a 10% rather than a 5% $CO_2$ gas mixture. The $[CaCl_2]$ was adjusted appropriately to maintain $Ca^{2+}$ activity from 1.8 mM to 2.34 mM(188).

The above interventions were applied separately and in various combinations. A pH electrode (BDH Ltd, UK) and pH meter (SE-500, Solex, Taiwan) were used to record superfusate pH at various times during experiments; the pH electrode was calibrated on a daily basis. Oxygen tension was estimated during experiments using an $O_2$ electrode (Licox CMP, Integra Neurosciences Ltd, UK).

## 2.2    Tissue collection and preparation

Cavernosal tissue was obtained from barrier maintained sexually mature male Dunkin-Hartley guinea-pigs weighing 500-950 g (Bantin & Kingsman Universal Ltd, UK). Animals were humanely killed by cervical dislocation according to UK Home Office guidelines. The penis was immediately dissected and placed into a dissection dish containing Ca-free Tyrode's solution. The penis was immobilised with three 25 gauge syringe needles (Terumo, Belgium) and excess connective tissue removed using straight nosed no. 5 micro-dissection forceps and fine scissors (INOX, Switzerland). Cavernosal smooth muscle strips were then prepared for isometric tension experiments (5 x 1 mm), or pieces of tissue obtained for isolated cell work ($1mm^3$). Tissue was stored in Ca-free Tyrode's at 4°C prior to use.

Table 2.1 Constituents of Tyrodes

## 2.3    Isometric tension measurement

### 2.3.1    Equipment and set-up

A horizontal Perspex superfusion trough (4 mm x 4 mm cross-section) was used that allowed the muscle strip to be immersed in a constant flow of solution (fig. 2.1). Flow speed was controlled with a gate clamp around the solution delivery tube which was adjusted at the start of every experiment to give a flow rate of 3 ml.min$^{-1}$.

The muscle strip was secured between two stainless steel mounting hooks; one fixed into the superfusion trough and a second connected to a force transducer (FT03, Grass Instrument Co, USA). This force transducer was mounted on a micromanipulator (Prior instruments, UK) with a Vernier scale on each plane of movement so that the transducer hook's position relative to the fixed hook could be recorded to give the length of the muscle strip. The system also permitted muscle length to be adjusted to yield maximum contractile force. The force transducer was connected to a variable gain Wheatstone bridge amplifier with a 5 Hz high frequency cut-off (Model TBM4M, World Precision Instruments, USA). Output was both monitored and recorded on a pen recording device with a low-pass filter of corner frequency 10 Hz (TA 240S, Gould Instruments Ltd, UK) and oscilloscope (DSO 420, Gould, UK).

A pair of platinum electrodes were embedded within the walls of the superfusion trough to deliver electrical field stimulation (EFS), and positioned such that the strip would lie between them. The electrodes were connected to an electrical stimulator (model 200, Palmer Bioscience, UK) and gating device (model 150, Palmer Bioscience, UK) which allowed reproducible manipulation of stimulation parameters. The stimulator and gating device were calibrated using a signal generator

(model TWG-501, Feedback, UK) and digital oscilloscope (Easyscope 420, Gould Instruments Ltd, UK) prior to use.

A water bath with a combined heater and pump (Thermoflow 471, Coniar Churchill Scientific supplies Ltd, UK) was used to warm perfusing solutions to 37±0.5 °C. This was mounted 1.5 m above the superfusion trough to enable warmed solution to be delivered to the trough under gravity. Warmed solutions were delivered to the trough via circulating water-jacketed 1.5 mm diameter tubing. After perfusing the tissue, solutions drained to waste. In experiments utilising low temperature superfusion fluids, a separate water bath (containing ice water if required) and delivery tubing system was used without a warming water jacket. Perfusing solution temperature was monitored periodically at the superfusion trough with a digital thermometer (model 915-1, Testo, UK). Solutions were bubbled with the appropriate gas mixture for at least 15 min prior to use.

A specially constructed experimental table was used with several features to minimise mechanical noise due to vibration. A welded steel frame with legs in buckets of sand was used with a 20 mm plywood top. This in turn supported a 25 mm steel plate mounted on neoprene and Teflon vibration absorbing pads (SK bearings, Cambridge, UK). Mounted on this was an aluminium modular top that allowed equipment to be firmly clamped in place.

At the end of experiments, the wet weight of the muscle strips was measured using a fine balance (model 205A, Precisa Balances Ltd, UK). This value along with the length of the strip was used to estimate the cross-sectional area (csa) using the formula:

$$csa \ (mm^2) = 1000 \ x \ mass \ (g)/[[density \ (g/ ml^{-1})] \ x \ [length \ (mm)]]$$

- o  Density was taken as 1.05 g.ml$^{-1}$.

Fig 2.1 Muscle strip experimental set up

### 2.3.2 Calibration of tension transducer

The orientation of the force transducer was manipulated such that small solder weights could be hung from the mounting hook to enable calibration. The mass of weights were confirmed on the fine balance and then each weight was suspended from the force transducer hook in turn. Corresponding deflections were recorded on the pen recorder. The height (mm) of each deflection above baseline (no weight) was plotted as a function of force (mN) calculated using the formula:

$$\text{Force (mN)} = \text{mass (g)} \times \text{gravitational constant (m.s}^{-2})$$

o The gravitational constant was taken as 9.81 $\text{m.s}^{-2}$

### 2.3.3 Muscle strip preparation and mounting

6/0 sutures (Sutures Ltd, UK) were tied with non-slipping surgical knots to each end of a muscle strip. The strip was then transferred to the superfusion trough with Tyrode's solution at 37 °C, flowing through at 3 $\text{ml.min}^{-1}$. One end of the strip was tied to a fixed mounting point in the base of the trough, and the other to the attachment hook of the tension transducer. The micromanipulators were adjusted so that the tissue was immersed in the flowing Tyrode's solution. There was no slack in the strip and the position was adjusted so that it was equidistant from each platinum electrode. Strip length was adjusted so that a stable baseline recording was achieved and reproducible phasic contractions in response to electrical field stimulation (EFS – see section 2.3.4) were obtained of a magnitude close to the maximum of the length-tension relationship. Typical strip length and weight was 5.5 mm and 0.015 g. Estimated CSA from these values was 2.5 $\text{mm}^2$.

## 2.3.4 Electrical field stimulation (EFS) experiments

*EFS contraction experiments*

Phasic contractions were elicited by periodic exposure of the muscle strips to electrical field stimulation (EFS). The optimum stimulation parameters in terms of stimulation voltage and frequency, duration of stimulation train and period between stimulations was ascertained experimentally and used for subsequent experiments.

All experiments commenced with 60 min. of periodic EFS to allow the muscle strip to equilibrate. Preparations were stimulated every 90 s with a 3 s pulse train at 32 Hz, 0.1 ms pulse width and at 50 V. Stimulation parameters were confirmed using an oscilloscope (DSO 240, Gould, UK). Tension in the strip was adjusted using the micromanipulators until a stable response was attained.

Strips were stimulated every 90 s at 32 Hz throughout each experiment. At various points during each experiment a force frequency relationship was determined by using stimulation frequencies from 8 to 60 Hz incrementally. The force-frequency relationship at the end of the 60 min. equilibration period acted as the control recording with similar force-frequency estimations being carried out during the ischaemic interventions and after a period of reperfusion in normal Tyrode's solution (figure 2.2).
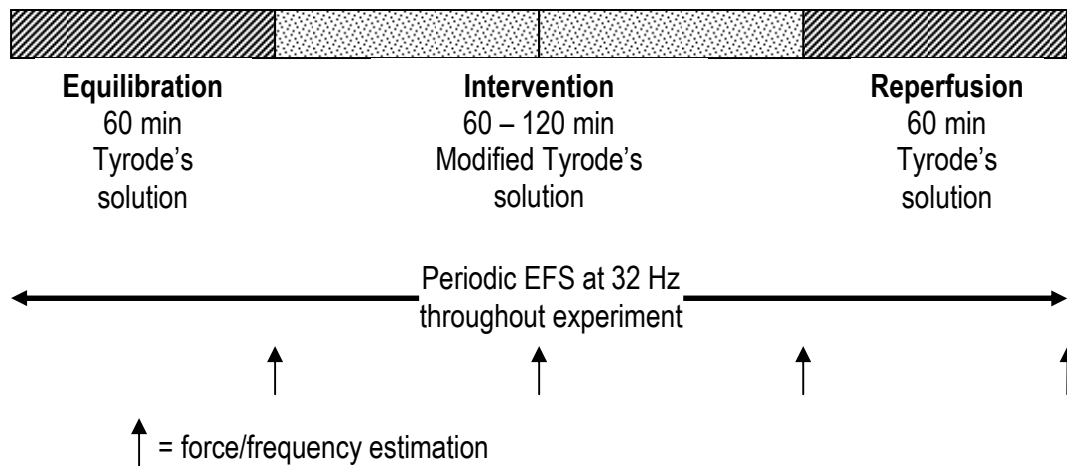
*Figure 2.2 - Experimental protocol for EFS contraction experiments*

*Stimulation at 32 Hz every 90 s throughout the experiment enabled the time point at which interventions had an effect to be determined whilst regular force/frequency estimations enabled these effects to be characterised.*

Recorded responses were measured using a 30 cm rule with 1 mm gradations to accuracy of ± 0.5 mm. Measurements were taken from baseline tension to the peak of each phasic contraction. Using calibration data, measurements were converted to force and normalised to unit cross-sectional area (csa) using the following equation:

$$\text{Deflection (mm)} / [\text{gradient of calibration graph (mN.mm}^{-1}) \times \text{csa (mm}^2)] = \text{force (mN.mm}^{-2})$$

In certain experiments, the time constant of the phasic contraction was measured as well as the maximum tension generated. To do this the pen recorder paper speed was increased from 2.5 mm.min$^{-1}$ to 25 mm.s$^{-1}$ for the final 60 Hz stimulation of each force-frequency estimation. The time-constant ($\tau$) for both the upstroke and downstroke of the phasic contraction were measured as shown in fig. 2.3.
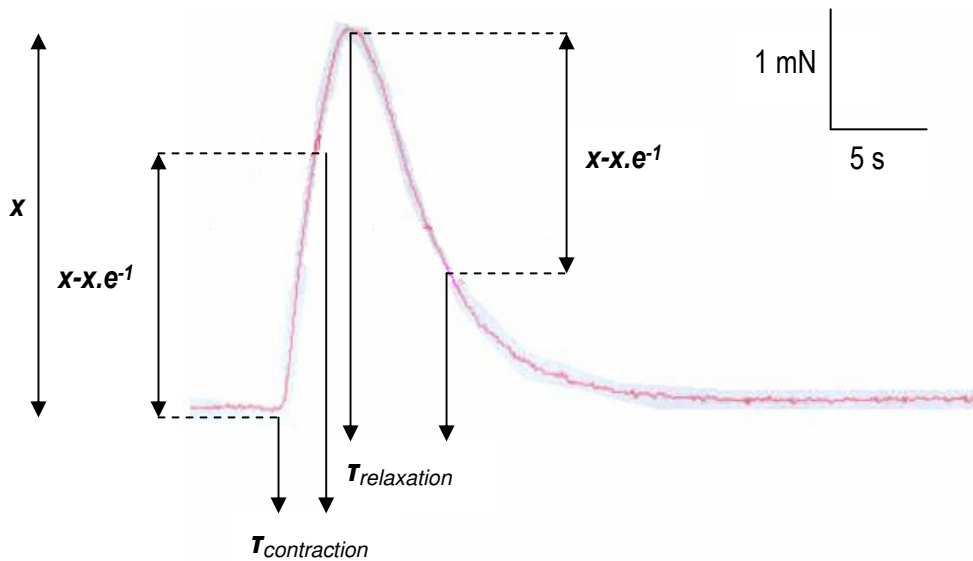
*Figure 2.3 - Method of measuring time-constant for phasic contractions*

$x$ = *maximum height of response (mm),* $\tau_{contraction}$ = *time constant of upstroke (s),* $\tau_{relaxation}$ = *time constant of downstroke (s).*

## EFS relaxation experiments

All experiments commenced with 60 min. of periodic EFS to allow the muscle strip to equilibrate.

EFS was then stopped and a stable baseline measurement confirmed for 5 min. Phasic

relaxations were elicited by periodic exposure of pre-contracted muscle strips to electrical field

stimulation. Strips were pre-contracted by exposure to 15 μM phenylephrine (PE) in Tyrode's

solution for 15 min. to elicit a tonic contracture. This concentration was chosen as being 10 times

the $EC_{50}$ for phenylephrine in this preparation, ascertained experimentally by another investigator

in our laboratory (unpublished work). 15 min. PE allowed the preparation to reach a stable

plateau contracture. 15 μM PE was chosen as the proposed experiments involved ischaemic

interventions that may be detrimental to the force of contraction generated in response to PE in a

time-dependent manner. A single concentration (15 μM PE) was chosen to measure the effect of

these interventions rather than a dose response curve due to the time involved in conducting the

latter. It was postulated that the effect of ischaemia may differ at the start of recording the

response to a cumulative dose of PE compared to the end. As relaxatory responses were also

being examined a maximal contracture was generated in order to minimise experimental error when measuring responses (10 times $EC_{50}$) rather than $EC_{50}$ or $EC_{80}$. Once this contracture had reached a plateau, a force frequency relationship was determined by using stimulation frequencies from 4 to 24 Hz incrementally. The phenylephrine was then washed out with normal Tyrode's solution (figure 2.4).



— = 15 µM phenylephrine
↑ = force/frequency estimation
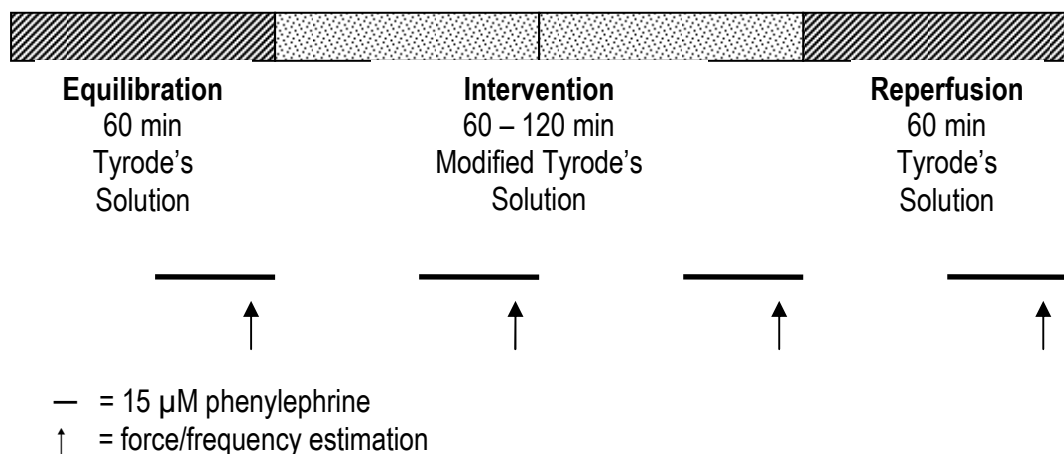
*Figure 2.4 - Experimental protocol for EFS relaxation experiments*

*Regular washout of phenylephrine during control and intervention was used to prevent muscle fatigue. After 15 min. of PE preparations had reached a plateau. Phasic relaxations were then elicited with an EFS stimulation train of 4-24 Hz.*

Recorded responses were measured using a 30 cm rule and converted to force per unit csa as previously described. The following measurements were taken from baseline tension (Fig. 2.5):

o   The maximum tension of each tonic contracture (PE peak).

o   The plateau tension of each tonic contracture (PE plateau). In cases where magnitude of the contracture was changing, this was taken as the contracture height above baseline after 16 min of phenylephrine.

o   The tension remaining above baseline after each EFS relaxation.

Tension remaining after EFS was expressed as a % of preceding PE plateau in all experiments and plotted using the Kaleidagraph™ program to obtain estimated minimum tension remaining (Ymin) and the frequency of stimulation resulting in half maximal relaxation ($f_{1/2}$).
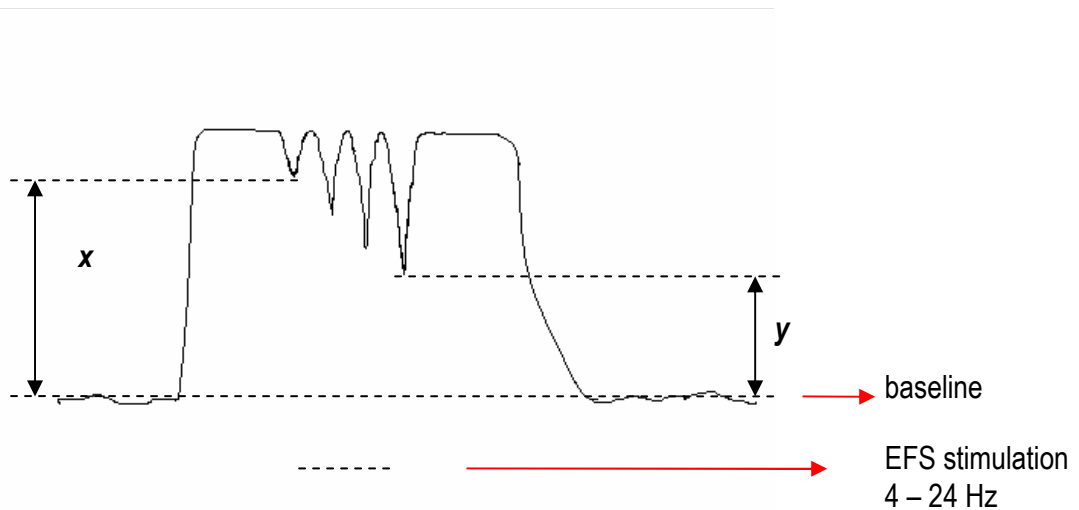


*Figure 2.5 - Method for measuring tension remaining after EFS-mediated relaxation*
*x –tension remaining after EFS stimulation at 4 Hz*
*y – tension remaining after EFS stimulation at 24 Hz*

In certain experiments, the time constants of the relaxation were measured. These experiments also involved pre-contracting the tissue with 15 µM PE after a period equilibration in Tyrode's solution at 37 °C. Once the contracture had reached a plateau, a single pulse train of EFS at 16 Hz ($EFS_{16Hz}$) was used to elicit a relaxation. A typical trace and the method of estimating the time-constants of the response are shown in fig 2.6.
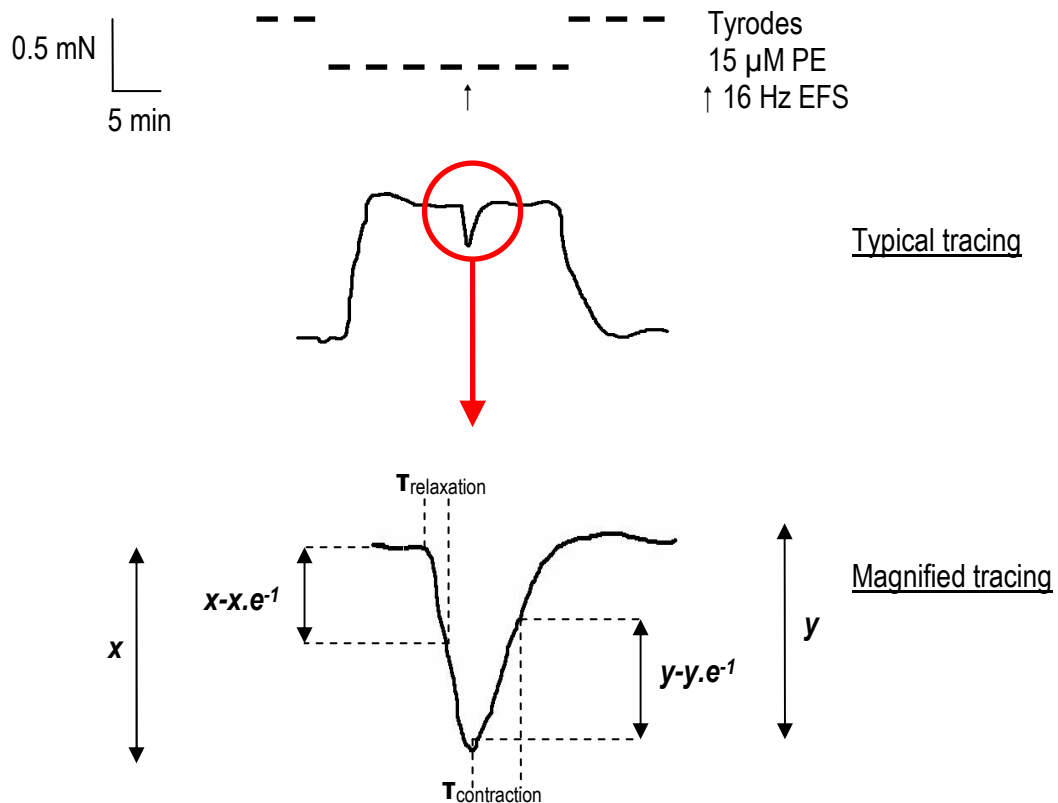
*Figure 2.6 - Method of measuring time-constant of EFS-mediated relaxation*

*x = maximum height of downstroke (mm), y = maximum height of upstroke (mm),*

*$\tau_{relaxation}$ = time constant of downstroke (s), $\tau_{contraction}$ = time constant of upstroke (s).*

2.3.5    Agonist-induced contracture and relaxation experiments

All experiments commenced with 60 min. of periodic EFS to allow the muscle strip to equilibrate.
EFS was then stopped and a stable baseline measurement confirmed for 5 min. Tonic
contractures were elicited by periodic exposure of the muscle strips to 15 µM phenylephrine.
Once this contracture had reached a plateau, agonist-induced relaxation was induced by
additional exposure of 1 µM carbachol to the pre-contracted muscle strips. The phenylephrine
and carbachol was then washed out with unmodified Tyrode's solution (Fig. 2.7).
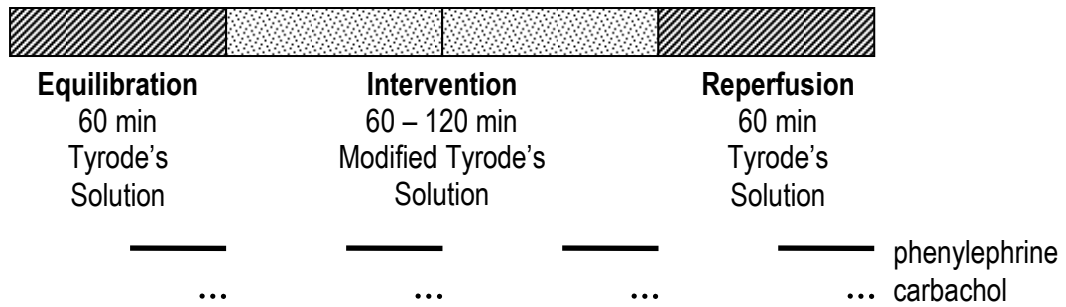
*Figure 2.7 - Experimental protocol for agonist-induced contractions and relaxations*

*Agonist-induced contractures reached a plateau with 15 min. of PE. Perfusing solutions were changed to PE and carbachol to examine the effect of the agonist-induced relaxation. 5 min. of carbachol was sufficient to elicit a plateau response.*

Recorded responses were measured using a 30 cm rule and converted to force per unit csa as previously described. The following measurements were taken from baseline tension (fig. 2.8):

- o  The maximum tension of each tonic contracture (PE peak).

- o  The plateau tension of each tonic contracture (PE plateau). In cases where magnitude of the contracture was changing, this was taken as the contracture height above baseline after 16 min of phenylephrine (fig. 2.8a).

- o  The minimum tension remaining above baseline after application of carbachol (C nadir)

- o  The plateau tension remaining after application of carbachol (C plateau). In cases where magnitude of the remaining contracture was changing, this was taken as the remaining contracture height above baseline after 1 min of carbachol (fig. 2.8b).
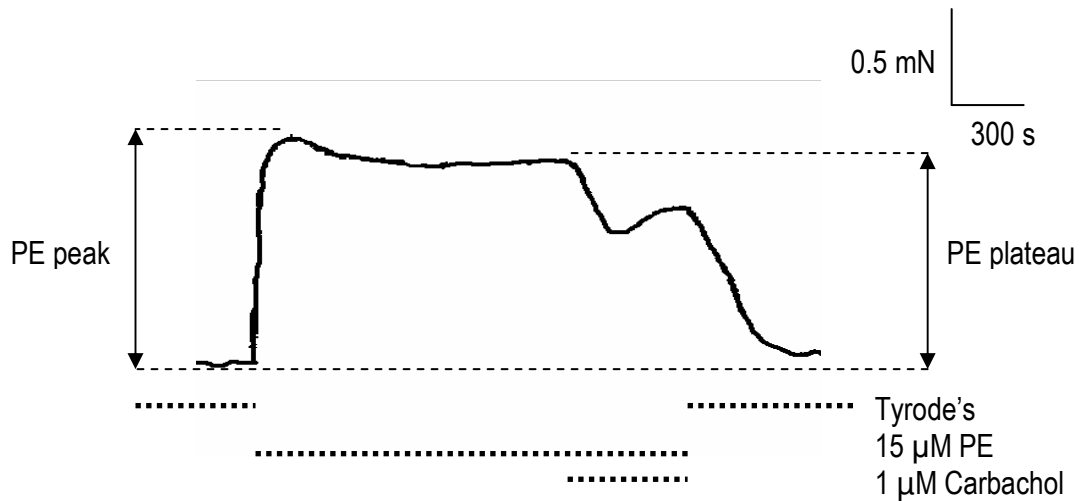
*Fig. 2.8a - Method of measuring agonist-induced contractures*

*PE peak = maximum height above baseline (mm), PE plateau = height above baseline after 16 min (mm).*
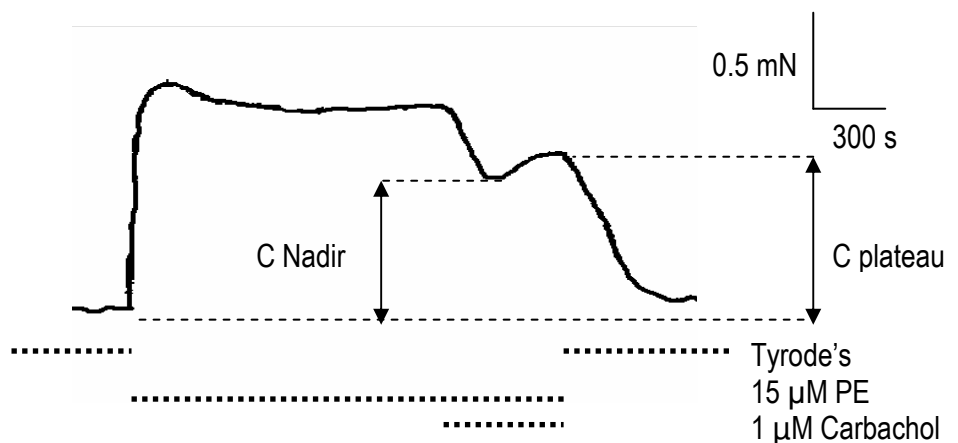


*Fig. 2.8b - Method of measuring agonist-induced relaxations*

*C Nadir = minimum height above baseline after application of carbachol (mm), C plateau = height above baseline after 5 min of carbachol (mm).*

In certain experiments, the time constants of the agonist-induced contracture were measured. A typical trace and the method of estimating the time-constants of the response are shown in figure 2.9.
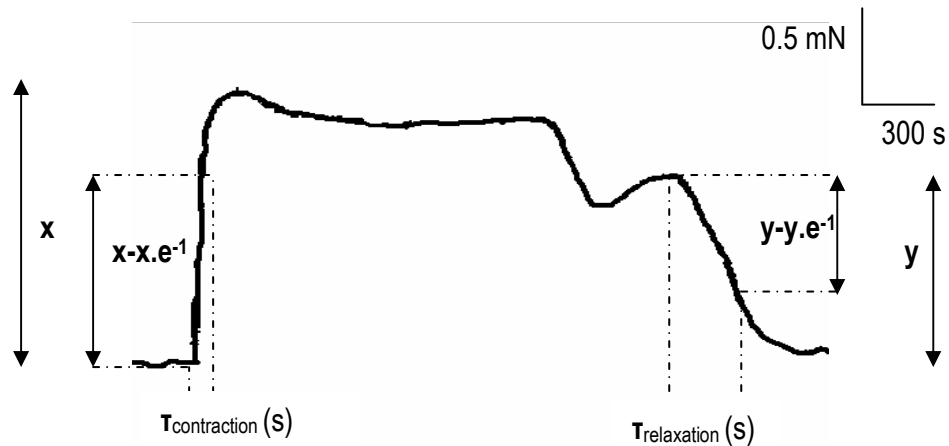
Fig. 2.9 - Method of measuring time-constants for tonic contractures

x = Peak PE contracture (mm), y = plateau PE contracture (mm), $\tau_{contraction}$ = time constant of upstroke (s), $\tau_{relaxation}$ = time constant of downstroke (s).

2.3.6    Reduced temperature interventions

The effect of reduced temperature on CSM function was examined in several experiments. The experimental protocols were similar to those described for the ischaemic interventions. The effects of Tyrode's solution at room temperature (21±1 °C) as well as chilled Tyrode's (10±3 °C) were recorded on the various aspects of CSM function described in sections 2.3.4 and 2.3.5. A tubing system without a warming jacket was used to supply superfusate to the muscle strips at a similar rate as the 37 °C Tyrode's solution (3ml.min$^{-1}$). Solution temperature was monitored at regular intervals throughout experiments at the superfusion chamber level using a digital thermometer (model 915-1, Testo, UK). Superfusate pH was monitored with a pH electrode (BDH Ltd, UK) and pH meter (SE-500, Solex, Taiwan). Chilled solutions were maintained in a polystyrene insulated water bath containing ice.

## 2.4 Estimation of stress/relaxation characteristics

Changes seen in the contractile and relaxatory responses at reduced temperature were postulated as being secondary to alterations in tissue biomechanics. In order to evaluate this, estimation of stress/relaxation characteristics were recorded at low temperature.

### 2.4.1 Equipment and set-up

A similar set up to that used for isometric tension measurement (section 2.3.1, figure 2.1) was used with the following the differences.

A solenoid arm with a stainless steel hook was used rather than a fixed mounting point. This solenoid arm was attached to a solenoid (model 6800HP, Cambridge Technology Inc, USA) mounted on a micromanipulator (Prior instruments, UK). A variable voltage supply and gating device (model TWG501, Feedback, UK) supplied current to this solenoid via a lever arm system (model 308B, Cambridge Technology Inc, USA). A change of voltage resulted in rotation of the solenoid and horizontal displacement of the hook (figure 2.10). Tension transducer output and solenoid output were connected to an a-d convertor (10 Hz sampling rate, Digidata 1200 interface, Axon Instruments Inc, USA), attached to a personal computer. The Clampex™ program (v8.0, Axon Instruments Inc, USA) was used to record data.

Fig 2.10 Stress relaxation experimental set up

A muscle strip was mounted between the force transducer and solenoid arm and the micromanipulators adjusted such that the strip was immersed in flowing Tyrode's solution. Tension in the strip was adjusted using the micromanipulators until the strip was taut. The ramp function of the variable voltage supply was used to ensure tension in the strip was within the linear region of the stress/strain relationship. The square wave function was used to examine the stress/relaxation relationship (figure 2.12).

At the end of each experiment the micromanipulator Vernier scales were used to measure the length and a fine balance used to estimate the mass of the strip. Cross-sectional area of each strip was calculated as previously described.

## 2.4.2   Experimental protocol

CSM strips were mounted as described in section 2.4.1. The strip was allowed to equilibrate in flowing Tyrode's solution at 37 °C for 15 min. (control conditions, figure 2.11). During this equilibration period, voltage supply to the solenoid was 0 V. The ramp function of the voltage supply was then selected and voltage increased to bring about linear movement of the solenoid arm hook and a cyclical increase and return to resting length of the tissue strip (length of complete cycle 100 s). Tension transducer output was observed to ensure strip length changes were within the linear portion of the length/tension relationship (fig. 2.12). The square wave function was then selected at the same voltage and three cycles of stress/relaxation were recorded. This process was repeated for another voltage on the same CSM strip.

The CSM strip was then allowed to equilibrate with Tyrode's at 13 °C for 15 min. (intervention, fig. 2.11). The above protocol was repeated and voltage supply/tension transducer output recorded.

A similar procedure was followed for examining the effect of return to 37 °C on stress/relaxation characteristics (reperfusion, fig. 2.11).



| **Control** | **Intervention** | **Reperfusion** |
| 37 °C Tyrode's Solution | 13 °C Tyrode's Solution | 37 °C Tyrode's Solution |

───  ───  ───  Ramp

………  ………  ………  Square wave
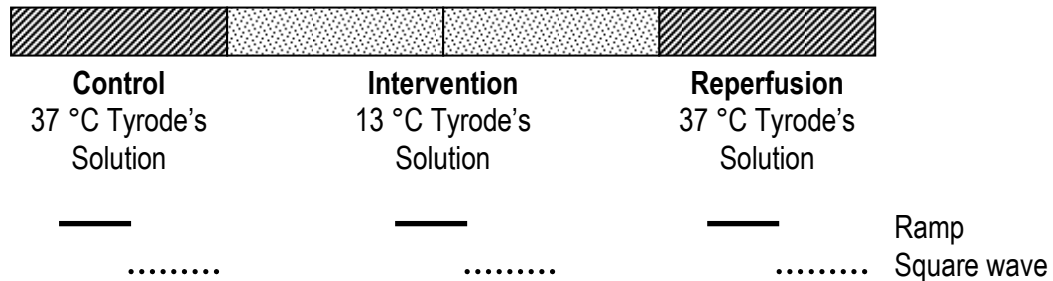
*Figure 2.11 – Experimental protocol for estimation of stress/strain characteristics of CSM*

*The ramp function was selected on the voltage supply and responses observed to ensure strip length changes were within the linear (Hookean) portion of the length/tension relationship*

2.4.3    Calibration of equipment

These experiments required the calibration of both the force transducer and the solenoid arm.

Calibration of the force transducer was identical to that in isometric force measurements (section 2.3.2). The change in signal magnitude with each mass was plotted as a function of force and the calibration slope calculated as previously described.

Calibration of the solenoid was carried out as follows. A dissection microscope and graticule (Nikon, Japan) were calibrated using a 30 cm rule with 1 mm gradations such that the number of graticule divisions per mm was known. The voltage across the solenoid was adjusted in 1 V increments. The resulting displacement of the solenoid hook was measured using the

microscope/graticule assembly. Change in length was plotted against change in variable voltage supply output on the Clampex program.

2.4.4    Data Analysis

The Clampfit™ (v8.0, Axon Instruments Inc, USA), Kaleidagraph™ (v3.5, Synergy Software, USA) and Excel™ (Microsoft, USA) programs were used to analyse recorded data. Typical output data are shown in figure 2.12. Data were recorded and converted to length (solenoid variable voltage output) and tension (tension transducer output) measurements using the calibration data (section 2.4.3). Tension was normalised to csa. The following data were calculated.

o   The instantaneous maximum stress due to an increase in length (*l*). This comprised the sum of steady-state (fig. 2.12, *C*) and viscous components (figures 2.12, *A*) and was expressed in Pascals (Pa).

o   The stiffness of the viscous component (calculated as instantaneous stress due to viscous component *A / *change in length *l*) expressed in Pa/mm.

o   The stiffness of the steady-state component (figures 2.12, *C*/*l*) expressed in Pa/mm.

o   The stiffness of the viscous component expressed as a proportion of the instantaneous maximum stiffness (*A*/*A*+*C*) expressed as a percentage.

o   The time-constant of the relaxation of the viscous component (figures 2.12, *A*) expressed in seconds (*k*).

o   Young's modulus (*e*) for the tissue, a constant obtained as the gradient of a straight line plot of steady state stress (figures 2.12, *C*) against strain (calculated as change in length *l* / resting length *L*) for each individual tissue strip. The straight line was fitted to the data using the least squares method.
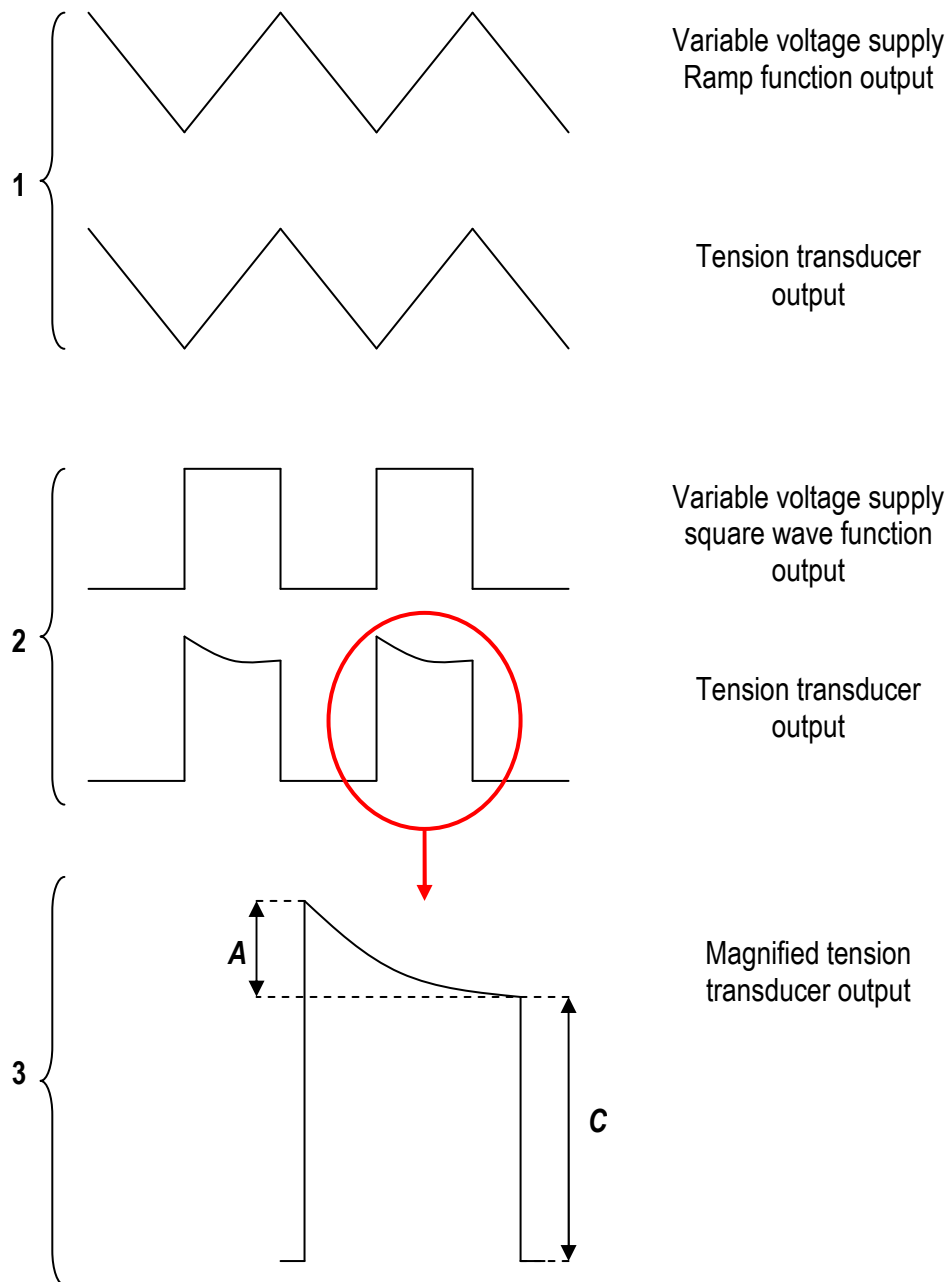
_Figure 2.12 – Typical output from variable voltage supply and tension transducer during estimation of stress/strain characteristics_

**1** – Ramp function of voltage supply used to ensure strip tension within linear ('Hookean') region of stress/strain relationship.
**2** – Square wave function of voltage supply used to examine the stress/relaxation characteristics of the tissue (tension transducer output magnified in 3).
**3** – Data used to estimate viscous (A) and steady state (C) stress/relaxation characteristics.

## 2.5 Isolated cell experiments (I)

### 2.5.1 Principles of epifuorescence microscopy

Epifuorescence microscopy was used to measure $[Ca^{2+}]_i$. The technique utilises the ability of certain compounds to emit light (fluoresce) in an ion concentration-dependent manner, in response to excitation by light of higher frequency. The emitted light has less energy and is therefore of a longer wavelength and different colour when compared to the excitation light. This phenomenon permits the use of light filters to isolate the emitted light and allow measurement of its intensity. The fluorescent indicators chosen for this purpose had two important attributes. Firstly, each was taken up by the cell in a non-invasive manner and predominantly localised in the cytosol. Secondly the fluorescence of each was quantitatively related to the concentration of the ion in question.

Cells were passively loaded with the lipid soluble acetoxymethyl ester (AM) of the indicator (sections 2.6.2 and 2.7.2). Once inside the cell, this ester would be hydrolysed to the active anionic indicator. Several factors were taken into account when choosing the method of fluorescence measurement.

i.      *Compartmentalisation*

The indicator (both the cell permeable ester and the anionic form) may accumulate within intracellular organelles where they would fluoresce independent of cytosolic ion concentration.

ii.    *Incomplete AM ester hydrolysis*

There may be residual AM ester in the extracellular space contributing to the detected fluorescence (should the AM ester be fluorescent as in the case of Fura-2 AM). In addition there may be incompletely hydrolysed indicator within the cell which would be insensitive to changes in ion concentration but would again contribute to the measured cell fluorescence.

iii.    *Leakage and photobleaching*

Anionic indicators may be actively removed from the cell by organic ion transporters, increasing the extracellular fluorescence. In addition, repeated fluorophore excitation and light emission is not a process that can go on indefinitely. Eventually the fluorophore will degrade, a process known as photobleaching.

iv.    *Signal buffering*

Indicators bind the ion of interest. If the intracellular indicator concentration is too high, the ion of interest will be buffered thus attenuating the magnitude and rate of change of the signal(189).

In order to compensate for some of the above factors (mainly iii), a ratiometric method of measurement was chosen. The indicators chosen exhibit an excitation spectral shift upon binding the ion of interest. By using a ratio of the fluorescence intensities at two different wavelengths, variations in the fluorescence signal itself (for the reasons listed above) can be cancelled out. The ratio of two fluorescence intensities with opposite ion-sensitive responses gives the largest range of ratio signals for a given indicator improving recording efficiency. By using a ratiometric method, factors such as leakage and photobleaching and variable cell thickness were compensated for.

Calibration of the system was achieved by experimentally deriving the dissociation constant ($K_d$). This would allow a given fluorescence signal in the same experimental system to be converted to an ion concentration.

## 2.5.2 Equipment and set-up

i. *Cell suspension chamber and microscope*

Isolated cells were placed in a Perspex cell bath mounted on a microscope stage such that fine manipulation of the chamber with respect to the objective lens could be achieved with adjustment of the stage controls. The base of the cell bath was made of a borosilicate microscope cover slip (thickness type 1, VWR, USA). The chamber was supplied with superfusing solution via 1mm tubing from four glass chambers placed 50 cm above the microscope. The cell bath, tubing and glass chambers were all water-jacketed and maintained at 37±0.5 °C using a water bath (model M3, Lauda, Germany). Three-way taps and a gate clamp controlled and maintained superfusate flow at 2ml.min$^{-1}$ to the bath. The cell bath was drained by suction using a peristaltic pump (Watson Marlow, UK) allowing a constant fluid level to be maintained. The cell bath was illuminated from above via a removable red light filter ($\lambda > 580$ nm) and observed using an inverted stage light microscope (Diaphot-TMD, Nikon Corporation, Japan). The apparatus was mounted on a nitrogen pressurised air table (model MICRO-g, Technical Manufacturing Corp, USA) and surrounded by a Faraday cage covered in a light-proof material (figure 2.13). Experiments were conducted in a darkened room.

A 75 W xenon short-arc bulb (XBO, Osram Ltd, Germany) with an independent high voltage power supply (Cairn research Ltd, UK) provided high-intensity broad-bandwidth light which was filtered, prior to transmission via a quartz fibre-optic cable. Filtration was achieved in two stages; polarisation with a static collimating filter followed by a motorised rotating wheel containing slots for up to eight radially placed filters of fixed wavelengths (Cairn Research Ltd). Magnetic and optical sensors within the filter housing enabled the central spectrophotometer unit (Cairn Research Ltd) to control the speed at which this filter wheel span (32 Hz) and synchronised this with the light detection mechanism.

Several mirrors, both plane and dichroic, were used to reflect the various light sources. The first dichroic mirror reflected the filtered illuminating light up through the microscope objective (x40 quartz objective, numerical aperture 1.3, oil lens, Nikon, Japan) to the microscope stage and cell bath where it was focussed on the cell in question. Emitted light passed back through this objective lens to pass straight through the first dichroic down to the plane microscope mirror. This reflected the emitted light to the collection system.

The microscope light source was positioned above the stage and filtered using a $\lambda$ > 580 nm red light filter. This light, used to position the cell, passed straight through the first dichroic mirror and was reflected by the microscope mirror to the collection system. This light source was extinguished during data acquisition.

The first stage of the collection system comprised a diaphragm which could be adjusted to reduce the field size and therefore reduce background emission. A second dichroic mirror acted as a

beam splitter. Higher wavelengths passed through this dichroic to a digital camera (Jai-PULNiX, USA) connected to a monitor (model 5512, Sanyo, USA). This image was used to observe the cell and adjust the diaphragm. Lower wavelengths were reflected up to a photomultiplier tube (PMT, Cairn Research Ltd) for signal detection.

iii.       *Signal detection and recording*

The PMT provided a current output which was a function of the light intensity entering it. Adjusting the voltage across the PMT enabled optimisation of the output with respect to the signal/noise ratio. In all recordings, two filters of differing wavelengths were placed in the motorised wheel. A high frequency internal clock within the spectrophotometer enabled rotation of each filter on the wheel to be synchronised with one of two sample-and-hold amplifiers. As emitted light from excitation at each filter frequency reached the PMT, the voltage output was integrated for the duration of the filter sweep, and the peak amplitude sampled. An analogue division circuit within the spectrophotometer enabled the signal from each amplifier to be converted to a signal ratio. This ratio signal along with the two individual sample-and-hold amplifier signals were recorded on a pen recorder (Gould TA 240S, UK) and a personal computer as well as displayed on a digital oscilloscope (Gould DSO 420, UK).

Fig 2.13 Isolated cell set up

2.5.3    Cavernosal cell isolation

Cavernosal tissue was dissected as described in section 2.2. An enzyme solution (Sigma, UK except collagenase Worthington, UK - table 2.2) was made up in the laboratory and aliquots stored at -20 °C for subsequent use. 0.7 ml of the thawed enzyme solution was added to 0.7 ml Ca-free HEPES buffered Tyrode's solution in a 2 ml eppendorf tube. 8-10 pieces of cavernosal tissue (1 mm$^3$) were placed in the enzyme mixture and stored for 12-15 hours at 4 °C. Tissue was then finely chopped with dissection scissors and the mixture transferred to a 7 ml screw top Perspex container along with a 5mm magnetic stirrer bar. This was placed in a 250 ml beaker containing water at 37.5 ± 0.5 °C on a stirrer for 6 min. Water temperature was monitored using a digital thermometer (model 915-1, Testo, UK). The resulting cell suspension was stored at 4 °C for subsequent use. All instruments and magnetic stirrers were soaked in a disinfecting solution (Haztab, Guest Medical, UK) and then washed in RO water prior to use.

*Table 2.2 - Constituents of enzyme mixture added to HEPES buffered Ca-free Tyrode's solution*

| Compound | Concentration (mg/ml) | Source |
|---|---|---|
| Collagenase type I (256 units/mg) | 20 | Worthington, UK |
| Hyaluronidase type I-S | 0.5 | Sigma, UK |
| Hyaluronidase type III | 0.5 | |
| Antitrypsin type II-S | 0.9 | |
| Bovine albumin | 5.0 | |

## 2.6  Isolated cell experiments (II)

### 2.6.1    Measurement of $[Ca^{2+}]_i$ by epiflourescence microscopy

The fluorescent indicator Fura-2 (Calbiochem-Novabiochem Corp, USA) was used as an index of $[Ca^{2+}]_i$. Fura-2 has a $K_d$ value that is close to typical basal $Ca^{2+}$ levels in mammalian cells (~100 nM), and has a high selectivity for $Ca^{2+}$ binding relative to $Mg^{2+}$. The fluorescence excitation spectrum of Fura-2 demonstrates an isoflourescence wavelength of 360 nm (fig. 2.14). As $[Ca^{2+}]_i$ increases, the spectrum shifts to the left resulting in:

i)        The emission intensity at 340 nm excitation increasing and

ii)       The emission intensity at 380 nm excitation decreasing.
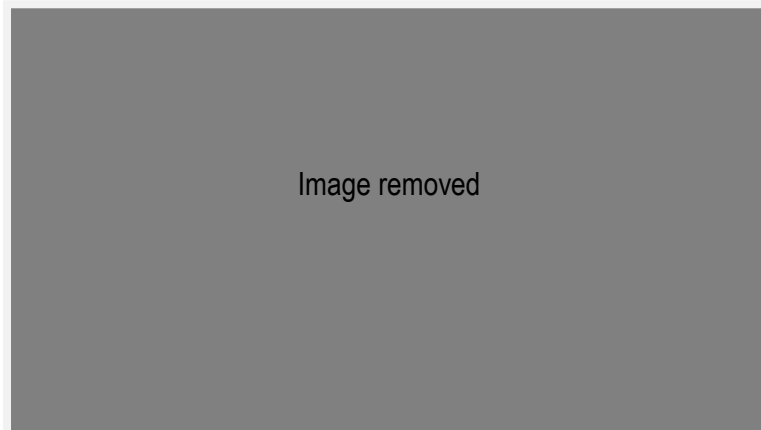
*Figure 2.14 - The fluorescence intensity spectra of Fura-2 detected at 510 nm at different $[Ca^{2+}]$ (modified from Invitrogen Molecular Probes handbook).*

Therefore, in these experiments 340 nm and 380 nm filters were placed in the filter wheel in the UV light path. The emission spectrum of fura-2 is maximal above 510 nm; hence emitted light was collected above this wavelength (fig 2.15). To achieve this, dichroic mirror 1 was a 410 nm mirror (allowing light > 410 nm to pass through) and dichroic mirror 2 was a 510 nm mirror to

reflect fluorescent light to the PMT tube (fig 2.13). The ratio of the 340/380nm emission was used as an index of $[Ca^{2+}]_i$.
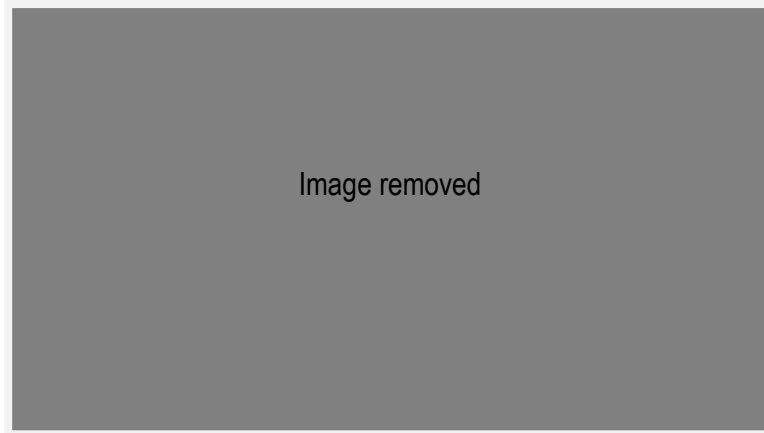


*Figure 2.15 - The fluorescence emission spectra of Fura-2 at different $[Ca^{2+}]$ at 340 nm excitation (modified from Invitrogen Molecular Probes handbook)*

2.6.2    Intracellular loading of Fura-2

The acetoxymethylester of Fura-2 (Fura-2 AM, Calbiochem-Novabiochem Corp, USA) was dissolved in DMSO to a concentration of 1 mM in the laboratory and stored at -20 °C. The lipid-soluble AM ester is able to passively diffuse across the cell membrane and once inside the cell, is cleaved by intracellular esterases to yield the charged cell-impermeant fluorescent $Ca^{2+}$ indicator (figure 2.16).
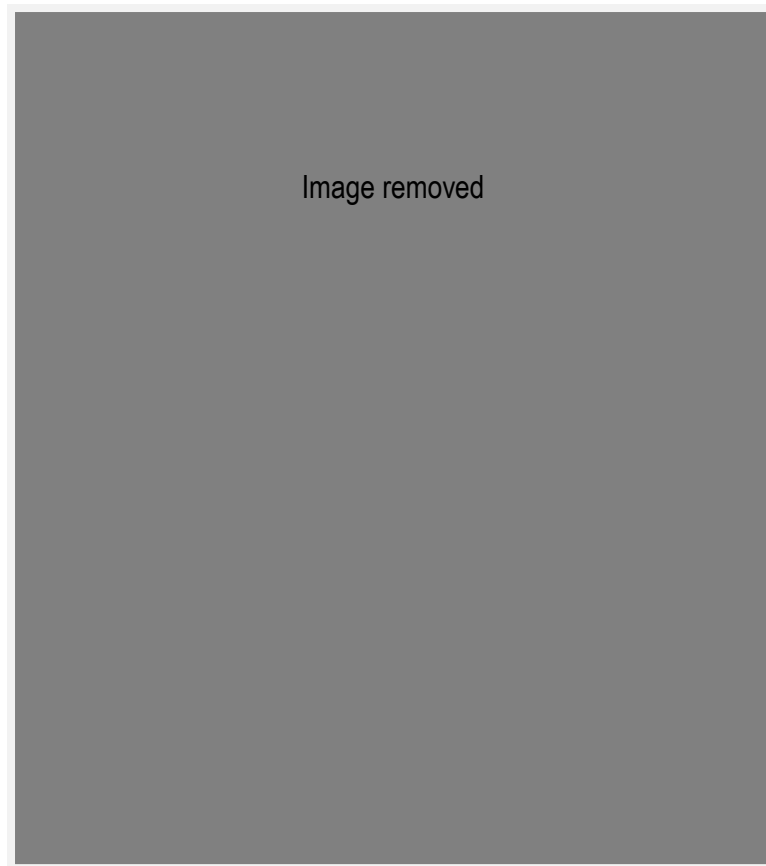
*Figure 2.16 -  The process of fura-2 AM hydrolysis liberating the Ca$^{2+}$ sensitive fluorophore (Invitrogen Molecular Probes handbook)*

Cells were loaded at room temperature by adding 5 µl of Fura-2 AM stock solution to 1 ml of cell suspension resulting in an indicator concentration of 5 µM. Cells were stored at 4 °C for 30 min to facilitate intracellular indicator loading.

2.6.3    Experimental procedure

The experimental rig was primed with oxygenated Tyrode's solution and the cell bath was washed with RO water and dried. Using a flamed-glass Pasteur pipette, two drops of loaded cell suspension were placed in the cell bath. The preparation was left for 30 min to allow cell adhesion to the base of the cell bath. The preparation was then superfused with Tyrode's solution

at a rate of 2 ml.min$^{-1}$. Many cells were washed away at this point but due to the high yield (~ 100 cells per high power field) from the isolation method described, enough cells remained for experimentation. Suitable cells were recognised as being spindle shaped with homogeneous cytoplasm and a smooth cell membrane. Additionally the presence of a 'halo' around the cell membrane under phase contrast illumination was seen as a favourable indicator of cell viability.

Once a suitable cell was identified, it was brought into focus and the stage adjusted to bring the cell into the centre of the field. The microscope red light filter was then slotted in place and the light collection diaphragm adjusted, guided by the monitor image, to optimise light collection from the cell. The microscope cage was then blacked out and the room lights turned off.

The light source was switched on to allow the appropriate excitation wavelengths to be reflected to the stage. The PMT voltage was adjusted to ensure full scale deflection of the 380 nm signal on the oscilloscope screen. Recording of the individual and ratio signals on both the computer and pen recorder were commenced. Once a stable signal was confirmed, background fluorescence was recorded by moving the cell out of position using the stage controls for 10 s without adjusting the size of the light collection diaphragm. The cell was then moved back into position and the experimental interventions commenced. At the conclusion of the planned interventions, background fluorescence was again recorded in a similar manner as previously described (figure 2.17a, 2.17b and 2.18).
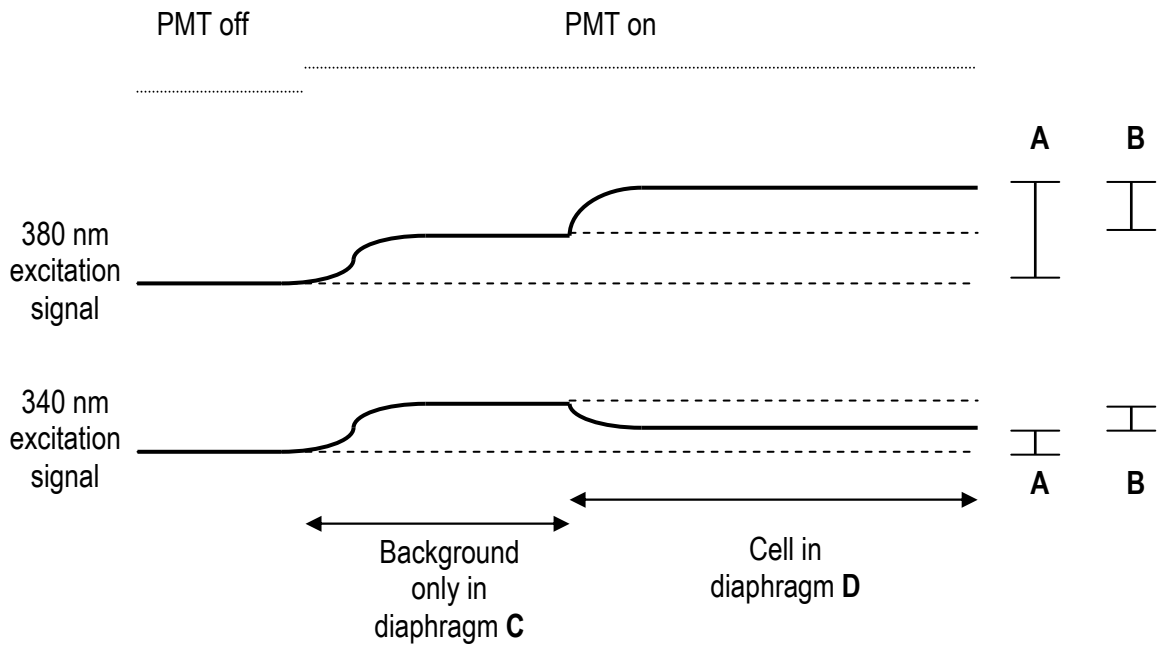
_Figure 2.17a – Diagram of emission signals showing rationale behind accounting for background_

_emission._

_**A** – Background emission included in emission signal, **B** – background emission removed from_

_recorded signal therefore isolating emitted light form the cell alone_
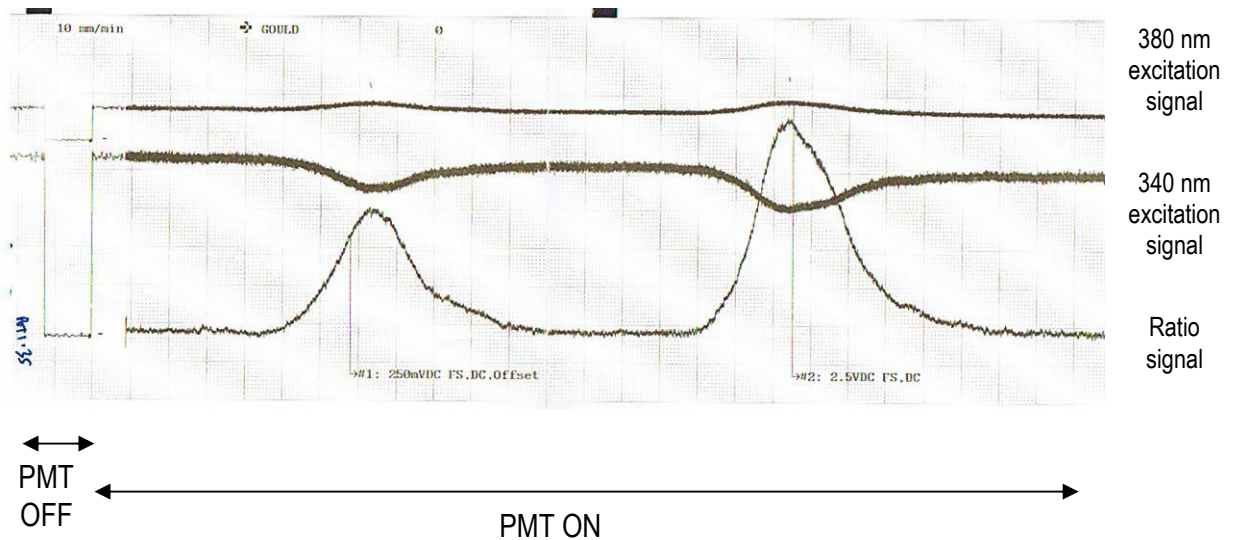


_Figure 2.17b – Typical emission signals showing changes recorded during cell stimulation_

_A good signal to noise ratio was a requirement for using a particular cell for experimentation._

_Additonal signs used in selecting cells included spindle-like shape, homogenous loading of_

_FURA-2 and a 'halo' on phase microscopy._

**Equilibration**
20 min
Tyrode's
Solution

**Intervention**
20 min
Modified Tyrode's
Solution

**Reperfusion**
20 min
Tyrode's
Solution

↑ = 3 µM phenylephrine
↑ = 120 mM KCl
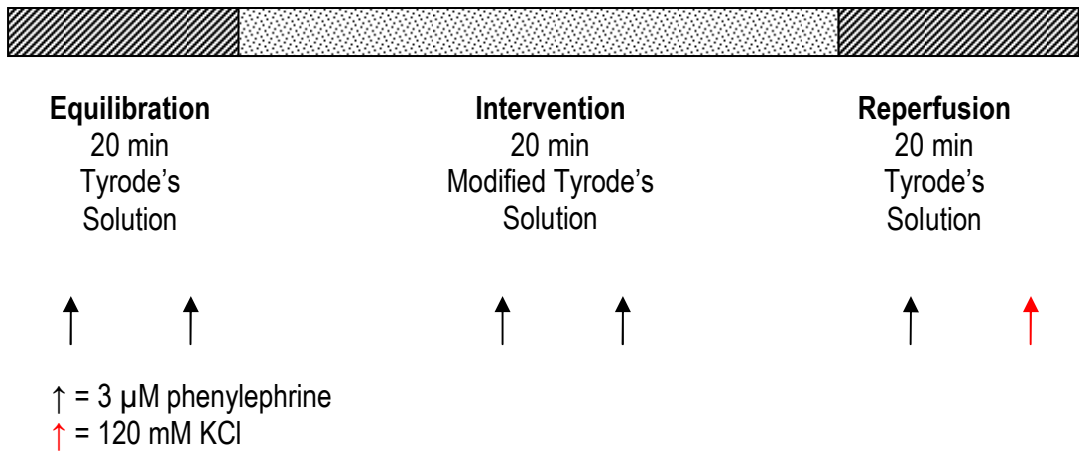
*Figure 2.18 – Experimental protocol for isolated cell intervention*

2.6.4    Calibration of the Fura-2 signal


The ratio of Fura-2 fluorescence at two different excitation wavelengths was used as an index of

the $[Ca^{2+}]_i$. The purpose of calibration was to determine the fluorescence signals and ratio at

known concentrations of $Ca^{2+}$ in the absence of cells. This *in vitro* calibration was performed in

conditions mimicking the intracellular environment (high $[K^+]$) using ethylene glycol tetra-acetic

acid (EGTA) as a $Ca^{2+}$ buffer to ensure $[Ca^{2+}]$ was within the physiological range (table 2.3).


*Table 2.3 - Constituents of FURA-2 signal calibration solution*

*The purity of EGTA was 94% determined from previous experiments making the actual*

*concentration of EGTA 4.7 mM(204).*


| Compound | Concentration (mM) |
|----------|---------------------|
| KCl | 120 |
| HEPES | 20 |
| NaCl | 10 |
| $MgCl_2$ | 1.0 |
| EGTA | 5.0 (actual 4.7) |


Aliquots of 1 M $CaCl_2$ solution were added to this solution at 37 °C (table 2.4). Each solution was

titrated with KOH to a pH of 7.1 using a pH meter (BDH, UK). A 2M KOH stock solution was

made from solid KOH. This compound is supplied as solid pellets of ~85% purity. This was taken

into account when calculating the weight of compound to be dissolved in RO water. The $[Ca^{2+}]$

was calculated using the following equation:

$$pCa = pK_{Ca} + \log ([EGTA] / [Ca\ EGTA])$$

- o pCa was the negative logarithm of $[Ca^{2+}]$
- o The $pK_{Ca}$ of the apparent EGTA dissociation constant ($K_{Ca}$) was taken as 6.64(188).
- o [EGTA] was the concentration of added EGTA.
- o [Ca EGTA] was taken as the concentration of added $CaCl_2$ when $\leq$ 4.0 mM.
- o The first solution had 0 mM added $CaCl_2$ and was used to calculate $R_{min}$.
- o The last solution had 6 mM added $CaCl_2$ to yield a solution with a $[Ca2+]_{free}$ > 1 mM. This was used to calculate $R_{max}$.

*Table 2.4 - Concentration of free $Ca^{2+}$ in calibrating solutions*

| [Ca EGTA] (mM) | [EGTA] (mM) | pCa | $[Ca^{2+}]_{free}$ (nM) |
|---|---|---|---|
| 0 | | | 0 |
| 0.5 | 4.2 | 7.56 | 27.3 |
| 1.0 | 3.7 | 7.21 | 61.9 |
| 2.0 | 2.7 | 6.77 | 169.7 |
| 2.5 | 2.2 | 6.58 | 260.3 |
| 3.0 | 1.7 | 6.39 | 404.3 |
| 4.0 | 0.7 | 5.88 | 1309.1 |
| 6.0 | | | >1000 |

The dissociation constant of Fura-2 for $Ca^{2+}$ in the system ($K_d$) was derived from the following equation(205):

$$K_d = [Ca^{2+}]_{free} (R_{max}-R) / \beta(R-R_{min})$$

- o $K_d$ is the dissociation constant of Fura-2 in the system.
- o R is the ratio signal at a given $[Ca^{2+}]_{free}$.

- $R_{min}$ is the ratio signal at 0 mM $[Ca^{2+}]_{free}$.

- $R_{max}$ is the ratio signal at saturating $[Ca^{2+}]_{free}$, in practice a $[Ca^{2+}]_{free}$ > 1 mM.

- $\beta$ is the emission signal ratio due to excitation at 380 nm of saturating $Ca^{2+}$ to 0 mM $Ca^{2+}$ ($F380_{max}$ / $F380_{min}$).

This equation was rearranged to yield a linear relationship for the estimation of $K_d$:

$$\log \beta[(R-Rmin)/(Rmax-R)] = -pCa + pK_d$$

$\log \beta[(R-Rmin)/(Rmax-R)]$ was plotted against $-pCa$ and $pK_d$ estimated as the pCa at which the $\log \beta[(R-Rmin)/(Rmax-R)] = 0$ (figure 2.19).
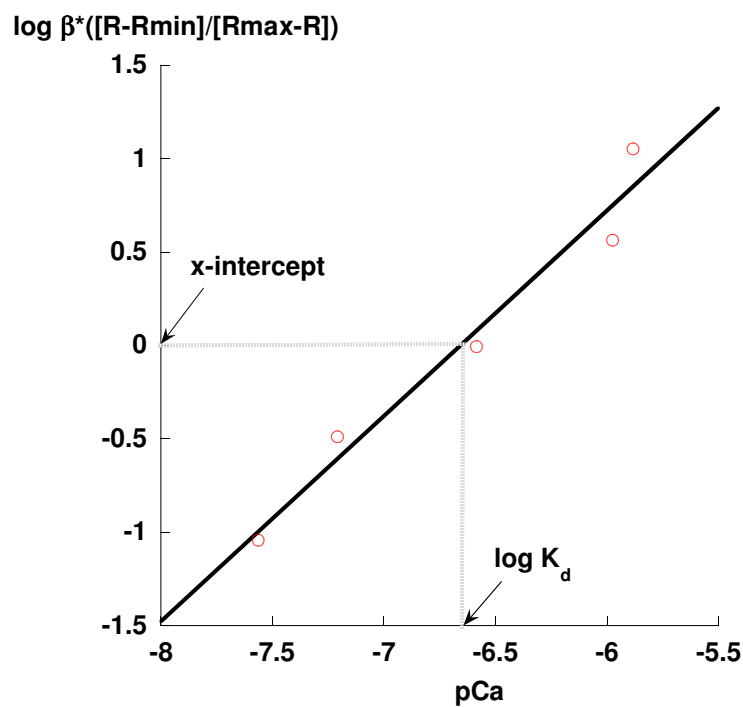


*Figure 2.19 – Sample Fura-2 calibration plot*

*The log $[Ca^{2+}]_{free}$ at the x-intercept corresponds to the log $K_d$ for Fura-2. Ischaemic interventions, in particular alterations in pH, affect the dissociation constant ($K_d$) for Fura-2. Data are therefore presented as ratio signals rather than $[Ca^{2+}]_i$ for accuracy(206).*

## 2.7 Statistical analysis

i) Data are expressed as the mean ± standard deviation of the data set. Several interventions caused tension generated to drop to 0 $mN.mm^{-2}$. These values are included in the data sets presented.

ii) Data sets are the result of $n$ experiments using tissue from $N$ animals.

iii) The computer program Kaleidagraph™ (v3.5, Synergy Software, USA) was used to parameterise straight lines and curves to fit experimental data using the least squares analysis method.

iv) Straight lines were fitted using the equation:

$$y = mx + c$$

o m is the gradient of the straight line.

o c is the point at which the line intercepts the y axis.

v) Curves were fitted using the equation:

$$(y_{max} \cdot x^a)/(x^a + (k_{half})^a)$$

o $y_{max}$ is the maximum of the curve.

o a is the power of the curve.

o $k_{half}$ is the value on the x axis corresponding to half $y_{max}$.

vi) For the purposes of statistical comparison between data sets, $k_{half}$ values are presented as $\log_{10} k_{half}$ ($pk_{half}$) as previous studies on lower urinary tract smooth muscle have shown this to be the normally distributed data set(188).

vii) Where parametric data were being analysed, statistical differences were tested using Student's $t$-tests. When data sets were compared to a single value (for example 100%), Mann-Whitney U tests were used to analyse variation. The null hypothesis was rejected when $p \leq 0.05$.

## 3.1 Results I – Basic tissue parameters

### 3.1.1 Isometric contractions elicited by electrical field stimulation (EFS)

#### 3.1.1.1 EFS-mediated contraction with time

Isometric nerve-mediated contractions elicited by EFS (range 8-60 Hz) were recorded and measured as described in section 2.3.4. Preparations were equilibrated in Tyrode's solution for 60 min. at 37 °C. At the end of this period, the mean nerve-mediated tension at 32 Hz (EFS$_{32Hz}$) was 0.56±0.37 mN.mm$^{-2}$ (N=4, n=6) and was 66±7% of the estimated maximal tension (T$_{max}$) from the force-frequency curves. The mean half-maximal frequency (f$_{1/2}$) under these control conditions was 22.2±3.7 Hz.

The maximum duration of proposed experiments was 240 min. including the equilibration period. Preparations were periodically stimulated at 32 Hz and the force-frequency relationship measured at set intervals during superfusion with Tyrode's solution (NT) to ascertain the stability of the preparation for the duration of the proposed experiments.

The force-frequency relationship as well as the mean EFS$_{32Hz}$ remained stable throughout the 240 min. of experimentation (figure 3.1). The large standard deviations reflect the variability in tension generated between muscle strips. However within each preparation tension was stable throughout the experimental period as shown by the T$_{max}$ and f$_{1/2}$ values (table 3.1).

8 16 24 32 40 60          8 16 24 32 40 60          8 16 24 32 40 60          EFS (Hz)

60 min.                         90 min.                        120 min.

1 mN

2 min.

8 16 24 32 40 60          8 16 24 32 40 60          EFS (Hz)

180 min.                        240 min.
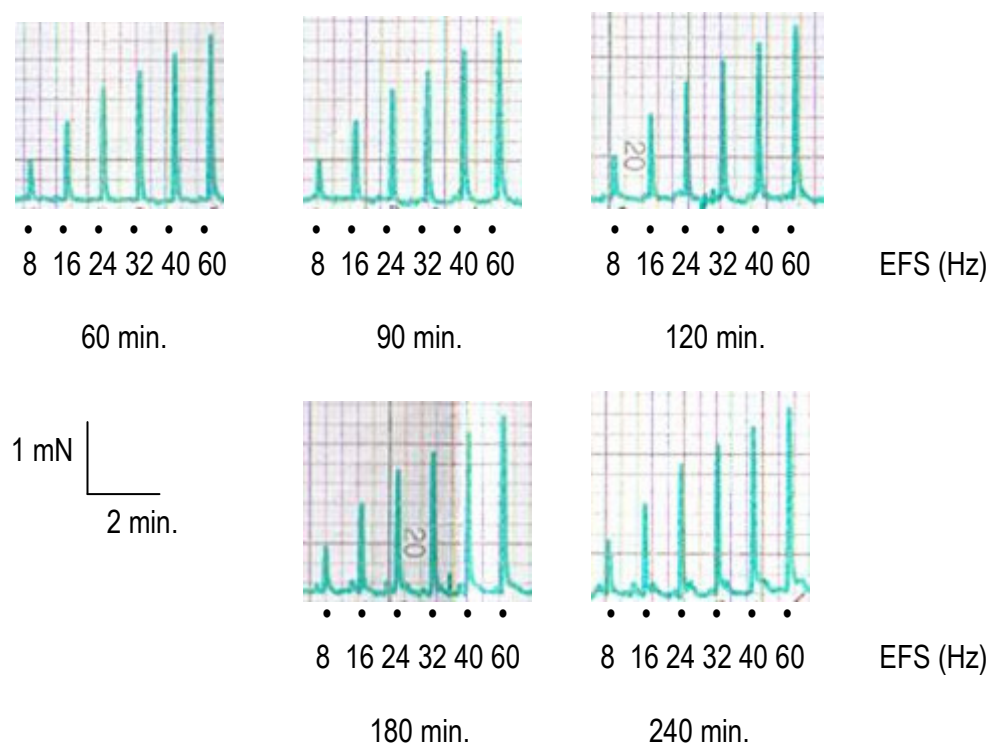
*Fig. 3.1 – Typical experimental tracing showing periodic force/frequency relationship over time in Tyrode's solution. EFS-mediated contractile responses were stable over the proposed time course of experiemts (240 min.)*

*Table 3.1 – Stability of contractile (EFS) responses in Tyrode's solution*

*NT = Normal Tyrode's solution*

| N=4, n=6 | 60 min NT | 90 min NT | 120 min NT | 180 min NT | 240 min NT |
|---|---|---|---|---|---|
| $EFS_{32Hz}$ (mN.mm$^{-2}$) | 0.56±0.37 | 0.60±0.42 | 0.63±0.47 | 0.66±0.52 | 0.65±0.50 |
| $EFS_{32Hz}$ as % control | - | 104±8 | 105±14 | 109±17 | 109±15 |
| $EFS_{32Hz}$ as % of $T_{max}$ (%) | 66±7 | 63±7 | 66±3 | 69±4 | 68±5 |
| $f_{1/2}$ (Hz) | 22.2±3.7 | 24.1±4.0 | 21.7±1.3 | 19.8±2.3 | 20.2±2.5 |

3.1.1.2 Effect of tetradotoxin on EFS-mediated contraction

To record the proportion of EFS-mediated contraction in the preparation that occurred via embedded motor nerves, the effect of the neurotoxin tetrodotoxin (TTX 1 μM) was examined. More than 95% of the phasic contraction in response to EFS (range 8-60 Hz) was reversibly abolished in the presence of TTX (figure 3.2).
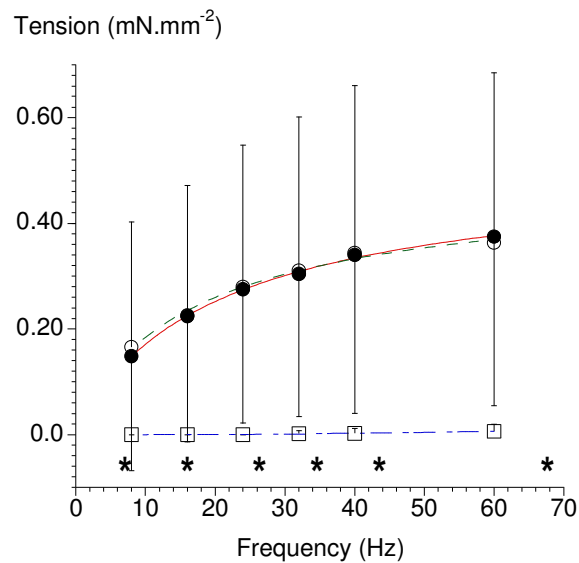


Figure 3.2 – Effect of 1 μM TTX on EFS-mediated contraction in CSM (N=8, n=12)

● – control, □ – 1 μM TTX, ○ – post-control, error bars show standard deviation of the mean

* significant reduction compared to control (p<0.05).

1 μM TTX abolished EFS-mediated responses indicating that phasic contractions in response to electrical stimulation as described were mediated via intrinsic motor nerves.

3.1.1.3 Effect of stimulation voltage on EFS-mediated contraction

To ascertain the proportion of embedded motor-nerve fibres stimulated with EFS, the effect of increasing stimulation voltage was examined on the preparation (table 3.2 and fig 3.3).

*Table 3.2 - Effect of stimulation voltage on EFS-mediated contractions*

*\* p<0.05 compared to 50 V*

*There was no significant increase in force of contraction above 50 V throughout the range of stimulation frequencies (8-60 Hz). In addition there was no difference in the $f_{1/2}$ at the different stimulation voltages. Subsequent EFS experiments were therefore carried out at 50 V.*

| N=4, n=7 | 40 V | 50 V | 60 V | 70 V | 80 V |
|---|---|---|---|---|---|
| $EFS_{24Hz}$ (mN.mm$^{-2}$) | 0.23±0.13* | 0.27±0.13 | 0.33±0.16 | 0.32±0.20 | 0.39±0.26 |
| $EFS_{24Hz}$ as % of $EFS_{24Hz}$ at 50 V | 82±11* | - | 124±22 | 118±31 | 151±68 |
| $f_{1/2}$ (Hz) | 20.0±13.7 | 25.2±13.3 | 19.6±6.5 | 22.8±6.8 | 24.0±7.6 |
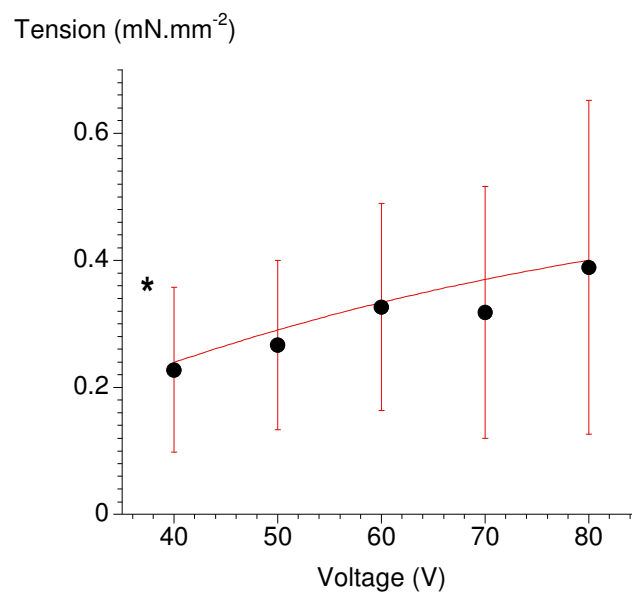


*Fig. 3.3 – Recruitment curve showing tension in response to $EFS_{24\ Hz}$ at varying stimulation voltages \* p<0.05 vs. 50 V*

*Findings were consistent throughout the frequency range (8-60 Hz). This indicates maximal nerve-recruitment at 50 V and above.*

3.1.2    Isometric contractures elicited by phenylephrine (PE)

3.1.2.1  PE-induced contractures with time

Isometric agonist-induced contractures were recorded and measured as described in section 2.3.5. Preparations were equilibrated in Tyrode's solution for 60 min. at 37 °C. At the end of this period, 15 µM PE was introduced and a contracture recorded. The mean peak tension in response to PE was $0.50\pm0.35$ mN.mm$^{-2}$ and mean plateau tension was $0.42\pm0.29$ mN.mm$^{-2}$ (N=11, n=14). The maximum duration of experiments measuring PE-induced contractures was 240 min. To ascertain the stability of the preparation, separate contractures were elicited in response to 15 µM PE for a similar time period (table 3.3).

*Table 3.3 - Stability of phenylephrine-induced contractile responses in Tyrode's solution*
*Peak and plateau PE responses remained stable throughout the experimental period. Plateau responses were on average 86% of the peak PE response (range 70-100%).*

| Intervention | Peak tension (mN.mm$^{-2}$) | Plateau tension (mN.mm$^{-2}$) | Plateau tension as % of peak tension |
|:---:|:---:|:---:|:---:|
| 60 min Tyrode's | $0.50\pm0.35$ | $0.42\pm0.29$ | $83\pm8$ |
| 90 min Tyrode's | $0.51\pm0.36$ | $0.44\pm0.31$ | $87\pm7$ |
| 120 min Tyrode's | $0.49\pm0.36$ | $0.43\pm0.31$ | $91\pm7$ |
| 180 min Tyrode's | $0.50\pm0.34$ | $0.43\pm0.30$ | $85\pm9$ |
| 240 min Tyrode's | $0.52\pm0.37$ | $0.44\pm0.33$ | $85\pm9$ |

3.1.2.2  Effect of nifedipine on phenylephrine-induced contractures

In order to examine the proportion of the phenylephrine-induced contracture which was due to $Ca^{2+}$ influx into the cells, the effect of the L-type calcium channel blocker nifedipine was examined. Muscle strips were maximally contracted with 15 µM phenylephrine and the contracture recorded as previously described. 100 µM nifedipine was then introduced into the superfusate and a similar PE-induced contracture recorded. This dose of nifedipine was chosen as it completely abolished the contracture seen in response to high KCl (100 mM).

The mean peak tension in response to PE was 1.60±0.90 mN.mm$^{-2}$ and mean plateau tension was 1.48±0.85 mN.mm$^{-2}$ (N=6, n=7, fig. 3.4). Peak and plateau contractile responses to 15 µM phenylephrine were significantly reduced in the presence of 100 µM nifedipine to 1.27±0.70 mN.mm$^{-2}$ and 1.15±0.67 mN.mm$^{-2}$ respectively (79±7% and 77±7% of control respectively).
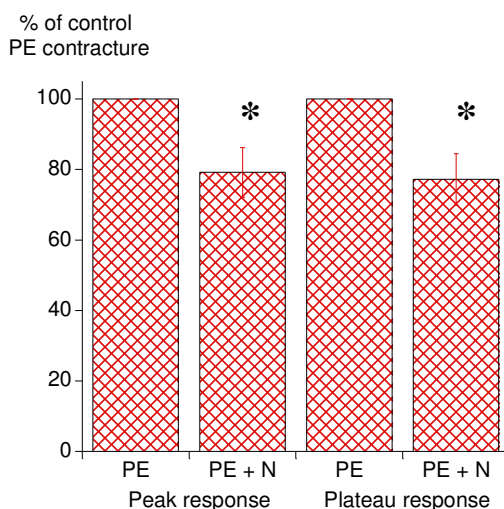


*Figure 3.4 – The effect of 100 µM nifedipine on PE-induced contractures.*

*PE – phenylephrine, N – nifedipine*

*\* significant reduction compared to control PE contracture (p<0.05)*

*These findings indicate that the majority of the agonist-induced contracture was independent of calcium influx via the L-type calcium channel.*

### 3.1.3    Isometric relaxations elicited by electrical field stimulation (EFS)

#### 3.1.3.1  EFS-mediated relaxation with time

Isometric relaxations elicited by EFS (range 4-24 Hz) in CSM strips pre-contracted with 15 µM PE were recorded and measured as described in section 2.3.4. Preparations were equilibrated in Tyrode's solution for 60 min. at 37 °C. At the end of this period, the mean tension remaining after nerve-mediated relaxation at 24 Hz ($EFS_{24Hz}$) was $0.37 \pm 0.15$ mN.mm$^{-2}$ (N=4, n=7) and was $57 \pm 16\%$ of the preceding plateau PE contracture. The mean half-maximal frequency ($f_{\frac{1}{2}}$) under these control conditions was $5.9 \pm 2.1$ Hz.

The maximum duration of proposed experiments was 240 min. including the equilibration period. Preparations were periodically pre-contracted and a force-frequency relationship recorded (EFS range 4-24) at set intervals during superfusion with Tyrode's solution (NT) to ascertain the stability of the preparation for the duration of the proposed experiments (figure 3.5). Increasing frequency of stimulation elicited progressively larger relaxatory responses in the pre-contracted strips.

However, in contrast to the EFS-mediated contractions (section 3.1.1), the EFS-relaxation force-frequency relationship was not stable throughout the proposed experimental period. This is shown by the left-shift of the force-frequency relationship with time (figure 3.6 and table 3.4). The $EFS_{24Hz}$ was the most stable parameter and is therefore used as the variable in subsequent experiments.

EFS (Hz)  4 8 16 24          4 8 16 24          4 8 16 24



60 min.          90 min.          120 min.     15 µM PE

EFS (Hz)        4 8 16 24        4 8 16 24

0.5 mN

5 min.



180 min.          240 min.     15 µM PE
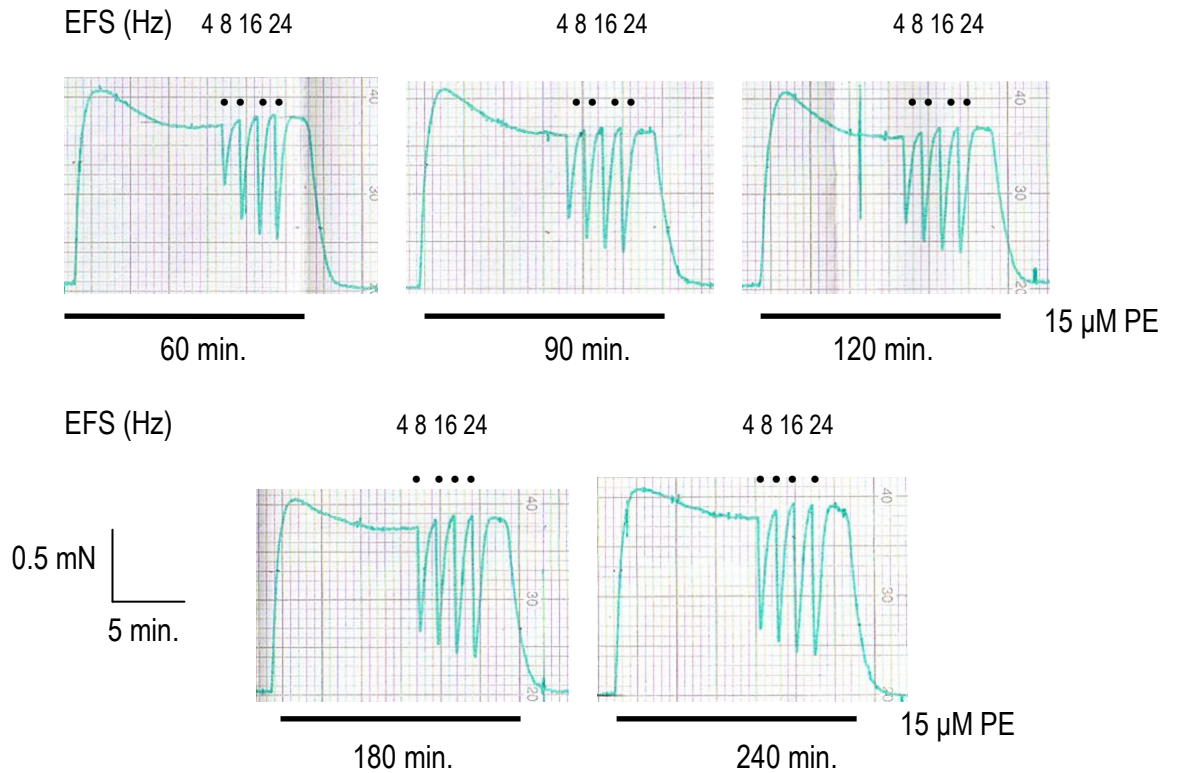
*Figure 3.5 – Typical experimental tracing showing EFS-mediated relaxatory responses over time*

*Consecutive contractures over 240 min. showing stability of 15 µM PE contracture with time.*

*Each stimulation train (EFS 4-24 Hz) elicited a progressively greater relaxatory response.*

*Tension remaining after the final 24 Hz stimulation was the most stable parameter.*

*Table 3.4 - Effect of Tyrode's solution on EFS relaxation*     NT = Unmodified Tyrode's solution

| N=4, n=7 | 60 min NT | 90 min NT | 120 min NT | 180 min NT | 240 min NT |
|---|---|---|---|---|---|
| PE plateau (mN.mm$^{-2}$) | 0.65±0.19 | 0.67±0.21 | 0.67±0.22 | 0.66±0.22 | 0.74±0.19 |
| EFS$_{24Hz}$ (mN.mm$^{-2}$) | 0.37±0.15 | 0.34±0.12 | 0.33±0.14 | 0.30±0.12 | 0.32±0.15 |
| EFS$_{24Hz}$ as % preceding PE plateau contracture | 57±16 | 52±18 | 51±19 | 48±20 | 45±20 |
| f$_{½}$ (Hz) | 5.9±2.1 | 4.2±3.0* | 3.6±2.0* | 2.5±2.2* | 2.4±2.3* |
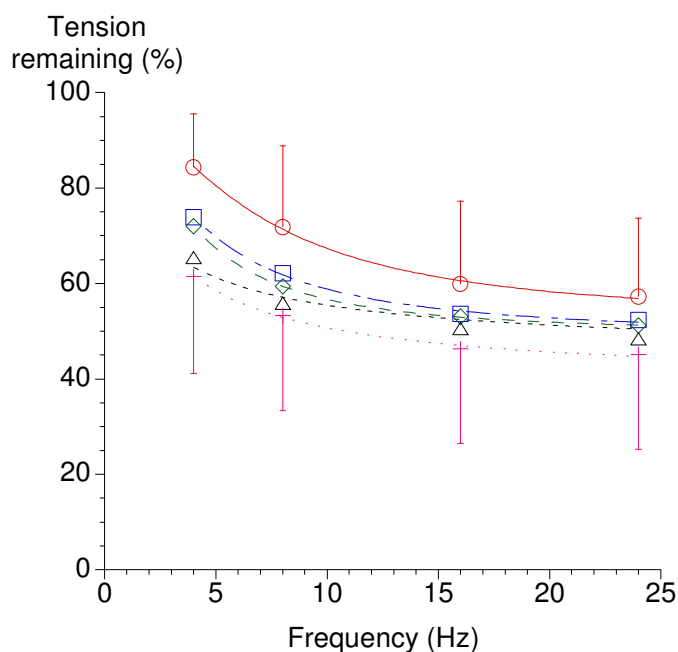
*Fig. 3.6 – Variation of EFS-mediated relaxation in CSM with time*

*○ – control, □ – 60 min NT, ◊ – 120 min NT, Δ – 180 min NT, + - 240 min NT*

*Stimulation trains during each consecutive contracture elicited larger relaxatory responses.*

3.1.3.2  EFS-mediated relaxation at differing levels of pre-contraction

Differing doses of PE were used to examine whether EFS-mediated relaxations were dependent upon the level of pre-contraction. Isometric relaxations elicited by EFS (range 4-24 Hz) in CSM strips pre-contracted with 15 µM PE or 1.5 µM PE were recorded and measured as described in section 2.3.4. Preparations were equilibrated in Tyrode's solution for 60 min. at 37 °C. At the end of this period, the mean plateau tension after pre-contraction with 15 µM PE was 1.03±0.56 mN.mm$^{-2}$ (N=3, n=6). A force-frequency relationship was subsequently recorded (EFS range 4-24). Tension remaining after nerve-mediated relaxation at 24 Hz (EFS$_{24Hz}$) was 0.68±0.47 mN.mm$^{-2}$ and was 62±12% of the preceding plateau PE contracture. Experiments were repeated using the same preparation pre-contracted with 1.5 µM PE. The mean plateau tension was

0.50±0.34 mN.mm$^{-2}$ (N=2, n=6) which was 46±9% of the plateau 15 µM PE contracture. Tension remaining after nerve-mediated relaxation at 24 Hz (EFS$_{24Hz}$) was 0.18±0.18 mN.mm$^{-2}$ and was 33±19% of the preceding plateau PE contracture (figure 3.7).
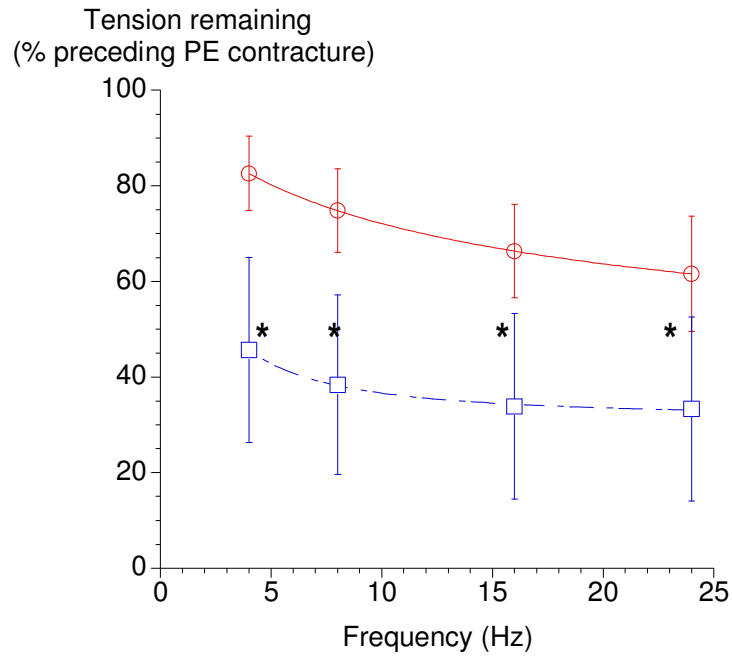


*Figure 3.7 – Effect of differing levels of pre-contraction on tension remaining after EFS relaxation*

*○ – pre-contraction with 15 µM PE, ▢ – pre-contraction with 1.5 µM PE*

*\* significant reduction compared to 15 µM PE (p<0.05)*

*Relaxation was proportionally greater with smaller PE pre-contraction.*

3.1.3.3  TTX on EFS-mediated relaxation

To record the proportion of EFS-mediated relaxation in the preparation that occurred via
embedded motor nerves, the effect of the neurotoxin tetrodotoxin (TTX 1 µM) was examined. On
average 88% (range 68-100%, N=4, n=7) of the phasic relaxation in response to EFS (range 4-24
Hz) was reversibly abolished in the presence of TTX (fig. 3.8).
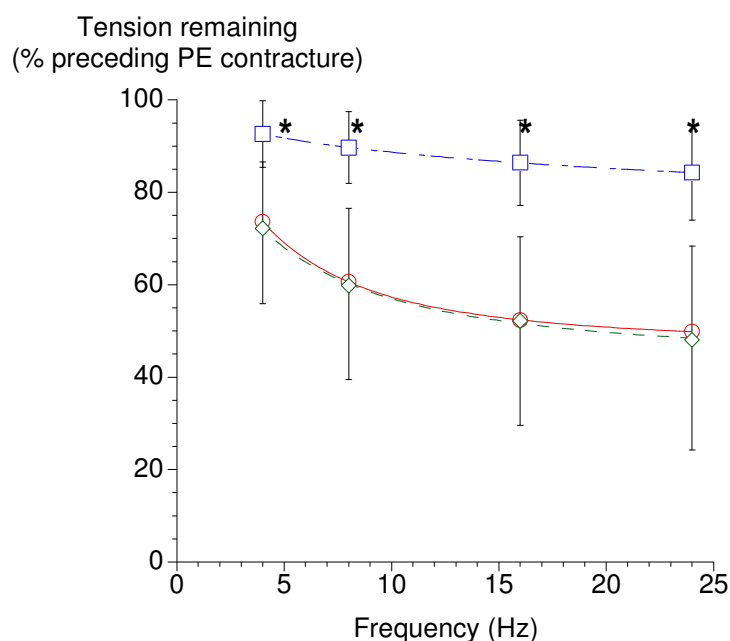


*Fig. 3.8 – Effect of 1 µM TTX on EFS mediated relaxation*

*○ – pre-control, □ – 1 µM TTX, ◊ – post-control*

*\* significant reduction compared to control and compared to preceding plateau PE*

*contracture(p<0.05).*

This TTX-resistant relaxation shows that there is an element of EFS-mediated relaxation which is
not mediated via embedded relaxatory nerves. This may be as a result of direct stimulation of the
endothelium or the muscle itself.

3.1.3.4  ODQ on EFS-mediated relaxation

To record the proportion of EFS-mediated relaxation in the preparation that was secondary to nitric oxide release, the effect of the highly selective inhibitor of soluble guanyl cyclase ODQ was examined. On average 90% (range 72-100%, N=4, n=6) of the phasic relaxation in response to EFS (range 4-24 Hz) was abolished in the presence of ODQ (figure 3.9).
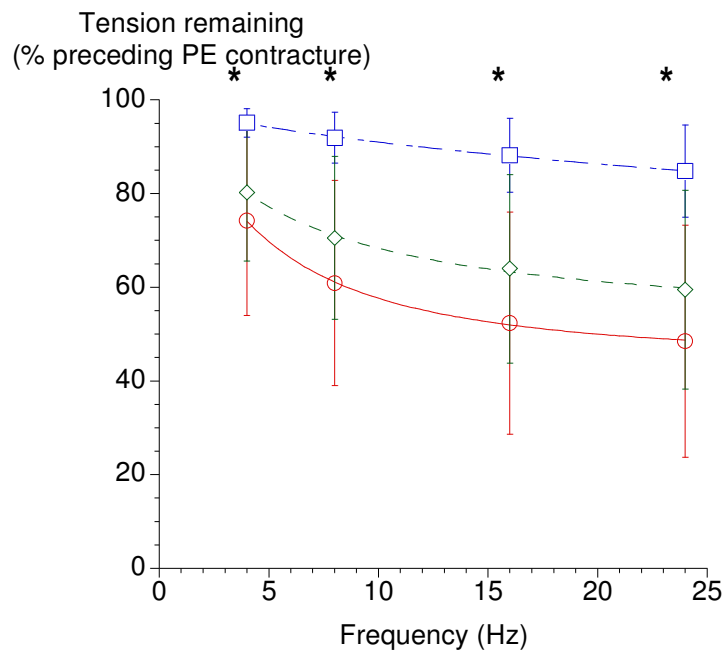


*Fig. 3.9 – Effect of ODQ on EFS mediated relaxation*

*○ – pre-control, □ – 10 μM ODQ, ◊ – post-control*

*\* significant reduction compared to control and to the 100% PE contracture(p<0.05)*

*This shows that the majority of relaxation in response to EFS is mediated via a cGMP specific pathway such as via nitric oxide production. Responses did not return to control values during the time course of reperfusion in these experiments. In a similar manner to the TTX responses, a proportion of relaxation persisted in the presence of ODQ and was significantly different from the preceding PE contracture. This ODQ-resistant relaxation shows that there is an element of EFS-mediated relaxation which is not mediated via a cGMP specific pathway.*

### 3.1.4 Isometric relaxations elicited by carbachol

### 3.1.4.1 Carbachol-induced relaxation with time

Isometric agonist-induced relaxations were recorded as described in section 2.3.5. Preparations were equilibrated in Tyrode's solution for 60 min. at 37 °C. At the end of this period, 15 μM phenylephrine (PE) was introduced and a contracture recorded. Once this contracture had reached a plateau, 1 μM carbachol was used to induce a relaxatory response in the pre-contracted muscle strip. The mean nadir tension remaining after application of carbachol was $0.11\pm0.09$ mN.mm$^{-2}$ (N=7, n=7) and mean plateau tension remaining was $0.11\pm0.09$ mN.mm$^{-2}$ (figure 3.10 and table 3.5).

*Table 3.5 - Stability of carbachol-induced relaxatory responses in Tyrode's solution*

*NT = unmodified Tyrode's solution, PE = phenylephrine*

*These responses were not significantly different from each other. Nadir and peak values were not significantly different throughout the experimental period*

| Intervention | Nadir tension remaining (mN.mm$^{-2}$) | Nadir tension as % preceding PE contracture (%) | Plateau tension remaining (mN.mm$^{-2}$) | Plateau as % preceding PE contracture (%) |
|---|---|---|---|---|
| 60 min NT | $0.11\pm0.09$ | $61\pm17$ | $0.11\pm0.09$ | $63\pm14$ |
| 90 min NT | $0.11\pm0.12$ | $55\pm21$ | $0.12\pm0.12$ | $57\pm19$ |
| 120 min NT | $0.10\pm0.11$ | $50\pm22$ | $0.11\pm0.12$ | $54\pm21$ |
| 180 min NT | $0.09\pm0.10$ | $40\pm25$ | $0.09\pm0.10$ | $44\pm23$ |
| 240 min NT | $0.08\pm0.10$ | $41\pm24$ | $0.10\pm0.10$ | $49\pm23$ |

60 min.
90 min.

15 µM PE
1 µM C

120 min.
180 min.

15 µM PE
1 µM C

1 mN

5 min.

240 min.

15 µM PE
1 µM C
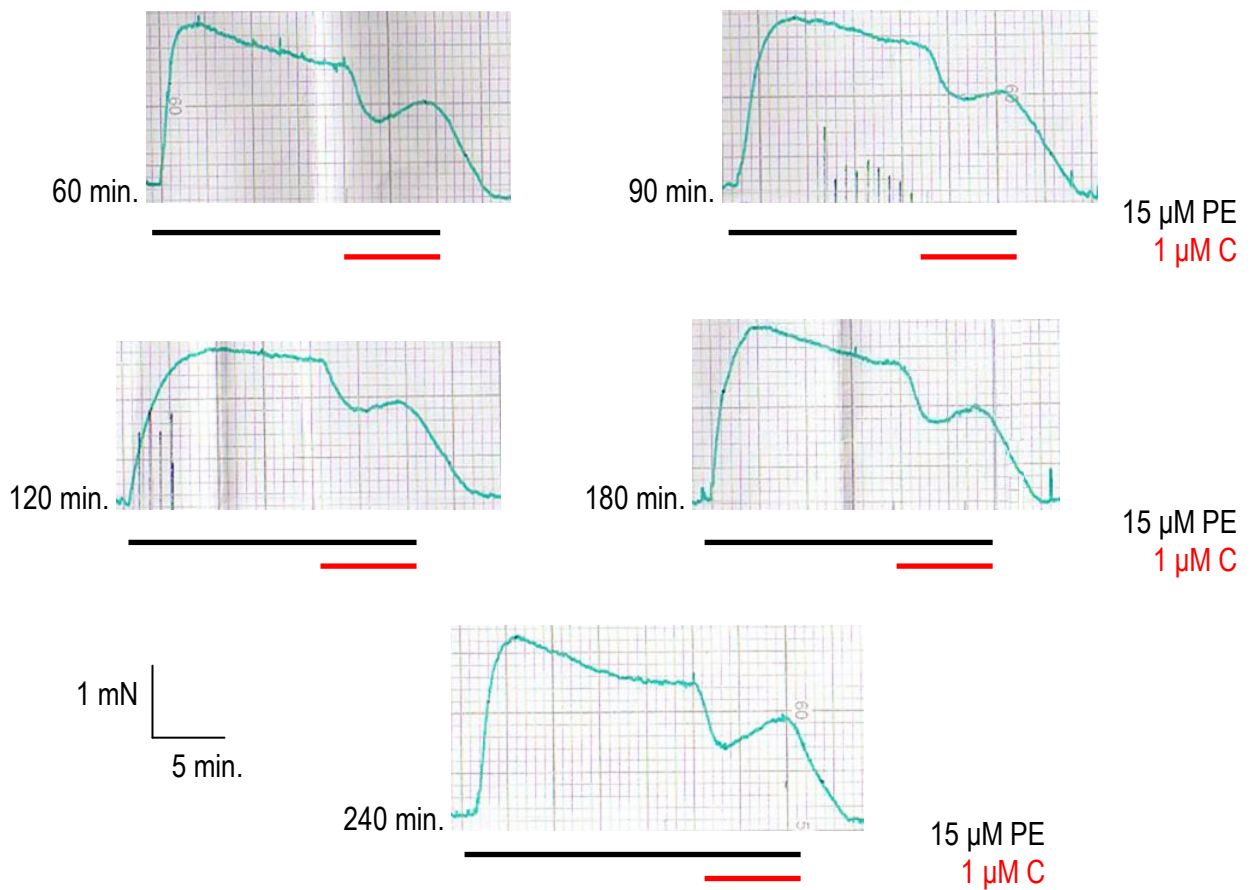
*Fig. 3.10 – Typical experimental tracing showing stability of phenylephrine induced contractures and carbachol-induced relaxations over time*

3.1.4.2  Carbachol-induced relaxation at differing levels of pre-contraction

Different doses of PE were used to examine whether carbachol-induced relaxations were dependent upon the level of pre-contraction. Relaxations elicited by 1 µM carbachol in CSM strips pre-contracted with 15 µM PE or 1.5 µM PE were recorded and measured as described in section 2.3.5. Preparations were equilibrated in Tyrode's solution for 60 min. at 37 °C. At the end of this period, the mean plateau tension after pre-contraction with 15 µM PE was $0.96\pm0.51$ mN.mm$^{-2}$ (N=3, n=6). The mean nadir tension remaining after application of carbachol was $0.67\pm0.42$ mN.mm$^{-2}$ and was $67\pm8\%$ of the preceding plateau PE contracture. Mean plateau

tension remaining after application of carbachol was 0.72±0.45 mN.mm$^{-2}$ and was 72±9% of the preceding plateau PE contracture.

The mean plateau tension after pre-contraction with 1.5 µM PE was 0.46±0.27 mN.mm$^{-2}$ (N=3, n=6) and was 46±9% of that generated after 15 µM PE. The mean nadir tension remaining after application of carbachol was 0.24±0.24 mN.mm$^{-2}$ and was 46±25% of the preceding plateau PE contracture. Mean plateau tension remaining after application of carbachol was 0.28±0.26 mN.mm$^{-2}$ and was 54±22% of the preceding plateau PE contracture (fig. 3.11).
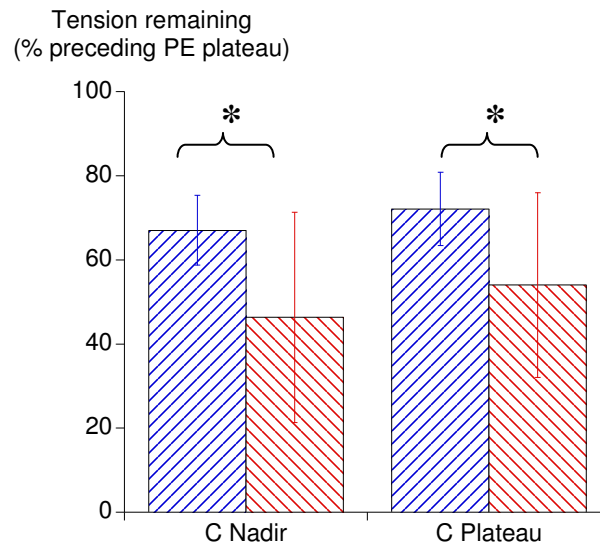


Fig. 3.11 – Effect of differing levels of pre-contraction on carbachol-induced relaxation

░ – 15 µM PE, ░ – 1.5 µM PE

* significant reduction compared to responses with 15 µM PE pre-contraction (p<0.05)

In a similar manner to EFS relaxation, 1.5 µM carbachol elicited a proportionally larger relaxatory response with a smaller PE pre-contracture.

3.1.5    Effect of repeated applications of PE on calcium transients is isolated CSM cells

CSM cell isolation was performed on fresh tissue as outlined in sections 2.6.2 and 2.6.3. In general, experimental protocols were as outlined in fig. 2.18. Cells were equilibrated in Tyrode's solution for 10 min. at 37 °C and constantly perfused with fresh solution during the course of the interventions.

Background fluorescence was recorded at the start and end of the experimental protocol. The mean ratio signal was 0.20±0.04 at the start and 0.23±0.03 at the end of the experiment ($[Ca^{2+}]$ 121±72 and 178±52 µM respectively). The mean PMT voltage required was 889±127 V. At the end of this period, 3 µM PE was introduced for 1 min. and the response recorded. Unmodified Tyrode's solution at 37 °C was used to perfuse isolated cells for 10 min. between subsequent stimulations as a 'washout' period. After a final washout period, 120 mM KCl was introduced and the response recorded. The maximum duration of experiments measuring PE-induced responses was 60 min. To ascertain the stability of the preparation, responses to 3 µM PE were recorded over a similar time period (figures 3.12, 3.13 and table 3.6).

*Table 3.6 - Effect of repeated stimulation with PE on isolated CSM cells*

*PE responses in isolated cells remained stable throughout the experimental period.*

| N=7, n=8 | 1st PE response | 2nd PE response | 3rd PE response | 4th PE response | 5th PE Response | 120 mM KCl |
|---|---|---|---|---|---|---|
| Peak ratio signal | 0.31±0.05 | 0.30±0.03 | 0.31±0.04 | 0.32±0.04 | 0.31±0.02 | 0.28±0.05 |
| Δ $[Ca^{2+}]$ (nM) | 327±90 | 308±59 | 318±72 | 336±68 | 325±42 | 275±89 |

380 nm

340 nm

ratio

----- 1 min. 3 µM PE

1st Ca²⁺ transient    2nd Ca²⁺ transient    3rd Ca²⁺ transient

380 nm

340 nm

ratio

----- 1 min. 3 µM PE    ----- 1 min. 120 mM KCl

4th Ca²⁺ transient    5th Ca²⁺ transient
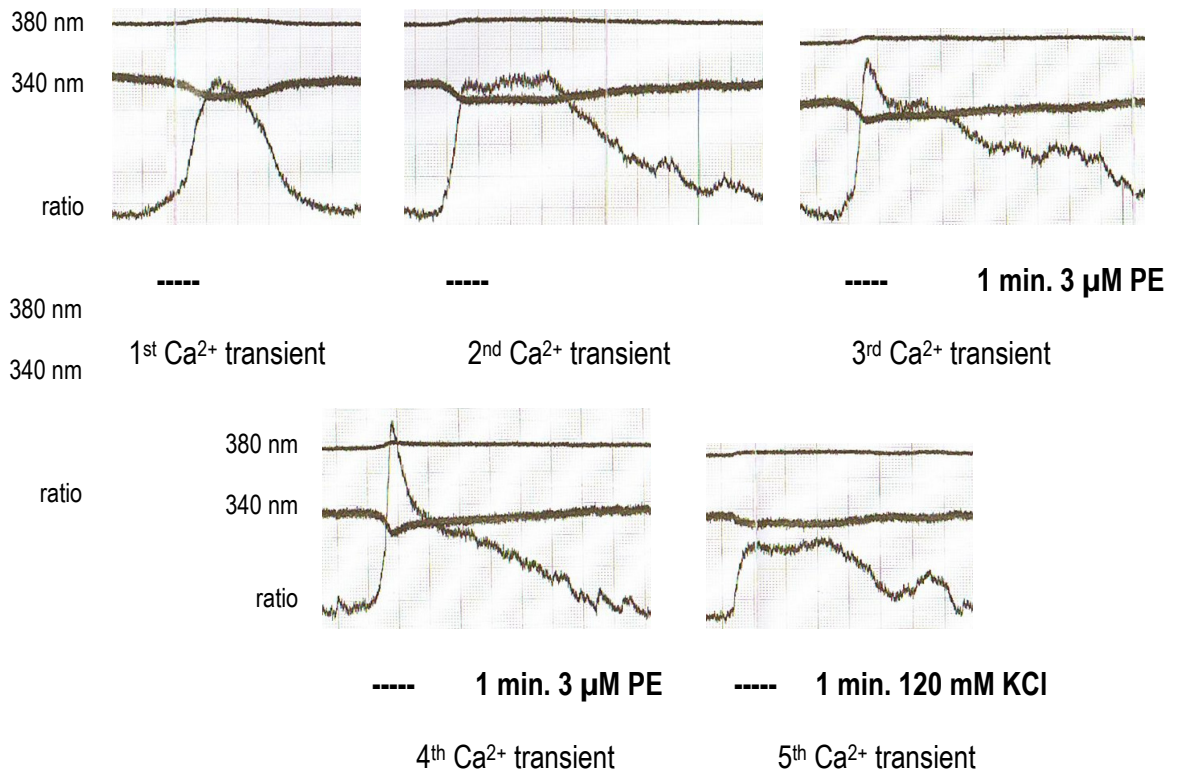
*Fig. 3.12 – Experimental tracing showing Ca²⁺ transients in response to consecutive 3 µM PE*

*To ensure cell stability, two consecutive PE responses were elicited under control conditions and*

*subsequent interventions compared to the second.*
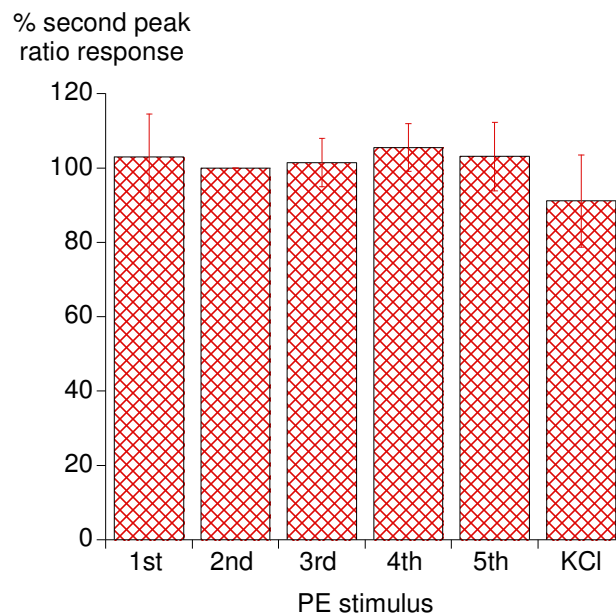


*Fig. 3.13 – Effect of consecutive applications of PE on calcium transients in isolated CSM cells*

*The final KCl response was 91±12% of the preceding PE response.*

### 3.1.6  Summary of basic tissue parameters

Dissection was straightforward after animals were sacrificed as outlined in section 2.2. No differences were observed between samples used on day 1 or day 2 after storage at 4 °C overnight in $Ca^{2+}$-free Tyrodes solution.

EFS-mediated contraction was stable over 240 min. 95% of contraction was via embedded motor nerves (TTX-sensitive). Maximal motor nerve recruitment was seen at 50 V.

Agonist-induced contractures were stable over 240 min. An initial peak response followed by a plateau was observed upon addition of 15 µM phenylephrine to the superfusate. The plateau contracture was on average 85% of the peak response. In addition, the majority of tension generated (87% of peak and 84% of plateau PE contracture) was insensitive to the L-type calcium channel blocker nifedipine. Alternative sources of calcium would be intracellular stores, intracellular calcium sensitisation and non-specific cation channels. These could have been investigated by using caffeine, Rho-kinase inhibitors and non-specific cation channel blockers (flufenamic acid and ruthenium red) respectively.

The majority of EFS-mediated relaxation is TTX sensitive (88%). However, there is a TTX insensitive proportion of EFS mediated relaxation which increased with increasing frequency of stimulation. Similarly relaxations were sensitive to ODQ and again there was a small ODQ insensitive proportion which increased with increasing frequency of stimulation. This may be secondary to direct EFS of the endothelium and may represent a nitric-oxide independent mechanism of relaxation.

EFS-mediated relaxation demonstrated a shift to the left of the force-frequency relationship over 240 min. $EFS_{24Hz}$ was stable when expressed as percentage of preceding PE contracture as long as the preceding PE contracture remained stable. However, the magnitude of EFS-mediated relaxation was dependent upon the level of pre-contraction. EFS-mediated relaxation had a proportionally greater effect with lower levels of pre-contraction. During the proposed experiments, it is postulated that the level of pre-contraction may be changing due to the ischaemic micro environment. Therefore observations on the effect of interventions on EFS-mediated relaxation can only be made when the normal relationship is altered. In summary this normal relationship is comprised of two aspects:

- At similar levels of pre-contraction, EFS-relaxation increases with time
- During interventions where the level of pre-contraction is reduced, EFS-mediated relaxation has a proportionally greater effect.

Carbachol-induced relaxation was stable over 240 min. However, the degree of relaxation in response to 1 µM carbachol was dependent upon the level of pre-contraction. In a similar manner to EFS-mediated relaxation, carbachol induced a proportionally greater relaxation at lesser levels of pre-contraction. Therefore, in experiments where the levels of pre-contraction may be reduced during the intervention, this relationship must be taken into account.

Isolated cell harvest was satisfactory with the protocol developed. PE-induced calcium transients were stable for the duration of proposed experiments.

*Table 3.7 – Summary of basic tissue parameters*

| Aspect of CSM function examined | Comments |
|---|---|
| EFS-mediated contraction | • Stable over 240 min.<br>• 95% of contraction via embedded motor nerves.<br>• Maximal nerve recruitment at 50 V and above. |
| PE-induced contraction | • Stable over 240 min.<br>• Initial peak response followed by plateau.<br>• Majority of response not sensitive to L-type calcium channel blockade. |
| EFS-mediated relaxation | • Left shift of the force-frequency relationship over 240 min.<br>• Dependent upon level of pre-contraction<br>• 88% TTX sensitive, 90% ODQ sensitive |
| Carbachol-induced relaxation | • Stable over 240 min.<br>• Dependent upon level of pre-contraction |
| Isolated cell contraction | • PE-induced $[Ca^{2+}]_i$ transients stable over 60 min. |

## 3.2 Results II – The effect of simulated ischaemia on nerve-mediated contraction

### 3.2.1 Effect of simulated ischaemia (HIAS) on nerve-mediated contraction

Simulated ischaemia (HIAS) consisted of simultaneous hypoxia, intra & extracellular acidosis and substrate depletion (absence of glucose and sodium pyruvate). This resulted in reduction of superfusate from pH $7.43\pm0.03$ to $6.98\pm0.02$ and reduction in $PO_2$ from $88.3\pm4.2$ kPa to $7.8\pm1.6$ kPa.

Isometric nerve-mediated contractions elicited by electrical field stimulation (EFS range 8-60 Hz) were recorded as described in section 2.3.4. Preparations were equilibrated in Tyrode's solution for 60 min. at 37 °C. At the end of this period, the mean nerve-mediated tension at 32 Hz ($EFS_{32Hz}$) was $0.25\pm0.13$ mN.mm$^{-2}$ (N=5, n=6) and was $45\pm1\%$ of the estimated maximal tension ($T_{max}$) from the force-frequency curves. The mean $f_{1/2}$ under these control conditions was $34.6\pm1.5$ Hz.

30 min. of HIAS significantly reduced the mean $EFS_{32Hz}$ to $0.14\pm0.15$ mN.mm$^{-2}$ ($53\pm30\%$ of control). This significant reduction was present at stimulation frequencies above 32 Hz. Further exposure reduced tension even more, until after 60 min. HIAS, $EFS_{32Hz}$ was significantly reduced to $20\pm13\%$ of control (figures 3.14 and 3.15, table 3.7). This reduction was significant throughout the frequency range of stimulation. $f_{1/2}$ was unchanged during simulated ischaemia. The EFS response did not recover upon reperfusion; after 60 min. of normal Tyrode's solution, $EFS_{32Hz}$ remained at $0.09\pm0.09$ mN.mm$^{-2}$ ($30\pm24\%$ of control).

8 16 24 32 40 40 60    8 16 24 32 40 60    8 16 24 32 40 60    8 16 24 32 40 60

Control            30 min. HIAS        60 min. HIAS        reperfusion
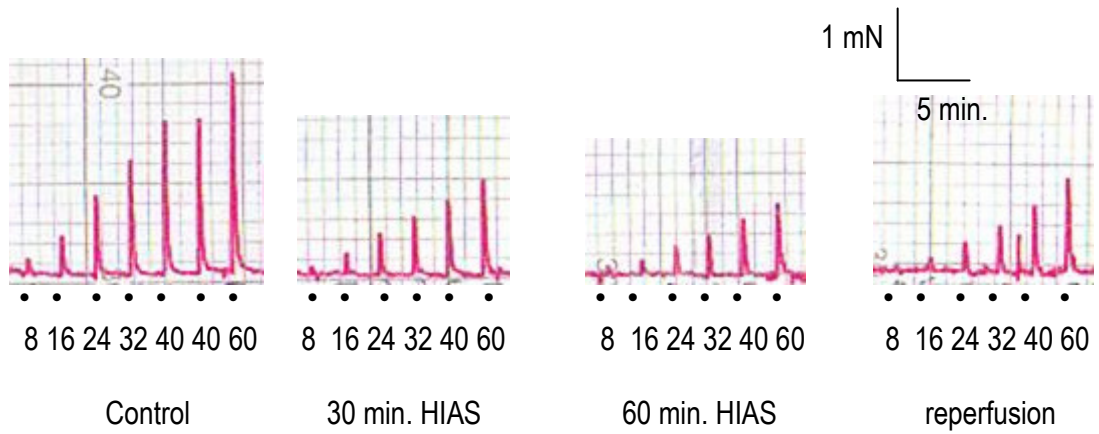
Figure 3.14 – Typical experimental tracing showing effect of 60 min. simulated ischaemia

followed by re-superfusion with normal Tyrode's solution for 60 min. on nerve-mediated

contraction
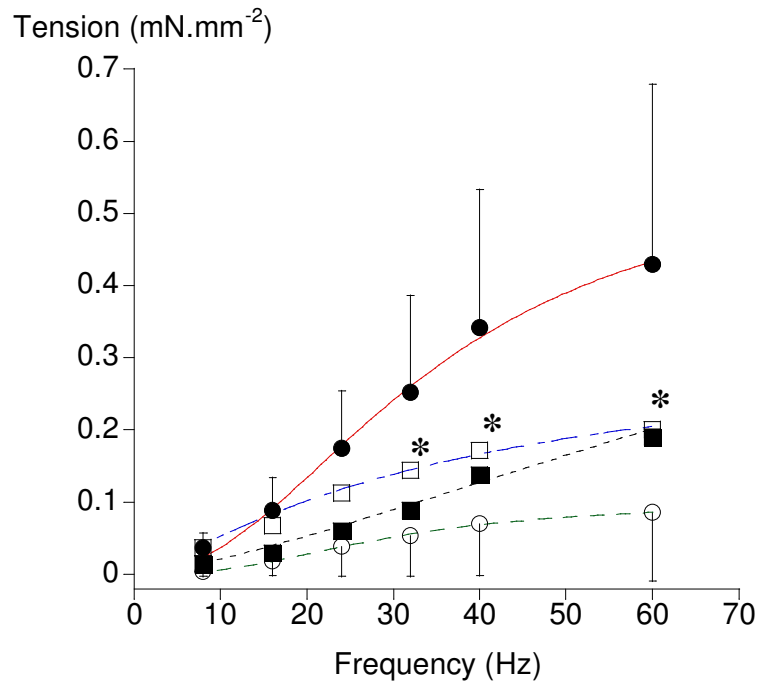


Figure 3.15 - Effect of 60 min. simulated ischaemia (HIAS) and reperfusion with normal Tyrode's

solution on nerve-mediated force-frequency response.

● – control, □ - 30 min HIAS, ○ – 60 min HIAS, ■ – reperfusion

*significant reduction 30 min. HIAS compared to control (p<0.05), error bars omitted for clarity

Tension was significantly and irreversibly ameliorated by simulated ischaemia.

*Table 3.8 - Effect of simulated ischaemia (HIAS) on nerve-mediated contraction*

* $p < 0.05$ compared to control

| N=5, n=6 | control | 30 min HIAS | 60 min HIAS | re-superfusion |
|---|---|---|---|---|
| extracellular pH | 7.43±0.03 | 6.98±0.02 | | 7.43±0.03 |
| $EFS_{32Hz}$ (mN.mm$^{-2}$) | 0.25±0.13 | 0.14±0.15* | 0.05±0.06* | 0.09±0.09* |
| $EFS_{32Hz}$ as % control | - | 53±30 * | 20±14 * | 30±24 * |
| $T_{max}$ (mN.mm$^{-2}$) | 0.56±0.29 | 0.28±0.28* | 0.13±0.13* | 0.49±0.29 |
| $f_{1/2}$ (Hz) | 34.6±1.5 | 46.3±44.5 | 31.0±6.07 | 65.6±48.0 |

Simulated ischaemia (HIAS) had a marked effect on nerve-mediated contraction. The individual effects of each component of simulated ischaemia were examined to try to elicit the most important factors in mediating this loss of contractile function.

3.2.2    Effect of isolated components of ischaemia on nerve-mediated contraction

3.2.2.1  Effect of substrate depletion (S) on nerve-mediated contraction

The effect of omission of glucose and Na pyruvate (S) from the superfusate on nerve-mediated contraction was examined. In the first set of experiments, the effect of 60 min. substrate depletion was recorded. At the end of the equilibration period, the mean $EFS_{32Hz}$ was $0.28\pm0.25$ mN.mm$^{-2}$ (N=4, n=5) and was $38\pm15\%$ of the $T_{max}$. The mean $f_{1/2}$ under these control conditions was $47.0\pm16.9$ Hz (table 3.9).

*Table 3.9 - Effect of 60 min. substrate depletion (S) on nerve-mediated contraction*

*60 min. of substrate depletion had no effect on nerve-mediated contraction. In addition, parameters after 60 min. of re-superfusion with normal Tyrode's were not significantly different from control.*

| N=4, n=5 | Control | 60 min S | 15 min reperfusion | 60 min reperfusion |
|---|---|---|---|---|
| $EFS_{32Hz}$ (mN.mm$^{-2}$) | $0.28\pm0.25$ | $0.32\pm0.25$ | $0.34\pm0.27$ | $0.27\pm0.22$ |
| $EFS_{32Hz}$ as % control | - | $127\pm17$ | $111\pm22$ | $106\pm18$ |
| $f_{1/2}$ (Hz) | $47.0\pm16.9$ | $31.8\pm13.7$ | $33.4\pm7.6$ | $40.6\pm13.5$ |

The next set of experiments examined the effect of 120 min. of substrate depletion (S). The mean $EFS_{32Hz}$ at the end of the equilibration period was $0.53\pm0.16$ mN.mm$^{-2}$ (N=4, n=6) and was $53\pm15\%$ of the estimated $T_{max}$ from the force-frequency curves. The mean $f_{1/2}$ under these control conditions was $33.3\pm19.4$ Hz (figure 3.16).

120 min. of substrate depletion also had no effect on the mean $EFS_{32Hz}$. However there was significant depression of tension generated in response to EFS at frequencies higher than this ($EFS_{40Hz}$, $EFS_{60Hz}$ and $EFS_{80Hz}$). This was reflected in a significant reduction in the $T_{max}$ after 120 min of substrate depletion (control $T_{max}$, $1.05\pm0.33$ mN.mm$^{-2}$ to 120 min. S $T_{max}$, $0.51\pm0.26$ mN.mm$^{-2}$) In addition, $f_{1/2}$ was also significantly reduced during this period (table 3.10, figure 3.16).

Upon re-superfusion with normal Tyrode's for 60 min., $f_{1/2}$ returned to control values (table 3.10). However, tension generated upon EFS did not recover. In fact nerve-mediated contractile responses were reduced further throughout the frequency range upon re-superfusion when compared to control contractions.

*Table 3.10 - Effect of 120 min. substrate depletion (S) on nerve-mediated contraction*

*\* p<0.05 compared to control*

| N=4, n=6 | Control | 60 min S | 120 min S | 15 min reperfusion | 60 min reperfusion |
|---|---|---|---|---|---|
| $EFS_{40Hz}$ (mN.mm$^{-2}$) | $0.65\pm0.20$ | $0.59\pm0.17$* | $0.44\pm0.22$* | $0.36\pm0.25$* | $0.30\pm0.22$* |
| $EFS_{40Hz}$ % of control | - | $90\pm6$ | $66\pm18$* | $42\pm31$* | $43\pm25$* |
| $EFS_{32Hz}$ (mN.mm$^{-2}$) | $0.53\pm0.16$ | $0.49\pm0.14$ | $0.40\pm0.19$ | $0.29\pm0.20$* | $0.25\pm0.19$* |
| $EFS_{32Hz}$ % of control | - | $93\pm7$ | $73\pm24$ | $50\pm25$* | $44\pm25$* |
| $T_{max}$ (mN.mm$^{-2}$) | $1.05\pm0.33$ | $0.89\pm0.26$* | $0.51\pm0.26$* | $0.67\pm0.38$ | $0.45\pm0.26$* |
| $f_{1/2}$ (Hz) | $33.3\pm19.4$ | $30.5\pm18.6$ | $15.6\pm7.5$* | $44.4\pm20.4$ | $31.9\pm9.8$ |
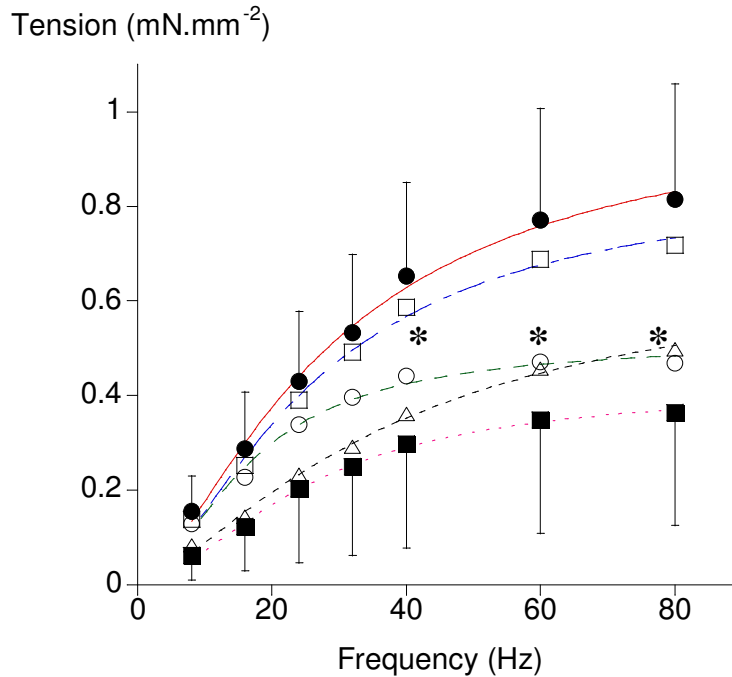
*Figure 3.16 - Effect of 120 min. substrate depletion (S) on nerve-mediated contraction*

*● – control, ▢ - 60 min S, ○ – 120 min S, Δ – 15 min reperfusion, ■ – 60 min reperfusion*

*significant reduction of 120 min. S compared to control (p<0.05), error bars omitted for clarity*

*Nerve-mediated contraction during substrate depletion (omission of glucose and Na pyruvate from supefusate) exhibited an initial resistance (for up to 60 min) to any detrimental effects. However, with increasing periods of substrate depletion (120 min.), it was not possible to maintain the magnitude of higher frequency nerve-mediated contractions. In addition, when this reduction of force occurred, reperfusion with normal Tyrode's caused a further reduction of contractile function throughout the frequency range.*

The time course of tension reduction during simulated ischaemia (HIAS) was shorter, and the magnitude of tension reduction greater, when compared to substrate depletion alone. This implies that substrate depletion alone was not the sole factor mediating reduction of nerve-mediated contractions during simulated ischaemia. The effects of the other components of simulated ischaemia were therefore examined followed by combinations of interventions.

3.2.2.2  Effect of hypoxia (H) on nerve-mediated contraction

The effect of using 95% nitrogen rather than 95% oxygen in the superfusate gas mixture on nerve-mediated contraction was examined. This resulted in a drop on $PO_2$ measured at the superfusion bath from 10±0.5 kPa to 4±0.3 kPa. The mean $EFS_{32Hz}$ at the end of the equilibration period was 0.47±0.21 mN.mm$^{-2}$ (N=5, n=6) and was 62±7% of the estimated $T_{max}$. The mean $f_{\frac{1}{2}}$ under these control conditions was 24.4±4.3 Hz (table 3.11).

*Table 3.11 - Effect of 120 min. hypoxia (H) on nerve-mediated contraction*

*60 and 120 min. of hypoxia had no effect on nerve-mediated contractions. After 60 min. of reperfusion, variables and parameters also remained at control values.*

| N=4, n=6 | Control | 60 min H | 120 min H | reperfusion |
|---|---|---|---|---|
| $EFS_{32Hz}$ (mN.mm$^{-2}$) | 0.47±0.21 | 0.42±0.21 | 0.40±0.23 | 0.41±0.22 |
| $EFS_{32Hz}$ as % control | - | 93±20 | 86±21 | 85±13 |
| $T_{max}$ (mN.mm$^{-2}$) | 0.66±0.33 | 0.64±0.30 | 0.63±0.29 | 0.70±0.36 |
| $f_{\frac{1}{2}}$ (Hz) | 24.4±4.3 | 28.6±10.1 | 30.3±10.1 | 33.2±7.5 |

3.2.2.3  Effect of intra- and extracellular acidosis (IA) on nerve-mediated contraction

Using 10% $CO_2$ rather than 5% $CO_2$ in the superfusate gas mixture generated an acidotic Tyrode's solution (pH 7.45±0.00 to pH 6.96±0.03). The effect of up to 120 min. acidosis (IA) on nerve-contraction in CSM was examined with data collected at 30, 60 and 120 min. The mean $EFS_{32Hz}$ at the end of the equilibration period was 0.49±0.48 mN.mm$^{-2}$ (N=5, n=6) and was 41±12% of the estimated $T_{max}$ from the force-frequency curves. The mean $f_{\frac{1}{2}}$ under these control conditions was 46.0±15.7 (figure 3.17a and table 3.12).

*Table 3.12 - Effect of 120 min. IA on nerve-mediated contraction*

*120 min. of simultaneous intra- and extra-cellular acidosis had no effect on nerve-mediated contraction. After 60 min. of reperfusion, parameters also remained at control values.*

| N=5, n=6 | Control | 30 min IA | 60 min IA | 120 min IA | reperfusion |
|---|---|---|---|---|---|
| pH | 7.45±0.00 | | 6.96±0.03 | | 7.45±0.00 |
| $EFS_{32Hz}$ (mN.mm$^{-2}$) | 0.49±0.48 | 0.48±0.50 | 0.48±0.52 | 0.48±0.53 | 0.51±0.58 |
| $EFS_{32Hz}$ as % control | - | 96±12 | 97±15 | 93±16 | 98±16 |
| $T_{max}$ (mN.mm$^{-2}$) | 1.04±0.66 | 1.23±1.08 | 1.11±1.10 | 0.91±0.68 | 1.01±0.72 |
| $f_{1/2}$ (Hz) | 46.0±15.7 | 46.4±10.4 | 38.6±5.7 | 38.5±12.0 | 41.8±13.4 |

3.2.2.4  Effect of intracellular acidification (I) on nerve-mediated contraction

As previously described, using 10% $CO_2$ rather than 5% $CO_2$ in the superfusate gas mixture generated an acidotic Tyrode's solution. By simultaneously increasing the amount of extracellular buffer ($HCO_3^-$) it was possible to create an intracellular acidification at normal extracellular pH (section 2.1.3). The effect of 120 min. intracellular acidification (I) on nerve-mediated contraction was examined.

The mean $EFS_{32Hz}$ at the end of the equilibration period was 0.59±0.60 mN.mm$^{-2}$ (N=5, n=6) and was 54±12% of the estimated $T_{max}$ from the force-frequency curves. The mean $f_{1/2}$ under these control conditions was 30.3±7.2 (figure 3.17b and table 3.13).

*Table 3.13 - Effect of 120 min. intracellular acidification (I) on nerve-mediated contraction*

*\* p<0.05 compared to control*

*30 min. of intracellular acidification significantly augmented nerve-mediated contraction in CSM and this effect was maintained at 60 and 120 min. intracellular acidification. $T_{max}$ and $f_{1/2}$ were unaltered during the intervention. Parameters returned to control values after 60 min. reperfusion in Tyrode's solution.*

| N=5, n=6 | Control | 30 min I | 60 min I | 120 min I | reperfusion |
|---|---|---|---|---|---|
| pH | 7.43±0.02 | | 7.45±0.01 | | 7.43±0.02 |
| $EFS_{32Hz}$ (mN.mm$^{-2}$) | 0.59±0.60 | 0.67±0.64* | 0.66±0.62* | 0.62±0.61* | 0.53±0.56 |
| $EFS_{32Hz\ a}$s % control | - | 116±5* | 115±6* | 107±7* | 89±9 |
| $T_{max}$ (mN.mm$^{-2}$) | 1.00±0.75 | 1.14±0.76 | 1.06±0.74 | 1.01±0.69 | 0.89±0.67 |
| $f_{1/2}$ (Hz) | 30.3±7.2 | 31.5±12.1 | 28.9±9.8 | 30.4±10.3 | 28.5±8.3 |

3.2.2.5  Effect of extracellular acidosis (A) on nerve-mediated contraction

By reducing the [$HCO_3^-$] in Tyrode's solution, it was possible to reduce the pH of the extracellular environment without a concomitant reduction in intracellular pH ($pH_e$ 7.39±0.03 to $pH_e$ 6.96±0.03)(186). The effect of up to 120 min. extracellular acidosis (A) on nerve-contraction in CSM was examined.

The mean $EFS_{32Hz}$ at the end of the equilibration period was 1.09±1.00 mN.mm$^{-2}$ (N=5, n=6) and was 49±18% of the estimated $T_{max}$. The mean $f_{1/2}$ under these control conditions was 39.0±21.2 Hz (figure 3.17c and table 3.14).

*Table 3.14 - Effect of 120 min. extracellular acidosis (A) on nerve-mediated contraction*

*\* p<0.05 compared to control*

*30 min. of extracellular acidosis significantly depressed nerve-mediated contractions and this effect was maintained at 120 min. extracellular acidosis. Parameters remained significantly depressed after 60 min. re-superfusion in Tyrode's solution.*

| N=5, n=6 | Control | 30 min A | 60 min A | 120 min A | reperfusion |
|---|---|---|---|---|---|
| pH | 7.39±0.03 | | 6.96±0.03 | | 7.39±0.03 |
| $EFS_{32Hz}$ (mN.mm$^{-2}$) | 1.09±1.00 | 0.76±0.85* | 0.75±0.86* | 0.72±0.88* | 0.94±1.04* |
| $EFS_{32Hz\,a}$s % control | - | 62±19* | 58±18* | 52±23* | 76±18* |
| $T_{max}$ (mN.mm$^{-2}$) | 2.29±1.59 | 1.64±1.41 | 1.55±1.33* | 1.49±1.33* | 1.58±1.43 |
| $f_{½}$ (Hz) | 39.0±21.2 | 39.2±12.6 | 35.2±8.1 | 36.7±6.4 | 29.2±6.5 |

Simultaneous intra- and extracellular acidosis had no effect on nerve-mediated contraction of CSM. However acidosis in the individual compartments had opposite actions; intracellular acidification augmented function whilst extracellular depressed it (figures 3.17a-c).

No single component in isolation mimicked the effect of simulated ischaemia (HIAS) on nerve-mediated contraction (60 min. HIAS reduced $EFS_{32Hz}$ to 20±14% of control with no significant recovery after 60 min. re-superfusion in normal Tyrode's). The effects of various factors in combination were therefore examined. Glucose and Na pyruvate omission from the superfusate (S) had the most marked effect, and therefore the combination of this with hypoxia (H) was recorded.

Fig. 3.17 – Acidosis on nerve contraction

### 3.2.3 Effect of combinations of components of simulated ischaemia on nerve-mediated contraction

#### 3.2.3.1 Effect of hypoxia and substrate depletion (HS)

At the end of the equilibration period, the mean $EFS_{32Hz}$ was $0.71 \pm 0.60$ mN.mm$^{-2}$ (N=7, n=7) and was $54 \pm 13\%$ of the estimated $T_{max}$ from the force-frequency curves. The mean $f_{1/2}$ under these control conditions was $30.9 \pm 9.2$ Hz.

Hypoxia and substrate depletion (HS) for 60 min. significantly reduced the mean $EFS_{32Hz}$ to $0.06 \pm 0.05$ mN.mm$^{-2}$ ($13 \pm 10\%$ of control). The $f_{1/2}$ was unchanged after 60 min. of HS depletion. Nerve-mediated contractile responses did not recover upon re-superfusion; after 60 min. of normal Tyrode's solution, $EFS_{32Hz}$ remained at $0.09 \pm 0.07$ mN.mm$^{-2}$ ($17 \pm 10\%$ of control, table 3.15 and figure 3.18). There was no significant difference between the effect of HIAS compared to simultaneous hypoxia and substrate depletion (HS) alone (table 3.16).

*Table 3.15 - Effect of hypoxia and substrate depletion (HS) on nerve-mediated contraction*
*\* p<0.05 compared to control*
*HS depletion significantly and irreversibly ameliorared nerve-mediated contraction.*

| N=7, n=9 | Control | 60 min HS | 15 min reperfusion | 60 min reperfusion |
|---|---|---|---|---|
| $EFS_{32Hz}$ (mN.mm$^{-2}$) | $0.71 \pm 0.60$ | $0.06 \pm 0.05^*$ | $0.09 \pm 0.07^*$ | $0.09 \pm 0.07^*$ |
| $EFS_{32Hz}$ as % control | - | $14 \pm 11^*$ | $18 \pm 12^*$ | $17 \pm 10^*$ |
| $T_{max}$ (mN.mm$^{-2}$) | $1.20 \pm 0.77$ | $0.12 \pm 0.11^*$ | $0.23 \pm 0.16^*$ | $0.21 \pm 0.13^*$ |
| $f_{1/2}$ (Hz) | $30.9 \pm 9.2$ | $31.8 \pm 8.8$ | $35.7 \pm 8.0$ | $32.4 \pm 8.8$ |
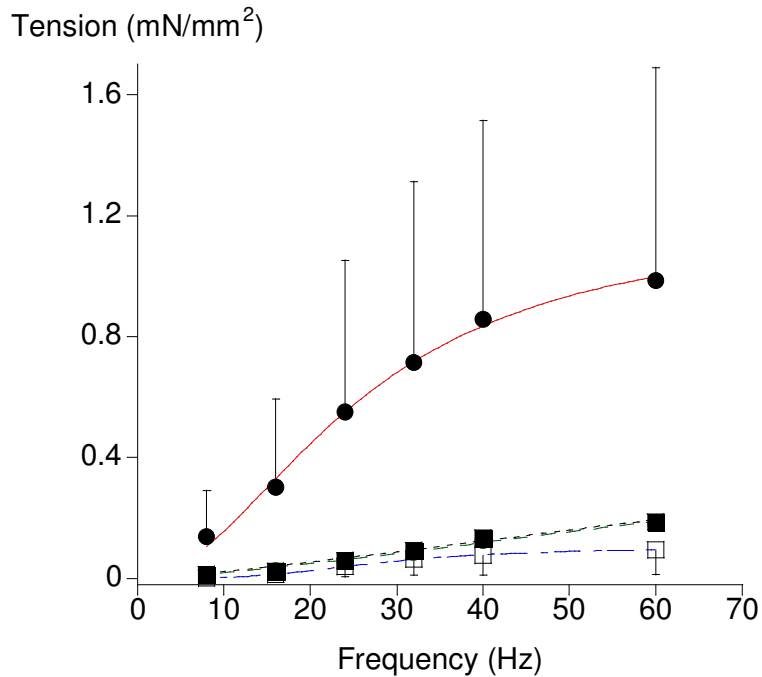
*Figure 3.18 - Effect of simultaneous hypoxia and substrate depletion (HS) on nerve contraction*

● *– control,* □ *- 60 min HS,* ○ *– 15 min reperfusion,* ■ *– 60 min reperfusion*

The depression of tension generated was present throughout the range of EFS.

*Table 3.16 - Effect of simulated ischaemia (HIAS) compared to simultaneous hypoxia & substrate depletion (HS) on nerve-mediated contraction* * $p < 0.05$ *compared to control*

These results showed that the combination of hypoxia and substrate depletion (HS) could be responsible for the depression of nerve-mediated contractile function seen during simulated ischaemia (HIAS).

| Intervention | | HIAS N=5, n=6 | HS N=7, n=7 |
|---|---|---|---|
| As % of control (%) | 30 min intervention | 53±30* | - |
| | 60 min intervention | 20±14* | 14±11* |
| | 60 min reperfusion | 30±24* | 17±10* |

In order to examine further the effect of intracellular acidification on nerve contraction, the effect of intra- or extracellular acidosis in the presence of hypoxia and substrate depletion was examined.

## 3.2.3.2 Effect of hypoxia, extracellular acidosis and substrate depletion (HAS)

At the end of the equilibration period, the mean $EFS_{32Hz}$ was $0.60\pm0.40$ mN.mm$^{-2}$ (N=5, n=6) and was $51\pm8\%$ of the estimated $T_{max}$ from the force-frequency curves. The mean $f_{1/2}$ under these control conditions was $31.9\pm4.9$ Hz (table 3.17 and fig 3.19c).

*Table 3.17 - Hypoxia, extracellular acidosis and substrate depletion (HAS) on nerve-contraction*
*Hypoxia, extracellular acidosis and substrate depletion (HAS) for 30 min. significantly reduced the mean $EFS_{32Hz}$ to $29\pm16\%$ of control. The reduction in tension generated persisted at 60 min. $f_{1/2}$ was unchanged during the intervention. The EFS response recovered partially upon reperfusion; after 60 min., $EFS_{32Hz}$ increased to $50\pm19\%$ of control. However, tension generated remained significantly less than control values.*

| N=5, n=6<br>* p<0.05 compared to control | Control | 30 min HAS | 60 min HAS | 60 min reperfusion |
|---|---|---|---|---|
| pH | 7.40±0.02 | 7.00±0.04 | | 7.40±0.02 |
| $EFS_{32Hz}$ (mN.mm$^{-2}$) | 0.60±0.40 | 0.13±0.05* | 0.10±0.03* | 0.27±0.13* |
| $EFS_{32Hz}$ as % control | - | 28.6±15.7* | 23.6±14.4* | 49.7±19.0* |
| $T_{max}$ (mN.mm$^{-2}$) | 1.14±0.66 | 0.30±0.13* | 0.24±0.08* | 0.61±0.09* |
| $f_{1/2}$ (Hz) | 31.9±4.9 | 28.1±8.5 | 38.9±11.1 | 27.8±2.2 |

3.2.3.3 Effect of hypoxia, intracellular acidification and substrate depletion (HIS)

At the end of the equilibration period, the mean $EFS_{32Hz}$ was 0.57±0.40 mN.mm$^{-2}$ (N=6, n=6) and was 49±8 % of the estimated $T_{max}$. The mean half-maximal frequency ($f_{1/2}$) under these control conditions was 33.7±5.4 Hz (table 3.18, fig. 3.19b).

*Table 3.18 - Hypoxia, intracellular acidification and substrate depletion (HIS) on nerve-contraction*
*\* p<0.05 compared to control. Hypoxia, intracellular acidification and substrate depletion (HIS) for*
*30 min. significantly reduced the mean $EFS_{32Hz}$ to 23±29% of control. $f_{1/2}$ was unchanged after 60*
*min. of HIS depletion. The EFS response did not recover upon reperfusion; after 60 min. of*
*normal Tyrode's, $EFS_{32Hz}$ remained at 26±23% of control.*

| N=6, n=6 | Control | 30 min HIS | 60 min HIS | reperfusion |
|---|---|---|---|---|
| pH | 7.45±0.01 | 7.50±0.01 | | |
| $EFS_{32Hz}$ (mN.mm$^{-2}$) | 0.57±0.40 | 0.08±0.07* | 0.04±0.05* | 0.11±0.08* |
| $EFS_{32Hz}$ as % control | - | 22.5±28.6 | 11.5±19.6 | 25.6±22.9 |
| $T_{max}$ (mN.mm$^{-2}$) | 1.11±0.65 | 0.19±0.22* | 0.09±0.12* | 0.27±0.23* |
| $f_{1/2}$ (Hz) | 33.7±5.4 | 25.9±30.7 | 21.2±17.7 | 37.3±13.6 |

In summary, the detrimental effect of hypoxia and substrate depletion (HS) on nerve-mediated contraction was similar to the effect of simulated ischaemia. Intra- or extracellular acidosis did not limit the reduction in tension although simultaneous extracellular acidosis did significantly increase tension upon reperfusion albeit not to control values (figures 3.19a-c). This may be due to inactivation of the mechanisms by which intracellular acidification augments nerve-mediated contractile function (section 3.2.2.4) by either hypoxia or substrate depletion. The effect of acidosis in combination with either hypoxia or substrate depletion was therefore examined.

Fig 3.19 Hypoxia, acidosis and substrate depletion on nerve-contraction

3.2.4 **Effect of combinations of intracellular and extracellular acidosis and substrate depletion on nerve-mediated contraction in CSM**

3.2.4.1 Effect of acidosis and substrate depletion (IAS)

At the end of the equilibration period, the mean $EFS_{32Hz}$ was $0.32\pm0.20$ mN.mm$^{-2}$ (N=6, n=6) and was $43\pm12$ % of the estimated $T_{max}$. The mean half-maximal frequency ($f_{1/2}$) under these control conditions was $38.8\pm14.7$ Hz (figure 3.20a and table 3.19).

*Table 3.19 - Effect of intracellular and extracellular acidosis and substrate depletion (IAS) on nerve-mediated contraction * p<0.05 compared to control*

*30 min acidosis and substrate depletion (IAS) significantly reduced the mean $EFS_{32Hz}$ to $73\pm16$ % of control. However, the estimated $T_{max}$ during the intervention was unchanged when compared to control values. This is in contrast to the lack of effect recorded with 60 min. substrate depletion (S) alone. At 60 min. of IAS depletion, $EFS_{32Hz}$ had returned to control values.*

| N=6, n=6 | Control | 30 min IAS | 60 min IAS | Reperfusion |
|---|---|---|---|---|
| pH | 7.43±0.02 | 6.98±0.01 | | 7.43±0.02 |
| $EFS_{32Hz}$ (mN.mm$^{-2}$) | 0.32±0.20 | 0.22±0.15* | 0.24±0.14 | 0.32±0.22 |
| $EFS_{32Hz}$ as % control | - | 72.7±15.5 | 81.1±19.2 | 100.1±12.4 |
| $T_{max}$ (mN.mm$^{-2}$) | 0.77±0.45 | 0.64±0.44 | 0.55±0.28 | 0.70±0.28 |
| $f_{1/2}$ (Hz) | 38.8±14.7 | 38.3±5.6 | 33.8±3.8 | 37.3±9.2 |

3.2.4.2  Effect of extracellular acidosis and substrate depletion (AS)

At the end of the equilibration period, the mean $EFS_{32Hz}$ was $0.63\pm0.41$ mN.mm$^{-2}$ (N=6, n=6) and was $51\pm9$ % of the estimated $T_{max}$. The mean half-maximal frequency ($f_{\frac{1}{2}}$) under these control conditions was $31.8\pm6.7$ Hz (figure 3.20b and table 3.20).

*Table 3.20 - Effect of extracellular acidosis and substrate depletion (AS) on nerve contraction*

*\* = p<0.05 compared to control*

*Extracellular acidosis and substrate depletion (AS) for 30 min. significantly reduced the mean $EFS_{32Hz}$ to $67\pm19$ % of control. This depression of nerve-mediated function was maintained at 60 min. AS depletion. Again this is in contrast to the lack of effect seen with 60 min. substrate depletion (S) in isolation. Parameters returned to control values upon reperfusion.*

| N=6, n=6 | Control | 30 min AS | 60 min AS | Reperfusion |
|---|---|---|---|---|
| pH | 7.40±0.02 | 6.94±0.02 | | 7.40±0.02 |
| $EFS_{32Hz}$ (mN.mm$^{-2}$) | 0.63±0.41 | 0.43±0.31* | 0.46±0.32* | 0.59±0.34 |
| $EFS_{32Hz}$ as % control | - | 67.4±19.1 | 71.3±20.6 | 96.5±10.4 |
| $T_{max}$ (mN.mm$^{-2}$) | 1.28±0.85 | 0.93±0.58 | 0.91±0.56* | 1.19±0.75 |
| $f_{\frac{1}{2}}$ (Hz) | 31.8±6.7 | 33.9±5.5 | 31.4±4.5 | 31.4±4.8 |

3.2.4.3  Effect of intracellular acidification and substrate depletion (IS)

At the end of the equilibration period, the mean $EFS_{32Hz}$ was $0.55\pm0.34$ mN.mm$^{-2}$ (N=5, n=6) and was $55\pm8$ % of the estimated $T_{max}$. The mean $f_{\frac{1}{2}}$ under these control conditions was $38.6\pm4.7$ Hz (figure 3.20c and table 3.21).

*Table 3.21 - Effect of intracellular acidification and substrate depletion (IS) on nerve-contraction*

*\* = p<0.05 compared to control*

*30 min. intracellular acidification and substrate depletion (IS) significantly increased the mean EFS$_{32Hz}$ to 112±7 % of control. This increase of nerve-mediated function was maintained at 60 min. Substrate depletion alone had no effect over a similar time course. Parameters returned to control values upon reperfusion.*

| N=6, n=6 | Control | 30 min IS | 60 min IS | Reperfusion |
|---|---|---|---|---|
| pH | 7.44±0.01 | 7.50±0.01 | | 7.44±0.01 |
| EFS$_{32Hz}$ (mN.mm$^{-2}$) | 0.55±0.34 | 0.61±0.37* | 0.63±0.37* | 0.60±0.37 |
| EFS$_{32Hz}$ as % control | - | 111.8±6.7 | 118.5±11.5 | 110.1±7.8 |
| T$_{max}$ (mN.mm$^{-2}$) | 0.96±0.55 | 0.99±0.52 | 1.01±0.54 | 1.04±0.53 |
| f$_{½}$ (Hz) | 28.6±4.7 | 28.2±10.2 | 26.7±8.6 | 31.0±10.1 |

These experiments show that substrate depletion does not affect the mechanism by which intracellular acidification augments and extracellular acidosis depresses nerve-mediated contraction in CSM. In addition, when both intra- and extracellular acidosis was combined with substrate depletion, an initial reduction in force of contraction at 30 min. followed by return to control values at 60 min. was recorded during the intervention. The mechanism(s) by which intracellular acidification maintains contractile function in the presence extracellular acidosis are therefore time-dependent. The effect of the combination of hypoxia and acidosis was examined next.

Fig 3.20 Acidosis and substrate depletion on nerve contraction

### 3.2.5 Combinations of hypoxia and acidosis on nerve-mediated contraction in CSM

### 3.2.5.1 Effect of hypoxia and intracellular and extracellular acidosis (HIA)

At the end of the equilibration period, the mean $EFS_{32Hz}$ was $0.31\pm0.08$ $mN.mm^{-2}$ (N=4, n=6) and was $56\pm9$ % of the estimated $T_{max}$. The mean $f_{1/2}$ under these control conditions was $29.5\pm6.3$ Hz. (figure 3.21a and table 3.22).

*Table 3.22 - Effect of hypoxia and acidosis (HIA) on nerve-mediated contraction*

*\* p<0.05 compared to control*

*30 min. hypoxia, intracellular and extracellular acidosis (HIA) significantly decreased the mean*

*$EFS_{32Hz}$ to $88\pm11$ % of control. This depression of nerve-mediated function was maintained at 60*

*min. HIA depletion. Parameters returned to control values upon reperfusion*

| N=4, n=6 | Control | 30 min HIA | 60 min HIA | Reperfusion |
|---|---|---|---|---|
| pH | $7.45\pm0.01$ | $7.42\pm0.02$ | | $7.45\pm0.01$ |
| $EFS_{32Hz}$ ($mN.mm^{-2}$) | $0.31\pm0.08$ | $0.28\pm0.09$* | $0.25\pm0.07$* | $0.31\pm0.10$ |
| $EFS_{32Hz}$ as % control | - | $88.0\pm11.3$ | $78.0\pm8.2$ | $98.7\pm9.5$ |
| $T_{max}$ ($mN.mm^{-2}$) | $0.57\pm0.14$ | $0.43\pm0.11$* | $0.40\pm0.10$* | $0.56\pm0.13$ |
| $f_{1/2}$ (Hz) | $29.5\pm6.3$ | $23.9\pm3.7$ | $25.5\pm2.8$ | $28.3\pm4.5$ |

3.2.5.2  Effect of hypoxia and extracellular acidosis (HA)

At the end of the equilibration period, the mean $EFS_{32Hz}$ was $0.36\pm0.38$ mN.mm$^{-2}$ (N=6, n=8) and was $53\pm8$ % of the estimated $T_{max}$. The mean $f_{1/2}$ under these control conditions was $29.3\pm4.4$ Hz (table 3.23 and figure 3.21c).

*Table 3.23 - Effect of hypoxia and extracellular acidosis (HA) on nerve-mediated contraction*

*\* p<0.05 compared to control*

*Hypoxia and extracellular acidosis (HA) for 60 min. had no significant effect on mean $EFS_{32Hz}$.*
*However the $T_{max}$ was significantly reduced during the ischaemic intervention with a reduction of*
*$f_{1/2}$ at 30 min. All variables returned to control values after 60 min. reperfusion.*

| N=6, n=8 | Control | 30 min HA | 60 min HA | Reperfusion |
|---|---|---|---|---|
| pH | 7.42±0.02 | 6.99±0.01 | | |
| $EFS_{32Hz}$ (mN.mm$^{-2}$) | 0.36±0.38 | 0.32±0.38 | 0.30±0.38 | 0.40±0.44 |
| $EFS_{32Hz}$ as % control | - | 87.6±20.2 | 79.2±21.6 | 115.5±19.7 |
| $T_{max}$ (mN.mm$^{-2}$) | 0.62±0.59 | 0.47±0.46* | 0.46±0.49* | 0.68±0.71 |
| $f_{1/2}$ (Hz) | 28.6±4.7 | 21.3±3.4* | 24.2±3.6 | 27.7±3.8 |

3.2.5.3 Effect of hypoxia and intracellular acidification (HI)

At the end of the equilibration period, the mean $EFS_{32Hz}$ was 0.34±0.43 mN.mm$^{-2}$ (N=5, n=6) and was 50±5 % of the estimated $T_{max}$. The mean half-maximal frequency ($f_{1/2}$) under these control conditions was 25.1±4.0 Hz (table 3.24 and figure 3.21b).

*Table 3.24 - Effect of hypoxia and intracellular acidification (HI) on nerve-mediated contraction*
*\* = significant reduction compared to control, # = significant increase compared to control, p<0.05*
*Hypoxia and intracellular acidification (HI) for 60 min. had no significant effect on mean $EFS_{32Hz}$.*
*However the $f_{1/2}$ was significantly reduced during the ischaemic intervention. All variables returned to control values after 60 min. reperfusion.*

| N=5, n=6 | Control | 30 min HI | 60 min HI | Reperfusion |
|---|---|---|---|---|
| pH | 7.40±0.00 | 7.48±0.02 | | |
| $EFS_{32Hz}$ (mN.mm$^{-2}$) | 0.34±0.43 | 0.35±0.38 | 0.34±0.36 | 0.33±0.40 |
| $EFS_{32Hz}$ as % control | - | 115.5±20.9 | 113.3±19.0 | 102.7±10.4 |
| $T_{max}$ (mN.mm$^{-2}$) | 0.56±0.68 | 0.50±0.50 | 0.47±0.47 | 0.59±0.62 |
| $f_{1/2}$ (Hz) | 25.1±4.0 | 20.6±3.7* | 19.8±3.8* | 29.3±3.9# |

During simultaneous intra and extracellular acidosis, it appears that intracellular acidification protects against reduction in tension seen with extracellular acidosis (section 3.2.2.3). The mechanism by which intracellular acidification augments nerve-mediated contractile function is sensitive to hypoxia. The above findings support this hypothesis. During simultaneous hypoxia and intracellular acidification, no augmentation of function was seen. Findings during simultaneous hypoxia, intra and extracellular acidosis (HIA) *vs.* hypoxia and extracellular acidosis were similar.

Fig 3.21 Hypoxia and acidosis on nerve contraction

### 3.2.6 Summary of results for nerve-mediated contraction in CSM

Simulated ischaemia (the combination of hypoxia, intra- and extracellular acidosis and substrate depletion) caused a significant, immediate and irreversible reduction in tension generated in response to EFS (HIAS - $EFS_{32Hz}$ 20±14% of control after 60 min. intervention). A similar response was seen in the presence of hypoxia and substrate depletion alone (HS - $EFS_{32Hz}$ 14±11% of control after 60 min. intervention). No further differences from HS values were seen when hypoxia and substrate depletion were combined with either intra- or extracellular acidosis (HAS - $EFS_{32Hz}$ 12±20% of control, HIS - $EFS_{32Hz}$ 13±11% of control after 60 min. intervention).

Looking at the individual elements of simulated ischaemia, 120 min. of hypoxia had no effect on nerve-mediated tension (H - $EFS_{32Hz}$ 93±20% of control). Simultaneous intra- and extracellular acidosis also had no effect (IA - $EFS_{32Hz}$ 97±15% of control after 120 min. intervention). However, intra- or extracellular acidosis in isolation had opposite effects. Intracellular acidification significantly and reversibly augmented nerve-mediated tension whereas extracellular acidosis significantly and irreversibly depressed it (I - $EFS_{32Hz}$ 115±6% of control, A - $EFS_{32Hz}$ 58±20% of control after 120 min. intervention).

Intracellular acidification was combined with other elements of simulated ischaemia to examine this increase in nerve-mediated tension. Augmentation of nerve-mediated tension was again seen when combining intracellular acidification with substrate depletion (IS - $EFS_{32Hz}$ 119±12% of control after 60 min. intervention). A similar period of substrate depletion alone had no effect on tension generated (although longer periods of substrate depletion significantly and irreversibly depressed nerve-mediated tension, $EFS_{32Hz}$ 74±24% of control after 120 min. S). In contrast to the inotropic effect of IS depletion, extracellular acidosis and substrate depletion depressed

tension generated (AS - $EFS_{32Hz}$ 71±21% of control after 60 min. intervention). Acidosis in both compartments in combination with substrate depletion initially depressed function followed by a return to control values at 60 min. of the intervention (IAS - $EFS_{32Hz}$ 73±16% and 81±19% of control after 30 min. and 60 min. of intervention respectively). This would suggest that the mechanism(s) by which intracellular acidification maintains contractile function in the presence extracellular acidosis are time-dependent.

Intracellular acidification was combined with hypoxia to further examine the augmentation seen with this component of ischaemia. No significant increase in tension was seen with this combination (HI - $EFS_{32Hz}$ 113±19% of control after 60 min. intervention). A reduction in tension to 79±22% of control was seen after 60 min. of both hypoxia and extracellular acidosis (HA). A similar reduction was seen with extracellular acidosis alone. Hypoxia and acidosis in both compartments resulted in a reduction in nerve-mediated tension (HIA - $EFS_{32Hz}$ 78±8% of control after 60 min. intervention). Again this was similar to the reduction in tension seen with extracellular acidosis alone, further evidence that hypoxia inactivates the mechanism by which intracellular acidification increases nerve-mediated tension. The effect of simulated ischaemia on nerve-mediated contraction in CSM is summarised in Table 3.25.

The next stage of investigation was to examine the effect of the various components of ischaemia on direct agonist-induced contraction of CSM. Subsequent experiments followed a similar format as that presented thus far on nerve-mediated contraction. The effect of simulated ischaemia on PE-induced contractures was recorded, followed by the individual components of ischaemia in turn; combinations of interventions were used to explore further the effects of simulated ischaemia. For presentation purposes data have been tabulated and presented in grapical form where appropriate.

*Table 3.25 - Effect of components of ischaemia applied in various combinations on nerve-mediated contraction in CSM*

* = significant reduction compared to control, # = significant increase compared to control, $p<0.05$

| Intervention | EFS$_{32Hz}$ after 60 min intervention (% control) | f$_{½}$ | Reperfusion |
|---|---|---|---|
| HIAS | 20±14* | no change | no recovery |
| HIAS had a rapid irreversible detrimental effect. | | | |
| HS | 14±11* | no change | no recovery |
| HAS | 13±11* | no change | no recovery |
| HIS | 12±20* | no change | no recovery |
| Detrimental effect of HIAS due to combined effect of hypoxia and substrate depletion (HS). | | | |
| H | 93±20 | shifted right after reperfusion | no change |
| IA | 97±15 | no change | no change |
| A | 58±20* | no change | some recovery |
| I | 115±6# | no change | back to control |
| Intracellular acidification rapidly augments contraction with no change in f$_{½}$. | | | |
| 60 min. S | 93±7* | no change | no change |
| 120 min. S | 74±24* | shifted left after 120 min | deterioration |
| T$_{max}$ suppressed during intervention. Reperfusion caused a further deterioration of function | | | |
| IAS | 81±19 | no change | no change |
| AS | 71±21* | no change | back to control |
| IS | 119±12# | no change | back to control |
| Intracellular acidification limited detrimental effect of extracellular acidosis with substrate depletion | | | |
| HIA | 78±8 | no change | back to control |
| HA | 79±22 | initially shifted to left | back to control |
| Tmax significantly suppressed during intervention, similar effect to extracellular acidosis | | | |
| HI | 113±19 | shifted to left | back to control |
| Augmentation of function by intracellular acidification is sensitive to hypoxia | | | |

## 3.3 Results III – The effect of ischaemia on agonist-induced contraction

### 3.3.1 Effect of simulated ischaemia (HIAS) on agonist-induced contraction in CSM

Isometric contractures in response to 15 µM phenylephrine (PE) were recorded as described in section 2.3.5. Preparations were equilibrated in Tyrode's solution for 60 min. at 37 °C. At the end of this period, PE was added to the superfusing solution and the resulting contracture recorded. The effect of 60 min. of simulated ischaemia was examined on both the peak and plateau PE contracture (Table 3.26).

*Table 3.26 - Effect of simulated ischaemia (HIAS) on PE contractures*

* $p < 0.05$ compared to control

| N=6, n=6 | Control | 30 min HIAS | 60 min HIAS | Reperfusion |
|---|---|---|---|---|
| Peak PE contracture (mN.mm$^{-2}$) | 0.74±0.53 | 0.55±0.42 | 0.21±0.11* | 0.70±0.48 |
| Peak PE contracture as % of control (%) | - | 83±31 | 35±19* | 99±23 |
| Plateau PE contracture (mN.mm$^{-2}$) | 0.70±0.53 | 0.18±0.17* | 0.16±0.08* | 0.60±0.43 |
| Plateau PE contracture as % of control (%) | - | 36±35* | 29±16* | 92±23 |

Simulated ischaemia (HIAS) caused a significant reduction in the size of the PE contracture which recovered completely upon reperfusion. This reduction was time-dependent - the peak contracture at 30 min. of simulated ischaemia was preserved whilst the steady state value was reduced to that remaining at 60 min, indicating some metabolic reserve prior to contractile failure (compare figs. 3.22 and 3.23). However, in contrast to the effect of HIAS on nerve-mediated contraction (section 3.2.1), PE contractures recovered completely upon reperfusion. The effect of HIAS on nerve-mediated contraction and PE contractures are summarised in fig. 3.24.
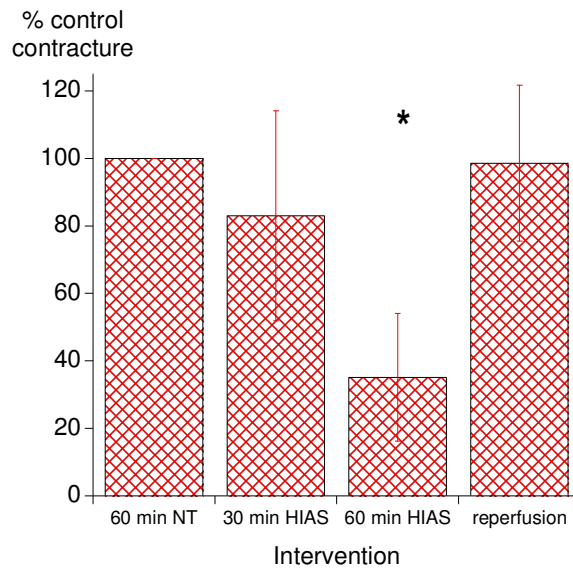
*Fig. 3.22 – The effect of simulated ischaemia (HIAS) on peak PE contractures*

*\* significant reduction compared to control (p<0.05)*

*The peak PE contracture was initially preserved.*
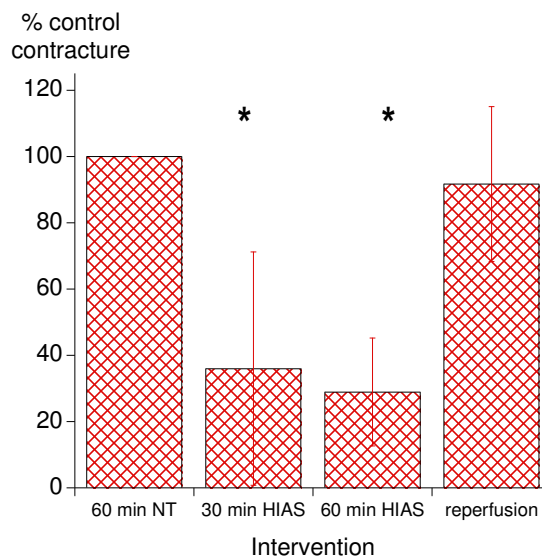


*Fig. 3.23 – The effect of simulated ischaemia (HIAS) on plateau PE contractures*

*\* significant reduction compared to control (p<0.05)*

*Plateau PE contracture was significantly ameliorated throughout the interververion.*
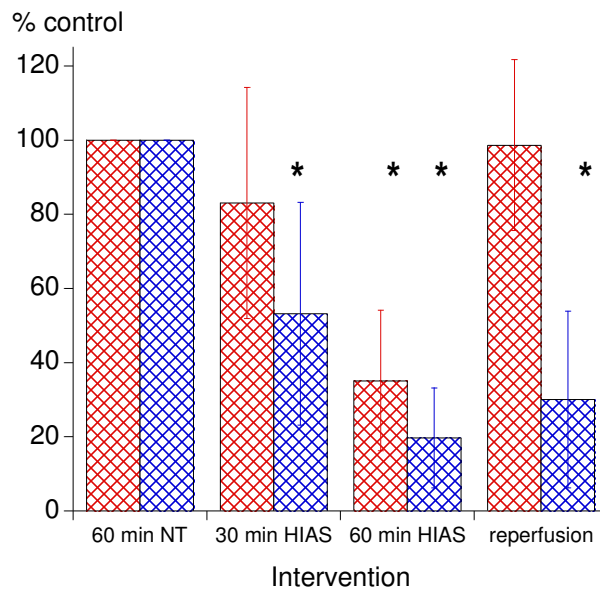
*Fig. 3.24 – The effect of simulated ischaemia (HIAS) on CSM contraction*

*red hatched bars peak PE contractures, blue hatched bars EFS$_{32Hz}$*

*\* significant reduction compared to control (p<0.05)*

*Agonist-induced contractures recovered completely upon reperfusion whereas nerve-mediated contractions did not.*

3.3.2    Effect of simulated ischaemia (HIAS) on agonist-induced contractures in the presence of nifedipine

Under control conditions, peak and plateau contractile responses to 15 µM phenylephrine were significantly reduced in the presence of 100 µM nifedipine to 79±7% and 77±7% of control respectively (section 3.1.2.2, page 98). Therefore around 20% of the agonist-induced contracture was dependent on $Ca^{2+}$ influx via the L-type $Ca^{2+}$ channel under control conditions. To further examine the effect of simulated ischaemia, PE-contractures in the presence of the L-type $Ca^{2+}$ channel blocker nifedipine were recorded (table 3.27 and fig. 3.25).

*Table 3.27 - Simulated ischaemia (HIAS) on PE contractures in presence of 100 µM nifedipine*

*\* p<0.05 compared to control*

| N=5, n=7 | control NT | 30 min HIAS | 60 min HIAS | Reperfusion |
|---|---|---|---|---|
| | in the presence of 100 µM nifedipine | | | |
| Peak PE contracture (mN.mm$^{-2}$) | 1.27±0.70 | 1.18±0.68 | 0.78±0.51 | 1.42±0.98 |
| Peak PE contracture as % of control (%) | - | 93±9 | 68±27 | 107±17 |
| Plateau PE contracture (mN.mm$^{-2}$) | 1.15±0.67 | 0.84±0.67 | 0.67±0.42* | 1.31±0.92 |
| Plateau PE contracture as % of control (%) | - | 77±21 | 66±31 | 110±21 |
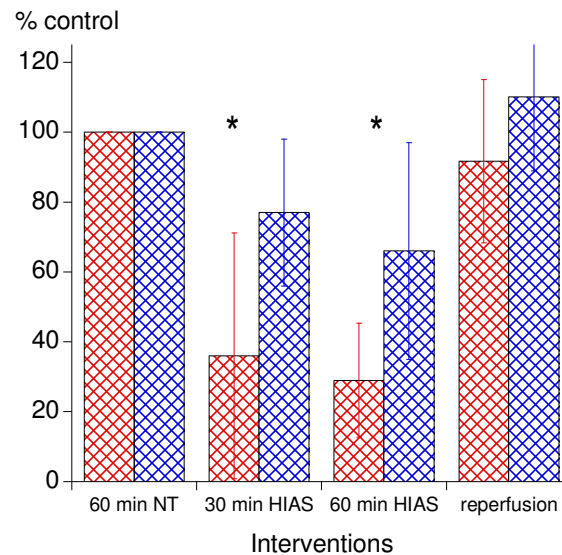


*Fig. 3.25 – Simulated ischaemia (HIAS) on agonist contractures in the presence of nifedipine*

*▨ plateau PE contractures ▨ plateau PE contractures in presence of 100 µM nifedipine*

*\*significant reduction compared to control (p<0.05)*

*The detrimental effect of simulated ischaemia was significantly ameliorated in the presence of*

*nifedipine. This suggests that the Ca$^{2+}$ channel is labile to the effects of ischaemia.*

### 3.3.3   Effect of simulated ischaemia (HIAS) on $Ca^{2+}$ transients in isolated CSM cells

Simulated ischaemia caused a significant reduction in PE induced contractures, an effect that appeared to be time dependent on agonist induced contractions. The L-type $Ca^{2+}$ channel is labile to the effects of simulated ischaemia with the detrimental effects of this intervention ameliorated by the presence of nifedipine. To examine the effect of ischaemia on $[Ca^{2+}]_i$ the following experiments were carried out.

CSM cell isolation was performed on fresh tissue as outlined in sections 2.6.2 and 2.6.3. Cells were equilibrated in Tyrode's solution for 10 min. at 37 °C and constantly perfused with fresh solution during the course of the interventions.

Background fluorescence was recorded at the start and end of the experimental protocol. The mean ratio signal was 0.18±0.02 at the start and 0.20±0.03 at the end of the experiment ($[Ca^{2+}]$ 97±37 nM and 127±45 nM respectively). The mean PMT voltage required was 817±46 V. At the end of this period, two responses with 3 µM PE were recorded, the second acting as the control calcium transient for comparison with simulated ischaemia exposures. 3 µM PE was determined experimentally as eliciting a maximal calcium transient. Unmodified Tyrode's solution at 37 °C was used to perfuse isolated cells for 10 min. between each intervention as a 'washout' period. The isolated cell was then subjected to 20 min. of simulated ischaemia (the combination of hypoxia, intra- and extracellular acidosis and substrate depletion). Two further PE responses were recorded during this intervention. 20 min. of intervention was used (in contrast to 30 min. and 60 min. responses in the muscle strip experiments) due to experimental limitations with cell stability over prolonged periods of experimentation. In addition the effect of interventions in the muscle strip experiments was apparent, in general, within 5-10 min. Unmodified Tyrode's solution

was then re-introduced for a period of 10 min. and a PE response recorded to examine the effect of reperfusion. A final response to 120 mM KCl was recorded at the end of the experiment (fig. 3.26, fig. 3.26a and table 3.28).
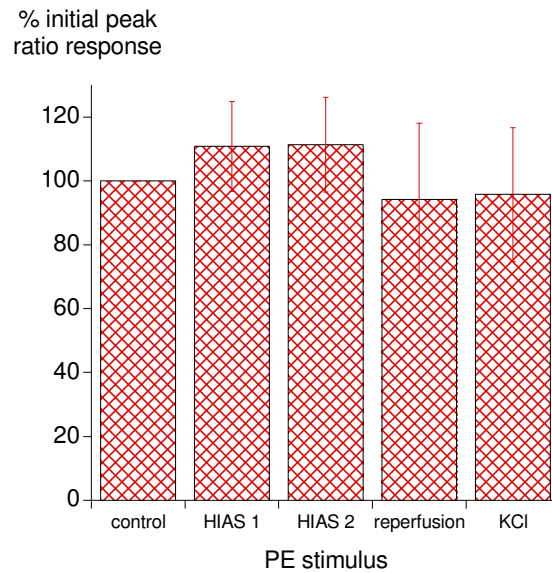


*Fig. 3.26 – Effect of simulated ischaemia (HIAS) on calcium transients in isolated CSM cells*

*PE responses were not significantly different from control values during the ischaemic intervention. These findings suggest that the decline in the PE contracture during simulated ischaemia is unrelated to changes in $[Ca^{2+}]_i$.*
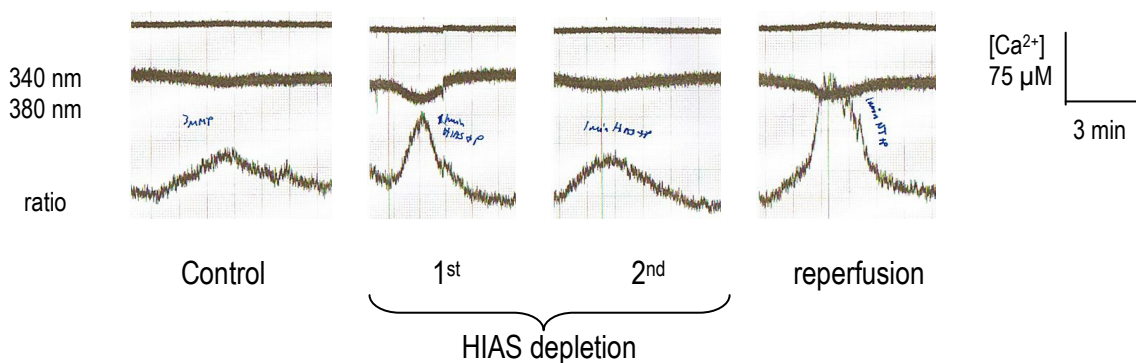


*Fig. 3.26a – Typical experimental tracing demonstrating the effect of HIAS on isolated CSM cells*

*Table 3.28 - Effect of simulated ischaemia on PE-induced Ca$^{2+}$ transients in isolated CSM cells*

| N=4, n=6 | Control | 1st HIAS response | 2nd HIAS Response | Reperfusion | 120 mM KCl |
|---|---|---|---|---|---|
| Peak ratio signal | 0.32±0.07 | 0.34±0.06 | 0.35±0.08 | 0.33±0.08 | 0.26±0.01 |
| Δ [Ca$^{2+}$] (nM) | 349±133 | 390±122 | 409±168 | 375±165 | 228±23 |

In a similar manner to preceding experiments, the effect of the separate components of

ischaemia on agonist-induced contractures was examined.

3.3.4     Effect of isolated components of ischaemia on agonist-induced contraction

3.3.4.1  Effect of substrate depletion (S) on agonist-induced contraction in CSM

The effect of 120 min. omission of Na pyruvate and glucose (S) from the superfusate was examined on both the peak and plateau PE contracture (figure 3.27 and table 3.32).
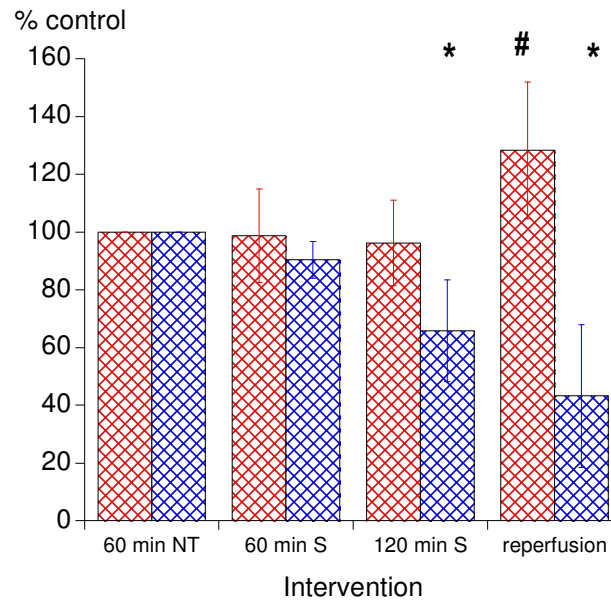


*Fig. 3.27 – The effect of substrate depletion (S) on CSM contraction*

*plateau PE contractures,      EFS$_{40Hz}$*

*\* significant reduction compared to control, # significant increase compared to control (p<0.05)*

*Substrate depletion had no effect on the magnitude of the PE response. On reperfusion for 60 min., both peak and plateau responses were greater than control. This is in contrast to the time-dependent detrimental effect of S on nerve-mediated contraction.*

3.3.4.2   Effect of substrate depletion (S) on isolated CSM cells


Background fluorescence was recorded at the start and end of the experimental protocol. The mean ratio signal was 0.17±0.01 at the start and 0.19±0.01 at the end of the experiment ([$Ca^{2+}$] 72±18 and 114±15 nM respectively). The mean PMT voltage required was 792±40 V. At the end of this period, two responses with 3 µM PE were recorded using the same protocol as in section 3.3.2. The isolated cell was then subjected to 20 min. of substrate depletion. Two further PE responses were recorded during this intervention. Unmodified Tyrode's solution was then re-introduced for a period of 10 min. and a PE response recorded to examine the effect of reperfusion. A final response to 120 mM KCl was recorded at the end of the experiment (fig. 3.28 and table 3.29). $Ca^{2+}$ transients were unaffected by substrate depletion. Due to time constraints, the number of experiments was small and conclusions cannot be drawn from these findings (N=2, n=3).
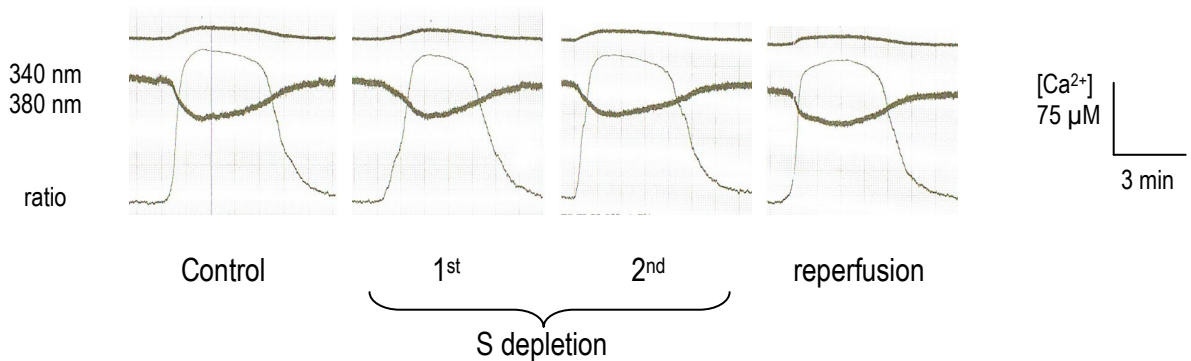


Fig. 3.28 – Typical experimental tracing demonstrating the effect of S on isolated CSM cells

$Ca^{2+}$ transients were not significantly different during the intervention.


Table 3.29 - Effect of substrate depletion on PE-induced transients in isolated CSM cells

| N=2, n=3 | Control | 1st S Response | 2nd S Response | Reperfusion | 120 mM KCl |
|---|---|---|---|---|---|
| Peak ratio signal | 0.44±0.09 | 0.40±0.07 | 0.39±0.06 | 0.42±0.07 | 0.29±0.10 |

### 3.3.4.3   Effect of hypoxia (H) on agonist-induced contraction in CSM

The effect of up to 120 min. hypoxia (H) was examined on peak and plateau PE contractures (fig. 3.29 and table 3.32).
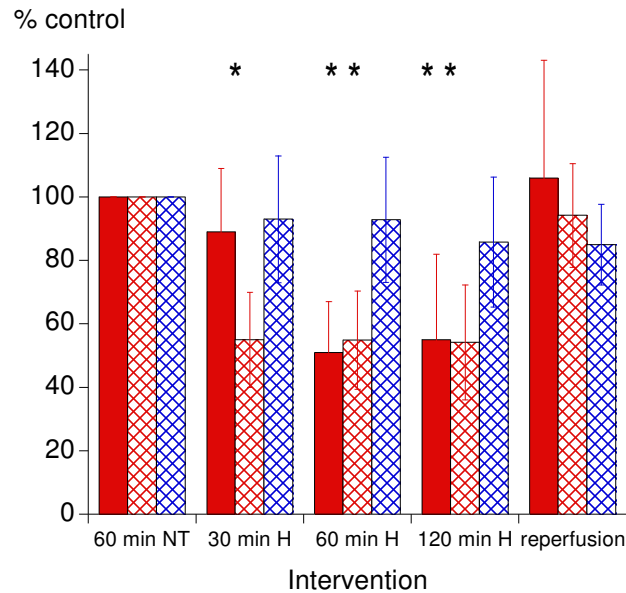


*Fig. 3.29 – The effect of hypoxia (H) on CSM contraction*

■ *peak PE contractures,* ▨ *plateau PE contractures,* ▨ *EFS$_{32Hz}$*

*\* significant reduction compared to control (p<0.05)*

*In a similar manner to the effect of HIAS, there appeared to be some early preservation of the peak PE response at 30 min. of hypoxia, with a significant effect on the peak response at 60 and 120 min. of the hypoxic intervention. Hypoxia significantly suppressed the plateau response at each interval. This is in contrast to the lack of effect of hypoxia on nerve-mediated contraction.*

3.3.4.4   Effect of intracellular and extracellular acidosis (IA) on agonist-contraction in CSM

The effects of 120 min. intra- and extra-cellular acidosis (IA) were examined on both peak and plateau PE contractures (Table 3.32).

IA had no effect on the magnitude of the PE response in a similar manner to the lack of effect of IA seen on nerve-mediated contraction.

3.3.4.5   Effect of acidosis (IA) on isolated CSM cells

Background fluorescence was recorded at the start and end of the experimental protocol. The mean ratio signal was $0.17\pm0.02$ at the start and $0.21\pm0.02$ at the end of the experiment ($[Ca^{2+}]$ $77\pm30$ and $138\pm38$ nM respectively). The mean PMT voltage required was $810\pm44$ V (fig. 3.30 and table 3.30).
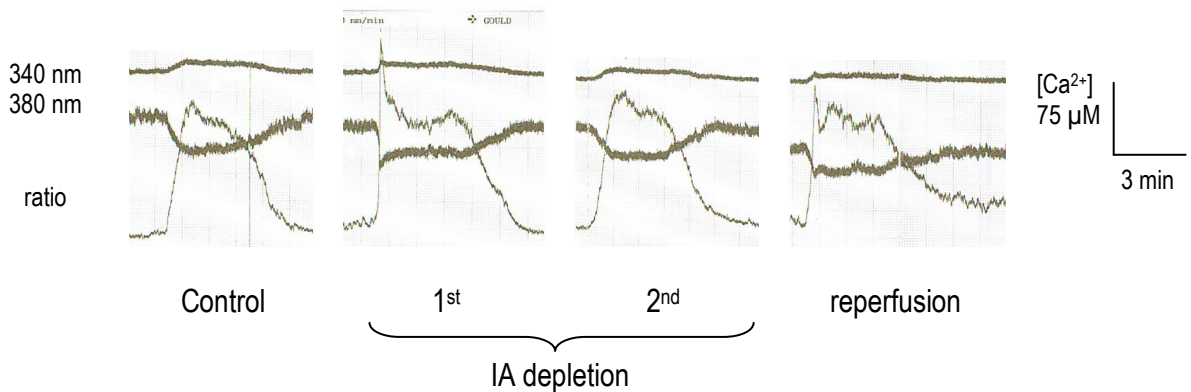


*Fig. 3.30 – Typical experimental tracing demonstrating the effect of IA on isolated CSM cells*

*Intra- and extracellular acidosis had no significant effect on calcium transients.*

*Table 3.30 - Effect of intra- and extracellular acidosis on calcium transients in isolated CSM cells*

| N=5, n=9 | Control | 1st IA response | 2nd IA Response | Reperfusion | 120 mM KCl |
|---|---|---|---|---|---|
| Peak ratio signal | $0.35\pm0.11$ | $0.38\pm0.15$ | $0.38\pm0.15$ | $0.36\pm0.12$ | $0.28\pm0.08$ |
| $\Delta [Ca^{2+}]$ (nM) | $426\pm267$ | $502\pm393$ | $498\pm402$ | $447\pm288$ | $273\pm156$ |

3.3.4.6   Effect of intracellular acidification (I) on agonist-induced contraction in CSM

The effect of 120 min. intracellular acidification (I) was examined on both peak and plateau PE contractures (table 3.32 and fig. 3.30a).
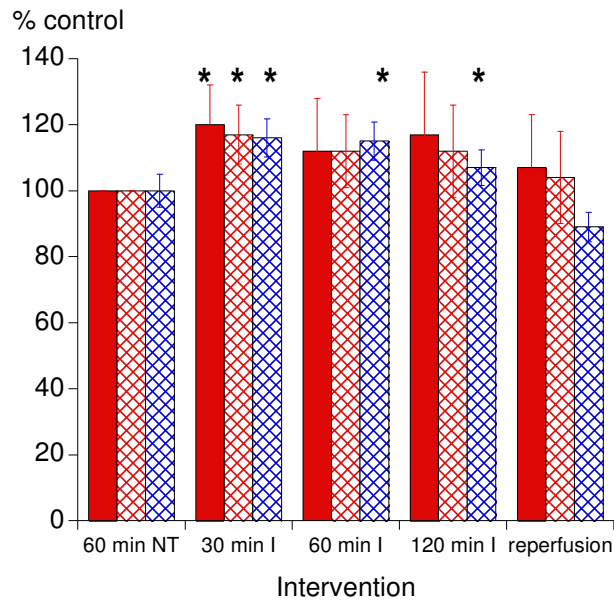


_Fig. 3.30a – The effect of intracellular acidification (I) on CSM contraction_

_peak PE contractures,_ _plateau PE contractures,_ _$EFS_{32Hz}$_

_* significant increase compared to control_

_Intracellular acidification significantly increased the magnitude of the PE contracture. This effect was transient, at 60 and 120 min. the increase was not maintained. This contrasts with the effect of intracellular acidification on nerve-mediated contraction, where the increase occurred throughout the 120 min. intervention. Responses returned to normal upon reperfusion._

3.3.4.7  Effect of intracellular acidification (I) on isolated cells

Background fluorescence was recorded at the start and end of the experimental protocol. The mean ratio signal was 0.18±0.02 at the start and 0.21±0.03 at the end of the experiment ($[Ca^{2+}]$ 93±32 and 150±49 µM respectively). The mean PMT voltage required was 799±61 V. At the end of this period, two responses with 3 µM PE were recorded. The isolated cell was then subjected to 20 min. of intracellular acidification and two further PE responses were recorded (figs. 3.31, 3.32 and table 3.31).

*Table 3.31 - Effect of intracellular acidification on calcium transients in isolated CSM cells*

*\* p<0.05 compared to control*

*Calcium transients were significantly and reversibly augmented during the period of intervention.*

| N=5, n=8 | Control | 1st I response | 2nd I response | Reperfusion | 120 mM KCl |
|---|---|---|---|---|---|
| Peak ratio signal | 0.34±0.07 | 0.41±0.09* | 0.41±0.09* | 0.34±0.07 | 0.29±0.08 |
| Δ $[Ca^{2+}]$ (nM) | 388±148 | 555±231 | 542±236 | 401±159 | 293±163 |
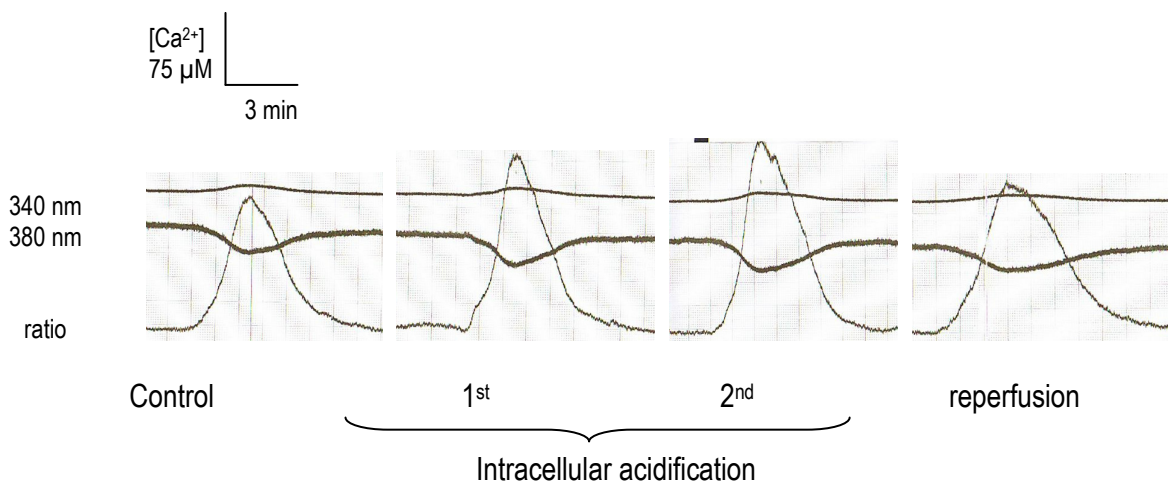


*Fig. 3.31 – Typical experimental tracing demonstrating the effect of intracellular acidification on isolated CSM cells*
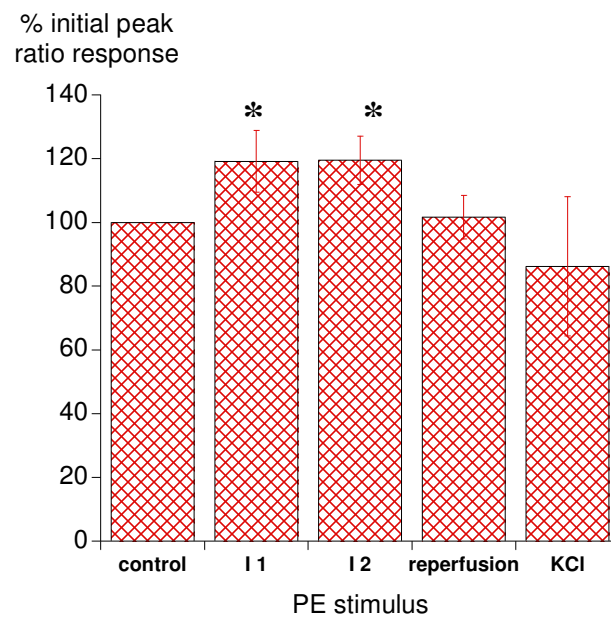
*Fig. 3.32 – Effect of intracellular acidification on $Ca^{2+}$ transients in isolated CSM cells*

*\*significant increase compared to control (p<0.05)*

*Increase in tension recorded during intracelleular acidification was secondary to a rise in $[Ca^{2+}]_i$.*

3.3.4.8   Effect of extracellular acidosis (A) on agonist-induced contraction in CSM

The effect of 120 min. extracellular acidosis (A) was recorded on both peak and plateau PE contractures (table 3.32 and figure 3.33).
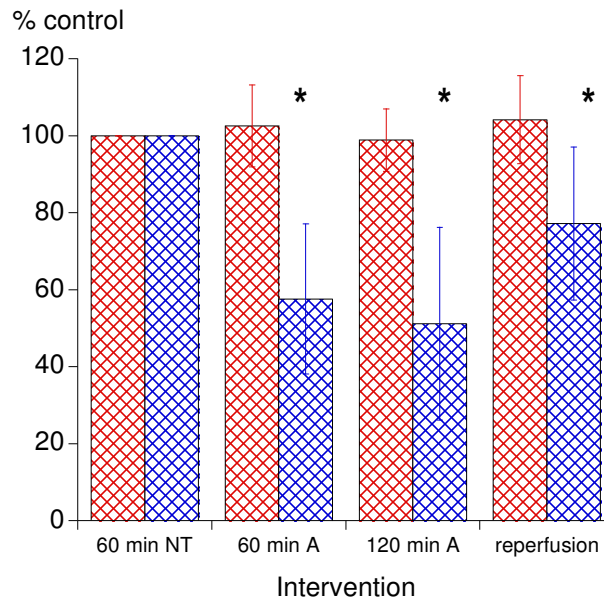


*Fig. 3.33 – The effect of extracellular acidosis (A) on CSM contraction*

▨ *plateau PE contractures,*▨ *EFS$_{32Hz}$*

 *\* significant reduction compared to control*

*Extracellular acidosis had no effect on the magnitude of either the peak or plateau PE contracture. This is in contrast to the significant reversible depression of nerve-mediated contraction seen with extracellular acidosis.*

In a similar manner to nerve-mediated contraction, the effects of the components of simulated ischaemia in various combinations were investigated on PE-induced contractures.

Table 3.32 Components of ischaemia on PE contractures

### 3.3.5 Effect of combinations of components of simulated ischaemia on agonist-induced contractions in CSM

### 3.3.5.1 Effect of hypoxia and substrate depletion on agonist-induced contraction in CSM

Combinations of interventions exerted a significant effect over a shorter time-frame than individual components of ischaemia in isolation. Due to the deleterious effects on muscle strip preparations, interventions were applied for a maximum of 60 min., in order to usefully record the effects of reperfusion. The effect of 60 min. hypoxia and substrate depletion (HS) was recorded on both peak and plateau PE contractures (Table 3.34).

HS depletion caused a significant reduction in the size of the PE contracture which recovered completely upon reperfusion. In a similar manner to the effect of HIAS, the effect was time-dependent as shown by the fact that the peak contracture at 30 min. of HS was not reduced. Again, in contrast to the effect of HS on nerve-mediated contraction, PE contractures recovered completely upon reperfusion (fig. 3.35a).

### 3.3.5.2 Effect of hypoxia and substrate depletion (HS) on isolated CSM cells

Background fluorescence was recorded at the start and end of the experimental protocol. The mean ratio signal was $0.15\pm0.04$ at the start and $0.19\pm0.01$ at the end of the experiment ([$Ca^{2+}$] $54\pm55$ and $109\pm23$ nM respectively). The mean PMT voltage required was $766\pm15$ V. At the end of this period, two responses with 3 µM PE were recorded. The isolated cell was then subjected to 20 min. combined hypoxia and substrate depletion. Two further PE responses were recorded during this intervention. Unmodified Tyrode's solution was then re-introduced for a period of 10

min. and a PE response recorded to examine the effect of reperfusion. A final response to 120

mM KCl was recorded at the end of the experiment (table 3.33 and figs. 3.34a and b).

*Table 3.33 - Effect of hypoxia and substrate depletion on calcium transients in isolated CSM cells*

*\* = significant reduction compared to control p<0.05*

*The second PE response was significantly depressed during HS depletion.*

| N=4, n=7 | Control | 1st HS Response | 2nd HS Response | Reperfusion | 120 mM KCl |
|---|---|---|---|---|---|
| Peak ratio signal | 0.33±0.08 | 0.32±0.07 | 0.28±0.08* | 0.29±0.09 | 0.24±0.03 |
| Δ [Ca$^{2+}$] (nM) | 361±157 | 346±137 | 277±144 | 289±177 | 189±54 |
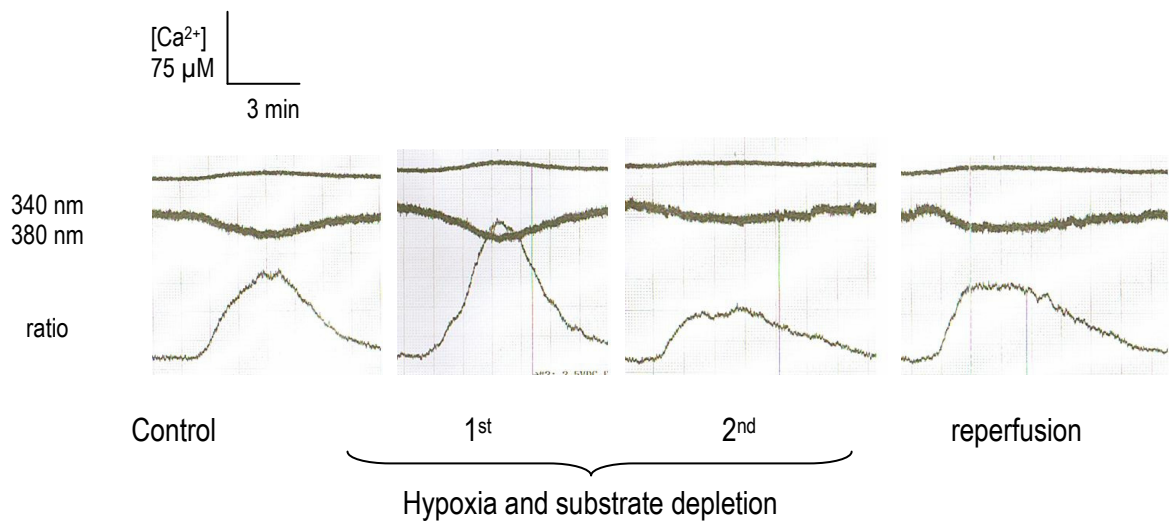


*Fig. 3.34a – Typical tracing showing effect of HS depletion on isolated CSM cell*
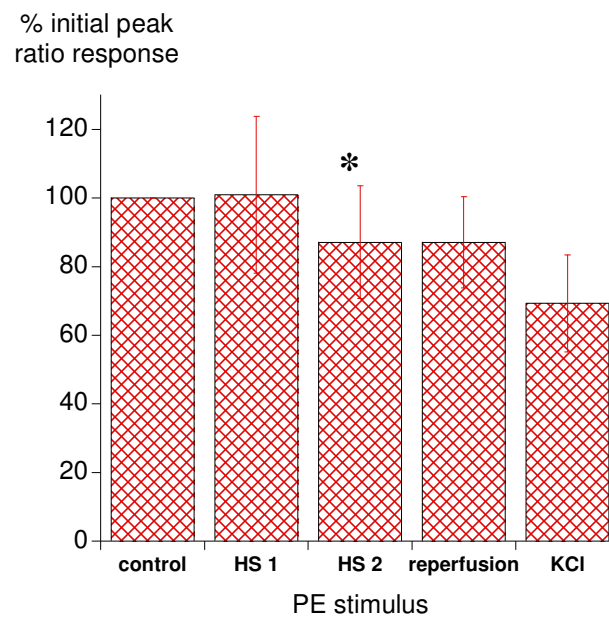
*Fig. 3.34b – Effect of hypoxia and substrate depletion on calcium transients in isolated CSM cells*

*significant reduction compared to control ($p < 0.05$)

### 3.3.5.3 Effect of hypoxia, extracellular acidosis and substrate depletion on PE contraction

The effect of 60 min. hypoxia, extracellular acidosis and substrate depletion (HAS) was recorded on both peak and plateau PE contractures (Table 3.34).

The effect of HAS on agonist-induced contraction was similar to the effect of HS depletion (section 3.3.5.1). HAS depletion caused a significant reduction in the PE contracture, however, the peak PE response at 30 min. was relatively preserved. Contractures recovered completely upon reperfusion in contrast to EFS responses (fig. 3.35b).

### 3.3.5.4 Effect of hypoxia, intracellular acidification and substrate depletion (HIS) on agonist contraction

The effect of 60 min. hypoxia, intracellular acidification and substrate depletion (HIS) was recorded on both peak and plateau PE contractures (Table 3.34).

HIS depletion caused a similar pattern of responses to HS and HAS interventions which recovered completely upon reperfusion. This is in contrast to the effect of HIS on nerve-mediated contraction (section 3.2.3.3) where tension did not recover after the HIS exposure (fig. 3.35c). It can be seen when comparing figures 3.35 a-c that the depression of function seen during HIS depletion was not as severe as that seen during either HS or HAS depletion.

Figure 3.35 – Combinations of elements of ischaemia on CSM contraction

Table 3.34 – combinations of components of simulated ischaemia on PE contractures

### 3.3.6 Combinations of acidosis and substrate depletion on PE-contractures

The effect of various combinations of intra- and extracellular acidosis and substrate depletion for 60 min. were recorded on both peak and plateau PE contractures (Table 3.35).

### 3.3.6.1 Effect of acidosis and substrate depletion (IAS)

No change in PE contracture was seen during the intervention. Upon reperfusion, a significant increase in tension was noted in the peak PE contracture (fig. 3.36a).

### 3.3.6.2 Effect of extracellular acidosis and substrate depletion (AS)

A significant reduction in tension was observed on peak PE responses at both 30 and 60 min. AS depletion. A trend in reduction was observed in the plateau PE contracture that was significant when tension was expressed as a percentage of control values. Responses returned to normal upon reperfusion. This is similar to the response of nerve-mediated contraction to extracellular acidosis and substrate depletion with a significant reversible amelioration of tension recorded (fig. 3.36b).

### 3.3.6.3 Effect of intracellular acidification and substrate depletion (IS)

No significant change in tension generated in response to PE was observed during the intervention. However, upon reperfusion, both peak and plateau responses were significantly augmented when compared to control. Nerve-mediated contraction was significantly increased in the presence of intracellular acidification. Agonist-induced contraction showed a trend towards increasing but did not reach significance (fig. 3.36c).

Figure 3.36 – Acidosis and substrate depletion on CSM contraction

Table 3.35 - Acidosis and substrate depletion on PE contractures

### 3.3.7 Effect of combinations of hypoxia and acidosis on agonist-induced contraction

The effect of various combinations of hypoxia, intracellular and extracellular acidosis for 60 min. were recorded on both peak and plateau PE contractures (Table 3.36).

#### 3.3.7.1 Effect of hypoxia and acidosis (HIA)

No significant change in tension generated in response to PE was recorded however a trend in reduction in tension during the intervention was observed. Responses remained at control levels upon reperfusion. A significant small reversible reduction in nerve-mediated contraction was noted during similar interventions (fig. 3.37a).

#### 3.3.7.2 Effect of hypoxia and extracellular acidosis (HA)

A significant reduction of the PE contracture was recorded with some preservation of the initial peak PE contracture. Responses returned to control levels upon reperfusion. A significant reversible reduction in nerve-mediated contraction was noted during similar interventions. This reduction in tension in nerve-mediated contraction was not as marked as that seen with agonist-induced contractures (fig. 3.37b).

#### 3.3.7.3 Effect of hypoxia and intracellular acidification (HI)

A trend towards a time-dependent reduction in the PE contracture was noted during the intervention with some preservation of the initial peak PE contracture. However, this did not reach significance. Responses remained at control levels upon reperfusion. No significant effect was noted with nerve-mediated contraction during similar interventions (fig. 3.37c).

Figure 3.37 – Hypoxia and acidosis on CSM contraction

Table 3.36 – Hypoxia and acidosis on PE contractures

### 3.3.8  Summary of results for agonist-induced contraction in CSM

Simulated ischaemia (the combination of hypoxia, intra- and extracellular acidosis and substrate depletion - HIAS) caused a significant and marked reduction in agonist-induced contraction (plateau $PE_{30}$ response 35±19%, plateau $PE_{60}$ response 29±16% of control). The degree of depression was similar to that seen in nerve-mediated contraction although there appeared to be some metabolic reserve as shown by early preservation of the peak PE response (peak $PE_{30}$ response 83±31%, peak $PE_{60}$ response 36±35% of control). $Ca^{2+}$ transients in isolated cells during similar interventions showed no difference from control values. However, the time-course of isolated cell procedures was much shorter and correlated with the period of preservation of peak PE responses during HIAS depletion. Nerve-mediated contraction did not recover upon reperfusion whereas agonist-induced contraction demonstrated a complete recovery. Experiments carried out in the presence of the $Ca^{2+}$-channel blocker nifedipine showed significantly less depression of agonist-induced contraction during simulated ischaemia (plateau $PE_{30}$ response 68±27%, plateau $PE_{60}$ response 66±31% of control).

As with nerve-mediated contractions, the combination of hypoxia and substrate depletion (HS) produced similar responses to simulated ischaemia (plateau $PE_{30}$ response 28±19%, plateau $PE_{60}$ response 30±20% of control). A significant reversible reduction in tension generated was recorded with initial preservation of the peak PE response (peak $PE_{30}$ response 89±23%, peak $PE_{60}$ response 28±19% of control). In a similar fashion, PE-induced $Ca^{2+}$ transients demonstrated an initial resistance with significant depression of the second PE-induced calcium transient during HS depletion. Again, in contrast to nerve-mediated contraction, complete recovery was observed upon reperfusion. Combined hypoxia, extracellular acidosis and substrate depletion (HAS) had a similar effect to hypoxia and substrate depletion (HS). Combined hypoxia, intracellular

acidification and substrate depletion (HIS) also had a similar effect however the initial preservation of the peak PE response was more marked (peak $PE_{30}$ response 102±4%, peak $PE_{60}$ response 52±24%, plateau $PE_{30}$ response 66±42%, plateau $PE_{60}$ response 55±25% of control). All interventions demonstrated complete recovery upon reperfusion.

Similar to the effect on nerve-mediated contraction, simultaneous intra- and extracellular acidosis had no overall effect on agonist-induced contractures, with no change upon reperfusion. Intracellular acidification caused a significant and reversible increase in nerve-mediated contraction and also augmented the PE contracture at 30 min. although then returned to control at 60 and 120 minutes. Intracellular acidification induced a significant and reversible increase in PE-induced $Ca^{2+}$ transients. Interestingly, the significant depression of nerve-mediated contraction observed with extracellular acidosis was not observed on PE-contractures.

Substrate depletion (omission of glucose and Na pyruvate) caused significant and irreversible depression of nerve-mediated contraction. No effect of this intervention was observed on agonist-induced contraction or PE-induced $Ca^{2+}$ transients in isolated cells. When combined with both intra- and extracellular acidosis (IAS) no change was observed on the PE contracture. Interestingly, the combination of extracellular acidosis and substrate depletion (AS) significantly reduced peak PE responses during the intervention with a trend in reduction of plateau responses also observed. This would suggest that there was some inotropic effect of intracellular acidification in agonist-induced contraction. No significant increase in contraction was observed during combined intracellular acidification and substrate depletion (IS). However, there was a significant increase in agonist-induced contraction upon reperfusion when compared to control.

Hypoxia caused a significant reduction in the PE contracture although some preservation of the initial peak PE response was recorded. This is in contrast to the lack of effect seen in nerve-mediated contractions. It is hypothesised that the reduction is a consequence of the increased energy required to generate the agonist-induced contracture as opposed to the nerve-mediated phasic contraction. When hypoxia was combined with both intra- and extracellular acidosis, a trend in reduction of the PE contracture was observed. This was not significant and returned to normal upon reperfusion. The combination of hypoxia and extracellular acidosis caused a marked reversible reduction in tension which was greater in magnitude than that seen with a similar intervention in nerve-mediated contraction. These findings are further evidence of the detrimental effect of hypoxia on agonist-induced contraction. The combination of hypoxia and intracellular acidification showed a trend towards reduction during the ischaemic intervention. This was not as marked as that seen with hypoxia and extracellular acidosis and again was not significant. This also lends evidence to the contraction enhancing effects of intracellular acidification in this preparation.

Table 3.37 summarises the effect of simulated ischaemia on calcium transients in isolated CSM cells. Both nerve-mediated and agonist-induced contraction in cavernosal smooth muscle strips is summarised in Table 3.38. Subsequent experiments examined the effect of simulated ischaemia on EFS-mediated relaxation.

*Table 3.37 - Summary of effect of ischaemia on Ca$^{2+}$ transients in isolated CSM*

*\* = significant reduction compared to control, # = significant increase compared to control, $p < 0.05$*

| Intervention | Peak ratio signal | | | | |
|---|---|---|---|---|---|
| | **Control** | **1st response** | **2nd response** | **Reperfusion** | **120 mM KCl** |
| Simulated ischaemia (HIAS) | 0.32±0.07 | 0.34±0.06 | 0.35±0.08 | 0.33±0.08 | 0.26±0.01 |
| Hypoxia & substrated depletion (HS) | 0.33±0.08 | 0.32±0.07 | 0.28±0.08* | 0.29±0.09 | 0.24±0.03 |
| Substrate depletion (S) | 0.44±0.09 | 0.40±0.07 | 0.39±0.06 | 0.42±0.07 | 0.29±0.10 |
| Intra- and extracellular acidosis (IA) | 0.35±0.11 | 0.38±0.15 | 0.38±0.15 | 0.36±0.12 | 0.28±0.08 |
| Intracellular acidification (I) | 0.34±0.07 | 0.41±0.09# | 0.41±0.09# | 0.34±0.07 | 0.29±0.08 |

*Table 3.38 - Effect of components of ischaemia in various combinations on contraction in CSM*

* = significant reduction compared to control, # = significant increase compared to control, $p < 0.05$

| Intervention | EFS$_{32Hz}$ after 60 min intervention (% control) | Plateau PE after 60 min intervention (% control) |
|---|---|---|
| HIAS | 20±14* | 29±16* |
| Rapid detrimental effect. Irreversible in EFS-mediated, reversible in PE-induced contraction. | | |
| HS | 14±11* | 30±20* |
| HAS | 13±11* | 21±3* |
| HIS | 12±20* | 55±25* |
| Detrimental effect of HIAS due to combined effect of hypoxia and substrate depletion (HS) | | |
| IA | 97±15 | 102±8 |
| A | 58±20* | 103±11 |
| I | 115±6# | 112±11 |
| Intracellular acidification reversibly augments contraction. Extracellular acidosis irreversibly inhibits nerve-mediated contraction | | |
| S | 74±24* | 99±16 |
| Substrate depletion caused an irreversible reduction in nerve-mediated contraction | | |
| IAS | 81±19 | 92±14 |
| AS | 71±21 | 78±9 |
| Extracellular acidosis and substrate depletion in isolation had no effect on PE-contracture, in combination, significant detrimental effect | | |
| IS | 119±12# | 103±17 |
| Intracellular acidification limited detrimental effect of substrate depletion | | |
| H | 93±20 | 55±15* |
| Hypoxia had marked reversible effect on PE contracture | | |
| HIA | 78±8 | 76±29 |
| HA | 79±22 | 35±17* |
| Extracellular acidosis augmented detrimental effect of hypoxia on contractile function | | |
| HI | 113±19 | 76±13 |
| Augmentation of function by intracellular acidification is sensitive to hypoxia. Intracellular acidification limited the detrimental effect of extracellular acidosis in the presence of hypoxia | | |

## 3.4    Results IV – The effect of ischaemia on nerve-mediated relaxation

### 3.4.1    Effect of simulated ischaemia (HIAS) on nerve-mediated relaxation in CSM

Isometric nerve-mediated relaxations elicited by EFS (range 4-24 Hz) in CSM strips pre-contracted with 15 µM PE were recorded and measured as described in section 2.3.4. Preparations equilibrated in Tyrode's solution for 60 min. at 37 °C. At the end of this equilibration period, the mean plateau PE response was $0.74\pm0.21$ mN.mm$^{-2}$. The plateau PE contracture was significantly reduced during the intervention (plateau PE$_{30\ min}$ $53\pm29$ % and plateau PE$_{60\ min}$ $44\pm22$ % of control). Tension remaining after nerve-mediated relaxation at 24 Hz (EFS$_{24Hz}$) was $48\pm15$ % of the preceding PE contracture (table 3.39 and fig. 3.38).

*Table 3.39 - Effect of simulated ischaemia (HIAS) on EFS-mediated relaxation*

*\* = significant reduction compared to control*

*30 min. of simulated ischaemia (HIAS) ameliorated nerve-mediated relaxation. This effect appeared more marked at 60 min. Responses returned to normal upon reperfusion.*

| N=5, n=6 | control | 30 min HIAS | 60 min HIAS | Reperfusion |
|---|---|---|---|---|
| Plateau PE contracture (mN.mm$^{-2}$) | $0.74\pm0.21$ | $0.37\pm0.22$* | $0.31\pm0.17$* | $0.73\pm0.19$ |
| Tension remaining after EFS$_{24Hz}$ (mN.mm$^{-2}$) | $0.35\pm0.12$ | $0.19\pm0.17$ | $0.18\pm0.16$ | $0.28\pm0.19$ |
| EFS$_{24Hz}$ as % preceding PE plateau contracture | $48\pm15$ | $45\pm14$ | $52\pm23$ | $38\pm20$ |
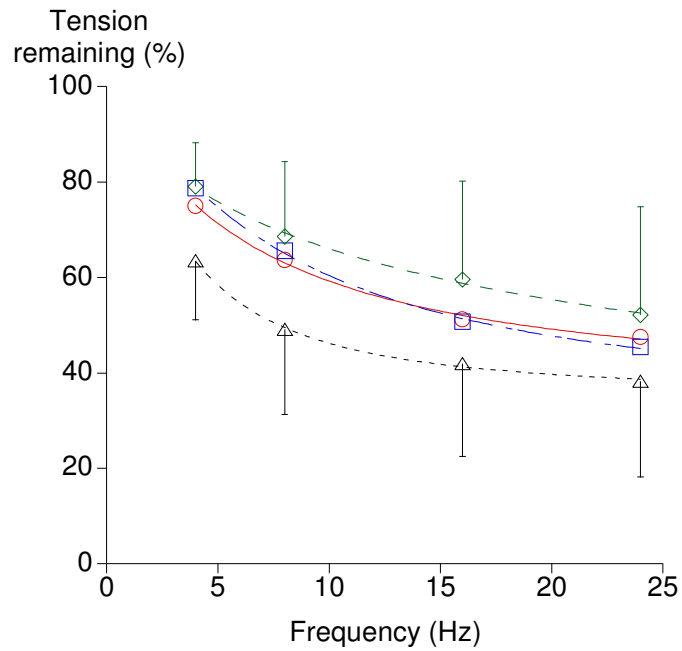
*Fig. 3.38 – Effect of simulated ischaemia on EFS-mediated relaxation in CSM*

○ *– control,* □ *– 30 min HIAS,* ◊ *– 60 min HIAS, Δ – reperfusion*

*Simulated ischaemia (HIAS) ameliorated nerve-mediated relaxation throughout the range of EFS stimulation. Responses returned to normal upon reperfusion. Nerve-mediated contractile responses were also ameliorated during simulated ischaemia (HIAS). However, contractile responses did not recover upon reperfusion whereas relaxatory responses did during the time course of these experiments.*

In a similar manner to preceding experiments, the effects of the components of ischaemia on EFS-mediated relaxation were examined.

## 3.4.2    Effect of isolated components of ischaemia on nerve-mediated relaxation

### 3.4.2.1  Effect of substrate depletion (S) on nerve-mediated relaxation

The plateau PE contracture was stable during the intervention. 60 min. of substrate depletion had no effect on nerve-mediated relaxation (table 3.40 and fig. 3.41a).

### 3.4.2.2 Effect of hypoxia (H) on nerve-mediated relaxation

The plateau PE contracture was significantly reduced during the intervention. 30 min. of hypoxia ameliorated nerve-mediated relaxation. At 60 min. relaxation was almost abolished with tension remaining similar to that recorded after EFS stimulation in the presence of ODQ (table 3.40, fig. 3.39-40).
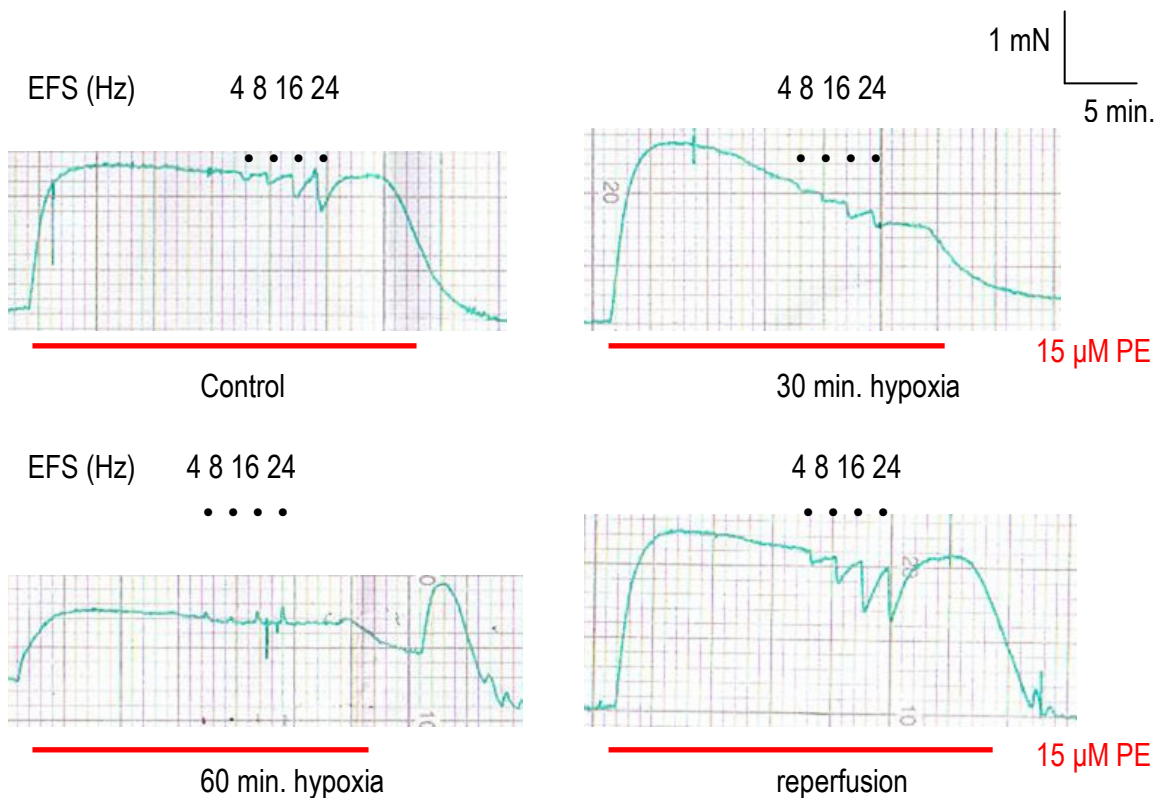


*Fig. 3.39 – Typical experimental tracing showing effect of hypoxia on nerve-mediated relaxation*
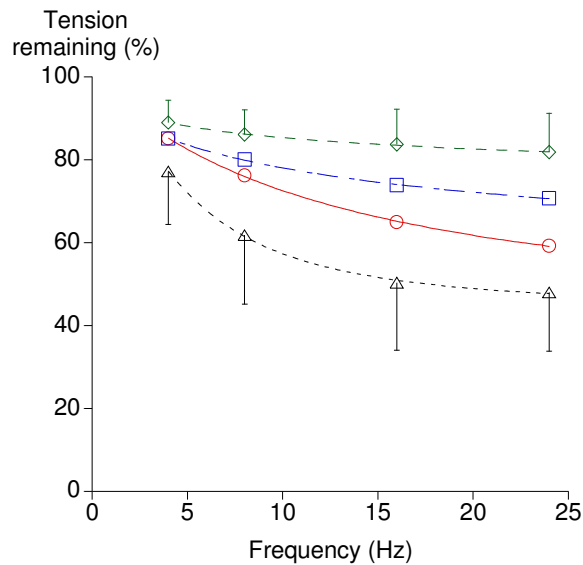
*Fig. 3.40 – Effect of hypoxia on EFS-mediated relaxation in CSM*

○ *– control,* □ *– 30 min H,* ◊ *– 60 min H, Δ – reperfusion*

3.4.3.2  Effect of acidosis (IA) on nerve-mediated relaxation

The plateau PE contracture was stable during the intervention. 60 min. of intra- and extracellular acidosis had no effect on nerve-mediated relaxation (table 3.40 and fig. 3.41b).

3.4.3.2  Effect of intracellular acidification (I) on nerve-mediated relaxation

The plateau PE contracture was stable during the intervention. 60 min. of intracellular acidification appeared to augment nerve-mediated relaxation. Relaxatory responses appeared to return to normal upon reperfusion (table 3.40 and fig. 3.41c).

3.4.3.3  Effect of extracellular acidosis (A) on nerve-mediated relaxation

The plateau PE contracture was stable during the intervention. 60 min. of extracellular acidosis had no effect on nerve-mediated relaxation. This is in contrast to the detrimental and irreversible effect similar interventions had upon nerve-mediated relaxation (table 3.40 and fig. 3.41d).

Figure 3.41 – Components of ischaemia on nerve relaxation

Table 3.40 – Components of ischaemia on EFS relaxation

### 3.4.3 Combinations of components of ischaemia on nerve-mediated relaxation in CSM

### 3.4.3.1 Effect of hypoxia and substrate depletion (HS) on nerve-mediated relaxation in CSM

The plateau PE contracture was significantly reduced during the intervention. 60 min. of hypoxia and substrate depletion ameliorated nerve-mediated relaxation in a time-dependent fashion in a similar manner to the effect of simulated ischaemia (table 3.41 and fig. 3.42a).

### 3.4.3.2 Effect of hypoxia, extracellular acidosis and substrate depletion (HAS) on nerve-mediated relaxation in CSM

The plateau PE contracture was significantly reduced during the intervention. 60 min. of hypoxia, extracellular acidosis and substrate depletion ameliorated nerve-mediated relaxation. Responses returned to normal upon reperfusion (table 3.41 and fig. 3.42b).

### 3.4.3.3 Effect of hypoxia, intracellular acidification and substrate depletion (HIS) on nerve-mediated relaxation in CSM

The plateau PE contracture was significantly reduced during the intervention. 60 min. of hypoxia, intracellular acidification and substrate depletion also ameliorated nerve-mediated relaxation. Responses returned to normal upon reperfusion (table 3.41 and fig. 3.42c).

Figure 3.42 – Combination of components of ischaemia on nerve relaxation

Table 3.41 – Combination of components of ischaemia on EFS relaxation

### 3.4.4 Effect of combinations of acidosis and substrate depletion on nerve-relaxation

### 3.4.4.1 Effect of intra- and extracellular acidosis and substrate depletion (IAS)

The plateau PE contracture was stable during the intervention. 60 min. of intra- and extracellular acidosis with substrate depletion ameliorated EFS-mediated relaxation at the lower end of the frequency range (4 and 8 Hz). Higher frequency stimulation (16 and 24 Hz) resulted in a normal relaxatory response (table 3.42 and fig. 3.43a).

### 3.4.4.2 Effect of extracellular acidosis and substrate depletion (AS)

The plateau PE contracture was significantly suppressed at 60 min. of the intervention. 60 min. of extracellular acidosis and substrate depletion appeared to augment nerve-mediated relaxation. This maybe artefactual and secondary to the fact that the preceding PE contracture was significantly reduced (table 3.42 and fig. 3.43b).

### 3.4.4.3 Effect of intracellular acidification and substrate depletion (IS)

The plateau PE contracture was stable during the intervention. 60 min. of intracellular acidification and substrate depletion augmented nerve-mediated relaxation. Responses returned to normal upon reperfusion (table 3.42 and fig. 3.43c).

Figure 3.43 – Acidosis and substrate depletion on EFS relaxation

Table 3.42 – Acidosis and substrate depletion on nerve relaxation

3.4.5    Effect of combinations of hypoxia and acidosis on nerve-relaxation in CSM

3.4.5.1  Effect of hypoxia and acidosis (HIA)

The plateau PE contracture was significantly suppressed during the intervention. 60 min. of hypoxia, intra- and extracellular acidosis ameliorated nerve-mediated relaxation. Responses returned to normal upon reperfusion (table 3.43 and fig. 3.44a).

3.4.5.2  Effect of hypoxia and extracellular acidosis (HA)

The plateau PE contracture was significantly suppressed during the intervention. 60 min. of hypoxia and extracellular acidosis ameliorated nerve-mediated relaxation. Responses returned to normal upon reperfusion (table 3.43 and fig. 3.44b).

3.4.5.3  Effect of hypoxia and intracellular acidification (HI)

The plateau PE contracture was stable during the intervention. 60 min. of hypoxia and intracellular acidification ameliorated nerve-mediated relaxation. Responses returned to normal upon reperfusion (table 3.43 and fig. 3.44c).

Figure 3.44 - Hypoxia and acidosis on EFS relaxation

Table 3.43 – Hypoxia and acidosis on EFS relaxation

### 3.4.6    The effect of ischaemia on nerve relaxation summary

Simulated ischaemia (the combination of hypoxia, intra- and extracellular acidosis and substrate depletion - HIAS) markedly reduced EFS-mediated relaxation. This is similar to the effect of HIAS depletion on nerve-mediated contraction. Interestingly, EFS-mediated relaxation recovered upon reperfusion whereas nerve-mediated contraction did not during the time course of these experiments. The combination of hypoxia and substrate depletion produced a similar response to simulated ischaemia (HIAS) on nerve-mediated relaxation and was again reversible upon reperfusion. No difference was seen when hypoxia and substrate depletion were combined with either intra- or extracellular acidosis. In summary, the combination of hypoxia and substrate depletion, with or without acidosis, markedly reduced the effect of nerve-mediated relaxation. Similar interventions severely and irreversibly reduced nerve-mediated contractile responses.

Combined intra- and extracellular acidosis had no effect on EFS-mediated relaxatory responses. Extracellular acidosis again had no effect. Intracellular acidification augmented the effect of nerve-mediated relaxation. This is similar to the effect of intracellular acidification on nerve-mediated contraction. The augmentation of response seen was reversible upon reperfusion.

30 min. of hypoxia markedly reduced nerve-mediated relaxation. At 60 min., relaxatory responses were almost abolished with residual relaxation in response to EFS similar to that seen during EFS relaxation in the presence of the soluble guanyl cyclase inhibitor ODQ. Simultaneous acidosis (intra- and extracellular acidosis in isolation and combination) did not ameliorate the inhibitory effect of hypoxia on nerve-mediated relaxation. All responses on nerve-mediated relaxation were reversible upon reperfusion with normoxic Tyrode's solution.

60 min. of substrate depletion had no effect on EFS-mediated relaxation. Longer periods of intervention were not examined. Simultaneous intra-and extracellular acidosis ameliorated relaxation in response to low frequency EFS, sparing responses to higher frequency stimulation. Extracellular acidosis and substrate depletion (AS) appeared to augment relaxation. However, this observation may be artefactual as the preceding PE contracture during AS depletion was significantly decreased. EFS-mediated contraction in sub-maximally precontracted muscle strips caused a proportionally increased EFS-mediated relaxatory response (EFS-relaxation in strips precontracted with 15 µM *vs.* 1.5 µM PE). In a similar manner to nerve-mediated contraction, the augmentation of relaxatory responses seen during intracellular acidification persisted in the presence of substrate depletion.

The effect of simulated ischaemia on nerve-mediated relaxation in CSM is summarised in Table 3.44. Following this the effect of ischaemia on agonist-induced relaxation was examined.

*Table 3.44 - Effect of components of ischaemia applied in various combinations on nerve-mediated relaxation in CSM*

| Intervention | Nerve-mediated contraction | Nerve-mediated relaxation |
|:---:|:---:|:---:|
| **HIAS** | suppressed, irreversible | suppressed, reversible |
| Rapid detrimental effect. Irreversible in nerve contraction, reversible in nerve relaxation | | |
| **HS** | suppressed, irreversible | suppressed, reversible |
| **HAS** | suppressed, irreversible | suppressed, reversible |
| **HIS** | suppressed, irreversible | suppressed, reversible |
| Detrimental effect of HIAS due to combined effect of hypoxia and substrate depletion (HS). Effect on nerve-mediated relaxation reversible | | |
| **IA** | no effect | no effect |
| **A** | suppressed, irreversible | no effect |
| **I** | augmented, reversible | augmented, reversible |
| Intracellular acidification reversibly augments nerve-mediated responses. Extracellular acidosis irreversibly inhibits nerve-mediated contraction | | |
| **S** | suppressed, irreversible | no effect |
| Substrate depletion caused an irreversible reduction in nerve-mediated contraction | | |
| **IAS** | suppression at low frequency, reversible | suppression at low frequency, reversible |
| **AS** | suppression, reversible | ? augmented,? no effect |
| Extracellular acidosis and substrate depletion suppressed nerve-mediated contraction | | |
| **IS** | augmented, reversible | augmented, reversible |
| Intracellular acidification limited detrimental effect of substrate depletion. Mechanism of augmentation not sensitive to substrate depletion | | |
| **H** | no effect | abolished, reversible |
| Hypoxia had marked reversible effect on relaxation | | |
| **HIA** | suppressed, reversible | suppressed, reversible |
| **HA** | suppressed, reversible | suppressed, reversible |
| **HI** | no effect | suppressed, reversible |
| Augmentation of nerve-mediated function by intracellular acidification is sensitive to hypoxia. | | |

## 3.5    Results V – The effect of ischaemia on agonist-induced relaxation

### 3.5.1    Effect of simulated ischaemia on agonist-induced relaxation

Isometric relaxation in response to 1 μM carbachol (C) muscle strips pre-contracted with 15 μM phenylephrine (PE) were recorded as described in section 2.3.5. Preparations equilibrated in Tyrode's solution for 60 min. at 37 °C. At the end of this period, PE was added to the superfusing solution and the resulting contracture recorded. Once this had reached a plateau, relaxation in response to carbachol was examined. The effect of 60 min. of simulated ischaemia was examined on both the nadir and plateau C relaxation. The plateau PE contracture was significantly reduced during the intervention (plateau $PE_{30 min}$ 36±35 % and plateau $PE_{60 min}$ 29±16 % of control). Tension was derived from height above baseline of the contracture remaining after the intervention (table 3.45 and fig. 3.45).
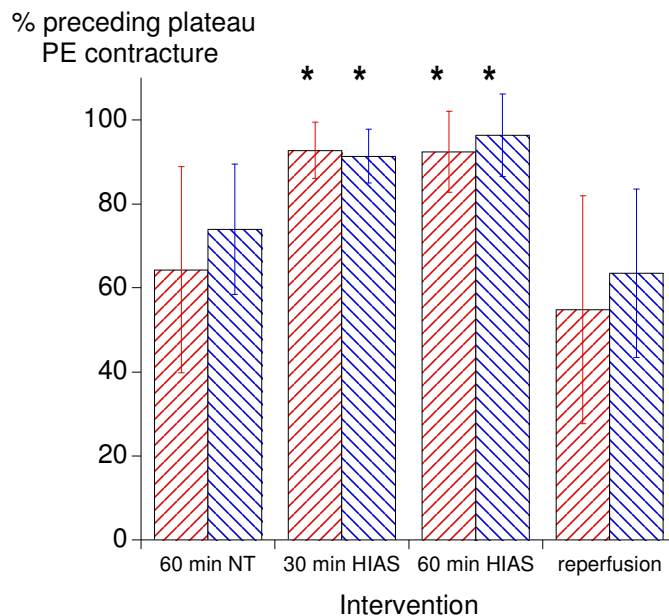


*Fig. 3.45 – The effect of simulated ischaemia (HIAS) on carbachol-induced relaxation in CSM*

🔴 *nadir carbachol relaxation,* 🔵 *plateau carbachol relaxation,*

*\* significant increase compared to control*

*Table 3.45 - Effect of simulated ischaemia (HIAS) on agonist-induced relaxation*

[#] *= p<0.05 compared to control*

*Simulated ischaemia (HIAS) abolished the relaxatory effect of carbachol. This effect recovered*

*completely upon reperfusion.*

| N=6, n=6 | Control | 30 min HIAS | 60 min HIAS | Reperfusion |
|---|---|---|---|---|
| Plateau PE contracture (mN.mm$^{-2}$) | 0.70±0.53 | 0.18±0.17* | 0.16±0.08* | 0.60±0.43 |
| Nadir C relaxation (mN.mm$^{-2}$) | 0.45±0.41 | 0.16±0.14 | 0.15±0.08 | 0.30±0.22 |
| Nadir C relaxation as % of preceding PE contracture | 64±25 | 93±7[#] | 92±10[#] | 55±27 |
| Plateau C relaxation (mN.mm$^{-2}$) | 0.52±0.43 | 0.18±0.13 | 0.16±0.09 | 0.37±0.25 |
| Plateau C relaxation as % of preceding PE contracture | 74±16 | 91±6[#] | 96±10[#] | 63±20 |

In a similar manner to preceding experiments, the effects of the individual components of

ischaemia on agonist-induced relaxation were examined.

3.5.2    Effect of isolated components of ischaemia on agonist-induced relaxation

The effects of the components of simulated ischaemia for 120 min. were recorded on both the nadir and plateau C relaxation.

3.5.2.1  Effect of substrate depletion (S) on agonist-induced relaxation in CSM

The plateau PE contracture was stable during the intervention. Substrate depletion had no effect on the agonist-induced relaxation (table 3.46 and fig. 3.47a).

3.5.3.1  Effect of hypoxia (H) on agonist-induced relaxation in CSM

The plateau PE contracture was significantly ameliorated during the intervention. 30 min. of hypoxia abolished agonist-induced relaxation. This effect persisted at 120 min. of the intervention. Carbachol-induced relaxation recovered completely upon reperfusion (table 3.46 and fig. 3.46).



Fig. 3.46 – The effect of hypoxia (H) on carbachol-induced relaxation in CSM

▨ nadir C relaxation, ▨ plateau C relaxation

* significant increase compared to control

3.5.2.2  Effect of acidosis (IA) on agonist-induced relaxation in CSM

The plateau PE contracture was stable during the intervention. Combined intra- and extracellular acidosis had no effect on agonist-induced relaxation (table 3.46 and fig. 3.47b).

3.5.2.3  Effect of extracellular acidosis (A) on agonist-induced relaxation in CSM

The plateau PE contracture was stable during the intervention. Extracellular acidosis had no effect on agonist-induced relaxation (table 3.46 and fig. 3.47c).

3.5.2.4  Effect of intracellular acidification (I) on agonist-induced relaxation in CSM

The plateau PE contracture was significantly augmented at 30 min. but not at 60 or 120 min. Intracellular acidification had no effect on agonist-induced relaxation (table 3.46 and fig. 3.47d).

Figure 3.47 – Components of ischaemia on carbachol relaxation

Table 3.46 - Components of ischaemia on carbachol relaxation

### 3.5.3 Effect of combinations of components of ischaemia on agonist-induced relaxation

The effects of ischaemia component combinations for 60 min. were recorded on both the nadir and plateau C relaxation.

### 3.5.3.1 Effect of hypoxia and substrate depletion on agonist-induced relaxation in CSM

The plateau PE contracture was significantly ameliorated during the intervention. Hypoxia and substrate depletion ameliorated agonist-induced relaxation at 30 min. although this effect was not significant. At 60 min. relaxation was abolished under these conditions. Responses returned to normal upon reperfusion (table 3.47 and fig. 3.48a).

### 3.5.3.2 Effect of hypoxia, extracellular acidosis and substrate depletion on agonist-relaxation

The plateau PE contracture was significantly ameliorated during the intervention. The combination of hypoxia, extracellular acidosis and substrate depletion abolished agonist-induced relaxation at 30 min. and 60 min. Responses recovered completely upon reperfusion (table 3.47 and fig. 3.48b).

### 3.5.3.3 Effect of hypoxia, intracellular acidification and substrate depletion on agonist-relaxation

The plateau PE contracture was significantly ameliorated during the intervention. Hypoxia, intracellular acidification and substrate depletion ameliorated agonist-induced relaxation during the intervention. This effect was not significant (table 3.47 and fig. 3.48c).

Figure 3.48 – Combination of components of ischaemia on carbachol relaxation

Table 3.47 - Combination of components of ischaemia on carbachol relaxation

3.5.4 Combinations of acidosis and substrate depletion on agonist-induced relaxation

The effects of combinations of acidosis and substrate depletion for 60 min. were recorded on both the nadir and plateau C relaxation.

3.5.4.1 Effect of acidosis and substrate depletion (IAS)

The plateau PE contracture was stable during the intervention. 60 min. of simultaneous intra- and extracellular acidosis with substrate depletion had no effect on agonist-induced relaxation (table 3.48 and fig. 3.49a).

3.5.4.2 Effect of extracellular acidosis and substrate depletion (AS)

The plateau PE contracture was stable during the intervention. Extracellular acidosis and substrate depletion had no effect on agonist-induced relaxation (table 3.48 and fig. 3.49b).

3.5.4.3 Effect of intracellular acidification and substrate depletion (IS)

The plateau PE contracture was stable during the intervention and demonstrated a significant increase upon reperfusion. Intracellular acidification and substrate depletion had no effect upon agonist-induced relaxation (table 3.48 and fig. 3.49c).

Figure 3.49 – Acidosis and substrate depletion on carbachol relaxation

Table 3.48 - Acidosis and substrate depletion on carbachol relaxation

3.5.5    Effect of combinations of hypoxia and acidosis on agonist relaxation in CSM

The effects of combinations of hypoxia and acidosis for 60 min. were recorded on both the nadir and plateau C relaxation.

3.5.5.1  Effect of hypoxia and acidosis (HIA)

The plateau PE contracture was stable during the intervention. Intra- and extracellular acidosis ameliorated the detrimental effect of hypoxia on agonist-induced relaxation (table 3.49 and fig. 3.50a).

3.5.5.2  Effect of hypoxia and extracellular acidosis (HA)

The plateau PE contracture was significantly depressed during the intervention. Hypoxia and extracellular acidosis had no significant effect on agonist-induced relaxation (table 3.49 and fig. 3.50b).

3.5.5.3  Effect of hypoxia and intracellular acidification (HI)

The plateau PE contracture was stable during the intervention. Intracellular acidification did not limit the detrimental effect of hypoxia; relaxation was abolished with this combination of interventions (table 3.49 and fig. 3.50c).

Figure 3.50 – Hypoxia and acidosis on carbachol relaxation

Table 3.49 - Hypoxia and acidosis on carbachol relaxation

### 3.5.6   Summary of the effect of ischaemia on CSM relaxation

Simulated ischaemia (the combination of hypoxia, intra- and extracellular acidosis and substrate depletion - HIAS) markedly reduced EFS-mediated relaxation and abolished agonist-induced responses. These detrimental effects were completely reversible upon return to normoxic Tyrodes solution. The effect on nerve-mediated contraction was secondary to the combination of hypoxia and substrate depletion (HS). However, agonist-induced relaxation was initially preserved with HS depletion with only a trend towards reduced relaxation at 30 min. Relaxation was abolished at 60 min. of this intervention. Hypoxia, intracellular acidification and substrate depletion (HIS) again showed a trend towards reduction of the carbachol relaxation during the intervention which was not significant. When hypoxia and substrate depletion were combined with extracellular acidosis, similar observations were made to those during simulated ischaemia (HIAS) with relaxation reversibly abolished at 30 and 60 min. In summary, the combination of hypoxia and substrate depletion, with or without acidosis, markedly reduced the effect of nerve-mediated relaxation. Agonist-induced relaxation was similarly affected by the combination of hypoxia, extracellular acidosis and substrate depletion.

Combined intra- and extracellular acidosis had no effect on EFS-mediated relaxatory responses. Extracellular acidosis again had no effect. Intracellular acidification reversibly augmented the effect of nerve-mediated relaxation. None of these interventions had any effect on agonist-induced relaxation.

30 min. of hypoxia markedly reduced nerve-mediated relaxation. At 60 min., relaxatory responses were almost abolished with residual relaxation in response to EFS similar to that seen during EFS relaxation in the presence of the soluble guanyl cyclase inhibitor ODQ. Agonist-induced relaxation was abolished at 30 min. and 60 min. of hypoxia. Simultaneous acidosis (intra- and extracellular

acidosis in isolation and combination) did not ameliorate the inhibitory effect of hypoxia on nerve-mediated relaxation. However, agonist-induced relaxation in the presence of similar interventions was affected. Simultaneous intra-and extracellular acidosis with hypoxia (HIA) ameliorated the effect of hypoxia on relaxatory responses. Carbachol relaxation during HIA depletion was similar to control. Experiments conducted in the presence of hypoxia and extracellular acidosis or intracellular acidification showed this preservation of relaxation in the presence of hypoxia to be secondary to a reduction of pH in the extracellular compartment.

60 min. of substrate depletion had no effect on EFS-mediated or agonist-induced relaxation. In a similar manner to nerve-mediated contraction, the augmentation of nerve-mediated relaxatory responses seen during intracellular acidification persisted in the presence of substrate depletion. Simultaneous substrate depletion with intra- and/or extracellular acidosis had no effect on agonist-induced relaxation.

The effect of simulated ischaemia on relaxation in CSM is summarised in table 3.50.

*Table 3.50 - Effect of components of ischaemia applied in various combinations on CSM*

*relaxation*

| Intervention | Nerve-mediated relaxation | Agonist-induced relaxation |
|:---:|:---:|:---:|
| **HIAS** | suppressed, reversible | abolished, reversible |
| | Rapid detrimental effect. Reversible upon reperfusion | |
| **HS** | suppressed, reversible | 30 min suppressed, 60 min abolished |
| **HAS** | suppressed, reversible | abolished, reversible |
| **HIS** | suppressed, reversible | suppressed, reversible |
| | Detrimental effect of HIAS due to combined effect of hypoxia, extracellular acidosis and substrate depletion (HAS). Effect reversible upon reperfusion | |
| **IA** | no effect | no effect |
| **A** | no effect | no effect |
| **I** | augmented, reversible | no effect |
| | Intracellular acidification reversibly augments nerve-mediated responses | |
| **S** | no effect | no effect |
| **IAS** | suppression at low frequency, reversible | no effect |
| **AS** | ? augmented,? no effect | no effect |
| | Extracellular acidosis and substrate depletion suppressed nerve-mediated contraction | |
| **IS** | augmented, reversible | no effect |
| | Intracellular acidification limited detrimental effect of substrate depletion on contraction. Mechanism of augmentation not sensitive to substrate depletion | |
| **H** | abolished, reversible | abolished, reversible |
| | Hypoxia had marked reversible effect on relaxation | |
| **HIA** | suppressed, reversible | no effect |
| **HA** | suppressed, reversible | no effect |
| **HI** | suppressed, reversible | abolished, reversible |
| | Extracellular acidosis limited effect of hypoxia on carbachol-induced relaxation | |

## 3.6 Results VI – The effect of low temperature on CSM contractile function

### 3.6.1 Generation of low temperature solutions

The effect on CSM contractile function of reducing the superfusing solution to $21\pm1.0$ °C (room temperature Tyrode's) or $10\pm3$ °C (chilled Tyrode's) was recorded (section 2.3.6). Tyrode's solution at 37 °C was gassed with a 95% $O_2$/5% $CO_2$ mixture (pH $7.39\pm0.01$). This solution at reduced temperature was acidotic (21 °C Tyrode's – pH $7.20\pm0.01$, 13 °C Tyrode's pH $6.95\pm0.04$). Reduced temperature interventions were therefore compared to similar experiments at 37 °C in acidotic Tyrode's solution (Tyrode's gassed with a 90% $O_2$/10% $CO_2$ mixture - pH $6.96\pm0.03$). This was chosen as the comparator due to time constraints. The alternative would be to alter extracellular buffer concentration to compensate for increased $CO_2$ solubility.

### 3.6.2 Effect of low temperature on nerve-mediated contractions

Isometric nerve-mediated contractions elicited by EFS (range 8-60 Hz) were recorded as described in section 2.3.4. Preparations were equilibrated in Tyrode's solution for 60 min. at 37°C. At the end of this period, the mean nerve-mediated tension at 32 Hz ($EFS_{32Hz}$) was $0.46\pm0.24$ mN.mm$^{-2}$ (N=6, n=10) and was $58\pm11$% of the estimated maximal tension ($T_{max}$) from the force-frequency curves. The mean half-maximal frequency ($f_{½}$) under these control conditions was $27.7\pm8.3$ Hz. The effect of temperature reduction to 21 °C on nerve-mediated contraction was examined (figs. 4.1 and 4.2 and table 4.1). For comparison, combined intra- and extracellular acidosis at 37 °C had no effect on the parameters measured during a similar time course (section 3.2.2.3).

*Table 4.1 - Effect of temperature reduction to 21 °C on nerve-mediated contraction*

*\* p<0.05 compared to control.*

*Reduction of superfusate temperature to 21 °C for 30 min. significantly reduced both the mean EFS$_{32Hz}$ to 56±14% and f$_{½}$ to 14.7±2.0 Hz. Parameters returned to control values upon reperfusion with Tyrode's solution at 37 °C for 60 min.*

| N=5, n=5 | Control | 30 min 21°C | 60 min 21°C | Reperfusion |
|:---:|:---:|:---:|:---:|:---:|
| pH | 7.39±0.01 | 7.20±0.01 | | 7.39±0.01 |
| EFS$_{32Hz}$ (mN.mm$^{-2}$) | 0.42±0.24 | 0.25±0.18 * | 0.26±0.17 * | 0.40±0.24 |
| EFS$_{32Hz}$ As % control | - | 56±14 * | 61±14 * | 95±21 |
| EFS$_{f½}$ as % of control (%) | - | 35 | 33 | 114 |
| f$_{½}$ (Hz) | 31.6±9.6 | 14.7±2.0 * | 14.3±1.6 * | 40.9±31.6 |



1 mN

2 min

| 8  16 24 32 40 60 | 8  16 24 32 40 60 | 8  16 24 32 40 60 | 8  16 24 32 40 60 |
|:---:|:---:|:---:|:---:|
| Control (37 °C) | 30 min at 21°C | 60 min 21°C | Reperfusion |
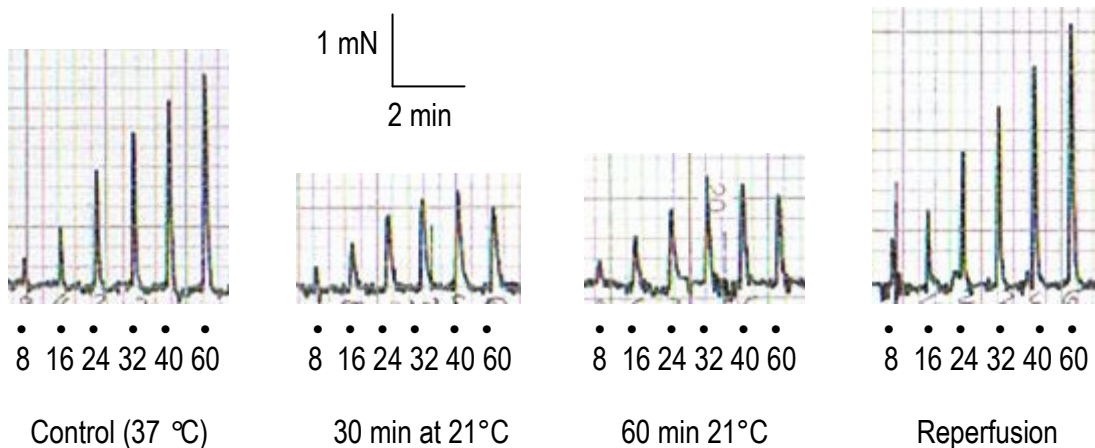
*Fig. 4.1 - Typical experimental tracing temperature reduction to 21 °C on nerve-mediated contraction (EFS 8-60 Hz)*

*Fig. 4.2 – Effect of temperature reduction to 21 °C on nerve-mediated contraction*

○ – control, ▢ - 30 min 21 °C , ◇ – 60 min 21 °C , Δ – reperfusion

* significant reduction compared to control (p<0.05)

When expressed as a percentage of $EFS_{f½}$ under control conditions, $EFS_{f½}$ after 30 min. of reduced temperature was significantly reduced at 21 °C to 35%.

Similar experiments were carried out examining the effect of temperature reduction to 13 °C on nerve-mediated contraction (figs. 4.3 and 4.4 and table 4.2).

*= p<0.05 compared to control*

*Reduction of superfusate temperature to 13 °C for 30 min. significantly reduced both the mean*

*EFS$_{32Hz}$ to 52±6% and f$_{1/2}$ to 10.5±2.4 Hz. Parameters returned to control values upon reperfusion*

*with Tyrode's solution at 37 °C for 60 min.*

| N=5, n=5 | Control | 30 min 13°C | 60 min 13°C | Reperfusion |
|---|---|---|---|---|
| pH | 7.38±0.01 | 6.95±0.04 | | 7.38±0.01 |
| EFS$_{32Hz}$ (mN.mm$^{-2}$) | 0.50±0.27 | 0.26±0.15 * | 0.25±0.17 * | 0.49±0.29 |
| EFS$_{32Hz}$ As % control | - | 52±6 * | 51±9 * | 99±15 |
| EFS$_{f1/2}$ as % of control (%) | - | 38 | 35 | 98 |
| f$_{1/2}$ (Hz) | 23.8±4.9 | 10.5±2.4 * | 11.2±2.7 * | 23.5±8.0 |



1 mN

2 min

8 16 24 32 40 60     8 16 24 32 40 60     8 16 24 32 40 60     8 16 24 32 40 60

Control (37 °C)          30 min at 13°C           60 min 13°C              Reperfusion
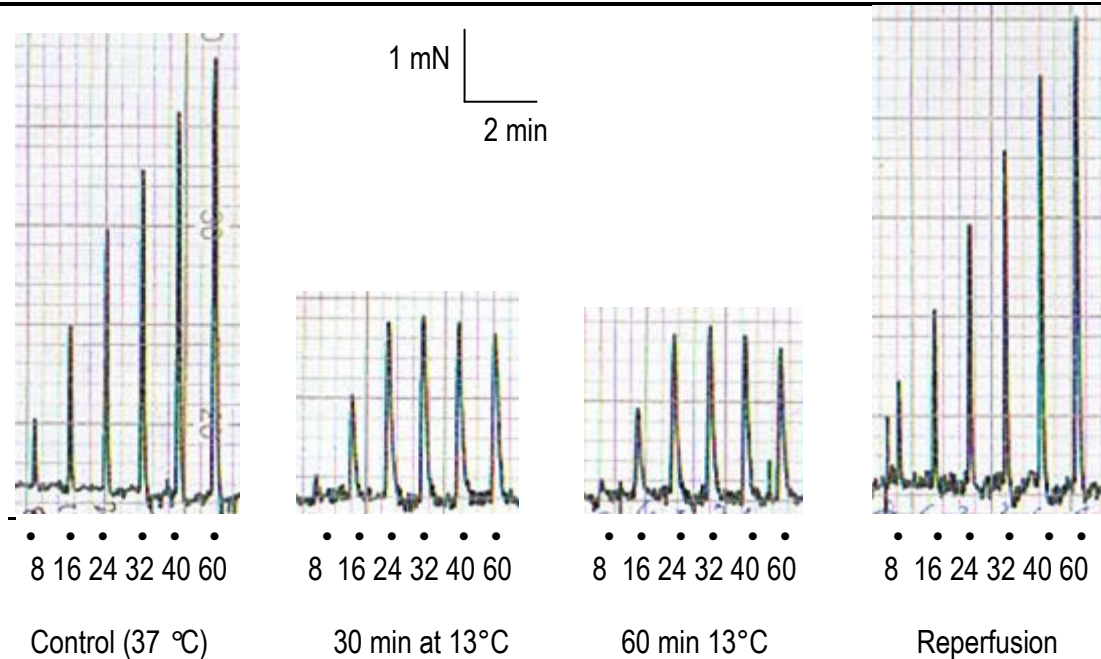
*Fig. 4.3 – Typical experimental tracing of effect of temperature reduction to 13 °C on nerve-mediated contraction (EFS 8-60 Hz)*
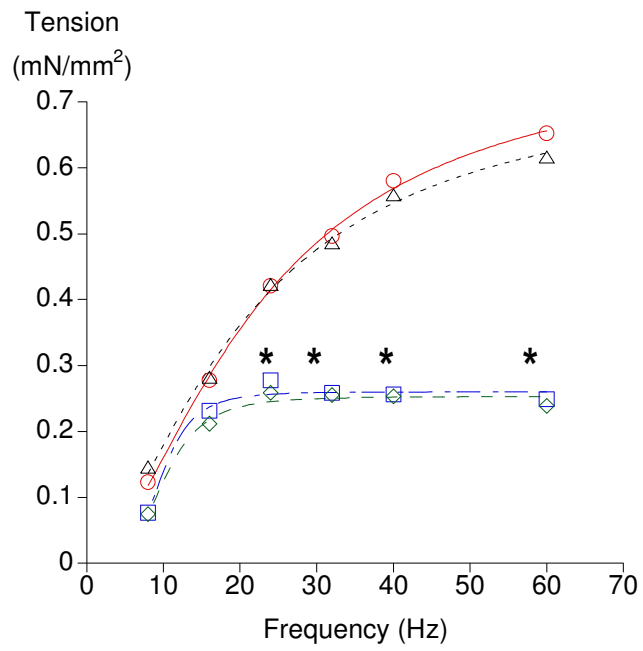
*Fig. 4.4 – Effect of temperature reduction to 13 °C on nerve-mediated contraction*

*○ – control, □ - 30 min 13 °C , ◇ – 60 min 13 °C , Δ – reperfusion*

*\* significant reduction compared to control (p<0.05)*

*When expressed as a percentage of $EFS_{f½}$ under control conditions, $EFS_{f½}$ after 30 min. of reduced temperature was significantly reduced at 13 °C to 38%.*

It was postulated that the amelioration of tension generated in response to EFS at reduced temperature could be secondary to reduced motor nerve recruitment. To investigate this possibility the effect of increasing voltage on EFS contractions was recorded. At 37 °C, increasing voltage (40-80 V) increased force of TTX-sensitive contraction. However, above 50 V, this increase in contractile force was not significant (section 3.1.1.3).
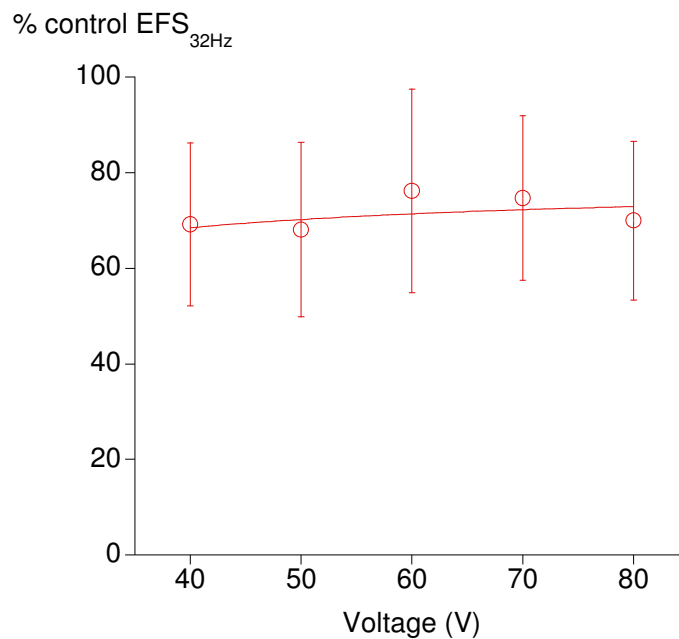


*Fig. 4.5 – Effect of reduced temperature to 21°C on EFS$_{32Hz}$ contraction at differing voltages*

*(N=4, n=6), Voltage range 40-80 V.*

*A reduction to 21 °C for 30 min. depressed the EFS response (8-60 Hz) in a consistent manner from 40 V to 80 V. EFS$_{32Hz}$ at 40 V were significantly reduced to 69±17% of control, at 50 V to 68±18% of control with EFS returning to normal upon reperfusion. Recordings were similar throughout the frequency range at 60 V, 70 V and 80 V. These findings are consistent with nerve recruitment not contributing to the reduced magnitude of EFS contractions at 21 °C.*

Experiments were repeated at 13 °C.
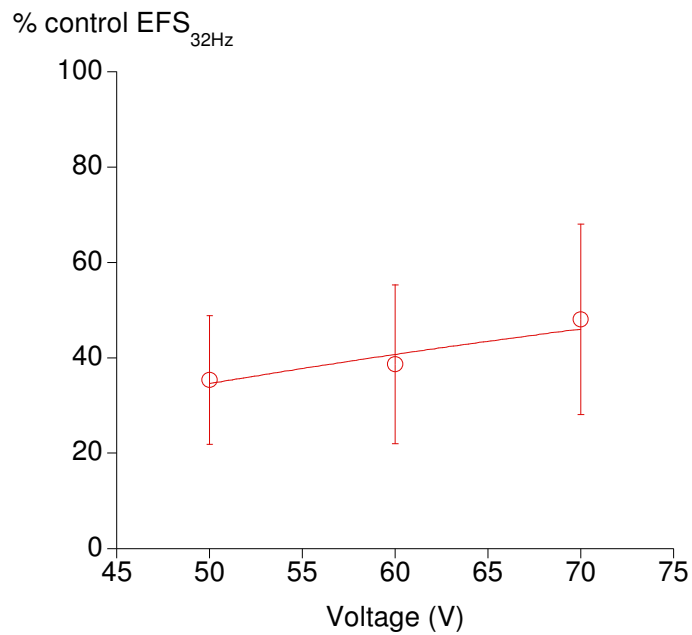
*Fig. 4.6 – Effect of reduced temperature to 13°C on EFS$_{32\,Hz}$ contraction at differing voltages*

*(N=4, n=6), Voltage range 50-70 V.*

*13 °C for 30 min. consistently reduced the EFS response between 50 V and 70 V. EFS$_{32Hz}$ at 50*

*V were significantly reduced to 35.4±13.5% of control with similar results recorded at 60 V and 70*

*V. All responses returned to normal upon reperfusion with Tyrode's at 37 °C. These findings are*

*consistent with nerve recruitment not contributing to the reduced magnitude of EFS contractions*

*at 13 °C.*

To assess whether low temperature affected the time course of the phasic contraction, the paper

speed was increased to 25 mm.s$^{-1}$ for the final 60 Hz stimulation of each force-frequency

estimation in these voltage experiments. The time-constant (τ) was measured as described in

section 2.3.4 (Table 4.3).

*p<0.05 compared to control*

*At 50 V, the time-constant of the relaxatory phase ($\tau_{relaxation}$) at 13°C almost doubled. significantly*

*prolonged from 5.5±0.7 s to 9.9±3.0 s. At 60 V and 70 V both the time-constant of the contractile*

*phase ($\tau_{contraction}$) and $\tau_{relaxation}$ were significantly prolonged. The time-constant of the relaxatory*

*phase was proportionately more prolonged compared to that of the contractile phase (60 V*

*$\tau_{contraction}$ 130±11% control, $\tau_{relaxation}$ 173±53% control). All responses returned to control values*

*upon reperfusion.*

| N=5, n=5 | | Control | Intervention | Reperfusion |
|---|---|---|---|---|
| | | 37 °C | 13 °C | 37 °C |
| 50 V | $\tau_{contraction}$ (s) | 2.6±0.4 | 2.7±0.6 | 2.3±0.2 |
| | $\tau_{relaxation}$ (s) | 5.5±0.7 | 9.9±3.0 * | 5.9±1.0 |
| 60 V | $\tau_{contraction}$ (s) | 2.3±0.2 | 3.0±0.4 * | 2.3±0.2 |
| | $\tau_{relaxation}$ (s) | 6.0±0.7 | 10.3±2.8 * | 6.5±0.8 |
| 70 V | $\tau_{contraction}$ (s) | 2.4±0.4 | 3.3±0.5 * | 2.4±0.4 |
| | $\tau_{relaxation}$ (s) | 6.6±0.6 | 10.1±2.5 * | 6.8±0.8 |

These findings may be due to changes in the biomechanical properties of the tissue and/or

molecular mechanisms mediating contraction and relaxation. This was further explored in section

3.6.6. Subsequent experiments examined the effect of reduced temperature on nerve-mediated

relaxation.

3.6.3    Effect of low temperature on nerve-mediated relaxation


Isometric nerve-mediated relaxations were elicited in response to EFS (range 4-24 Hz) in pre-

contracted muscle strips as described in section 2.3.4. Preparations equilibrated in Tyrode's

solution for 60 min. at 37 °C. At the end of this equilibration period, the mean plateau PE

response was $0.44\pm0.20$ mN.mm$^{-2}$. The plateau PE contracture was stable during the

intervention. Tension remaining after nerve-mediated relaxation at 24 Hz (EFS$_{24Hz}$) was

$0.26\pm0.15$ mN.mm$^{-2}$ ($58\pm21$ % of the preceding PE contracture). Reduction in superfusate

temperature to 21°C on nerve-mediated relaxation was examined (table 4.4 and fig. 4.7).
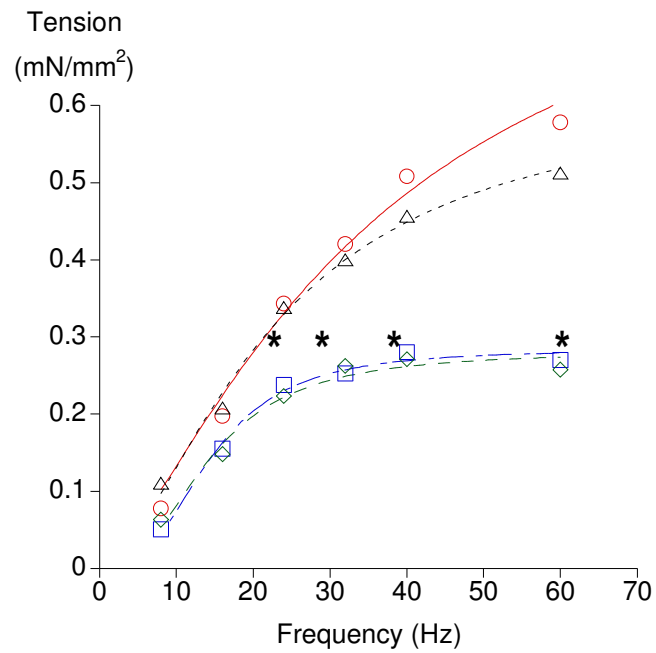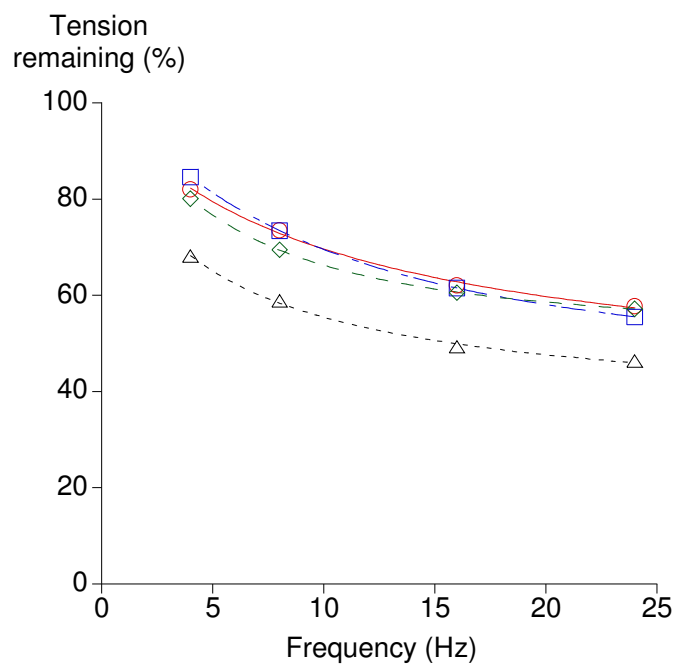


*Fig. 4.7 – Effect of reduced temperature to 21 °C on nerve-mediated relaxation*

*○ – control, □ - 30 min 21 °C , ◊ – 60 min 21 °C , Δ – reperfusion*

*The trend for nerve-mediated relaxation was to increase in magnitude with time (section 3.1.3.1).*

*Reduction in superfusate temperature to 21 °C suppressed this trend; relaxatory responses*

*remained at control values for the duration of the intervention. Return to 37 °C brought about a*

*return to the normal trend.*

_Table 4.4 - Effect of reduced temperature to 21°C on nerve-mediated relaxation_

| N=7, n=8 | Control 37 °C | 30 min 21 °C | 60 min 21°C | Reperfusion 37 °C |
|---|---|---|---|---|
| Plateau PE contracture ($mN.mm^{-2}$) | 0.44±0.20 | 0.50±0.24 | 0.42±0.20 | 0.47±0.24 |
| Tension remaining after $EFS_{24Hz}$ ($mN.mm^{-2}$) | 0.26±0.15 | 0.29±0.16 | 0.25±0.14 | 0.23±0.17 |
| $EFS_{24Hz}$ as % preceding PE plateau contracture | 58±21 | 56±24 | 57±26 | 46±24 |

A reduction of superfusate temperature to 13°C was subsequently examined (fig. 4.8 and table 4.5).

Preparations were equilibrated in Tyrode's solution for 60 min. at 37 °C. At the end of this equilibration period, the mean plateau PE response was 0.64±0.28 $mN.mm^{-2}$. The plateau PE contracture was stable during the intervention. Tension remaining after nerve-mediated relaxation at 24 Hz ($EFS_{24Hz}$) was 0.41±0.16 $mN.mm^{-2}$ (65±7 % of the preceding PE contracture). The effect of reduction to 13°C on nerve-mediated relaxation was recorded. In comparison, 60 min of intra- and extracellular acidosis (IA) had no effect on nerve-mediated relaxation (section 3.4.2.3, page 171).

*Table 4.5 - Effect of reduction to 13°C on nerve-mediated relaxation*

*Amelioration of EFS relaxation was more marked than that noted during a reduction of Tyrode's to 21°C.*

| N=7, n=8 | Control 37 °C | 30 min 13 °C | 60 min 13°C | Reperfusion 37 °C |
|---|---|---|---|---|
| Plateau PE contracture (mN.mm$^{-2}$) | 0.64±0.28 | 0.66±0.35 | 0.59±0.34 | 0.67±0.29 |
| Tension remaining after EFS$_{24Hz}$ (mN.mm$^{-2}$) | 0.41±0.16 | 0.50±0.25 | 0.44±0.22 | 0.39±0.18 |
| EFS$_{24Hz}$ as % preceding PE plateau contracture | 65±7 | 77±10 | 77±9 | 58±11 |
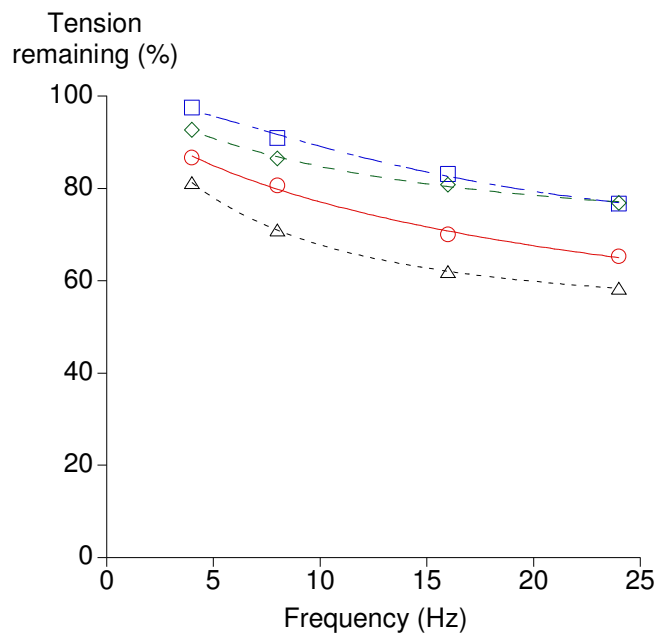


*Fig. 4.8 – Effect of reduced temperature to 13°C on nerve-mediated relaxation*

○ – control, ▢ - 30 min 13 °C , ◇ – 60 min 13 °C , Δ – reperfusion

*Reduction in superfusate temperature to 13 °C significantly depressed nerve-mediated*

*relaxation. Responses returned to normal upon reperfusion at 37 °C.*

Low temperature superfusate reduced the magnitude of nerve-mediated relaxation in CSM. In

addition, the time course of EFS relaxation appeared to be markedly affected at these reduced

temperatures. To examine this, a similar set of experiments were conducted as described in

section 2.3.4. These also involved pre-contracting the tissue with 15 μM PE after a period

equilibration in Tyrode's solution at 37 °C. Once the contracture had reached a plateau, a single

pulse train of EFS at 16 Hz was used to elicit a relaxation ($EFS_{16Hz}$). This protocol was repeated

at low temperature and upon reperfusion (table 4.6).

*Table 4.6 - Effect of reduced temperature to 13°C on time constants of $EFS_{16\,Hz}$ relaxations*

*\* p<0.05 compared to control*

*The time-constant of relaxation ($\tau_{relaxation}$) was unaffected by low temperature superfusion fluids.*

*However, contraction following EFS mediated relaxation was significantly prolonged at 13 °C and*

*returned to control values upon reperfusion.*

| N=4, n=6 | Control | Intervention | Reperfusion |
|---|---|---|---|
| | 37 °C | 13 °C | 37 °C |
| $\tau_{relaxation}$ (s) | 11.0±1.1 | 16.0±7.7 | 12.7±3.7 |
| $\tau_{contraction}$ (s) | 64.7±14.2 | 125.3±33.4 * | 54.0±12.8 |

3.6.4    Effect of low temperature on agonist-induced contractures

Isometric agonist-induced contractures were recorded as described in section 2.3.5. At the end of

the equilibration period, mean peak tension achieved was 0.57±0.22 $mN.mm^{-2}$ and mean plateau

tension was 0.48±0.18 $mN.mm^{-2}$ (N=6, n=6). The effect of a reduction in superfusate temperature

to 21 °C for 60 min was recorded (table 4.7). In comparison up to 120 min. of intra- and extracellular acidosis on PE-contractures had no effect on the magnitude of PE contractures (section 3.3.4.4 - page 165 and table 3.32 - page 166).

*Table 4.7 - Effect of reduction of temperature to 21°C on agonist-induced contractures*

*A reduction of temperature to 21°C had no effect on the magnitude of the PE contracture.*

| Intervention | Peak tension (mN.mm$^{-2}$) | Plateau tension (mN.mm$^{-2}$) |
|---|---|---|
| 60 min 37 °C Tyrodes | 0.57±0.22 | 0.48±0.18 |
| 30 min 21 °C Tyrodes | 0.59±0.23 | 0.54±0.24 |
| 60 min 21 °C Tyrodes | 0.52±0.21 | 0.51±0.22 |
| Reperfusion at 37 °C | 0.58±0.21 | 0.52±0.20 |

The effect of a reduction to 13 °C was also examined. The mean peak tension achieved after equilibration was 0.59±0.21 mN.mm$^{-2}$ (N=5, n=5) and mean plateau tension was 0.51±0.21 mN.mm$^{-2}$ (table 4.8).

*Table 4.8 - Effect of reduction of temperature to 13°C on agonist-induced contractures*

*A reduction to 13 °C for 60 min had no effect on the magnitude of the PE contracture.*

| Intervention | Peak tension (mN.mm$^{-2}$) | Plateau tension (mN.mm$^{-2}$) |
|---|---|---|
| 60 min 37 °C Tyrodes | 0.59±0.21 | 0.51±0.21 |
| 30 min 21 °C Tyrodes | 0.64±0.25 | 0.58±0.27 |
| 60 min 21 °C Tyrodes | 0.56±0.27 | 0.55±0.27 |
| Reperfusion at 37 °C | 0.70±0.27 | 0.58±0.26 |

To examine whether low temperature had an effect on the duration of these agonist-induced contractures, the time-constants were measured as shown in section 2.3.5 and fig. 2.9 (page 80).

*Table 4.9 - Effect of reduction of temperature to 21 °C on tonic contracture time-constants*

*\* p<0.05 compared to control*

*Both the time-constant of the contractile phase ($\tau_{contraction}$) and that of the relaxatory phase ($\tau_{relaxation}$) were significantly prolonged during superfusion with Tyrode's solution at 21 °C with the former parameter more severely affected. Time-constants of agonist-induced contractures during simultaneous intra- and extracellular acidosis were unaffected.*

| N=5, n=5 | 37 °C | 30 min 21 °C | 60 min 21 °C | reperfusion |
|---|---|---|---|---|
| $\tau_{contraction}$ (s) | 83±41 | 120±41 * | 195±62 * | 173±218 |
| $\tau_{relaxation}$ (s) | 270±56 | 413±135 * | 405±97 * | 263±113 |

*Table 4.10 - Effect of reduction of temperature to 13 °C on tonic contracture time-constants*

*\* p<0.05 compared to control*

*Again both the time-constant of the contractile phase ($\tau_{contraction}$) and that of the relaxatory phase ($\tau_{relaxation}$) were significantly prolonged during superfusion with reduced temperature Tyrode's solution with the former parameter more severely affected.*

| N=5, n=5 | 37 °C | 30 min 13 °C | 60 min 13 °C | 37 °C |
|---|---|---|---|---|
| $\tau_{contraction}$ (s) | 68±31 | 105±17 * | 165±57 * | 68±31 |
| $\tau_{relaxation}$ (s) | 270±41 | 420±81 * | 435±98 * | 263±53 |

3.6.5    Effect of low temperature on agonist-induced relaxation

Isometric relaxation in response to 1 µM carbachol (C) muscle strips pre-contracted with 15 µM phenylephrine (PE) were recorded as described in section 2.3.5. Preparations equilibrated in Tyrode's solution for 60 min. at 37 °C. At the end of this period, PE was added to the superfusing solution and the resulting contracture recorded. Once this had reached a plateau, relaxation in response to carbachol was recorded. The effect of 60 min. of reduction to 21 °C and 13 °C was examined on both the nadir and plateau C relaxation (tables 4.11 and 4.12). For comparison, simultaneous intra- and extracellular acidosis at 37 °C had no effect on carbachol relaxation (section 3.5.2.3 and table 3.46 – page 207).

*Table 4.11 – Effect of reduced temperature to 21°C on agonist-induced relaxation*

*The plateau PE contracture was stable during the intervention. No change in agonist-induced relaxation was observed during reduction of superfusate temperature to 21 °C.*

| N=6, n=6 | Control 37 °C | 30 min 21 °C | 60 min 21 °C | Reperfusion 37 °C |
|---|---|---|---|---|
| Plateau PE contracture ($mN.mm^{-2}$) | 0.48±0.18 | 0.54±0.24 | 0.51±0.22 | 0.52±0.20 |
| Nadir C relaxation ($mN.mm^{-2}$) | 0.30±0.14 | 0.29±0.13 | 0.30±0.14 | 0.29±0.15 |
| Nadir C relaxation as % of preceding PE contracture | 63±22 | 56±18 | 62±23 | 57±24 |
| Plateau C relaxation ($mN.mm^{-2}$) | 0.33±0.15 | 0.29±0.13 | 0.30±0.14 | 0.31±0.15 |
| Plateau C relaxation as % of preceding PE contracture | 69±19 | 57±19 | 63±24 | 63±23 |

*Table 4.12 – Effect of reduced temperature to 13°C on agonist-induced relaxation*

*The plateau PE contracture was stable during the intervention. No change in agonist-induced relaxation was observed during reduction of superfusate temperature to 13 °C.*

| N=5, n=5 | Control 37 °C | 30 min 13 °C | 60 min 13 °C | Reperfusion 37 °C |
|---|---|---|---|---|
| Plateau PE contracture (mN.mm$^{-2}$) | 0.59±0.21 | 0.64±0.25 | 0.56±0.27 | 0.70±0.27 |
| Nadir C relaxation (mN.mm$^{-2}$) | 0.34±0.17 | 0.34±0.22 | 0.34±0.23 | 0.30±0.19 |
| Nadir C relaxation as % of preceding PE contracture | 65±15 | 57±18 | 57±21 | 49±19 |
| Plateau C relaxation (mN.mm$^{-2}$) | 0.34±0.17 | 0.35±0.21 | 0.34±0.23 | 0.33±0.19 |
| Plateau C relaxation as % of preceding PE contracture | 66±16 | 58±18 | 58±23 | 54±18 |

3.6.6    Effect of low temperature on stiffness of CSM

In order to examine whether the changes in CSM function identified were due to changes in the biomechanical properties of the tissue at low temperature, the stress / strain characteristics in chilled Tyrode's were compared as described in section 2.4.2.

Strips were placed under similar strains during control, intervention and reperfusion phases of the experiments (0.5±0.8 %, 0.5±0.7 % and 0.6±0.9 % respectively). During each phase of the experiment a linear relationship between stress and strain was confirmed as described in section 2.4.2. A diagrammatic representation of a typical strip response to an instantaneous stress is shown in fig. 4.9.
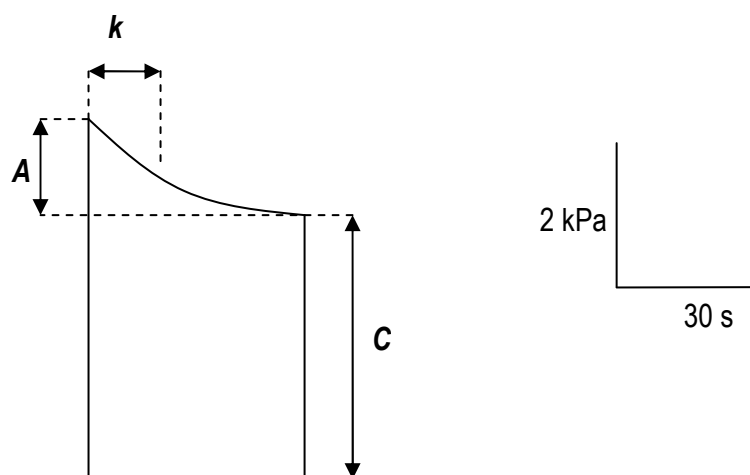
*Fig. 4.9 – Diagram of typical strip response to instantaneous stress*
*__A__ – Magnitude of viscous component of strain. __C__ – Magnitude of steady-state component of strain. __k__ – time-constant of relaxation following instantaneous stress.*

The viscous component of instantaneous stress (fig. 4.9 – __A__) was significantly reduced at low temperature (control 37 °C, 26.9±10.4 kPa/mm *vs.* intervention 13 °C, 24.7±9.9 kPa/mm) returning to control values upon reperfusion (table 4.13). The time-constant of the relaxation to steady-state stress (fig. 4.9 – __k__) was unaffected by low temperature and remained at control values upon reperfusion.

The steady-state component of stress (fig. 4.9 – __C__) was significantly increased at low temperature (control 37 °C, 47.8±38.5 kPa/mm vs. intervention 13 °C, 53.4±43.5 kPa/mm) returning to control values upon reperfusion.

When __A__ was expressed as a percentage of the total instantaneous stress (__A+C__), no difference was seen during intervention or upon reperfusion (table 4.13).

Young's modulus (e) was increased at cold temperature and returned towards control values upon reperfusion. However these changes were not statistically significant (control 37 °C, 57.0±6.4, intervention 13 °C, 71.6±17.2, reperfusion 37 °C, 45.4±20.2).

*Table 4.13 – Stress/strain characteristics of CSM at low temperature, 13°C*

*\* p<0.05 compared to control*

*These findings indicate that CSM becomes stiffer at low temperature and that this increase in stiffness is matched by a concurrent reduction in the viscous component of the tissue. The time-constant of relaxation at reduced temperatures is unchanged; changes in contraction and relaxation characteristics seen in sections 3.6.2, 3.6.3 and 3.6.4 cannot be explained by changes in the biomechanical properties of the tissue at reduced temperatures.*

| N=6, n=12 | Control 37 °C | Intervention 13 °C | Reperfusion 37 °C |
|---|---|---|---|
| Strain (%) | 0.5±0.8 | 0.5±0.7 | 0.6±0.9 |
| viscous component instantaneous stress - A (kPa/mm) | 26.9±10.4 | 24.7±9.9* | 27.3±11.3 |
| steady-state component stress - C (kPa/mm) | 47.8±38.5 | 53.4±43.5* | 43.4±36.4 |
| A / (A+C) (%) | 26±10 | 23±9 | 29±12 |
| *Young's modulus – e* | 57.0±6.4 | 71.6±17.2 | 45.4±20.2 |
| *Time-constant stress-relaxation – k (s)* | 10.3±3.7 | 9.6±3.5 | 9.6±3.5 |

3.6.7    Effect of reduced temperature on CSM function – results summary

Modification of the experimental set-up was straightforward and enabled low temperature solutions to be delivered to the superfusion chamber in a reliable and reproducible manner. A reduction in pH occurred because of the increased solubility of perfusing gas mixture $CO_2$ in the reduced temperature superfusate. Low temperature interventions were therefore compared to the effect of acidosis on CSM. The findings summarised below were more marked at 13 °C when compared to 21 °C.

Reduction in superfusate temperature significantly suppressed nerve-mediated contraction. This was not due to reduced recruitment of nerve fibres at low temperature. In addition, the time-course of phasic nerve-mediated contractions was prolonged, slowing responses significantly. This was not due to changes in the biomechanical parameters measured at 21 °C or 13 °C. In contrast, the magnitude of agonist-induced contraction was unaltered by reduction in temperature. However, there was a significant reduction in the speed of the response with both the contractile and relaxatory components of the PE-contracture affected.

Nerve-mediated relaxation was significantly ameliorated at low temperatures. The phasic relaxation was also prolonged with the 'contractile' aspect (the return to pre-contracted tension following EFS-mediated relaxation) slowed to a greater degree than the initial relaxatory response. No change in magnitude of agonist-induced relaxation was observed.

This prolongation of responses at reduced temperature was not due to a change in the biomechanical properties of the tissue. The time-constant of the instantaneous stress/relaxation relationship remained constant at reduced temperatures. Although CSM became stiffer at low

temperature, this was matched by a concurrent reduction in the viscous component of the tissue. The effects of reduced temperature on CSM are summarised in table 4.14.

*Table 4.14 - The effect of reduced temperature on CSM*

| Parameter | Effect of reduced temperature |
|:---:|:---:|
| **Nerve-mediated contraction** | |
| Force-frequency relationship | Significant reversible depression of magnitude of nerve-mediated contraction. Reversible shift of $f_{\frac{1}{2}}$ to the left. |
| Force-voltage relationship | Depression of nerve-mediated contraction not attributable to decreased nerve recruitment |
| Time-constants | Time-constants prolonged at low-temperature |
| **Nerve-mediated relaxation** | |
| Force-frequency relationship | Reversible depression of nerve-mediated relaxation |
| Time-constants | Time-constants prolonged at low-temperature |
| **Agonist-induced contraction** | |
| Magnitude of peak and plateau responses | No effect |
| Time-constants | Time-constants prolonged at low temperature |
| **Agonist-induced relaxation** | |
| Magnitude of nadir and plateau responses | No effect |
| **Stress/strain characteristics** | |
| Viscous component | Reduced in magnitude, no change in stress-relaxation time-constants |

**4.0** **Discussion**

4.1 **Experimental limitations**

Experiments utilising muscle strips used small tissue preparations of approximately 1 mm in width and 4-6 mm in length. Adequate superfusion of the tissue was ensured by using such small samples. This was particularly important when examining the effect of the elements of ischaemia as any inadvertent metabolic depletion secondary to suboptimal superfusion may have affected the results recorded. There was considerable variability in tension generated between muscle strips from the same animal. This may be a consequence of the amount of connective tissue in the sample(207, 208). However, tension generated during interventions was compared to control and reperfusion responses within the same muscle strip, utilising a method of internal control.

Relaxatory responses were dependent upon the level of pre-contraction of the specimen(193). During interventions that affected this level of pre-contraction, changes to the relaxatory response had to be commented upon with care. During control experiments in unmodified Tyrode's solution, carbachol-induced relaxation was stable in magnitude. EFS-mediated relaxation invariably demonstrated a shift to the left of the relaxation-frequency relationship with increasing time. Responses during interventions were therefore compared to the trends seen during control experiments. For example if an intervention abolished or ameliorated relaxation whereas during control experiments these relaxations were increased with time, this intervention was interpreted to have had an effect. Therefore, subtle changes to CSM relaxatory function were difficult to elucidate. Other researchers postulated that this shift to the left of the relaxation/frequency relationship may be secondary to inducible NOS (iNOS) production. However, in our own study this left shift was not seen with carbachol induced relaxation. The decision was therefore made to

use the methodology described rather than attempt to manipulate iNOS production. However future experiments may include investigation of the mechanism of this progressive augmentation of nerve-mediated relaxation (with the addition of aminoguanidine for example)(71).

Several other researchers added additional chemicals to perfusing solutions to suppress aspects of contraction or relaxation that were not being examined. These include:

- L-NAME and L-NOARG    inhibit nitric oxide synthase

- Indomethacin     inhibit cycloxygenase, preventing prostanoid production

- Scopolamine    inhibit acetylcholine

- Guanethidine    inhibit NA release from adrenergic nerves

In these experiments the decision was made not to use these agents. The effect of ischaemia was examined on overall CSM function; blocking various mechanisms may have deleterious effects that were not translatable to the clinical condition.

CSM cell isolation proved to be time-consuming. The technique in this type of smooth muscle had not been established and required attempts with various protocols before a consistently useful method was found. Functioning cell harvest was excellent with 20-30 cells per high-powered field being available for subsequent experiments. Unfortunately, proposed examination of the effect of interventions on intracellular pH (BCECF loading) and $NADP^+$/NADPH ratios (autofluorescence) was not carried out due to time constraints.

Isolated cell experiments were undertaken on a modified microscope stage with a warmed perfusion chamber. The surface area of the chamber was large and the depth of superfusing fluid

thin. This raises the possibility of significant diffusion of room air into the superfusing solution during interventions. Hypoxic interventions on isolated cells may not be directly comparable to muscle strip experiments because of this. Due to the small amounts of fluid on the microscope at any one time, measurement of $PO_2$ was not possible.

## 4.2 Results overview

The aim of this thesis was to ascertain the contribution of the various components of ischaemia to contractile failure in cavernosal smooth muscle and to characterise the cellular mechanisms underlying this failure. Observations made during these experiments were in five main areas:

1. The use of this preparation to examine the effect of ischaemia

2. The effect of simulated ischaemia on cavernosal smooth muscle and the components contributing to contractile failure

3. The effect of hypoxia on relaxatory responses

4. The effect of acidosis on contractile function

5. The effect of reduced temperature on CSM function

The following discussion will focus on each of these areas in turn.

### 4.2.1 Validity of using guinea-pig CSM

Initial experiments were to establish whether this preparation could be used to study the effects of ischaemia. In the first instance it was important to examine whether the preparation was stable over the time course of the experiments proposed.

For EFS-mediated isometric tension experiments, stimulation parameters used (preparations were stimulated every 90 s with a 3 s pulse train at 8-60 Hz, 0.1 ms pulse width and at 50 V) provided a stable preparation over 240 minutes. In addition, over 95% of the tension generated using these stimulation parameters was via embedded motor nerves rather than direct muscle stimulation. However, there were marked differences in absolute tension values generated by different muscle strips, even if they were from the same animal. This may have been due to differences in smooth muscle content or embedded nerve density(207, 208). The former is more likely as similar differences were noted during PE contracture experiments. Over 700 muscle strip experiments were carried out, the findings of which form the bulk of this body of work. Very little spontaneous activity was recorded in muscle strips during this time, a possible advantage over other animal models described(182).

In order to contrast with experiments examining nerve-mediated contraction, direct muscle  the proposed duration of experiments (240 min). Responses consisted of an initial peak response followed by a plateau contracture, typically 85% of the initial peak recorded. The majority of this PE-induced contracture is postulated as utilising intracellular $Ca^{2+}$ stores rather than influx of extracellular $Ca^{2+}$ as demonstrated by the large proportion of nifedipine-resistant tension generated in response to PE. Both the peak and plateau response were ameliorated to a similar degree by nifedipine. This is similar to findings in rabbit and human CSM. Sparwasser *et al.* used CSM retrieved during penile implant insertion for erectile dysfunction(176, 177). After incubation in $Ca^{2+}$-free solution, phenylephrine-induced contractures were reduced to 64±6 % of control. Ryanodine further ameliorated PE-contractures to 30±6 % of control with the addition of caffeine further reducing contraction to 11 %. Further experiments on agonist-induced contraction in guinea-pig CSM could explore the following with a view to defining the underlying mechanisms of contraction:

1. Alternative routes of calcium entry

   a. Use of $Ca^{2+}$-free superfusate

   b. Non-specific cation channel antagonists (flufenamic acid and ruthenium red)

   c. $Na^+/Ca^{2+}$ exchanger antagonists

2. Calcium sensitisation

   a. Rho-kinase inhibitors

3. Intracellular calcium stores

   a. Caffeine

   b. TMB-8, a putative intracellular Ca2+ release inhibitor(209).

Nerve mediated relaxation was examined by subjecting pre-contracted muscle strips to EFS. Strips were periodically contracted as opposed to continuously superfused with phenylephrine in order to minimise fatigue in the strip due to prolonged periods in a maximally contracted state. Increasing frequency of stimulation elicited progressively larger relaxations in the pre-contracted strips. This relaxation was largely abolished in the presence of TTX indicating that the relaxation was nerve-mediated. In addition, ODQ produced a similar reduction in EFS-mediated relaxation indicating that the relaxation was mediated via nitric oxide. Interestingly there was a degree of relaxation that persisted in the presence of ODQ. The mechanism of this ODQ resistant relaxation was not elucidated. Sources of nitric oxide independent relaxation include the endothelial 15-lipoxygenase-1 (15-LO-1) metabolites of arachidonic acid(210).

The force-frequency relationship was not stable over the time course of experiments examining EFS-mediated relaxation (240 min). The curve shifted to the left with time indicating that the relaxatory mechanisms became more sensitive to EFS over time. Inducible nitric oxide synthase (iNOS) has implicated in this augmentation of relaxation with time. However, Nangle et al. saw no

increase in the maximal EFS mediated relaxation in mice lacking the iNOS gene when compared to wild type(211). The magnitude of relaxation was dependent upon the level of pre-contraction(212). Several interventions examined in these experiments augmented or suppressed this level of pre-contraction. Therefore interpretation of the effect of interventions on relaxatory responses was more complex than those made on nerve-mediated and agonist-induced contraction. Tension remaining after stimulation at 24 Hz was the most stable parameter and was therefore used in subsequent experiments to examine the effect of ischaemia on this aspect of CSM function. In addition, the effect of interventions were compared to the trend in EFS relaxation observed under normal conditions, i.e. that the frequency response relationship demonstrated a left shift and increase in maximal relaxation with time.

Relaxation in cavernosal smooth muscle is mediated via both cavernosal nerves and the endothelium lining the lacunar spaces within the corporal bodies(86). To examine the effect of ischaemia on the overall relaxatory system, the cholinergic agonist carbachol was used. The response of pre-contracted strips was stable over the proposed time course of these experiments (240 min). Again responses were dependent upon the level of pre-contraction. As pre-contraction increased, carbachol relaxation was proportionately smaller in magnitude.

Single cell harvest was satisfactory with over 90% of cells selected for intervention responding to agonists in a stable manner. As outlined in experimental limitations (section 4.1), hypoxia may not have been as reproducible as in muscle strip experiments due to diffusion of room air into the superfusing fluid on the microscope stage.

4.2.2 The effect of simulated ischaemia and the components contributing to contractile failure

*Simulated Ischaemia*

Simulated ischaemia (the combination of hypoxia, acidosis and substrate depletion - HIAS) significantly reduced the magnitude of both nerve-mediated and agonist-induced contraction. In addition, the effect on nerve-mediated contraction was irreversible upon reperfusion over the time course of the experimental protocol.

The effect on nerve-mediated contraction was immediate (fig. 3.15, 30 min HIAS $EFS_{32Hz}$ - 53±30% control) and increased with longer periods of ischaemia (60 min HIAS $EFS_{32Hz}$ - 20±13% control). This was similar to the significant effect of HIAS on the plateau agonist-induced contracture (tension generated 36±35% control after 30 min HIAS; 29±16% control after 60 min HIAS). By contrast, the peak agonist contracture was relatively preserved initially (tension generated 83±30% control after 30 min HIAS; 35±19% control after 60 min HIAS). This indicates that the muscle has, at least initially, some metabolic reserve and/or mechanism of limiting contractile failure secondary to simulated ischaemia.

This concept was further explored by examining the effect of ischaemia on agonist-induced contraction in the presence of the L-type $Ca^{2+}$-channel blocker nifedipine. Intracellular stores contributed to the majority of the PE contracture under normal conditions (peak PE response 87±12% and plateau PE response 84±13% of control in the presence of nifedipine). Contractile responses were relatively preserved in the presence of nifedipine during the period of ischaemia (plateau PE response after 30 min HIAS 77±21% and plateau PE response after 60 min HIAS 66±31% of control in the presence of nifedipine). This raises the possibility that dysfunction of the L-type $Ca^{2+}$-channel contributes to the contractile failure seen during ischaemia. De Jongh *et al*.

postulated that receptor dysfunction was secondary to the production of reactive oxygen species (ROS) and showed that contraction in porcine detrusor strips was ameliorated in the presence of cumene hydroperoxide (CHP)(213). However, other researchers have shown that localised production of ROS may enhance L-type $Ca^{2+}$-channel activity. Amberg *et al.* used cerebral artery myocytes and co-localised L-type $Ca^{2+}$-channel sparklet activity with endogenous ROS production(214).

The initial preservation of peak PE response during ischaemia (which was preserved in the presence of nifedipine) would infer a degree of metabolic reserve. The concentration of high-energy phosphates (e.g. ATP) is reduced in CSM when compared to bladder detrusor for example(215). The normal cycle of penile erection and detumescence creates a closed compartment in the penis, CSM may be adapted to function more effectively whilst utilising anaerobic respiration than other smooth muscles. In addition, alternative mechanisms of increasing $[Ca^{2+}]_i$ may be utilised by cavernosal smooth muscle, at least initially, as shown by preservation of the peak PE response(176, 177, 216, 217).

At the end of 60 min reperfusion, nerve-mediated responses demonstrated no significant recovery in tension generated. In contrast, the agonist-induced response recovered completely after a similar period. This would infer that ischaemia induced some degree of nerve damage during the course of the experiment. It is difficult to say whether this was during the ischaemic episode or a reperfusion type injury. The fact that the peak-PE contracture was preserved at 30 min HIAS whereas the nerve-mediated response was significantly impaired at this time point would infer that the damage occurs during the ischaemic episode (fig. 5.1). Pessina *et al.* examined the effect of combined hypoxia and substrate depletion of human, monkey and guinea-pig detrusor strips(218, 219). Glycogen stores measured biochemically were reduced during

ischemic interventions. In addition, nerve-mediated contraction was irreversibly ameliorated during the course of experiments before any reduction in agonist-induced contraction was noted. The irreversible nerve damage was most marked in the guinea-pig model which had the lowest glycogen reserve of the three tissue sources studied. Glycogen stores were localised in the smooth muscle but not in intramural nerve ganglia. Juan *et al.* showed a significant reduction in nerve density following an ischaemic insult with some recovery noted 14 days post injury(220). Our own experimental findings support a differential effect of ischaemia, with nerves being the most susceptible initially with smooth muscle damage occurring later in the ischaemic episode.

Simulated ischaemia had a similar deleterious effect on relaxatory responses. Nerve-mediated relaxation was significantly reduced during the ischaemic intervention (fig. 3.38). However, in contrast to nerve-mediated contraction, relaxation recovered completely upon reperfusion(71). This suggests that relaxatory nerves are more resistant to ischaemic damage, a finding which would contribute to the pathogenesis of ischaemic priapism and the contractile failure observed in this condition(71). These findings are similar to those of Muneer *et al.* using a rabbit model of priapism. Relaxatory mechanisms were more resistant to ischaemia than CSM contraction. Agonist relaxation was similarly affected with responses significantly and reversibly reduced during simulated ischaemia.

*Hypoxia and substrate depletion*

Identical responses to those outlined above were seen when muscle strips were subjected to the combination of hypoxia and substrate depletion (HS depletion). It appears that the ability of CSM to contract and relax is severely affected by hypoxia and absence of glucose and Na pyruvate from the superfusate(218, 221). The exception to this finding was agonist-induced relaxation, which was initially preserved in the presence of HS depletion. The combination of hypoxia,

substrate depletion and extracellular acidosis did mimic simulated ischaemia in this aspect of CSM function. The presence of these conditions in corporal blood aspirates from men with low-flow priapism is well documented(35). However, they do not occur simultaneously during the ischaemic episode. Substrate depletion is a late finding, with undetectable blood glucose usually seen after 6-12 hours of priapism (fig. 5.2 - time course of blood gas changes in corporal aspirates during prolonged penile erection)(35). This would help to explain why response to current treatments for priapism are much improved early in the disease process prior to reduction in CSM response to PE and irreversible contractile nerve damage has occurred (usually during the first 6 hours)(222).

Simulated ischaemia had no effect on isolated CSM cells. However, the combination of hypoxia and substrate depletion significantly suppressed the second $Ca^{2+}$ transient during the ischaemic intervention. The differences observed between muscle strip and single cell experiments may be secondary to the longer intervention time in the muscle strip *vs.* isolated cell experiments (20 min. *vs.* 60 min.). In addition, the degree of hypoxia may have been less in single cell experiments due to differences in the experimental set-up as previously discussed. The reduction in $[Ca^{2+}]_i$ can also be attributed to utilisation of intracellular glycogen stores. Less ATP is liberated during anaerobic respiration which would reduce the amount of myosin-phosphorylation and therefore decrease force of contraction.
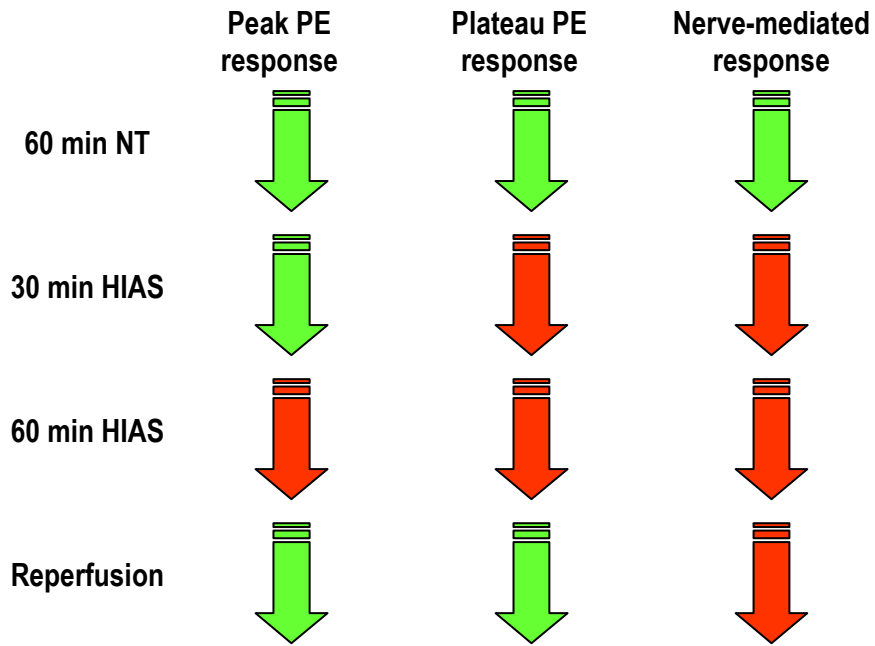
*Fig. 5.1 – Response of cavernosal smooth muscle contractile function to simulated ischaemia*

*Green arrows – no effect, red arrows – significant depression compared to control*
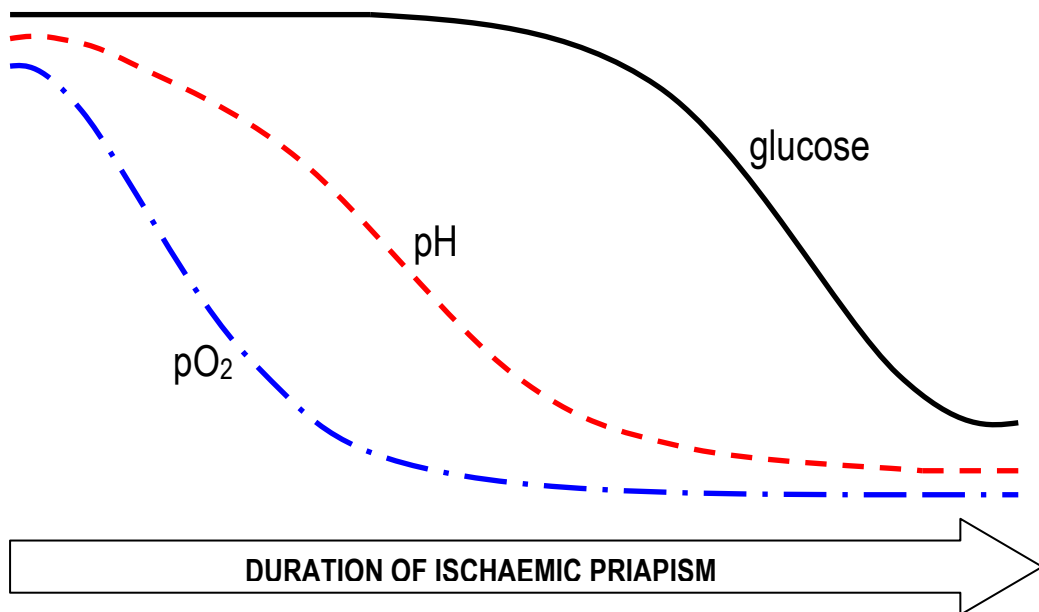


*Fig. 5.2 - Blood gas changes in corporal aspirates during prolonged penile erection*

adapted from Muneer *et al (71)*

<u>Substrate depletion</u>

60 min. of substrate depletion in isolation had no effect on EFS-mediated contraction with tension remaining at control levels upon reperfusion. 120 min. of the same intervention resulted in a significant reduction in higher frequency nerve-mediated contraction (significant suppression of tension generated in response to $EFS_{40Hz}$ and above). In addition, reperfusion resulted in a further deterioration in EFS mediated contractile function throughout the frequency range(221). Interestingly, a similar finding was not seen on agonist-induced contraction, with tension remaining at control levels during 120 min. of the intervention and upon reperfusion. This would infer that absence of glucose and Na pyruvate has a specific effect on contractile nerves rather than the smooth muscle itself. This effect is not immediate as shown by preservation of responses at 60 min. of intervention and after reperfusion. This would imply that this is a metabolic effect rather than disruption of excitation-contractile coupling due to the absence of glucose and Na pyruvate(223). No similar effect was noted on nerve-mediated relaxation although only 60 min. of this intervention was examined. 120 min. of substrate depletion had no effect on agonist-induced relaxation.

<u>Hypoxia</u>

120 min. of hypoxia had no effect on EFS-mediated contraction. A similar period of hypoxia had a significant reversible deleterious effect on the PE contracture (plateau PE contracture at 30 min. 57±12%, 60 min. 55±15% and 120 min. 54±18% of control). In a similar manner to the effect of HIAS depletion, peak responses demonstrated some initial preservation of tension generated (peak PE contracture at 30 min. 89±20%, 60 min. 51±16% and 120 min. 55±27% of control). It is postulated that the agonist-induced contracture requires more energy than nerve-mediated phasic contractions (figs. 3.1 and 3.10)(133, 223).

When examining experimental recordings, with tension on the $y$ axis and time along the $x$ axis, it can be seen that the area under the experimental tracing would be a function of energy expenditure. Agonist-induced contractures are more expensive in terms of energy expenditure; this may explain the differential effect of hypoxia on nerve and agonist contraction. Metabolic reserves are depleted at a faster rate with agonist-induced contraction or are unable to be replenished at the same rate; hypoxia therefore exhibits its deleterious effects at an earlier stage than is observed in nerve-mediated contraction.

It is hypothesised that the combination of hypoxia and substrate depletion exacerbates this depletion of metabolic reserves and therefore is the key change in the corporal micro-environment contributing to contractile failure seen in ischaemic priapism(71, 218). These findings are similar to those reported by Kim *et al*. when examining the effect of hypoxia on CSM contractile responses (183). Noradrenaline- and endothelin-evoked contractions were significantly attenuated after 180 min of hypoxia. Responses returned to normal upon return to control conditions. Tone induced by a high-K solution was also measured, with a sustained relaxation of tone observed during up to 180 min of hypoxia. This was fully reversible on return to control conditions. It was hypothesised that contractile failure was a result of inhibition of oxidative phosphorylation (reduction in ATP/ADP ratio) resulting in loss of homeostasis of $Ca^{2+}$(183).

4.2.3    The effect of hypoxia on CSM relaxation

Hypoxia reversibly abolished relaxation in CSM. When examining the effect on carbachol-induced relaxation, the deleterious effect was evident at both 30 min. and 60 min. of the intervention. Responses returned to control upon reperfusion. EFS-mediated relaxation demonstrated a significant reduction at 30 min. Nerve-mediated responses were abolished at 60 min. of EFS

stimulation in pre-contracted muscle strips demonstrating similar responses to those recorded in response to EFS-stimulation in the presence of ODQ. This compound is a highly selective and irreversible inhibitor of sGC. Soluble guanyl cyclase activated by NO, catalyses the production of cGMP from GTP. Inhibition of sGC (with ODQ) effectively blocks the action of nitric oxide. These findings show that hypoxia inhibits NO-mediated relaxation. A possible mechanism would be the fact that oxygen is a substrate in the production of nitric oxide from the semi-essential amino acid arginine (fig. 1.5). The fact there was some initial preservation of relaxation with nerve-mediated responses may indicate that this mechanism of relaxation is more efficient in terms of nitric oxide requirements.

This hypothesis is supported by work by Kim *et al* (section 1.6.1)(122). In summary this group of investigators measured intracavernosal $pO_2$ in both flaccid and the erect penis from human volunteers. Oxygen tension was similar to venous blood in the flaccid state (25-43 mmHg) and increased rapidly during penile erection to levels in excess of 100 mmHg. *In vitro* experiments on both rabbit and human CSM (from patients undergoing penile implant insertion for erectile dysfunction) showed a progressive inhibition of EFS-mediated and agonist-induced relaxation in the presence of decreasing $pO_2$ levels. Relaxation in response to exogenous NO was preserved in the presence of hypoxia. In addition, NOS activity and production of cGMP was reduced in the presence of hypoxia.

Simultaneous hypoxia and acidosis made no difference to the deleterious effect of hypoxia alone on nerve-mediated relaxation. However, the same combination ameliorated the deleterious effect of hypoxia on agonist-induced relaxation. This effect was attributable to the simultaneous presence of hypoxia and extracellular acidosis.

4.2.4    The effect of acidosis on CSM function

Acidosis generated by changing the superfusate gas mixture to 10% $CO_2$ rather than 5% $CO_2$ results in a reduction of pH in both the intra and extra-cellular compartments. 120 min of acidosis generated in this manner had no overall effect on nerve-mediated or peak/plateau agonist-induced contraction. In addition no effect was observed on nerve-mediated or agonist induced relaxation. This lack of effect is in contrast to that reported by other investigators(71, 184, 188). On scrutinising experimental technique it became apparent that other researchers often generated either intracellular acidification or extracellular acidosis. The effects of these two conditions were therefore examined independently.

Intracellular acidification was generated by again changing the superfusate gas mixture to 10% $CO_2$ rather than 5% $CO_2$ as well as increasing the amount of the extracellular buffer [$HCO_3^-$](188). The [$CaCl_2$] was adjusted appropriately to maintain $Ca^{2+}$ activity. Intracellular acidification immediately and significantly increased tension in response to EFS (EFS$_{32Hz}$ at 30, 60 and 120 min. to 116±5%, 115±6% and 107±7% respectively). In addition, this occurred throughout the frequency range with no change in the estimated frequency of contraction to achieve half maximal contraction ($f_{1/2}$ at control, 30, 60, and 120 min. - 30±7Hz, 32±12Hz, 29±10Hz, 30±10Hz respectively). This represents a true increase in tension rather than a shift to the left of the force-frequency relationship (figs. 3.17)(188, 195). Tension returned to control values upon reperfusion. Agonist-induced contraction was also augmented in the presence of intracellular acidification. At 30 min. peak and plateau PE contracture significantly increased to 120±12% and 117±9% of control respectively. Similarly at 60 min. the plateau PE was significantly increased to 112±11% of control. This augmentation of contractile function was not sustained, peak 60 min. response and the 120 min. PE contracture were no different to control values. The similar effect on both

nerve and muscle implies that the augmentation of function is an effect on the muscle itself(188, 195).

A decrease of extracellular pH was achieved by reducing the $[HCO_3^-]$ of the superfusate(188). In contrast to intracellular acidification, extracellular acidosis significantly decreased the magnitude of nerve-mediated contraction (tension in response to $EFS_{32Hz}$ at 30, 60 and 120 min. of extracellular acidosis was significantly reduced to 62±19%, 58±18% and 52±23% of control respectively)(194). This change in tension during the intervention occurred throughout the frequency range with no change in $f_{1/2}$ ($f_{1/2}$ at control, 30, 60, and 120 min. - 39±21Hz, 39±12Hz, 35±8Hz, 37±6Hz respectively). Some recovery was seen upon reperfusion with normal Tyrode's with $EFS_{32Hz}$ increasing to 76±18% of control. However this was again significantly less than control levels. Extracellular acidosis had no effect on agonist-induced contraction. This differential effect of extracellular acidosis on nerve and muscle implies that the effect is on the nerve or on the neuro-muscular junction rather than the smooth muscle itself(188).

In summary, intracellular acidification augmented contraction by an effect on the smooth muscle itself and extracellular acidosis depressed it, possibly by an effect on the nerve or neuro-muscular junction. The fact that these contrasting effects on CSM contractile function cancel each other out (the lack of effect seen with combined intra-and extracellular acidosis) implies that the underlying mechanisms are different. To further explore this, the effect of acidosis in either compartment combined with other components of simulated ischaemia was examined.

The combination of hypoxia and acidosis resulted in a significant reduction in nerve-mediated contraction whereas hypoxia or acidosis in isolation had no effect on nerve-mediated contraction (fig. 5.3a). Further examination of hypoxia in combination with either intra- or extracellular

acidosis demonstrated that the augmentation of CSM function seen with intracellular acidification was inactivated in the presence of hypoxia (figs. 5.3b and c). Experiments on the combination of acidosis and substrate depletion showed that the absence of glucose and sodium pyruvate from the superfusate did not ameliorate the augmentation in function seen with intracellular acidification. These findings mirrored those seen when examining the effect of hypoxia and acidosis on PE contractures. The augmentation of contraction seen with intracellular acidification was therefore an oxygen dependent mechanism.
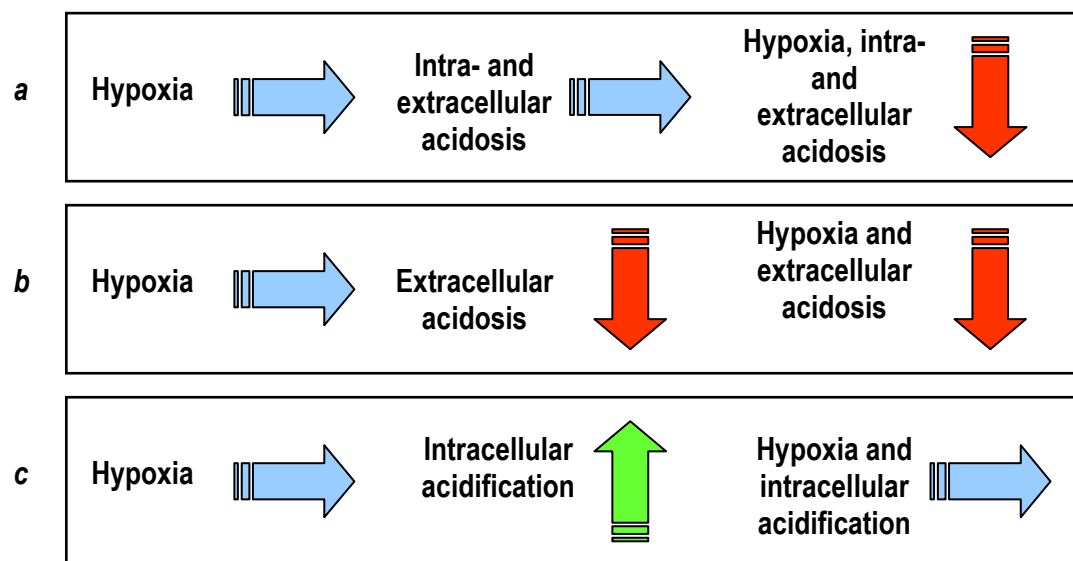


*Fig. 5.3 – Response of CSM contractile function to the combination of hypoxia and acidosis*
*arrows represent effect of intervention:*
*blue - no effect, green – significant increase, red – significant decrease compared to control*

Baxter *et al.* demonstrated an increase in rat coronary artery contraction in response to a reduction in $pH_i$ without a concurrent increase in $[Ca^{2+}]_i$. An increase in myofilament sensitivity to $Ca^{2+}$ was postulated as the underlying mechanism(224). Wu *et al.* found an increase in agonist evoked $[Ca^{2+}]_i$ transients during a decrease in pHi in guinea-pig detrusor smooth muscle(188). They suggested that the increase in carbachol and caffeine induced $Ca^{2+}$ transients was secondary to an enhancement of $Ca^{2+}$ uptake into intracellular stores as a result of raised resting

$[Ca^{2+}]_i$. Althought this could certainly explain the increase in contraction noted in our own experiments, an increase in resting $Ca^{2+}$ was not seen.

4.2.5    The effect of reduced temperature on CSM function

A recognised treatment of ischaemic priapism is the use of ice packs on the penis and washout of the corporal bodies with fluids used for intravenous infusion, typically normal saline (0.9% NaCl)(30, 60, 62). These fluids are invariably cold or at room temperature. There is no evidence within the literature to support the use of these measures. Cavernosal smooth muscle function was examined at low temperatures to test the hypothesis that these conditions are actually detrimental to CSM function.

Carbon dioxide solubility is inversely related to temperature(225, 226). Cooled Tyrode's solution resulted in an increase in dissolved $CO_2$ and a reduction of solution pH. CSM responses at low temperature were compared to those in an acidotic Tyrode's solution at 37 °C to ensure that any changes seen were not attributable to this reduction in pH. An alternative methodology would have been to adjust the pH of perfusing solutions at low temperature with NaOH using a pH meter.

The magnitude of nerve-mediated contraction was almost immediately suppressed at both 21 °C and 13 °C as compared to responses at 37 °C. This effect was dependent upon the frequency of stimulation and was completely reversible on return to 37 °C. Ebong *et al*. reported a significant reduction in force of contraction in rat vas deferens at similar temperatures(227). Contractions were completely inhibited by the α-adrenergic antagonist phentolamine. In this same study, agonist-induced contraction was augmented at room temperature. It was postulated that

reduction in EFS-mediated contraction was via a pre-synaptic mechanism. Burdyga et al. reported the effect of cooling on both rat and guinea-pig ureter(202). Differences were noted in the response of ureteric cooling between species. In the rat a significant increase in force of contraction was secondary to an increase in the $Ca^{2+}$ transient, in turn secondary to a prolongation of the action potential. Cooling in guinea-pig ureter significantly reduced force of contraction. Differences were attributed to discrepancies in ion channel distribution. In particular the $Ca^{2+}$-activated $Cl^-$ current, present in rat but not guinea-pig, was affected by reduced temperature.

In contrast to responses at 37°C, increasing frequency of stimulation did not produce an increase in nerve-mediated tension above $f_{1/2}$ at 37°C(228). The inference is that reduction in nerve-mediated contraction was not secondary to a reduction in nerve recruitment as shown by the effect of increasing voltage on tension generated. At 37°C, tension generated was found to be optimal at 50 V. At reduced temperatures, increasing the stimulation voltage above this level did not elicit any increased response to EFS at reduced temperature. Acidosis for a similar time period had no effect on the contractile response to EFS.

At low temperatures, the time-course of nerve-mediated phasic contractions was prolonged. This effect was more marked during the return to baseline tension as opposed to the upstroke of the contractile response, although both were significantly increased. The duration of contractile responses returned to control values upon reperfusion with Tyrode's at 37°C. Mitsui et al. showed that both myosin light chain kinase (MLCK) and myosin light chain phosphatase (MLCP) activity was significantly reduced at low temperature; the latter being affected to a greater degree. This in turn resulted in a larger proportion of MLC phosphorylation and slowing of relaxation(229).

The trend measured for nerve-mediated relaxation under control conditions at 37°C was to increase in magnitude with time. Experiments conducted at low temperature suppressed this trend; nerve-mediated relaxation remained at control values throughout the low temperature intervention. As with nerve-mediated contraction, the effect was greater at 13°C as compared to 21°C. Relaxatory responses to EFS at low temperatures were prolonged compared to those at 37°C(230, 231). This effect was significant during the 'contractile' phase of relaxation, i.e. the return to the pre-contracted state of the muscle strip. Again, alterations in MLCK/MLCP kinetics could explain this change(202).

In summary, a reduction in temperature reduced both the magnitude of nerve-mediated responses and increased the time course of these responses. These effects were greater during tissue contraction than relaxation. In order to examine whether these effects were mediated via the nerve or were a direct muscle effect, similar experiments at low temperature were conducted on the PE and carbachol induced contractures and relaxations respectively.

A reduction to 21°C or 13°C had no effect on the magnitude of agonist-induced contraction. A reduction in temperature had no effect on the magnitude of agonist-induced relaxation. Due to experimental limitations it was not possible to accurately measure the time course of these relaxatory responses. These observations would imply that the significant reduction seen in nerve-mediated contraction is secondary to some action on the nerves themselves or the neuromuscular junction(232). This effect is not secondary to a reduction in nerve recruitment at low temperatures.

The time course of PE-induced contractures was significantly prolonged at low temperature. Both the rise to peak tension and return to baseline upon washout of PE were significantly affected.

This is a similar finding to that during EFS contraction and would imply that this is an effect of low temperature on the muscle itself(233). To further explore this finding, experiments were conducted to examine the biomechanical properties of CSM at low temperature. These found that the viscous component of stress was reduced at low temperature for a given strain. In addition the steady state stress at low temperature was significantly increased, indicating that the tissue became stiffer at low temperature. However, the time course for the stress relaxation that occurred after an instantaneous strain was placed upon the muscle strip remained unchanged during the low temperature intervention, indicating that the mechanical ability of the tissue to relax was unaffected at low temperature(234). The slowing of both nerve-mediated function and agonist-induced contractures cannot be explained by changes in the biomechanical properties measured here. These may be due to alterations in CSM mechanism of contraction at low temperature(201, 202).

## 4.3    Conclusions and further research

Contractile failure in cavernosal smooth muscle during ischaemia is secondary to the combination of hypoxia and reduction in availability of the energy substrates glucose and sodium pyruvate. This depression of function is irreversible on the contractile nerves at an earlier stage than on relaxatory nerves and the smooth muscle itself and results in a decrease of $[Ca^{2+}]_i$. This would propagate any ischaemic priapic state. Reversal of these conditions should form part of any treatment regime for patients who have ischaemic priapism.

Intracellular acidification augments CSM contractile function in an oxygen-dependent mechanism that results in an increase in $[Ca^{2+}]_i$. Extracellular acidosis depresses contractile function. The site

of action of this depression is the nerve or the neuromuscular junction. Hypoxia alone depresses relaxatory responses. This can be limited by simultaneous extracellular acidosis.

Overall this thesis provides evidence for the two hypotheses proposed. Substrate depletion is central to the contractile failure seen in cavernosal smooth muscle during ischaemia. Prolonged ischaemia is detrimental to contractile function before relaxatory responses. In addition, nerve-mediated contraction is irreversibly affected before a similar effect on relaxatory nerves.

Low temperature interventions do not improve CSM function with nerve-mediated function significantly reduced at low temperature as well as slowing CSM contractile responses. It may be beneficial to use oxygenated washout fluids at body temperature which contain energy substrates such as glucose and Na pyruvate to treat ischaemic priapism.

This is the first study to characterise the use of guinea-pig samples to study CSM function. Both the muscle strip and single cell models of ischaemic priapism can be used to further elucidate the mechanisms by which the combination of hypoxia and substrate depletion exerts its deleterious effects. The augmentation of contractile function by intracellular acidification is also extremely interesting and may yield a therapeutic target in the treatment of priapism should agents that mimic these effects be identified. In addition, the mechanism of ODQ resistant relaxation may provide a therapeutic target for men with erectile dysfunction.

**5.0    Bibliography**

1.      Eland IA, van der Lei J, Stricker BH, Sturkenboom MJ. Incidence of priapism in the general population. Urology. 2001;57(5):970-2. Epub 2001/05/19.

2.      Kulmala RV, Lehtonen TA, Tammela TL. Priapism, its incidence and seasonal distribution in Finland. Scandinavian journal of urology and nephrology. 1995;29(1):93-6. Epub 1995/03/01.

3.      Adeyoju AB, Olujohungbe AB, Morris J, Yardumian A, Bareford D, Akenova A, et al. Priapism in sickle-cell disease; incidence, risk factors and complications - an international multicentre study. BJU international. 2002;90(9):898-902. Epub 2002/12/04.

4.      Parker RCT. Priapus2003.

5.      Hinman F. Priapism: Report of Cases and a Clinical Study of the Literature with Reference to Its Pathogenesis and Surgical Treatment. Annals of surgery. 1914;60(6):689-716. Epub 1914/12/01.

6.      Hinman F, Jr. Priapism; reasons for failure of therapy. The Journal of urology. 1960;83:420-8. Epub 1960/04/01.

7.      Pautler SE, Brock GB. Priapism. From Priapus to the present time. The Urologic clinics of North America. 2001;28(2):391-403. Epub 2001/06/14.

8.      Bastuba MD, Saenz de Tejada I, Dinlenc CZ, Sarazen A, Krane RJ, Goldstein I. Arterial priapism: diagnosis, treatment and long-term followup. The Journal of urology. 1994;151(5):1231-7. Epub 1994/05/01.

9.      Witt MA, Goldstein I, Saenz de Tejada I, Greenfield A, Krane RJ. Traumatic laceration of intracavernosal arteries: the pathophysiology of nonischemic, high flow, arterial priapism. The Journal of urology. 1990;143(1):129-32. Epub 1990/01/01.

10.     Lue TF, Hellstrom WJ, McAninch JW, Tanagho EA. Priapism: a refined approach to diagnosis and treatment. The Journal of urology. 1986;136(1):104-8. Epub 1986/07/01.

11.     Ramos CE, Park JS, Ritchey ML, Benson GS. High flow priapism associated with sickle cell disease. The Journal of urology. 1995;153(5):1619-21. Epub 1995/05/01.

12.     Engin G, Tunaci M, Acunas B. High-flow priapism due to cavernous artery pseudoaneurysm: color Doppler sonography and magnetic resonance imaging findings. European radiology. 1999;9(8):1698-9. Epub 1999/10/20.

13.     Foda MM, Mahmood K, Rasuli P, Dunlap H, Kiruluta G, Schillinger JF. High-flow priapism associated with Fabry's disease in a child: a case report and review of the literature. Urology. 1996;48(6):949-52. Epub 1996/12/01.

14.     Garcia-Consuegra J, Padron M, Jaureguizar E, Carrascosa C, Ramos J. Priapism and Fabry disease: a case report. European journal of pediatrics. 1990;149(7):500-1. Epub 1990/04/01.

15.     Burnett AL, Bivalacqua TJ. Glucose-6-phosphate dehydrogenase deficiency: an etiology for idiopathic priapism? The journal of sexual medicine. 2008;5(1):237-40. Epub 2007/11/01.

16.     Finley DS. Glucose-6-phosphate dehydrogenase deficiency associated stuttering priapism: report of a case. The journal of sexual medicine. 2008;5(12):2963-6. Epub 2008/10/01.

17.     Backenroth R, Landau EH, Goren M, Raas-Rothschild A. Fabry disease and G6PD in three family members with priapism: is the nitric oxide pathway to blame? The journal of sexual medicine. 2010;7(4 Pt 1):1588-91. Epub 2010/01/28.

18.     Ilkay AK, Levine LA. Conservative management of high-flow priapism. Urology. 1995;46(3):419-24. Epub 1995/09/01.

19.     Park JK, Jeong YB, Han YM, Kim HJ. High-flow priapism caused by injury of the bilateral cavernosal artery after needle trauma in a patient with low-flow priapism. BJU international. 2003;92 Suppl 3:e7-e8. Epub 2003/12/01.

20.     Wallis CJ, Hoag N, Pommerville PJ, Huk ME. Recurrent idiopathic high-flow priapism treated with selective arterial embolization after repeated initial treatments for low-flow priapism. Canadian Urological Association journal = Journal de l'Association des urologues du Canada. 2009;3(1):60-3. Epub 2009/03/19.

21.     deHoll JD, Shin PA, Angle JF, Steers WD. Alternative approaches to the management of priapism. International journal of impotence research. 1998;10(1):11-4. Epub 1998/05/30.

22.     Steers WD, Selby JB, Jr. Use of methylene blue and selective embolization of the pudendal artery for high flow priapism refractory to medical and surgical treatments. The Journal of urology. 1991;146(5):1361-3. Epub 1991/11/11.

23.     Gujral S, MacDonagh RP, Cavanagh PM. Bilateral superselective arterial microcoil embolisation in delayed post-traumatic high flow priapism. Postgraduate medical journal. 2001;77(905):193-4. Epub 2001/02/27.

24.     Hatzichristou D, Salpiggidis G, Hatzimouratidis K, Apostolidis A, Tzortzis V, Bekos A, et al. Management strategy for arterial priapism: therapeutic dilemmas. The Journal of urology. 2002;168(5):2074-7. Epub 2002/10/24.

25.     Kress O, Heidenreich A, Klose KJ, Wagner HJ, Alfke H. Superselective embolization with coils in high-flow priapism. Cardiovascular and interventional radiology. 2002;25(4):326-9. Epub 2002/09/27.

26.      Volkmer BG, Nesslauer T, Kuefer R, Kraemer S, Goerich J, Gottfried HW. High-flow priapism: a combined interventional approach with angiography and colour Doppler. Ultrasound in medicine & biology. 2002;28(2):165-9. Epub 2002/04/09.

27.      Brock G, Breza J, Lue TF, Tanagho EA. High flow priapism: a spectrum of disease. The Journal of urology. 1993;150(3):968-71. Epub 1993/09/01.

28.      Pohl J, Pott B, Kleinhans G. Priapism: a three-phase concept of management according to aetiology and prognosis. British journal of urology. 1986;58(2):113-8. Epub 1986/04/01.

29.      A. J. Wein LRK, A. C. Novick, A. W. Partin, and C. A. Peters. Campbell-Walsh Urology. 9th ed: Saunders-Elsevier; 2007.

30.      Kumar P MS, Ralph DJ. The Surgical Management of Priapism. Current Sexual Health Reports. 2007;1(4):125-8.

31.      Broderick GA, Harkaway R. Pharmacologic erection: time-dependent changes in the corporal environment. International journal of impotence research. 1994;6(1):9-16. Epub 1994/03/01.

32.      Bochinski DJ, Deng DY, Lue TF. The treatment of priapism--when and how? International journal of impotence research. 2003;15 Suppl 5:S86-90. Epub 2003/10/11.

33.      Adogu AA. Stuttering priapism in sickle cell disease. British journal of urology. 1991;67(1):105-6. Epub 1991/01/01.

34.      Muneer A, Minhas S, Arya M, Ralph DJ. Stuttering priapism--a review of the therapeutic options. International journal of clinical practice. 2008;62(8):1265-70. Epub 2008/05/16.

35.      Muneer A, Minhas S, Freeman A, Kumar P, Ralph DJ. Investigating the effects of high-dose phenylephrine in the management of prolonged ischaemic priapism. The journal of sexual medicine. 2008;5(9):2152-9. Epub 2008/05/10.

36.      Bennett N, Mulhall J. Sickle cell disease status and outcomes of African-American men presenting with priapism. The journal of sexual medicine. 2008;5(5):1244-50. Epub 2008/03/04.

37.      Champion HC, Bivalacqua TJ, Takimoto E, Kass DA, Burnett AL. Phosphodiesterase-5A dysregulation in penile erectile tissue is a mechanism of priapism. Proceedings of the National Academy of Sciences of the United States of America. 2005;102(5):1661-6. Epub 2005/01/26.

38.      Schreibman SM, Gee TS, Grabstald H. Management of priapism in patients with chronic granulocytic leukemia. The Journal of urology. 1974;111(6):786-8. Epub 1974/06/01.

39.      Wilson SK, Klionsky BL, Rhamy RK. A new etiology of priapism: Fabry's disease. The Journal of urology. 1973;109(4):646-8. Epub 1973/04/01.

40.      Greenberg WM. Mechanism of neuroleptic-associated priapism. The American journal of psychiatry. 1988;145(3):393-5. Epub 1988/03/01.

41.     Sadeghi-Nejad H, Jackson I. New-onset priapism associated with ingestion of terazosin in an otherwise healthy man. The journal of sexual medicine. 2007;4(6):1766-8. Epub 2007/04/25.

42.     Stimmel GL, Gutierrez MA. Counseling patients about sexual issues. Pharmacotherapy. 2006;26(11):1608-15. Epub 2006/10/27.

43.     Guvel S, Kilinc F, Torun D, Egilmez T, Ozkardes H. Malignant priapism secondary to bladder cancer. Journal of andrology. 2003;24(4):499-500. Epub 2003/06/27.

44.     Hettiarachchi JA, Johnson GB, Panageas E, Drinis S, Konno S, Das AK. Malignant priapism associated with metastatic urethral carcinoma. Urologia internationalis. 2001;66(2):114-6. Epub 2001/02/27.

45.     Kvarstein B. Bladder cancer complicated with priapism. A case report. Scandinavian journal of urology and nephrology Supplementum. 1996;179:155-6. Epub 1996/01/01.

46.     Lomaga MA, Hayter C. Priapism as a possible acute side effect of radical radiotherapy for prostate cancer. The Canadian journal of urology. 2004;11(2):2205-6. Epub 2004/06/09.

47.     Sonmez NC, Coskun B, Arisan S, Guney S, Dalkilic A. Early penile metastasis from primary bladder cancer as the first systemic manifestation: a case report. Cases journal. 2009;2:7281. Epub 2010/02/27.

48.     Weitzner S. Secondary carcinoma in the penis. Report of three cases and literature review. The American surgeon. 1971;37(9):563-7. Epub 1971/09/01.

49.     Baba H, Maezawa Y, Furusawa N, Kawahara N, Tomita K. Lumbar spinal stenosis causing intermittent priapism. Paraplegia. 1995;33(6):338-45. Epub 1995/06/01.

50.     Coraddu M, Floris F, Corrias A, Nurchi GC, Lobina GF, Dettori P. Spontaneous priapism produced by stenosis of the lumbar canal. Acta neurologica. 1989;11(6):428-33. Epub 1989/12/01.

51.     Cuenca PJ, Tulley EB, Devita D, Stone A. Delayed traumatic spinal epidural hematoma with spontaneous resolution of symptoms. The Journal of emergency medicine. 2004;27(1):37-41. Epub 2004/06/29.

52.     Gordon SA, Stage KH, Tansey KE, Lotan Y. Conservative management of priapism in acute spinal cord injury. Urology. 2005;65(6):1195-7. Epub 2005/05/26.

53.     Ravindran M. Cauda equina compression presenting as spontaneous priapism. Journal of neurology, neurosurgery, and psychiatry. 1979;42(3):280-2. Epub 1979/03/01.

54.     Vaidyanathan S, Watt JW, Singh G, Hughes PL, Selmi F, Oo T, et al. Management of recurrent priapism in a cervical spinal cord injury patient with oral baclofen therapy. Spinal cord. 2004;42(2):134-5. Epub 2004/02/07.

55.     el-Amin EO. Issues in management of scorpion sting in children. Toxicon : official journal of the International Society on Toxinology. 1992;30(1):111-5. Epub 1992/01/01.

56.     Lapan DI, Graham AR, Bangert JL, Boyer JT, Conner WT. Amyloidosis presenting as priapism. Urology. 1980;15(2):167-70. Epub 1980/02/01.

57.     Talaulicar PM. Persistent priapism in rabies. British journal of urology. 1977;49(6):462. Epub 1977/11/01.

58.     Bochinski DJ, Dean RC, Lue TF. Erectile dysfunction and priapism. Nature clinical practice Urology. 2004;1(1):49-53; quiz 1 p following Epub 2006/02/14.

59.     Costa WS, Felix B, Cavalcanti AG, Medeiros J, Jr., Sampaio FJ. Structural analysis of the corpora cavernosa in patients with ischaemic priapism. BJU international. 2010;105(6):838-41; discussion 41. Epub 2009/09/16.

60.     Pryor J, Akkus E, Alter G, Jordan G, Lebret T, Levine L, et al. Priapism. The journal of sexual medicine. 2004;1(1):116-20. Epub 2006/01/21.

61.     Mulhall JP, Honig SC. Priapism: etiology and management. Academic emergency medicine : official journal of the Society for Academic Emergency Medicine. 1996;3(8):810-6. Epub 1996/08/01.

62.     Montague DK, Jarow J, Broderick GA, Dmochowski RR, Heaton JP, Lue TF, et al. American Urological Association guideline on the management of priapism. The Journal of urology. 2003;170(4 Pt 1):1318-24. Epub 2003/09/23.

63.     Gibel LJ, Reiley E, Borden TA. Intracorporeal cavernosa streptokinase as adjuvant therapy in the delayed treatment of idiopathic priapism. The Journal of urology. 1985;133(6):1040-1. Epub 1985/06/01.

64.     Hubler J, Szanto A, Konyves K. Methylene blue as a means of treatment for priapism caused by intracavernous injection to combat erectile dysfunction. International urology and nephrology. 2003;35(4):519-21. Epub 2004/06/17.

65.     Janetschek G, Promegger R, Weimann S. Local fibrinolysis and perfusion in the treatment of priapism of the corpora cavernosa and corpus spongiosum. Scandinavian journal of urology and nephrology. 1993;27(4):545-7. Epub 1993/01/01.

66.     Martinez Portillo F, Hoang-Boehm J, Weiss J, Alken P, Junemann K. Methylene blue as a successful treatment alternative for pharmacologically induced priapism. European urology. 2001;39(1):20-3. Epub 2001/02/15.

67.     Okpala I, Westerdale N, Jegede T, Cheung B. Etilefrine for the prevention of priapism in adult sickle cell disease. British journal of haematology. 2002;118(3):918-21. Epub 2002/08/16.

68.     Teloken C, Ribeiro EP, Chammas M, Jr., Teloken PE, Souto CA. Intracavernosal etilefrine self-injection therapy for recurrent priapism: one decade of follow-up. Urology. 2005;65(5):1002. Epub 2005/05/11.

69.     Govier FE, Jonsson E, Kramer-Levien D. Oral terbutaline for the treatment of priapism. The Journal of urology. 1994;151(4):878-9. Epub 1994/04/01.

70.     Lowe FC, Jarow JP. Placebo-controlled study of oral terbutaline and pseudoephedrine in management of prostaglandin E1-induced prolonged erections. Urology. 1993;42(1):51-3; discussion 3-4. Epub 1993/07/01.

71.     Muneer A, Cellek S, Dogan A, Kell PD, Ralph DJ, Minhas S. Investigation of cavernosal smooth muscle dysfunction in low flow priapism using an in vitro model. International journal of impotence research. 2005;17(1):10-8. Epub 2004/04/09.

72.     Spycher MA, Hauri D. The ultrastructure of the erectile tissue in priapism. The Journal of urology. 1986;135(1):142-7. Epub 1986/01/01.

73.     Nixon RG, O'Connor JL, Milam DF. Efficacy of shunt surgery for refractory low flow priapism: a report on the incidence of failed detumescence and erectile dysfunction. The Journal of urology. 2003;170(3):883-6. Epub 2003/08/13.

74.     Ralph DJ, Garaffa G, Muneer A, Freeman A, Rees R, Christopher AN, et al. The immediate insertion of a penile prosthesis for acute ischaemic priapism. European urology. 2009;56(6):1033-8. Epub 2008/10/22.

75.     Brant WO, Garcia MM, Bella AJ, Chi T, Lue TF. T-shaped shunt and intracavernous tunneling for prolonged ischemic priapism. The Journal of urology. 2009;181(4):1699-705. Epub 2009/02/24.

76.     Burnett AL, Pierorazio PM. Corporal "snake" maneuver: corporoglanular shunt surgical modification for ischemic priapism. The journal of sexual medicine. 2009;6(4):1171-6. Epub 2009/02/12.

77.     Ebbehoj J. A new operation for priapism. Scandinavian journal of plastic and reconstructive surgery. 1974;8(3):241-2. Epub 1974/01/01.

78.     Ercole CJ, Pontes JE, Pierce JM, Jr. Changing surgical concepts in the treatment of priapism. The Journal of urology. 1981;125(2):210-1. Epub 1981/02/01.

79.     Grayhack JT, McCullough W, O'Conor VJ, Jr., Trippel O. Venous Bypass to Control Priapism. Investigative urology. 1964;1:509-13. Epub 1964/03/01.

80.     R Q. Cure d'un cas de priapisme par anastomose cavernospongieuse. Acta Urol Belg 1964;32:5-13.

81.     Winter CC. Cure of idiopathic priapism: new procedure for creating fistula between glans penis and corpora cavernosa. Urology. 1976;8(4):389-91. Epub 1976/10/01.

82.     H E. Clinical anatomy: Blackwell Scientific Publications; 1992.

83.     TF L. Sexual function and dysfunction. In: Walsh PC RA, Vaughan ED, Wein AJ, editor. Campbell's Urology. 8th ed: Saunders; 2002. p. 1589-604.

84.     Minhas S PJ, Ralph DJ. Male Sexual Function. In: Mundy AR FJ, Neal DE, George NJR, editor. The Scientific Basis of Urology: Taylor & Francis Ltd; 2004. p. 343-65.

85.     Sexual Medicine.  Sexual Dysfunctions in Men and Women. Paris: Health Publications; 2004.

86.     Andersson KE, Wagner G. Physiology of penile erection. Physiological reviews. 1995;75(1):191-236. Epub 1995/01/01.

87.     Pickard RS, Powell PH, Zar MA. The effect of inhibitors of nitric oxide biosynthesis and cyclic GMP formation on nerve-evoked relaxation of human cavernosal smooth muscle. British journal of pharmacology. 1991;104(3):755-9. Epub 1991/11/01.

88.     Sathananthan AH, Adaikan PG, Lau LC, Ho J, Ratnam SS. Fine structure of the human corpus cavernosum. Archives of andrology. 1991;26(2):107-17. Epub 1991/03/01.

89.     Steers WD. Neural pathways and central sites involved in penile erection: neuroanatomy and clinical implications. Neuroscience and biobehavioral reviews. 2000;24(5):507-16. Epub 2000/07/06.

90.     Giuliano F, Rampin O. Central neural regulation of penile erection. Neuroscience and biobehavioral reviews. 2000;24(5):517-33. Epub 2000/07/06.

91.     Skagerberg G, Bjorklund A, Lindvall O, Schmidt RH. Origin and termination of the diencephalo-spinal dopamine system in the rat. Brain research bulletin. 1982;9(1-6):237-44. Epub 1982/07/01.

92.     Skagerberg G, Lindvall O. Organization of diencephalic dopamine neurones projecting to the spinal cord in the rat. Brain research. 1985;342(2):340-51. Epub 1985/09/09.

93.     Lue TF, Takamura T, Schmidt RA, Palubinskas AJ, Tanagho EA. Hemodynamics of erection in the monkey. The Journal of urology. 1983;130(6):1237-41. Epub 1983/12/01.

94.     Shirai M, Ishii N, Mitsukawa S, Matsuda S, Nakamura M. Hemodynamic mechanism of erection in the human penis. Archives of andrology. 1978;1(4):345-9. Epub 1978/09/01.

95.     Wagner G, Metz P. Impotence (erectile dysfunction) due to vascular disorders. An overview. Journal of sex & marital therapy. 1980;6(4):223-33. Epub 1980/01/01.

96.     Lue TF. Erectile dysfunction. The New England journal of medicine. 2000;342(24):1802-13. Epub 2000/06/15.

97.     Christ GJ, Spray DC, el-Sabban M, Moore LK, Brink PR. Gap junctions in vascular tissues. Evaluating the role of intercellular communication in the modulation of vasomotor tone. Circulation research. 1996;79(4):631-46. Epub 1996/10/01.

98.     Costa P, Soulie-Vassal ML, Sarrazin B, Rebillard X, Navratil H, Bali JP. Adrenergic receptors on smooth muscle cells isolated from human penile corpus cavernosum. The Journal of urology. 1993;150(3):859-63. Epub 1993/09/01.

99.     Levin RM, Wein AJ. Adrenergic alpha receptors outnumber beta receptors in human penile corpus cavernosum. Investigative urology. 1980;18(3):225-6. Epub 1980/11/01.

100.    Andersson KE. Pharmacology of penile erection. Pharmacological reviews. 2001;53(3):417-50. Epub 2001/09/08.

101.    Traish AM, Gupta S, Toselli P, de Tejada IS, Goldstein I, Moreland RB. Identification of alpha 1-adrenergic receptor subtypes in human corpus cavernosum tissue and in cultured trabecular smooth muscle cells. Receptor. 1995;5(3):145-57. Epub 1995/01/01.

102.    Traish AM, Moreland RB, Huang YH, Goldstein I. Expression of functional alpha2-adrenergic receptor subtypes in human corpus cavernosum and in cultured trabecular smooth muscle cells. Receptors & signal transduction. 1997;7(1):55-67. Epub 1997/01/01.

103.    Traish AM, Netsuwan N, Daley J, Padman-Nathan H, Goldstein I, Saenz de Tejada I. A heterogeneous population of alpha 1 adrenergic receptors mediates contraction of human corpus cavernosum smooth muscle to norepinephrine. The Journal of urology. 1995;153(1):222-7. Epub 1995/01/01.

104.    El-Gamal OM, Sandhu DP, Terry T, Elliott RA. alpha-Adrenoceptor subtypes in isolated corporal tissue from patients undergoing gender re-assignment. BJU international. 2006;97(2):329-32. Epub 2006/01/25.

105.    Dausse JP, Leriche A, Yablonsky F. Patterns of messenger RNA expression for alpha1-adrenoceptor subtypes in human corpus cavernosum. The Journal of urology. 1998;160(2):597-600. Epub 1998/07/29.

106.    Hieble JP, Bylund DB, Clarke DE, Eikenburg DC, Langer SZ, Lefkowitz RJ, et al. International Union of Pharmacology. X. Recommendation for nomenclature of alpha 1-adrenoceptors: consensus update. Pharmacological reviews. 1995;47(2):267-70. Epub 1995/06/01.

107.    Hedlund H, Andersson KE. Comparison of the responses to drugs acting on adrenoreceptors and muscarinic receptors in human isolated corpus cavernosum and cavernous artery. Journal of autonomic pharmacology. 1985;5(1):81-8. Epub 1985/03/01.

108. Kerfoot WW, Park HY, Schwartz LB, Hagen PO, Carson CC, 3rd. Characterization of calcium channel blocker induced smooth muscle relaxation using a model of isolated corpus cavernosum. The Journal of urology. 1993;150(1):249-52. Epub 1993/07/01.

109. Andersson KE, Hedlund P, Alm P. Sympathetic pathways and adrenergic innervation of the penis. International journal of impotence research. 2000;12(S1):S5-S12. Epub 2000/06/13.

110. Simonsen U, Prieto D, Hernandez M, Saenz de Tejada I, Garcia-Sacristan A. Prejunctional alpha 2-adrenoceptors inhibit nitrergic neurotransmission in horse penile resistance arteries. The Journal of urology. 1997;157(6):2356-60. Epub 1997/06/01.

111. Takahashi R, Nishimura J, Hirano K, Naito S, Kanaide H. Modulation of Ca2+ sensitivity regulates contractility of rabbit corpus cavernosum smooth muscle. The Journal of urology. 2003;169(6):2412-6. Epub 2003/05/29.

112. Somlyo AP, Somlyo AV. Signal transduction and regulation in smooth muscle. Nature. 1994;372(6503):231-6. Epub 1994/11/17.

113. Karaki H, Ozaki H, Hori M, Mitsui-Saito M, Amano K, Harada K, et al. Calcium movements, distribution, and functions in smooth muscle. Pharmacological reviews. 1997;49(2):157-230. Epub 1997/06/01.

114. Kimura K, Ito M, Amano M, Chihara K, Fukata Y, Nakafuku M, et al. Regulation of myosin phosphatase by Rho and Rho-associated kinase (Rho-kinase). Science. 1996;273(5272):245-8. Epub 1996/07/12.

115. Saenz de Tejada I, Carson MP, de las Morenas A, Goldstein I, Traish AM. Endothelin: localization, synthesis, activity, and receptor types in human penile corpus cavernosum. The American journal of physiology. 1991;261(4 Pt 2):H1078-85. Epub 1991/10/01.

116. Bell CR, Sullivan ME, Dashwood MR, Muddle JR, Morgan RJ. The density and distribution of endothelin 1 and endothelin receptor subtypes in normal and diabetic rat corpus cavernosum. British journal of urology. 1995;76(2):203-7. Epub 1995/08/01.

117. Dai Y, Pollock DM, Lewis RL, Wingard CJ, Stopper VS, Mills TM. Receptor-specific influence of endothelin-1 in the erectile response of the rat. American journal of physiology Regulatory, integrative and comparative physiology. 2000;279(1):R25-30. Epub 2000/07/18.

118. Parkkisenniemi UM, Klinge E. Functional characterization of endothelin receptors in the bovine retractor penis muscle and penile artery. Pharmacology & toxicology. 1996;79(2):73-9. Epub 1996/08/01.

119. Holmquist F, Kirkeby HJ, Larsson B, Forman A, Alm P, Andersson KE. Functional effects, binding sites and immunolocalization of endothelin-1 in isolated penile tissues from man

and rabbit. The Journal of pharmacology and experimental therapeutics. 1992;261(2):795-802. Epub 1992/05/01.

120.	Holmquist F, Persson K, Garcia-Pascual A, Andersson KE. Phospholipase C activation by endothelin-1 and noradrenaline in isolated penile erectile tissue from rabbit. The Journal of urology. 1992;147(6):1632-5. Epub 1992/06/01.

121.	Christ GJ, Lerner SE, Kim DC, Melman A. Endothelin-1 as a putative modulator of erectile dysfunction: I. Characteristics of contraction of isolated corporal tissue strips. The Journal of urology. 1995;153(6):1998-2003. Epub 1995/06/01.

122.	Kim N, Vardi Y, Padma-Nathan H, Daley J, Goldstein I, Saenz de Tejada I. Oxygen tension regulates the nitric oxide pathway. Physiological role in penile erection. The Journal of clinical investigation. 1993;91(2):437-42. Epub 1993/02/01.

123.	Sattar AA, Salpigides G, Vanderhaeghen JJ, Schulman CC, Wespes E. Cavernous oxygen tension and smooth muscle fibers: relation and function. The Journal of urology. 1995;154(5):1736-9. Epub 1995/11/01.

124.	Burnett AL, Lowenstein CJ, Bredt DS, Chang TS, Snyder SH. Nitric oxide: a physiologic mediator of penile erection. Science. 1992;257(5068):401-3. Epub 1992/07/17.

125.	Moreland RB, Albadawi H, Bratton C, Patton G, Goldstein I, Traish A, et al. O2-dependent prostanoid synthesis activates functional PGE receptors on corpus cavernosum smooth muscle. American journal of physiology Heart and circulatory physiology. 2001;281(2):H552-8. Epub 2001/07/17.

126.	Khan MA, Calvert RC, Sullivan ME, Thompson CS, Mumtaz FH, Morgan RJ, et al. Normal and pathological erectile function: the potential clinical role of endothelin-1 antagonists. Current drug targets. 2000;1(3):247-60. Epub 2001/07/24.

127.	Saenz de Tejada I, Kim N, Lagan I, Krane RJ, Goldstein I. Regulation of adrenergic activity in penile corpus cavernosum. The Journal of urology. 1989;142(4):1117-21. Epub 1989/10/01.

128.	Somlyo AP, Somlyo AV. Smooth muscle: excitation-contraction coupling, contractile regulation, and the cross-bridge cycle. Alcoholism, clinical and experimental research. 1994;18(1):138-43. Epub 1994/02/01.

129.	Hedlund P, Alm P, Andersson KE. NO synthase in cholinergic nerves and NO-induced relaxation in the rat isolated corpus cavernosum. British journal of pharmacology. 1999;127(2):349-60. Epub 1999/06/29.

130.    Levin RM, Hypolite J, Broderick GA. Comparative studies on intracellular calcium and NADH Fluorescence of the rabbit corpus cavernosum. Neurourology and urodynamics. 1994;13(5):609-18. Epub 1994/01/01.

131.    Paul RJ. Smooth muscle energetics and theories of cross-bridge regulation. The American journal of physiology. 1990;258(2 Pt 1):C369-75. Epub 1990/02/01.

132.    Rhee AY, Brozovich FV. Force maintenance in smooth muscle: analysis using sinusoidal perturbations. Archives of biochemistry and biophysics. 2003;410(1):25-38. Epub 2003/02/01.

133.    Wendt IR, Paul RJ. Energy cost of contraction in rat urinary bladder smooth muscle during anoxia. Clinical and experimental pharmacology & physiology. 2003;30(8):565-9. Epub 2003/08/02.

134.    Kim YD, Cho MH, Kwon SC. Myoplasmic [ca], crossbridge phosphorylation and latch in rabbit bladder smooth muscle. The Korean journal of physiology & pharmacology : official journal of the Korean Physiological Society and the Korean Society of Pharmacology. 2011;15(3):171-7. Epub 2011/08/24.

135.    Hedlund P, Ny L, Alm P, Andersson KE. Cholinergic nerves in human corpus cavernosum and spongiosum contain nitric oxide synthase and heme oxygenase. The Journal of urology. 2000;164(3 Pt 1):868-75. Epub 2000/08/23.

136.    Saenz de Tejada I, Goldstein I, Krane RJ. Local control of penile erection. Nerves, smooth muscle, and endothelium. The Urologic clinics of North America. 1988;15(1):9-15. Epub 1988/02/01.

137.    Traish AM, Carson MP, Kim N, Goldstein I, Saenz de Tejada I. Characterization of muscarinic acetylcholine receptors in human penile corpus cavernosum: studies on whole tissue and cultured endothelium. The Journal of urology. 1990;144(4):1036-40. Epub 1990/10/01.

138.    Traish AM, Palmer MS, Goldstein I, Moreland RB. Expression of functional muscarinic acetylcholine receptor subtypes in human corpus cavernosum and in cultured smooth muscle cells. Receptor. 1995;5(3):159-76. Epub 1995/01/01.

139.    Cartledge JJ, Minhas S, Eardley I, Morrison JF. Endothelial and neuronal-derived nitric oxide mediated relaxation of corpus cavernosal smooth muscle in a rat, in vitro, model of erectile function. International journal of impotence research. 2000;12(4):213-21. Epub 2000/11/18.

140.    Sjostrand NO, Klinge E. What function have cholinergic nerves in the smooth muscle of the male genital tract? Acta physiologica Scandinavica Supplementum. 1977;452:89-91. Epub 1977/01/01.

141.    Burnett AL. Priapism pathophysiology: clues to prevention. International journal of impotence research. 2003;15 Suppl 5:S80-5. Epub 2003/10/11.

142.    Burnett AL, Tillman SL, Chang TS, Epstein JI, Lowenstein CJ, Bredt DS, et al. Immunohistochemical localization of nitric oxide synthase in the autonomic innervation of the human penis. The Journal of urology. 1993;150(1):73-6. Epub 1993/07/01.

143.    Ceccatelli S, Lundberg JM, Zhang X, Aman K, Hokfelt T. Immunohistochemical demonstration of nitric oxide synthase in the peripheral autonomic nervous system. Brain research. 1994;656(2):381-95. Epub 1994/09/12.

144.    Hohler B, Olry R, Mayer B, Kummer W. Nitric oxide synthase in guinea pig sympathetic ganglia: correlation with tyrosine hydroxylase and neuropeptides. Histochemistry and cell biology. 1995;104(1):21-8. Epub 1995/07/01.

145.    Song ZM, Brookes SJ, Gibbins IL, Costa M. NADPH-diaphorase and other neuronal markers in nerves and ganglia supplying the guinea-pig vas deferens. Journal of the autonomic nervous system. 1994;48(1):31-43. Epub 1994/06/01.

146.    Bloch W, Klotz T, Sedlaczek P, Zumbe J, Engelmann U, Addicks K. Evidence for the involvement of endothelial nitric oxide synthase from smooth muscle cells in the erectile function of the human corpus cavernosum. Urological research. 1998;26(2):129-35. Epub 1998/06/19.

147.    Stanarius A, Uckert S, Machtens SA, Stief CG, Wolf G, Jonas U. Immunocytochemical distribution of nitric oxide synthase in the human corpus cavernosum: an electron microscopical study using the tyramide signal amplification technique. Urological research. 2001;29(3):168-72. Epub 2001/08/03.

148.    Burnett AL. Nitric oxide regulation of penile erection: biology and therapeutic implications. Journal of andrology. 2002;23(5):S20-6. Epub 2002/09/19.

149.    Moncada S, Higgs A, Furchgott R. International Union of Pharmacology Nomenclature in Nitric Oxide Research. Pharmacological reviews. 1997;49(2):137-42. Epub 1997/06/01.

150.    Azadzoi KM, Kim N, Brown ML, Goldstein I, Cohen RA, Saenz de Tejada I. Endothelium-derived nitric oxide and cyclooxygenase products modulate corpus cavernosum smooth muscle tone. The Journal of urology. 1992;147(1):220-5. Epub 1992/01/01.

151.    Burnett AL, Chang AG, Crone JK, Huang PL, Sezen SE. Noncholinergic penile erection in mice lacking the gene for endothelial nitric oxide synthase. Journal of andrology. 2002;23(1):92-7. Epub 2002/01/10.

152.    Burnett AL. Role of nitric oxide in the physiology of erection. Biology of reproduction. 1995;52(3):485-9. Epub 1995/03/01.

153.    Busse R, Fleming I. Pulsatile stretch and shear stress: physical stimuli determining the production of endothelium-derived relaxing factors. Journal of vascular research. 1998;35(2):73-84. Epub 1998/05/20.

154.	Cornwell TL, Pryzwansky KB, Wyatt TA, Lincoln TM. Regulation of sarcoplasmic reticulum protein phosphorylation by localized cyclic GMP-dependent protein kinase in vascular smooth muscle cells. Molecular pharmacology. 1991;40(6):923-31. Epub 1991/12/01.

155.	Archer SL, Huang JM, Hampl V, Nelson DP, Shultz PJ, Weir EK. Nitric oxide and cGMP cause vasorelaxation by activation of a charybdotoxin-sensitive K channel by cGMP-dependent protein kinase. Proceedings of the National Academy of Sciences of the United States of America. 1994;91(16):7583-7. Epub 1994/08/02.

156.	Lincoln TM. Cyclic GMP and mechanisms of vasodilation. Pharmacology & therapeutics. 1989;41(3):479-502. Epub 1989/01/01.

157.	Furukawa K, Ohshima N, Tawada-Iwata Y, Shigekawa M. Cyclic GMP stimulates Na+/Ca2+ exchange in vascular smooth muscle cells in primary culture. The Journal of biological chemistry. 1991;266(19):12337-41. Epub 1991/07/05.

158.	Lincoln J, Crowe R, Blacklay PF, Pryor JP, Lumley JS, Burnstock G. Changes in the VIPergic, cholinergic and adrenergic innervation of human penile tissue in diabetic and non-diabetic impotent males. The Journal of urology. 1987;137(5):1053-9. Epub 1987/05/01.

159.	Hedlund P, Alm P, Ekstrom P, Fahrenkrug J, Hannibal J, Hedlund H, et al. Pituitary adenylate cyclase-activating polypeptide, helospectin, and vasoactive intestinal polypeptide in human corpus cavernosum. British journal of pharmacology. 1995;116(4):2258-66. Epub 1995/10/01.

160.	Hedlund P, Larsson B, Alm P, Andersson KE. Distribution and function of nitric oxide-containing nerves in canine corpus cavernosum and spongiosum. Acta physiologica Scandinavica. 1995;155(4):445-55. Epub 1995/12/01.

161.	Ottesen B, Wagner G, Virag R, Fahrenkrug J. Penile erection: possible role for vasoactive intestinal polypeptide as a neurotransmitter. British medical journal. 1984;288(6410):9-11. Epub 1984/01/07.

162.	Kim YC, Kim JH, Davies MG, Hagen PO, Carson CC, 3rd. Modulation of vasoactive intestinal polypeptide (VIP)-mediated relaxation by nitric oxide and prostanoids in the rabbit corpus cavernosum. The Journal of urology. 1995;153(3 Pt 1):807-10. Epub 1995/03/01.

163.	Cara AM, Lopes-Martins RA, Antunes E, Nahoum CR, De Nucci G. The role of histamine in human penile erection. British journal of urology. 1995;75(2):220-4. Epub 1995/02/01.

164.	Kim YC, Davies MG, Lee TH, Hagen PO, Carson CC, 3rd. Characterization and function of histamine receptors in corpus cavernosum. The Journal of urology. 1995;153(2):506-10. Epub 1995/02/01.

165.    Furukawa K, Nagao K, Ishii N, Uchiyama T. Responses to serotonin (5HT) in isolated corpus cavernosum penis of rabbit. International journal of impotence research. 2003;15(4):267-71. Epub 2003/08/23.

166.    Hayes ES, Adaikan PG. The effects of 5HT(1) agonists on erection in rats in vivo and rabbit corpus cavernosum in vitro. International journal of impotence research. 2002;14(4):205-12. Epub 2002/08/02.

167.    Tong YC, Broderick G, Hypolite J, Levin RM. Correlations of purinergic, cholinergic and adrenergic functions in rabbit corporal cavernosal tissue. Pharmacology. 1992;45(5):241-9. Epub 1992/01/01.

168.    Simonsen U, Garcia-Sacristan A, Prieto D. Penile arteries and erection. Journal of vascular research. 2002;39(4):283-303. Epub 2002/08/21.

169.    Cohen RA, Vanhoutte PM. Endothelium-dependent hyperpolarization. Beyond nitric oxide and cyclic GMP. Circulation. 1995;92(11):3337-49. Epub 1995/12/01.

170.    Angulo J, Cuevas P, Fernandez A, Gabancho S, Videla S, Saenz de Tejada I. Calcium dobesilate potentiates endothelium-derived hyperpolarizing factor-mediated relaxation of human penile resistance arteries. British journal of pharmacology. 2003;139(4):854-62. Epub 2003/06/19.

171.    Sato M, Kawatani M. Effects of noradrenaline on cytosolic concentrations of Ca(2+) in cultured corpus cavernosum smooth muscle cells of the rabbit. Neuroscience letters. 2002;324(2):89-92. Epub 2002/05/04.

172.    Yang Z, Wang X, Zhu G, Zhou Z, Wang Y, Chen D, et al. Effect of surgical castration on expression of TRPM8 in urogenital tract of male rats. Molecular biology reports. 2012;39(4):4797-802. Epub 2011/09/29.

173.    Pietrobon D, Di Virgilio F, Pozzan T. Structural and functional aspects of calcium homeostasis in eukaryotic cells. European journal of biochemistry / FEBS. 1990;193(3):599-622. Epub 1990/11/13.

174.    Levin RM, Hypolite JA, Broderick GA. Evidence for a role of intracellular-calcium release in nitric oxide-stimulated relaxation of the rabbit corpus cavernosum. Journal of andrology. 1997;18(3):246-9. Epub 1997/05/01.

175.    Gregoire G, Loirand G, Pacaud P. Ca2+ and Sr2+ entry induced Ca2+ release from the intracellular Ca2+ store in smooth muscle cells of rat portal vein. The Journal of physiology. 1993;472:483-500. Epub 1993/12/01.

176.    Sparwasser C, Drescher P, Eckert R, Madsen PO. Ryanodine-sensitive intracellular Ca2+ stores in isolated rabbit penile erectile tissue. Urological research. 1995;22(6):393-8. Epub 1995/01/01.

177.    Sparwasser C, Schmelz HU, Drescher P, Eckert R, Madsen PO. Role of intracellular Ca2+ stores in smooth muscle of human penile erectile tissue. Urological research. 1998;26(3):189-93. Epub 1998/08/07.

178.    Friel DD, Tsien RW. Phase-dependent contributions from Ca2+ entry and Ca2+ release to caffeine-induced [Ca2+]i oscillations in bullfrog sympathetic neurons. Neuron. 1992;8(6):1109-25. Epub 1992/06/01.

179.    Eisner DA, Lederer WJ. Na-Ca exchange: stoichiometry and electrogenicity. The American journal of physiology. 1985;248(3 Pt 1):C189-202. Epub 1985/03/01.

180.    Juenemann KP, Lue TF, Abozeid M, Hellstrom WJ, Tanagho EA. Blood gas analysis in drug-induced penile erection. Urologia internationalis. 1986;41(3):207-11. Epub 1986/01/01.

181.    Kim JJ, Moon DG, Koh SK. The role of nitric oxide in vivo feline erection under hypoxia. International journal of impotence research. 1998;10(3):145-50; discussion 51. Epub 1998/10/27.

182.    Broderick GA, Gordon D, Hypolite J, Levin RM. Anoxia and corporal smooth muscle dysfunction: a model for ischemic priapism. The Journal of urology. 1994;151(1):259-62. Epub 1994/01/01.

183.    Kim NN, Kim JJ, Hypolite J, Garcia-Diaz JF, Broderick GA, Tornheim K, et al. Altered contractility of rabbit penile corpus cavernosum smooth muscle by hypoxia. The Journal of urology. 1996;155(2):772-8. Epub 1996/02/01.

184.    Saenz de Tejada I, Kim NN, Daley JT, Royai R, Hypolite J, Broderick GA, et al. Acidosis impairs rabbit trabecular smooth muscle contractility. The Journal of urology. 1997;157(2):722-6. Epub 1997/02/01.

185.    Moon DG, Lee DS, Kim JJ. Altered contractile response of penis under hypoxia with metabolic acidosis. International journal of impotence research. 1999;11(5):265-71. Epub 1999/12/20.

186.    Munarriz R, Park K, Huang YH, Saenz de Tejada I, Moreland RB, Goldstein I, et al. Reperfusion of ischemic corporal tissue: physiologic and biochemical changes in an animal model of ischemic priapism. Urology. 2003;62(4):760-4. Epub 2003/10/11.

187.    Kumar P MS, Ralph DJ. Models for the study of priapism. Curr Sex Health Reports. 2006;3(4):151-3.

188.    Wu C, Fry CH. The effects of extracellular and intracellular pH on intracellular Ca2+ regulation in guinea-pig detrusor smooth muscle. The Journal of physiology. 1998;508 ( Pt 1):131-43. Epub 1998/06/06.

189.     Wu C, Fry CH. Na(+)/Ca(2+) exchange and its role in intracellular Ca(2+) regulation in guinea pig detrusor smooth muscle. American journal of physiology Cell physiology. 2001;280(5):C1090-6. Epub 2001/04/05.

190.     Lynch RM, Paul RJ. Energy metabolism and transduction in smooth muscle. Experientia. 1985;41(8):970-7. Epub 1985/08/15.

191.     Paul RJ, Krisanda JM, Lynch RM. Vascular smooth muscle energetics. Journal of cardiovascular pharmacology. 1984;6 Suppl 2:S320-7. Epub 1984/01/01.

192.     Krebs HA. The citric acid cycle and the Szent-Gyorgyi cycle in pigeon breast muscle. The Biochemical journal. 1940;34(5):775-9. Epub 1940/05/01.

193.     Barron JT, Kopp SJ, Tow J, Parrillo JE. Fatty acid, tricarboxylic acid cycle metabolites, and energy metabolism in vascular smooth muscle. The American journal of physiology. 1994;267(2 Pt 2):H764-9. Epub 1994/08/01.

194.     Liston TG, Palfrey EL, Raimbach SJ, Fry CH. The effects of pH changes on human and ferret detrusor muscle function. The Journal of physiology. 1991;432:1-21. Epub 1991/01/01.

195.     Burdyga TV, Taggart MJ, Wray S. An investigation into the mechanism whereby pH affects tension in guinea-pig ureteric smooth muscle. The Journal of physiology. 1996;493 ( Pt 3):865-76. Epub 1996/06/15.

196.     Chu YH, Wu CC, Wang HW. Effect of cooling on electrical field stimulation and norepinephrine-induced contraction in isolated hypertrophic human nasal mucosa. American journal of rhinology. 2006;20(5):471-5. Epub 2006/10/27.

197.     Gonzalez O, Santacana GE. Effect of low temperature on tracheal smooth muscle contractile and relaxing responses evoked by electrical field stimulation. Puerto Rico health sciences journal. 2001;20(3):237-44. Epub 2002/01/05.

198.     Sabeur G. Effect of temperature on the contractile response of isolated rat small intestine to acetylcholine and KCl: calcium dependence. Archives of physiology and biochemistry. 1996;104(2):220-8. Epub 1996/01/01.

199.     Harker CT, Bowman CJ, Taylor LM, Jr., Porter JM. Cooling augments human saphenous vein reactivity to electrical stimulation. Journal of cardiovascular pharmacology. 1994;23(3):453-7. Epub 1994/03/01.

200.     Mustafa SM, Thulesius O. Cooling-induced bladder contraction: studies on isolated detrusor muscle preparations in the rat. Urology. 1999;53(3):653-7. Epub 1999/03/30.

201.     Burdyga TV, Magura IS. Effects of temperature and Na0+ on the relaxation of phasic and tonic tension of guinea-pig ureter muscle. General physiology and biophysics. 1988;7(1):3-15. Epub 1988/02/01.

202.	Burdyga TV, Wray S. On the mechanisms whereby temperature affects excitation-contraction coupling in smooth muscle. The Journal of general physiology. 2002;119(1):93-104. Epub 2002/01/05.

203.	Cooklin M, Wallis WR, Sheridan DJ, Fry CH. Conduction velocity and gap junction resistance in hypertrophied, hypoxic guinea-pig left ventricular myocardium. Experimental physiology. 1998;83(6):763-70. Epub 1998/10/23.

204.	Fry CH LS. Calibration of Ion-selective electrodes. Ion-selective electrodes for biological systems: Harwood academic publishers; 2001. p. 55-75.

205.	Grynkiewicz G, Poenie M, Tsien RY. A new generation of Ca2+ indicators with greatly improved fluorescence properties. The Journal of biological chemistry. 1985;260(6):3440-50. Epub 1985/03/25.

206.	Lattanzio FA, Jr., Bartschat DK. The effect of pH on rate constants, ion selectivity and thermodynamic properties of fluorescent calcium and magnesium indicators. Biochemical and biophysical research communications. 1991;177(1):184-91. Epub 1991/05/31.

207.	Maia RS, Babinski MA, Figueiredo MA, Chagas MA, Costa WS, Sampaio FJ. Concentration of elastic system fibers in the corpus cavernosum, corpus spongiosum, and tunica albuginea in the rabbit penis. International journal of impotence research. 2006;18(2):121-5. Epub 2005/10/15.

208.	Pinheiro AC, Costa WS, Cardoso LE, Sampaio FJ. Organization and relative content of smooth muscle cells, collagen and elastic fibers in the corpus cavernosum of rat penis. The Journal of urology. 2000;164(5):1802-6. Epub 2000/10/12.

209.	Takahara A, Yoshida K, Suzuki-Kusaba M, Hisa H, Satoh S. Effects of nifedipine and TMB-8 on angiotensin II-induced mesenteric vasoconstriction in dogs. Archives internationales de pharmacodynamie et de therapie. 1994;328(3):288-96. Epub 1994/11/01.

210.	Aggarwal NT, Gauthier KM, Campbell WB. Endothelial nitric oxide and 15-lipoxygenase-1 metabolites independently mediate relaxation of the rabbit aorta. Vascular pharmacology. 2012;56(1-2):106-12. Epub 2011/12/27.

211.	Nangle MR, Cotter MA, Cameron NE. An in vitro study of corpus cavernosum and aorta from mice lacking the inducible nitric oxide synthase gene. Nitric oxide : biology and chemistry / official journal of the Nitric Oxide Society. 2003;9(4):194-200. Epub 2004/03/05.

212.	Michel MC, Sand C. Effect of pre-contraction on beta-adrenoceptor-mediated relaxation of rat urinary bladder. World journal of urology. 2009;27(6):711-5. Epub 2009/05/19.

213.     de Jongh R, Haenen GR, van Koeveringe GA, Dambros M, De Mey JG, van Kerrebroeck PE. Oxidative stress reduces the muscarinic receptor function in the urinary bladder. Neurourology and urodynamics. 2007;26(2):302-8. Epub 2006/09/26.

214.     Amberg GC, Earley S, Glapa SA. Local regulation of arterial L-type calcium channels by reactive oxygen species. Circulation research. 2010;107(8):1002-10. Epub 2010/08/28.

215.     Levin RM, Hypolite JA, Longhurst PA, Gong C, Briscoe J, Broderick GA. Metabolic studies on the rabbit corpus cavernosum. Journal of andrology. 1993;14(5):329-34. Epub 1993/09/01.

216.     Rivera L, Brading AF. The role of Ca2+ influx and intracellular Ca2+ release in the muscarinic-mediated contraction of mammalian urinary bladder smooth muscle. BJU international. 2006;98(4):868-75. Epub 2006/09/19.

217.     Sward K, Josefsson M, Lydrup ML, Hellstrand P. Effects of metabolic inhibition on cytoplasmic calcium and contraction in smooth muscle of rat portal vein. Acta physiologica Scandinavica. 1993;148(3):265-72. Epub 1993/07/01.

218.     Pessina F, McMurray G, Wiggin A, Brading AF. The effect of anoxia and glucose-free solutions on the contractile response of guinea-pig detrusor strips to intrinsic nerve stimulation and the application of excitatory agonists. The Journal of urology. 1997;157(6):2375-80. Epub 1997/06/01.

219.     Pessina F, Solito R, Maestrini D, Gerli R, Sgaragli G. Effect of anoxia-glucopenia and re-superfusion on intrinsic nerves of mammalian detrusor smooth muscle: importance of glucose metabolism. Neurourology and urodynamics. 2005;24(4):389-96. Epub 2004/12/18.

220.     Juan YS, Chuang SM, Kogan BA, Mannikarottu A, Huang CH, Leggett RE, et al. Effect of ischemia/reperfusion on bladder nerve and detrusor cell damage. International urology and nephrology. 2009;41(3):513-21. Epub 2008/11/11.

221.     Corbett AD, Lees GM. Depressant effects of hypoxia and hypoglycaemia on neuro-effector transmission of guinea-pig intestine studied in vitro with a pharmacological model. British journal of pharmacology. 1997;120(1):107-15. Epub 1997/01/01.

222.     Munarriz R, Wen CC, McAuley I, Goldstein I, Traish A, Kim N. Management of ischemic priapism with high-dose intracavernosal phenylephrine: from bench to bedside. The journal of sexual medicine. 2006;3(5):918-22. Epub 2006/09/01.

223.     Wendt IR. Effects of substrate and hypoxia on smooth muscle metabolism and contraction. The American journal of physiology. 1989;256(4 Pt 1):C719-27. Epub 1989/04/01.

224.     Baxter KA, Laher I, Church J, Hsiang YN. Acidosis augments myogenic constriction in rat coronary arteries. Annals of vascular surgery. 2006;20(5):630-7. Epub 2006/10/03.

225.    Bradley AF, Severinghaus JW, Stupfel M. Variations of serum carbonic acid pK with pH and temperature. Journal of applied physiology. 1956;9(2):197-200. Epub 1956/09/01.

226.    Bradley AF, Severinghaus JW, Stupfel M. Effect of temperature on PCO2 and PO2 of blood in vitro. Journal of applied physiology. 1956;9(2):201-4. Epub 1956/09/01.

227.    Ebong OO. Influence of lowered temperature upon the response of prostatic and epididymal portion of the rat isolated vas deferens to field stimulation. Clinical and experimental pharmacology & physiology. 1986;13(1):9-16. Epub 1986/01/01.

228.    Stjarne L, Alberts P. Influence of temperature on stimulus-secretion coupling in the sympathetic nerves and on neuromuscular transmission, in guinea-pig vas deferens. Acta physiologica Scandinavica. 1985;125(2):181-94. Epub 1985/10/01.

229.    Mitsui T, Kitazawa T, Ikebe M. Correlation between high temperature dependence of smooth muscle myosin light chain phosphatase activity and muscle relaxation rate. The Journal of biological chemistry. 1994;269(8):5842-8. Epub 1994/02/25.

230.    Cooke JP, Shepherd JT, Vanhoutte PM. The effect of warming on adrenergic neurotransmission in canine cutaneous vein. Circulation research. 1984;54(5):547-53. Epub 1984/05/01.

231.    Vanhoutte PM, Cooke JP, Lindblad LE, Shepherd JT, Flavahan NA. Modulation of postjunctional alpha-adrenergic responsiveness by local changes in temperature. Clinical science. 1985;68 Suppl 10:121s-3s. Epub 1985/01/01.

232.    Foldes FF, Kuze S, Vizi ES, Deery A. The influence of temperature on neuromuscular performance. Journal of neural transmission. 1978;43(1):27-45. Epub 1978/01/01.

233.    Jaworowski A, Arner A. Temperature sensitivity of force and shortening velocity in maximally activated skinned smooth muscle. Journal of muscle research and cell motility. 1998;19(3):247-55. Epub 1998/05/16.

234.    Stephens NL, Cardinal R, Simmons B. Mechanical properties of tracheal smooth muscle: effects of temperature. The American journal of physiology. 1977;233(3):C92-8. Epub 1977/09/01.